BERICHTE
aus dem Fachbereich Geowissenschaften
der Universität Bremen

Nr. 103

Kerntopf, Beate

DINOFLAGELLATE DISTRIBUTION PATTERNS AND PRESERVATION IN THE EQUATORIAL ATLANTIC AND OFFSHORE NORTH-WEST AFRICA.

Berichte, Fachbereich Geowissenschaften, Universität Bremen, Nr. 103,
137 S., Bremen 1997

ISSN 0931-0800

Die "Berichte aus dem Fachbereich Geowissenschaften" werden in unregelmäßigen Abständen vom Fachbereich 5, Universität Bremen, herausgegeben.
Sie dienen der Veröffentlichung von Forschungsarbeiten, Doktorarbeiten und wissenschaftlichen Beiträgen, die im Fachbereich angefertigt wurden.

Die Berichte können bei:

Frau Gisela Boelen

Sonderforschungsbereich 261

Universität Bremen

Postfach 330 440

D 28334 BREMEN

Telefon: (49) 421 218-4124

Fax: (49) 421 218-3116

angefordert werden.

Zitat:
Kerntopf, B.
Dinoflagellate Distribution Patterns and Preservation in the Equatorial Atlantic and Offshore North-West Africa.
Berichte, Fachbereich Geowissenschaften, Universität Bremen, Nr. 103, 137 Seiten, Bremen, 1997.

ISSN 0931-0800

DINOFLAGELLATE DISTRIBUTION PATTERNS AND PRESERVATION IN THE EQUATORIAL ATLANTIC AND OFFSHORE NORTH-WEST AFRICA

Dissertation
zur Erlangung des
Doktorgrades der Naturwissenschaften

im Fachbereich 5 - Geowissenschaften
der Universität Bremen

vorgelegt von

Beate Kerntopf
Bremen

1997

For my Father:

H. G. Kerntopf

* 11.12.1915

† 14.08.1996

"No one could have dreamed
that we were being scrutinized,
as someone with a microscope
studies creatures that swarm
and multiply in a drop of water."

"....when, suddenly, the lid fell off!"

JEFF WAYNE's musical version of "THE WAR OF THE WORLDS"

CONTENTS:

List of Abbreviations

AABW	Antarctic Bottom Water
BC	Brazil Current
BCC	Benguela Coastal Current
BOC	Benguela Oceanic Current
CC	Canary Current
CNRY	Canary Current Coastal
E	east
ETRA	Eastern Tropical Atlantic
EUC	Equatorial Undercurrent
GC	Guinea Current
HCO	Holocene Climatic Optimum
ITCZ	Intertropical Convergence Zone
LGM	Last Glacial Maximum
LM	light microscope
MAS	accelerator-mass-spectrometer
MA SST	mean annual sea surface temperature
MAT	Modern Analogue Technique
MOW	Mediterranean outflow water
MUC	multicorer
N	north
NACW	North Atlantic Central Water
NADW	North Atlantic Deep Water
NATR	North Atlantic Tropical Gyre
NAST	North Atlantic Subtropical Gyre
NAST (E)	North Atlantic Subtropical Gyre (East)
NAST (W)	North Atlantic Subtropical Gyre (West)
NBCC	North Brazilian Coastal Current
NE	north-east
NEC	North Equatorial Current
NECC	North Equatorial Counter Current
NW	north-west
S	south
SACW	South Atlantic Central Water
SAIW	South Atlantic Intermediate Water
SAST	South Atlantic Subtropical Gyre
SE	south-east
SEC	South Equatorial Current
SECC	South Equatorial Counter Current
SEM	scanning electron microscope
SST	sea surface temperature
SW	south-west
Tc	cold season sea surface temperature
Tw	warm season sea surface temperature
W	west
WTRA	Western Tropical Atlantic
#	specimen number

1. INTRODUCTION

Dinoflagellates are eukaryotic and biflagellate organisms. They have a unique type of nucleus, the dinokaryon. The chromosomes are lacking histones and are permanently condensed. This is the apomorphic character of the Dinophyta *sensu* MÖHN (1984) and of the division Dinoflagellata (BÜTSCHLI, 1885) *sensu* FENSOME et al. (1993).

Free-living dinoflagellates are adapted to all major aquatic environments (freshwater lakes, brackish neritic water, and fully marine oceanic water) and are found in all climatic/biogeographic zones from tropic to arctic, where they live as planktic or benthic organisms. Many species are cosmopolitan.

The total variety of dinoflagellate life cycles are quite complex and numerous, with one basic sexual cycle being haplontic with haplontic vegetative cells and diploid zygotes. The sexual cycle may include the formation of gametes, which may fuse and produce a planozygote and subsequently a hypnozygote, i.e. lead to encystment and production of a resting cyst (Fig.1). After some time excystment occurs, and meiosis may happen before or after excystment. Asexual reproduction of vegetative Dinoflagellata usually happens as "closed" mitosis.

1.1. DINOFLAGELLATE LIFE STAGES

1.1.1. THE VEGETATIVE STAGE

The external cellular covering of vegetative dinoflagellates, the amphiesma, is a complicated and multi-layered structure with various membranes, organic phragmas, and a single layer of vesicles. These vesicles may either contain cellulosic plates (armoured or thecate dinoflagellates: orders Prorocentrales LEMMERMANN, 1910, Dinophysiales KOFOID, 1926, Peridiniales HAECKEL, 1894, Gonyaulacales TAYLOR, 1980) or be empty and flexible (unarmoured, athecate, or "naked" dinoflagellates: order Gymnodiniales APSTEIN, 1909). Within the coccoid dinoflagellates (order Thoracosphaerales TANGEN, 1982) the cell is covered with a calcified layer, embedded in between an inner and outer organic phragma.

Of the three basic "types" of vegetative dinoflagellates only the thecate and coccoid dinoflagellate cells are covered with a rigid "shell". The terms "vegetative-thecate dinoflagellates" and "vegetative-coccoid dinoflagellates" are suggested for these organisms, which will be comprised within the term "shelled vegetative dinoflagellates" to make a clear distinction from the unarmoured, athecate dinoflagellates.

Free-living dinoflagellate cells range in size from 5 µm to more than 1,500 µm. Most vegetative dinoflagellates are equipped with two dissimilar flagella for propulsion.

1.1.1.1. VEGETATIVE-THECATE DINOFLAGELLATES

A substantial terminology is applied to the description the morphological features of vegetative-thecate dinoflagellates. Fig.2 shows the main features and the major directional terms.

The cells are covered with numerous plates of cellulose. They fit tightly together and the line of junction between two plates is called a suture. The **thecal plates** can may vary in shape, thickness and ornamentation. The number and position of the thecal plates constitute the **tabulation**. The tabulation is thought to be a fairly stable feature and is used as a major taxonomic criterion in distinguishing genera and species. There exist various systems of tabulation, but the mostly adopted system was proposed by KOFOID (1907, 1909) for the Peridiniales.

The part of the cell which points "ahead", i.e. in the direction of swimming, is called the **anterior**, the **apical part** or, when looking at a theca, the **epitheca**. The opposite part or "end" is termed the **posterior**, the **antapical part**, or the **hypotheca**. A longitudinal groove, the **sulcus**, is running perpendicular to a spiral girdle, the **cingulum**, which encircles the cell in a more or less equatorial position. The sulcus is positioned on the **ventral side**, the **dorsal side** lying opposite. The flagella arise from pores at the anterior end (e.g. *Prorocentrum* EHRENBERG, 1834) or from the ventral surface of the organism where the sulcus and cingulum intersect (e.g. *Dinophysis* EHRENBERG 1839, *Gonyaulax* DIESING 1866). The longitudinal flagellum is "whip-like" and beats posteriorly, whereas the transverse flagellum is ribbon-like with multiple waves beating to the left in the cingulum.

Dinoflagellates vary greatly in their nutritional modes. They may be autotrophs, mixotrophs, and/or heterotrophs (saprophytic, phagocytic, and/or parasitic organisms). Photosynthetic dinoflagellates (autotrophs) are equipped with chloroplasts where, in addition to several unique dinoflagellate pigments, chlorophylls *a* and c_2 are present.

Fig.1: Thecate Dinoflagellate Main Life Cycles (i.a. after Evitt, 1985; Below, 1987)

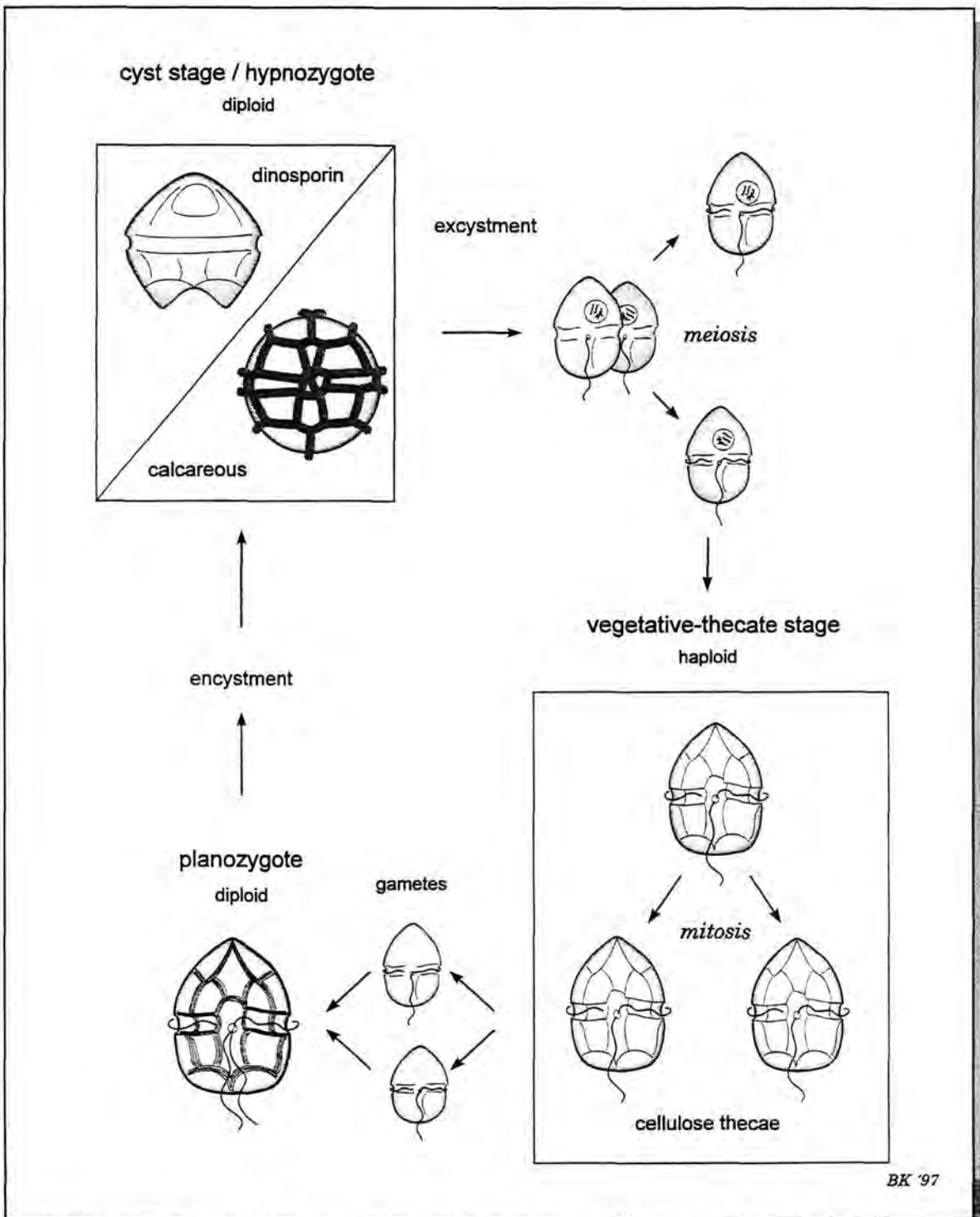

Fig. 1: Vegetative-thecate dinoflagellate main life cycles (i.a. after EVITT, 1985; BELOW, 1987). The sexual cycle may include the formation of gametes, planozygotes, and hypnozygotes (i.e. resting cysts). Asexual reproduction may happen as mitosis (i.e. cell division).

Fig.2: Thecate Dinoflagellate Morphology and Terminology

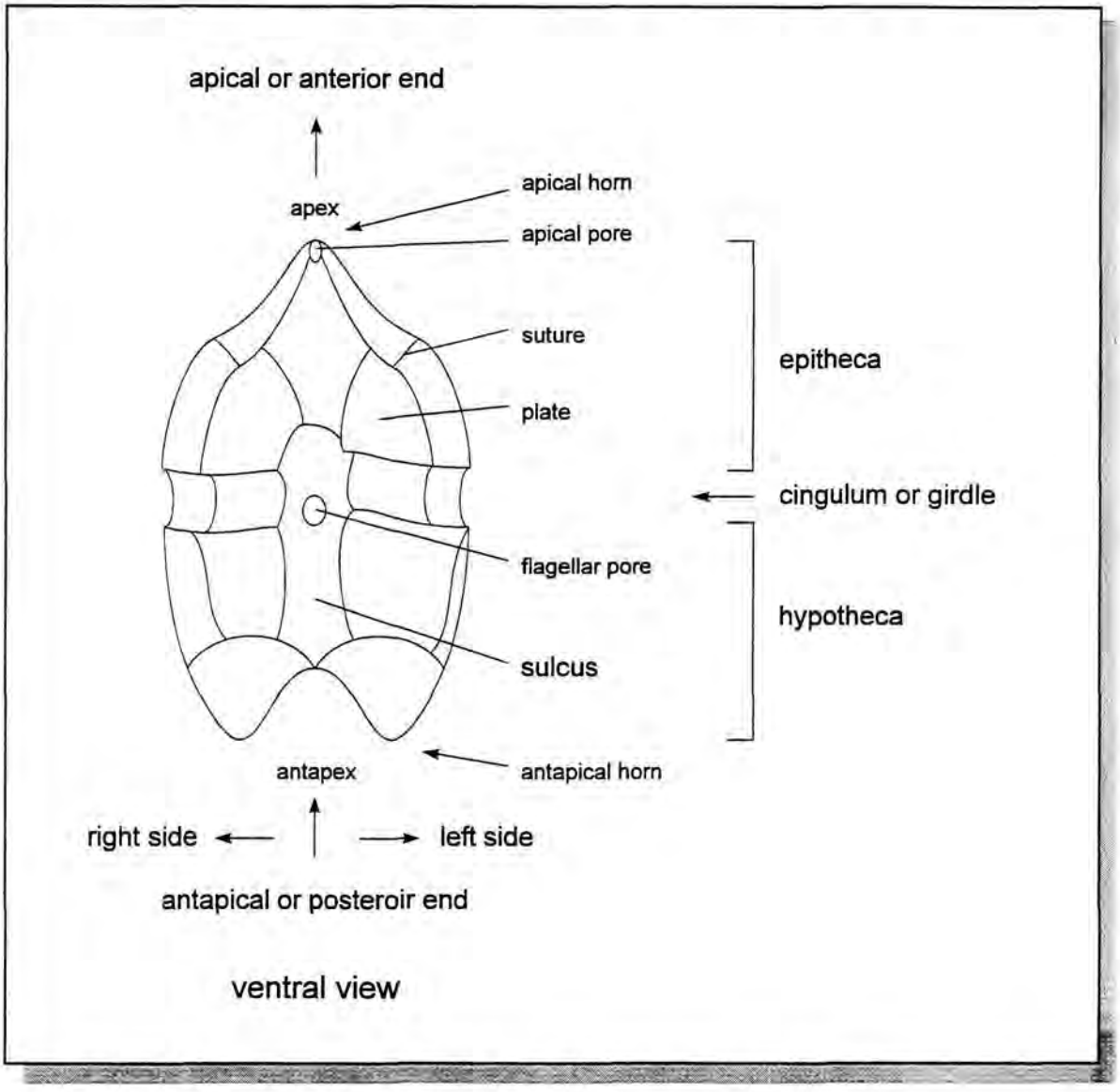

Fig. 2: Basic thecal morphology and directional terms used for descriptions (modified after EVITT, 1985).

The autotrophic mode of nutrition predominates, and the vegetative-thecate dinoflagellates are commonly regarded as part of the phytoplankton. In marine plankton, they are among the more important primary producers. Their productivity at temporary blooms may be extremely high and cause red tides. Some marine species produce toxins, which might cause various types of shellfish poisoning.

1.1.1.2. VEGETATIVE-COCCOID DINOFLAGELLATES

Thoracosphaerids, i.e. specimens of the species *Thoracosphaera heimii* (LOHMANN) KAMPTNER 1927, are members of the calcareous nannoplankton of the major oceans. The genus *Thoracosphaera* was first described by KAMPTNER (1927) from plankton and sediment samples. He placed them within the coccolithophorids, but their systematic position has been questionable ever since.

Fig.3: Vegetative-coccoid *Thoracosphaera heimii* Main Cell Cycle

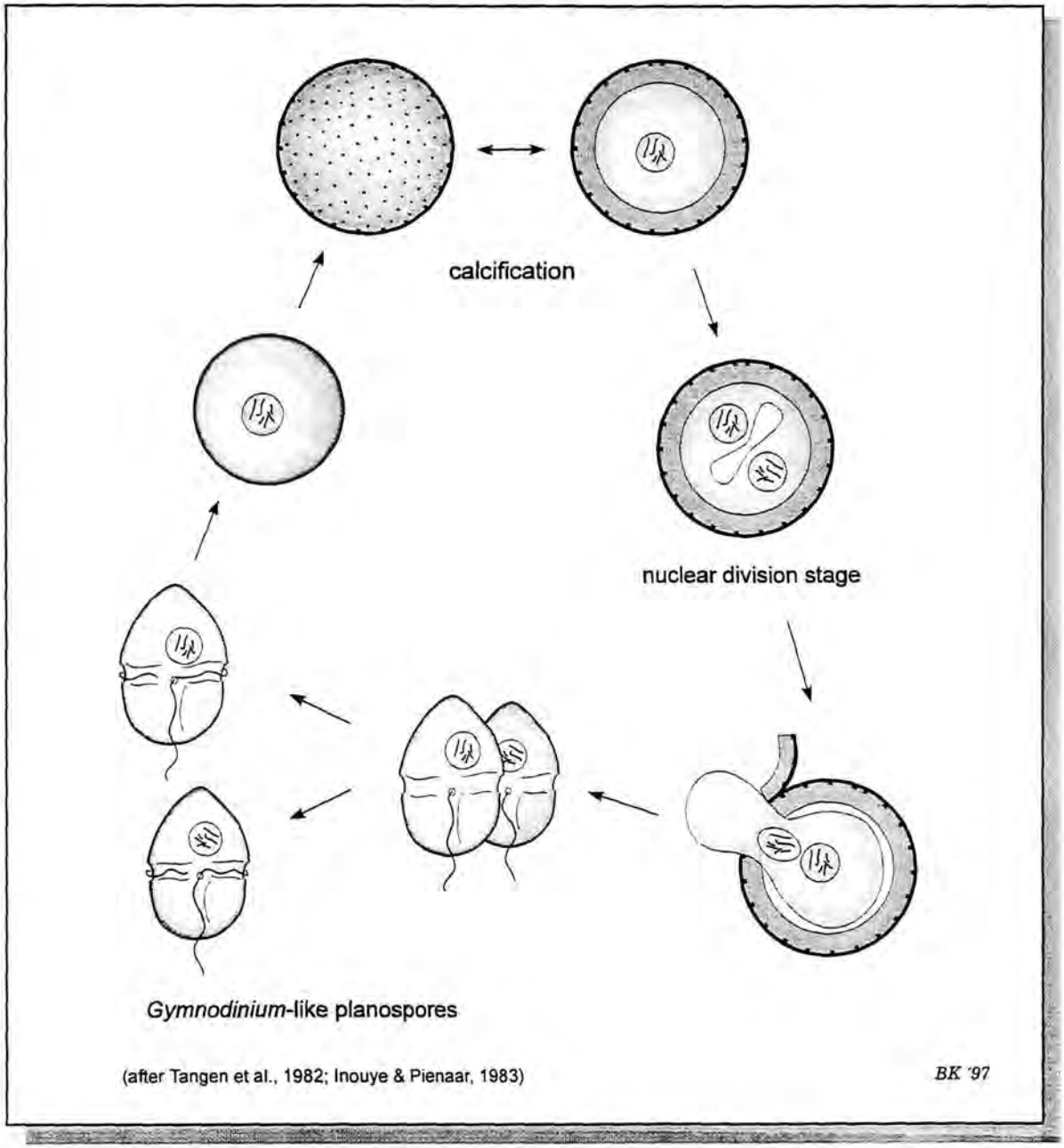

Fig. 3: Main cell cycle of vegetative-coccoid *Thoracosphaera heimii* (adapted from TANGEN et al., 1982; INOUYE & PIENAAR, 1983).

TANGEN et al. (1982) and INOUYE & PIENAAR (1983) successfully isolated *Th. heimii* into culture and established its classification within the new order Thoracosphaerales TANGEN, 1982 of the class Dinophyceae.

Observations of the life cycle (Fig.3) and morphology of their clones showed that the calcareous cell wall is present in the vegetative-coccoid life stage. The nucleus within a vegetative cell undergoes nuclear division to produce a vegetative-coccoid cell with two nuclei. An opening or aperture is formed by ring-shaped corrosion or dissolution of the calcite from the inner shell surface (TANGEN et al., 1982). The binucleate cell is released through this circular aperture, and the then free-living, motile, and still binucleate cell divides into two dinospores.

The binucleate cell and the dinospores may have, or have not, flagella. The dinospores change their shape and become biflagellate athecate planospores (INOUYE & PIENAAR, 1983). The calcified cell develops directly from the planospores. No sexual fusion was observed by INOUYE & PIENAAR (1983). All life stages possess chloroplasts and a dinokaryotic nucleus.

The Thoracosphaerales are therefore coccoid marine dinoflagellates capable of primary calcification of the cell wall in the vegetative life phase (vegetative-coccoid dinoflagellates). The calcified cell of *Th. heimii* is not a resting cyst at all, which is most unusual in the class Dinophyceae.

1.1.2. THE CYST STAGE

Only a few living genera of dinoflagellates are able to produce cysts. The cyst wall consists of one or more layers and may furthermore be composed of cellulose, calcite, or an organic sporopollenin-like material, i.e. "dinosporin" (FENSOME et al., 1993). Cysts with cellulosic wall material are very delicate and rarely found. Most dinoflagellate cysts have a dinosporin or calcitic wall.

In the present study, the terms "dinoflagellate cysts", "dinocysts", or "cysts" are used to describe resting cysts. They represent "...a dormant stage in which normal life processes are greatly reduced..." (FENSOME et al., 1993, p.6). Dinocysts may result from sexual fusion, these cysts are hypnozygotes. After encystment, the dinocysts possibly are either morphologically very different from the vegetative stage or closely resemble it.

Cysts may show a reflected tabulation or **paratabulation**. To distinguish between cysts and thecae the prefix "para" is applied to most morphological terms of the cysts. Where a paracingulum is present the apical part of the cell is called the epitract, the antapical portion is called hypotract.

The release of the protoplasm from the cyst (excystment) occurs through an "escape hole", the **archaeopyle**. This is formed by the complete or partial removal of one or several paraplates, the **operculum**, of the epitract. The form and position of the archaeopyle is a determined feature and constant within the known species.

1.1.2.1. DINOSPORIN CYSTS

Generally, two major groups of dinosporin cysts are recognized (WALL et al., 1977; LEWIS et al., 1990; POWELL et al., 1990; EDWARDS et al., 1991; VERSTEEGH, 1994). One group may be related to the autotrophic family Gonyaulacaceae LINDEMANN, 1928. Vegetative-thecate species of this family are known to produce the so-called "G-cysts". The other group is formed by vegetative-thecate species of the heterotrophic genus *Protoperidinium* BERGH, 1882, and therefore is called the "P-cysts".

1.1.2.2. CALCAREOUS CYSTS

Living calcareous cysts are produced as hypnozygotes by a closely related group of orthoperidinioid dinoflagellates capable of primary calcification of the cyst wall. The knowledge of cyst-theca relationships has grown considerably owing to recent incubation experiments with isolated specimens. The motile thecate cells have been identified as belonging to the genera *Ensiculifera* BALECH, 1967 (WALL & DALE, 1968a; MATSUOKA et al., 1990), *Pentapharsodinium* INDELICATO & LOEBLICH III, 1986 (MONTRESOR et al., 1993), and *Scrippsiella* BALECH, 1959 (WALL & DALE, 1968a; WALL et al., 1970; MONTRESOR & ZINGONE, 1988; AKSELMAN & KEUPP, 1990; GAO & DODGE, 1991; LEWIS, 1991; MONTRESOR et al., 1994).

1.2. DINOFLAGELLATE PRESERVATION

The two basic life stages, vegetative and encysted, are usually investigated separately. The distribution pattern of vegetative dinoflagellates has been recorded in biological studies of plankton organisms. Although the motile vegetative-thecate cells are abundant and widely distributed, they lack a mineralized test and, after death, are easily destroyed by bacterial activity. Therefore, the vegetative-thecate dinoflagellates are less readily preserved for study than other phytoplankton groups such as the coccolithophorids or diatoms. The vegetative-coccoid species *Th. heimii*, with its calcareous shell, is the only exception of this rule. *Th. heimii*-shells in the sediments represent vegetative dinoflagellate remains which may reflect dinoflagellate productivity in corresponding surface water masses (DALE & DALE, 1992).

Merely the *Th. heimii*-shells and the dinosporin or calcareous resting cysts are preserved in the sediments and known in the fossil record, at least from the Triassic onwards (JAFAR, 1979; JANOFSKE, 1992; FENSOME et al., 1996). Dinoflagellate cysts are an important group of microfossils used by palaeontologists for the interpretation of sediment biostratigraphy. The ecology of planktic, vegetative dinoflagellates and the

environmental conditions favouring cyst production are of general interest in research. But, not all vegetative-thecate dinoflagellate species produce cysts. Only about 20% of living species are known to form cysts (EDWARDS et al., 1991). Of these, the proportion of motile cells forming cysts is variable and ranges from 0.2% to 50% (DALE, 1983; DALE & DALE, 1992). To date, for the tropical Atlantic Ocean, only a few attempts have been made to correlate plankton distribution data with cyst data from sediments (DODGE & HARLAND, 1991; DODGE, 1994).

Therefore, the fossil record of dinoflagellates represents only the thanatocoenosis of *Th. heimii*-shells together with a few cyst-producing vegetative species. Thus, dinoflagellate fossils give only rudimentary evidence of the biocoenosis of vegetative dinoflagellate populations, but nevertheless carry information related to a variety of palaeo-environmental conditions in surface waters.

For a better understanding of fossil dinoflagellates, one should be obliged to include as many aspects of Recent dinoflagellate life stages as possible in one single study. Therefore, this study is primarily an exploratory one. The major aim is to investigate the standing stock of free-living dinoflagellates in the tropical fully oceanic Atlantic, i.e. to include diverse dinoflagellate life stages into one qualitative inventory. Species composition, abundance, and distribution of Recent dinoflagellates are described from the plankton and from the sediment surface of the equatorial Atlantic and offshore NW Africa.

Even though the coverage of the Atlantic is only rudimentary, relationships may be established between distribution patterns of planktic dinoflagellates and the oceanographic parameters of the corresponding surface waters (such as temperature, salinity, productivity, and the current system). These plankton data will be compared with cyst data from the bottom sediments, in order to provide ecological information that may define probable palaeo-environmental indicators for subsequent biostratigraphic investigations.

1.3. DINOFLAGELLATE DISTRIBUTION PATTERNS

A substantial part of the ocean's primary productivity is provided by dinoflagellates. Living dinoflagellates of all life stages have been found in all major aquatic environments, but the majority (90%) are marine planktic or benthic forms (TAYLOR, 1987b). In tropical and temperate oceanic waters, the phytoplankton population is dominated by coccolithophorids and dinoflagellates; dinoflagellates contribute up to 70% of the shelled phytoplankton (LOHMANN, 1912; HENTSCHEL, 1936; TAYLOR, 1976, 1987b; GOULD & FRYXELL, 1988). While diatoms tend to dominate phytoplankton populations under high nutrient conditions, such as in upwelling areas, they may add up to more than 90% of the shelled phytoplankton (LOHMANN, 1912; HENTSCHEL, 1936; HEAD et al., 1996; JICKELLS et al., 1996).

The development of dinoflagellate species associations is generally related to light, sea surface temperature (SST), sea surface salinity (SSS), nutrient supply (divergence/ upwelling), grazing (by other, heterotrophic dinoflagellates and by zooplankton), and the distributing current system (TAYLOR, 1987b; STEIDINGER & TANGEN, 1996). The different currents within the water column play an important role in the distribution of dinoflagellates (DALE & DALE, 1992).

Generally, there are two basic trends in dinoflagellate distribution patterns: environmental and climatic (WALL et al., 1977; HARLAND, 1983, 1988; TAYLOR, 1987b; DODGE & HARLAND, 1991; EDWARDS et al., 1991; DALE & DALE, 1992; EDWARDS, 1992; EDWARDS & ANDRLE, 1992; DODGE, 1994; DODGE & MARSHALL, 1994; STEIDINGER & TANGEN, 1996). Species assemblages are associated with nearshore, neritic or fully oceanic environments (environmental or inshore-offshore trend); some species prefer tropical, south-subtropical or more north-temperate to arctic regions (latitudinal or climatic trend). They are recorded in all climatic/biogeographic "provinces" or "zones" from tropic to arctic regions, but species diversity is the largest in tropical environments (TAYLOR, 1987b).

- **Vegetative-thecate dinoflagellates:** TAYLOR (1987a) gives a synopsis of previously offered general aspects of the biology, ecology and distribution of marine vegetative-thecate dinoflagellates. Recently an overview of common species distribution data was given by STEIDINGER & TANGEN (1996).

While a considerable amount of distribution data is available for the North Atlantic Ocean (including its coastal areas, i.a. DODGE, 1982, 1993, 1994; DODGE & HARLAND, 1991; DODGE & MARSHALL 1994), for the South-West Atlantic south of 20°S (e.g. BALECH, 1988), as well as for more restricted areas as the Caribbean (e.g. WOOD, 1968), there is a

remarkable blank in the dinoflagellate records of the equatorial Atlantic Ocean. Other plankton surveys provide only limited data by including merely certain dinoflagellate families or genera (e.g. HALLEGRAEFF & LUCAS, 1988; CARBONELL-MOORE, 1994a, 1996a,b; DODGE & MARSHALL 1994); or samples may have been obtained without recording the corresponding oceanographic parameters, and planktic distribution patterns are inadequately related to mean annual parameters.

In tropical oceans, less than 10% of the vegetative-thecate dinoflagellate species are able to produce cysts, and the cyst assemblages are overwhelmingly dominated by calcareous forms (DALE, 1976; DALE, 1983; DODGE & HARLAND, 1991; DALE & DALE, 1992).

- **Vegetative-coccoid dinoflagellates:** *Th. heimii* has been reported from the plankton and bottom sediments of the temperate to tropical oceans (KAMPTNER, 1927, 1963, 1967; FÜTTERER, 1976, 1977). After the culture studies of TANGEN et al. (1982), they were described in calcareous nannoplankton biocoenosis of sediment trap samples from the equatorial Atlantic (STEINMETZ, 1991) and the central Sargasso Sea, where they contribute up to 36,000 specimens/m²·day to the sediment flux (DALE & DALE, 1992).

The abundance of vegetative-coccoid *Th. heimii*-shells in the sediments may be directly interpreted as indicator for their primary productivity in the adjacent sea surface masses (DALE & DALE, 1992).

- **Dinosporin cysts:** Recent workers (WALL et al., 1977; REID & HARLAND, 1977; HARLAND, 1983, 1988; DODGE & HARLAND, 1991; EDWARDS et al., 1991; EDWARDS, 1992; EDWARDS & ANDRLE, 1992; MARRET, 1994) confirmed the two basic trends in cyst distribution patterns: environmental and climatic. Dinosporin cysts are recorded abundantly from the cold temperate Atlantic of higher latitudes and from its coastal areas (e.g. HARLAND, 1983, 1988; DODGE & HARLAND, 1991; MATTHIESSEN, 1991; DALE & DALE, 1992; EDWARDS, 1992; EDWARDS & ANDRLE, 1992; DE VERNAL et al., 1992; DODGE, 1994). In the tropical Atlantic, they are mainly found in coastal and estuarine environments (WALL et al., 1977; MARRET, 1994). "Oceanic assemblages" described from pelagic sediments have been probably transported there by bottom water masses from more coastal areas (DALE & DALE, 1992).

High amounts of P-cysts are considered to occur in upwelling and/or coastal areas where nutrients are high (WALL et al., 1977; LEWIS et al., 1990; POWELL et al., 1990). The ratio between G-cysts and P-cysts is assumed to be related to changes in productivity. But throughout the published data no uniform equation for this ratio can be found. The various authors use different ratios for their purposes: e.g. HARLAND (1973) uses the number of the different species to calculate the P/G ratio; EDWARDS et al. (1991) define their G/P ratio as the ratio of the total number of specimens of the two cyst affinities; whereas POWELL et al. (1990) and VERSTEEGH (1994) used the number of specimens to obtain, even though totally different, P/G equations. Some dinocyst analyses (e.g. DODGE, 1994) show no clear distinction between G-cysts or P-cysts distribution. This ratio, let it be G/P- or P/G-ratio, includes, in the estimation of dinoflagellate productivity, only a small number of cyst forming species and an unknown proportion of cyst forming specimens. The specimen density of other species, autotrophic and heterotrophic, are not included in this interpretation.

- **Calcareous cysts:** Until quite recently, only dinosporin cysts were observed by palaeontologists. Mineralized cysts, e.g. calcareous cysts, were destroyed by hydrochloric (HCl) and hydrofluoric acid (HF) routinely used in palynological preparation methods. Owing to their small size (10-50 µm) the calcareous cysts were washed through sieves during preparation for foraminiferal studies, and for nannoplankton studies they are generally too large to be included.

The relative amount of calcareous dinocysts may vary considerably in coastal sediments. MONTRESOR et al. (1994) reported the highest amount so far; 27-79% of the entire dinocysts assemblage in the Gulf of Naples were calcareous forms. Abundances from temperate coastal areas (DALE, 1976; BOLCH & HALLEGRAEFF, 1990; LEWIS, 1991; ELLEGARD et al., 1994; BLANCO, 1995; NEHRING, 1995) may be much lower.

However in the fully oceanic Atlantic Ocean the relative amount of calcareous dinocysts increases from higher to lower latitudes (DALE & DALE, 1992). Small amounts were recorded in the higher latitudes (0-12% in Nordic Seas; DALE & DALE, 1992) and large amounts in lower latitudes (82-100% in the central Sargasso Sea and the tropical Atlantic; DALE & DALE, 1992). This contrasts sharply with the cyst signal previously recorded from low-latitude coastal areas (WALL et al., 1977; MARRET, 1994) and from the cold-temperate high-latitude Atlantic

Ocean (HARLAND, 1983, 1988; DODGE & HARLAND, 1991; MATTHIESSEN, 1991; DALE & DALE, 1992; DODGE, 1994). These assemblages consist almost entirely of dinosporin cysts.

In the tropical Atlantic few calcareous cyst species are found in great abundances: e.g. *Calciodinellum operosum* DEFLANDRE, 1947, *Orthopithonella granifera* (FÜTTERER) KEUPP & KOHRING, 1993, *"Sphaerodinella" albatrosiana* (KAMPTNER) KEUPP & VERSTEEGH, 1989, *"Sph." tuberosa* (KAMPTNER) KEUPP & VERSTEEGH, 1989, and the calcareous cyst of *Scrippsiella trochoidea* (STEIN) LOEBLICH III, 1978, i.e. *Rhabdothorax erinaceus* (KAMPTNER) KAMPTNER, 1958. They contribute at least several thousands of calcareous cysts/m²·day to the sediment flux (DALE & DALE, 1992). The flux of vegetative-coccoid *Th. heimii*-shells, however, is roughly ten times greater. Relatively few specimens in a population of thecate dinoflagellates produce resting cysts, whereas up to one division per day was observed in thoracosphaerid cultures (Dale, 1983).

2. MATERIAL AND METHODS

2.1. SAMPLES

The studied material was obtained during RV METEOR cruises M 20/1 in November/ December 1991 (WEFER et al., 1993) and M 23/3 during March/April 1993 (WEFER et al., 1994). Plankton samples were collected from the surface water of ~4.5m depth, and sediment samples were recovered via multi-corer from the ocean floor surface. For sample examination both light microscope (LM) and scanning electron microscope (SEM) were used.

-Plankton Samples: The plankton samples were recovered during cruise M 23/3 and site positions were located in three sections (Fig.4). The first section covers the equatorial Atlantic between 24°W and 12°W (samples 22-S08 to 22-S16), the second and third sections cover the western margin of the upwelling region offshore NW Africa extending from the equator at 12°W towards NW to 11.5°N/21°W (samples 22-S16 to 22-S23) and N to the Canary Isles (samples 22-S23 to 22-S37). As the plankton samples were collected, the corresponding oceanographic parameters were routinely recorded and are listed in Tables 1 and 2.

Plankton samples were pumped on board ship with a membrane vacuum pump from a water depth of ~4.5m. The larger zooplankton organisms were separated by passing the water through a 250 µm mesh sieve. The plankton was then concentrated on cellulose nitrate or polycarbonate membrane filters of pore size 5 µm. The filters were dried over night (at ~30°C) and stored in air-tight containers.

On board ship the polycarbonate membrane filters were cut into halves, one half was embedded in Canada Balm on standard slides for preliminary LM examinations.

The cellulose nitrate membrane filters and the remaining half of the polycarbonate membrane filters were mounted on stubs with adhesive tape and sputtered with gold for SEM examination. The filters were traversed several times and a minimum of 200 specimens of shelled phytoplankton organisms were counted directly from the SEM screen.

Dinoflagellates of various life stages were observed. Whole coccospheres and aggregates of coccoliths of the same species were recorded. Diatoms were found less frequently. Dinoflagellates, coccospheres, and diatoms contributed to the shelled phytoplankton and the relative abundances of the different phytoplankton groups was estimated. Most filters were clogged with organic mucus, therefore it was not possible to calculate the absolute specimen densities.

The plankton filters were closely investigated for dinoflagellate cells. Various species of vegetative-thecate dinoflagellates, their calcareous cysts, and the vegetative-coccoid *Th. heimii*-shells were recorded.

- Sediment Samples: During cruise M 20/1, sediment surface samples were obtained via multicorer. Site positions were offshore NW Africa; site GeoB 1602-7 was located off Cape Blanc within the transition of coastal upwelling-open ocean systems (FISCHER & WEFER, 1996). Sites GeoB 1606-7 and GeoB 1607-8 were positioned in the eastern equatorial Atlantic, i.e. in the western part of the Guinea Basin beneath the westward flowing South Equatorial Current (SEC) and the eastern equatorial upwelling area (FISCHER & WEFER, 1996) (Fig.5).

Average sedimentation rates are 3 cm/ky for the area off Cape Blanc (ANDERSEN, 1996) and 2cm/ka for the Guinea Basin (WEFER et al., 1993). The sample parameters are listed in Table 3. All sediment surface samples have a high carbonate content and were not affected by dissolution; the major lithological unit in all cores is nannofossil-foraminiferal ooze or foraminiferal ooze (WEFER et al., 1993).

On board ship the cores of the multicorer were cut in 1cm slices (oriented perpendicular to the core's long axis), the slices were stored in wet condition at 4°C. To prevent partial solution of the delicate calcareous dinoflagellates further treatment of the sediment samples was carried out in an alkalic environment (H_2O + NH_3, pH~10). The samples were washed through a 63 µm mesh sieve and the fraction <63 µm was collected in beakers. The material <5 µm was then separated by decantation after hydraulic sedimentation of the larger particles (FÜTTERER, 1990). The 5-63 µm sediment fraction was stored in 30% alcoholic solution.

From the upper 5 samples of each core, smear slides were taken and mounted within Canada Balm for preliminary LM examinations.

The preparation technique of JANOFSKE (1990) was modified to mount the samples on SEM stubs with an unexposed and developed black and white photographic film strip as adhesive (Fig.6). Prior to this a grid had been scratched onto the gelatinous side of the film strip. Film strip size is about 0.25 cm^2 and the grid squares are 1 mm^2 each. The strip was fixed on the SEM stub with adhesive tape, the gelatinous side up.

Table 1: M23/3 plankton sample parameters of the equatorial Atlantic.

SAMPLE-NO.	22-S08	22-S10	22-S11	22-S13	22-S14	22-S16	22-S17	22-S18
Latitude	01° 13' S	00° 00'	00° 00'	00° 00'	00° 00'	00° 00'	02° 44' N	03° 08' N
Longitude	24° 09' W	23° 30' W	17° 45' W	16° 51' W	13° 26' W	11° 58' W	13° 10' W	13° 31' W
Date	28.03.1993	29.03.1993	31.03.1993	31.03.1993	01.04.1993	01.04.1993	03.04.1993	03.04.1993
Time (UTC)	15:00	17:30	09:27	14:44	09:54	17:44	12:29	15:29
Bathymetry [m]	4327	3711	6035	3874	4212	4581	4541	4677
Air Temperature [°C]	27.8	27.5	26.9	27.5	23.8	27.1	27.5	28.0
Air Pressure [hPa]	1009.6	1009.7	1011.9	1009.8	1012.9	1009.5	1010.3	1007.8
Sea Surface Temperature [°C]	27.8	27.7	27.4	27.6	26.9	27.5	28.8	29.4
Sea Surface Salinity [‰]	36.25	36.24	35.83	35.87	36.08	36.07	35.05	35.00
Sample Volume [l]	130	130	140	140	140	112	140	140

Table 2: M23/3 plankton sample parameters of the East Atlantic offshore NW Africa and at the Canary Isles.

SAMPLE-NO.	22-S20	22-S21	22-S23	22-S26	22-S27	22-S32	22-S33	22-S34	22-S36	22-S37
Latitude	08° 29' N	08°50 N'	11° 29' N	14° 13' N	18° 11' N	21° 43' N	22° 23' N	22° 27' N	29° 06' N	29° 09' N
Longitude	18° 23' W	18° 42' W	21° 03' W	20° 14' W	19° 05' W	18° 01' W	17° 49' W	17° 48' W	15° 27' W	15° 27' W
Date	05.04.1993	05.04.1993	06.04.1993	07.04.1993	08.04.1993	09.04.1993	09.04.1993	09.04.1993	11.04.1993	11.04.1993
Time (UTC)	09:37	12:21	12:59	14:57	14:32	10:33	14:21	14:48	10:11	14:23
Bathymetry [m]	4735	4640	4972	4181	3118	1454	2165	2267	3608	3613
Air Temperature [°C]	25.2	25.5	22.8	21.8	19.6	19.8	19.8	19.8	17.9	17.8
Air Pressure [hPa]	1012.3	1012.4	1013.1	1011.3	1011.5	1013.9	1013.2	1013.1	1022.8	1020.9
Sea Surface Temperature [°C]	26.1	25.7	24.0	21.7	20.1	19.3	19.5	19.4	18.6	18.6
Sea Surface Salinity [‰]	35.75	35.70	35.59	35.90	36.03	36.37	36.68	36.64	36.82	36.80
Sample Volume [l]	140	140	140	112	10	28	28	42	84	84

Fig.4: Plankton Sample Site Positions

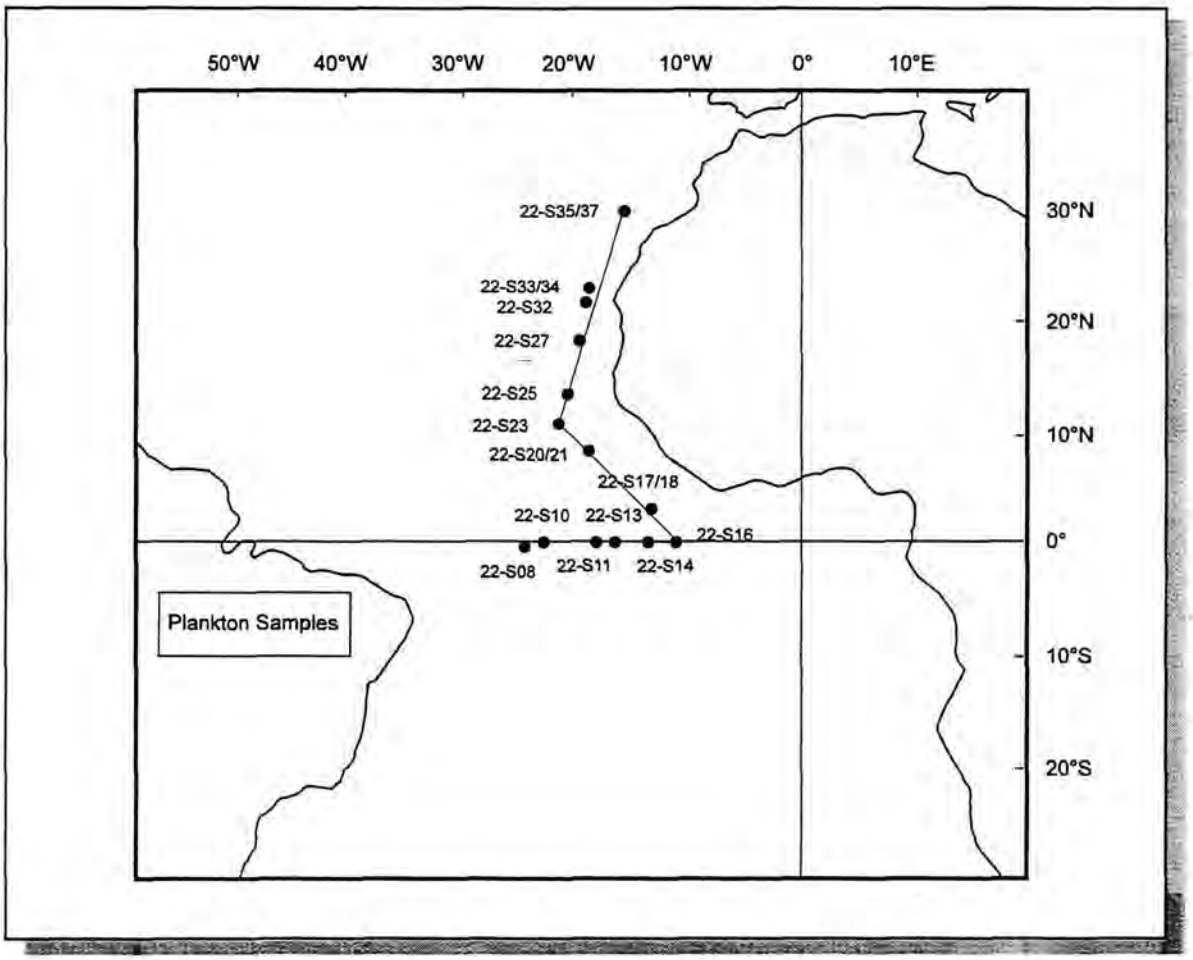

Fig. 4: Map of plankton sample site positions of cruise M 23/3. Sections cover the equatorial Atlantic, the area offshore NW Africa influenced by upwelling, and the ocean area at the Canary Isles.

The 5-63 µm sediment samples were shaken well to get a homogeneous suspension and a few drops were put on the film strip. Then, the stubs were air dried, washed to remove all particles not embedded in the gelatinous layer of the strip and dried again. This method gives an even layer of sediment particles mounted on an SEM stub.

After having been sputtered with gold, the SEM stubs were examined for dinoflagellates. No thecal remains and no dinosporin cysts could be found, whereas calcareous cysts and *Th. heimii*-shells were found in great numbers. To get a semi-semi-quantitative abundance of the individual species, a certain amount of grid squares were examined. For each sample, specimens of dinoflagellate remains, at least a total of 200, were counted directly from the SEM screen and the specimen density on the SEM stub was calculated. The species abundances of the uppermost centimetre of each sediment core is considered to reflect the present sedimentary process.

SEM examinations were carried out with a CamScan CS44 Scanning Electron Microscope.

Samples and micrographs are stored at the department *Historische Geologie/ Paläontologie* (i.e. Historical Geology/ Palaeontology) of the *Fachbereich 5-Geowissenschaften* (i.e. Geosciences Faculty) at the University of Bremen.

Fig.5: Sediment Sample Site Positions

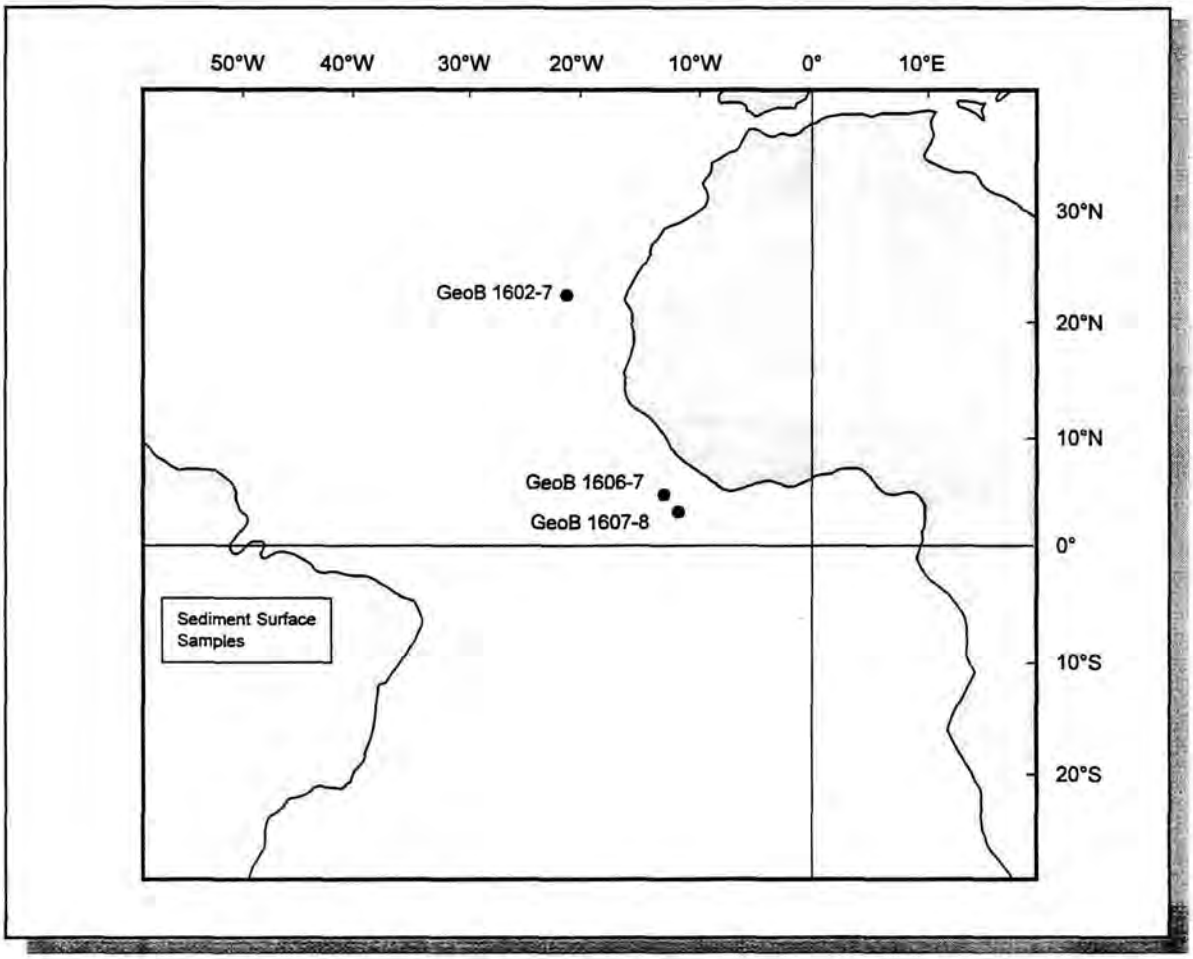

Fig. 5: Map of surface sediment sample site positions of cruise M 20/1. Samples were recovered via multicorer from offshore NW Africa (GeoB 1602-7 MUC, off Cape Blanc) and from the eastern equatorial Atlantic (GeoB 1606-7 MUC, GeoB 1607-8 MUC, in the Guinea Basin).

Table 3: M20/1 multicorer sediment sample parameters.

SITE GEOB-NO.	1602-7	1606-7	1607-8
	OFF CAPE BLANC	GUINEA BASIN	
Latitude	21° 10.9' N	03° 03.9' N	01° 48.2' N
Longitude	20° 42.7' W	11° 54.9' W	11° 16.4' W
Date	27.11.1991	03.12.1991	04.12.1991
Time Bottom Contact (UTC)	21:22	09:30	21:56
Bathymetry [m]	4098	4451	4318
Core Recovery [cm]	31	30	35

Fig.6: Sediment Samples on SEM Stubs

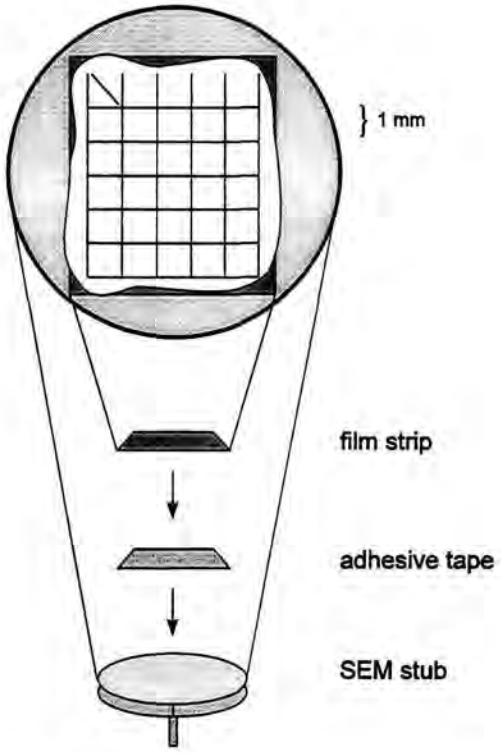

Fig. 6: Mounting of sediment samples on SEM stubs. The 5-63 µm fraction of the sediment samples is mounted on the SEM stubs by means of an especially prepared film strip and adhesive tape.

2.2. TAXONOMY

Two different classification systems exist for both the vegetative and the cyst stages. Traditionally, biologists use a classification largely based on the non-fossilizable, motile, vegetative cells in the plankton. Palaeontologists have established a classification based on the morphology of fossil cysts. Recently, a phylogenetically-based classification scheme was suggested by FENSOME et al. (1993) combining the two different systems. Even though vegetative stages and cysts should be included in one general classification of dinoflagellates, there still are some problems in combining them.

Extensive use of the SEM allowed the examination of plankton filters and sediment samples at both low and high magnifications. A collection of several thousands of electron micrographs have been accumulated. The most distinct and instructive micrographs have been selected, and an atlas of scanning electron micrographs of various dinoflagellate species is presented with the photographic plates in the appendix.

- **Vegetative-thecate dinoflagellates:** In the present study, the "outline of classification" for the vegetative-thecate dinoflagellates is mainly based on TAYLOR (1987) and FENSOME et al. (1993). Classification on family level is based on various authors (i.a. FENSOME et al., 1993; STEIDINGER & TANGEN, 1996).

The descriptions of vegetative-thecate dinoflagellates are given on genus level only. STEIDINGER & TANGEN (1996) offer common

genera and species descriptions. Descriptions were adapted from WOOD (1968), TAYLOR (1976), ABÉ (1981), DODGE (1982), SOURNIA (1986), BALECH (1988), and from various other authors quoted.

Descriptions are presented by order then alphabetically by family and genera.

- **Vegetative-coccoid dinoflagellates:** LOHMANN (1920) first described the vegetative-coccoid species as *Syracosphaera heimi* LOHMANN, 1920. KAMPTNER (1927) established the new genus *Thoracosphaera* with the type species *Thoracosphaera pelagica*, he already mentioned a close resemblance of *Th. pelagica* to *S. heimi*. Later, KAMPTNER (1944) considered these descriptions as conspecific and combined them under the name *Thoracosphaera heimii* (LOHMANN) KAMPTNER.

KAMPTNER (1927) first included the then *Th. pelagica* and other "*Thoracosphaera*"-species within the coccolithophorids. Later, FÜTTERER (1976, 1977) based their classification among the peridinoid dinoflagellates. He emphasised that all "Thoracosphaeroideae" are calcareous dinocysts, owing to the presence of an archaeopyle with most species; even though another major criterion, reflected tabulation by means of crystallite ridges, is absent with all species. But, the outer shell of *Thoracosphaera heimii*, the type species of this genus, does not possess any visible operculum or other distinctive features with dinoflagellate affinities. On the other hand, no evidence was provided to support the coccolithophorid classification.

At last, clonal culture studies by TANGEN et al. (1982) and INOUYE & PIENAAR (1983) confirmed that *Th. heimii* is a dinophyte and not a coccolithophorid. The calcareous shell wall is present in the vegetative-coccoid life phase, and therefore this species is not a resting cyst at all. A new order was established "for primarily coccoid marine dinoflagellates that possess a calcified cell wall in the vegetative life phase" (TANGEN et al., 1982). No archaeopyle with an operculum, as defined for dinoflagellate cysts, was observed. This order represents a distinctly different group of dinoflagellates with apertural differences from and ultrastructural similarities to calcareous cysts. As yet, the order contains only one family with a single type species of the genus *Thoracosphaera*.

- **Calcareous cysts:** The taxonomic positions of various calcareous dinoflagellate cysts are uncertain and there still are unsolved problems of relating living species to fossil ones. There exist only a few studies of their biostratigraphy compared with other groups of microfossils or nannofossils. Diagenetic alterations may change the characteristics of fossil species and thus create "new diagenetic species" (FÜTTERER, 1977). Natural variations in the cyst wall morphology of some recent and fossil species add to the general taxonomic confusion. Their skeletal elements may be quite variable in shape and size, even if their ultrastructural arrangement appears to be the same for two or more species.

Fossil, calcareous dinocysts were first described by DEFLANDRE (1947, 1948) from the Miocene of El Medhi, Algeria. He misinterpreted *Calciodinellum operosum* DEFLANDRE, 1947 as a fossil vegetative dinoflagellate species and accordingly established the family Calciodinellaceae.

After germination experiments with modern calcareous dinoflagellates, WALL & DALE (1968b) concluded that Quaternary calcareous dinoflagellates are peridinoid resting cysts, and that Mesozoic and Tertiary calciodinellids very probably have the same affinities. FÜTTERER (1976, 1977) observed various morphological similarities of "*Thoracosphaera*" *albatrosiana* KAMPTNER, 1963 with *C. operosum* and suggested that specimens of this species were calcareous dinocysts as well.

On the other hand, the calcareous shell wall of the Thoracosphaerid type species (*Thoracosphaera heimii*) proved to be present in the vegetative-coccoid life phase; thus it is not a resting cyst at all (TANGEN et al., 1982; INOUYE & PIENAAR, 1983). The new order Thoracosphaerales was established and yet this order contains only one family with a single species of the genus *Thoracosphaera*. Other species of calcareous spheres formerly referred to this genus, presumably real dinocysts, were known only by their calcareous wall remains. Very recently, the corresponding motile planktic stages and the respective cell cycles were established in clonal culture studies for some of these species (MONTRESOR et al., 1997; JANOFSKE, pers. comm.).

BUJAK & DAVIS (1983) emended the family Calciodinellaceae to include all this data and positioned peridiniinean dinoflagellates with calcareous cysts within this family. Since then, biologists and palaeontologists have traditionally classified calcareous dinocysts within the family Calciodinellaceae (FÜTTERER, 1990; JANOFSKE, 1990, 1992; JANOFSKE & KEUPP, 1992; KEUPP & KOHRING, 1993, 1994; KEUPP & MUTTERLOSE, 1984; KEUPP & VERSTEEGH, 1989; KOHRING, 1993;

LEWIS, 1991; MONTRESOR et al., 1993, 1994; VERSTEEGH, 1993; WILLEMS, 1985, 1988, 1990, 1992, 1994; ZÜGEL, 1994).

The first examinations of calcareous dinocysts were carried out with a light microscope (LM), and some ultrastructural characteristics were given in terms of LM, e.g. crystallographic orientation of the c-axes of calcite crystals (KAMPTNER, 1967). In and after the seventies, modern work was mainly done by using a scanning electron microscope (SEM) and describing the morphological properties of the skeletal crystallites. The morphological orientation of the elongated calcite crystals were assumed to be analogous with the crystallographic orientation. And a taxonomy based on these SEM descriptions was established. KEUPP (1987) proposed the subdivision of the family Calciodinellaceae into three subfamilies according to crystallite orientation in the outer wall layer (Orthopithonelloideae KEUPP, 1987: radial orientation; Obliquipithonelloideae KEUPP, 1987: irregularly arranged, oblique to tangential orientation; Pithonelloideae KEUPP, 1987: uniform oblique orientation). Another subfamily (Fuettererelloideae KOHRING, 1993: tangential orientation) was later added by KOHRING (1993).

KEUPP & VERSTEEGH (1989) divided the subfamily Orthopithonelloideae into two tribes: the Orthopithonelleae KEUPP & VERSTEEGH, 1989 and the Calciodinelleae KEUPP & VERSTEEGH, 1989. The tribe Calciodinelleae comprises cyst species with a large archaeopyle formed by the detachment of the apical and intercalary paraplates. The crystallographic c-axes of the crystallites were assumed to be radially oriented. The following genera were included in this tribe: *Calciodinellum* DEFLANDRE, 1947, *Calcigonellum* DEFLANDRE, 1948, *Calcipterellum* DEFLANDRE, 1948, and the newly established genus *Sphaerodinella* KEUPP & VERSTEEGH, 1989. All more or less spherical cyst species of this tribe with missing or rudimentary paratabulation and a large, polygonal archaeopyle were included in the new genus, and type species was "*Sphaerodinella*" *albatrosiana* (KAMPTNER) KEUPP & VERSTEEGH, 1989 (formerly known as "*Thoracosphaera*" *albatrosiana* KAMPTNER, 1963).

Recent work done by JANOFSKE (1996) on the crystallographic orientation of the skeletal crystallites of modern calcareous dinocysts raises questions on the entire taxonomy of calcareous cysts. It was shown that in most cases the crystallographic c-axes were not the equivalent of the morphological axes.

The c-axes of "*Sph.*" *albatrosiana* wall crystallites were strictly oriented tangential. Additionally, in LM and in SEM examinations it was observed that in all aspects of skeletal ultrastructure "*Sph.*" *albatrosiana* shows complete correspondence with *Calciodinellum operosum* (KARWATH, unpubl. data; JANOFSKE, pers. comm.). Various authors (FÜTTERER, 1976, 1977; KEUPP, 1984; KEUPP et al., 1991; DALE, 1983; DALE & DALE, 1992; KOHRING, 1993) discussed the ultrastructural and morphological similarities of *C. operosum* and "*Sph.*" *albatrosiana*, and their undoubtedly close systematic relationship based on "the continuous transition, in skeletal architecture and ultrastructure" (FÜTTERER, 1976). Recent incubation experiments by MONTRESOR et al. (1997) give circumstantial evidence for their close systematic relationship: isolated *C. operosum*-like cysts from the Mediterranean were germinated to produce *Scrippsiella*-like motile thecate dinoflagellates. Thecal clones in turn encysted and produced any transition between plain "*Sph.*" *albatrosiana*-like cysts and *C. operosum*-like cysts with well defined ridges >3 µm.

Therefore, the type species of the tribe Calciodinelleae and the type species of the genus *Sphaerodinella* are not members of the subfamily Orthopithonelloideae at all, but belong to the subfamily Fuettererelloideae (crystals with the c-axes parallel to the cysts surface, i.e. tangential orientation).

Furthermore, LM examinations of "*Sphaerodinella*" *tuberosa* (KAMPTNER) KEUPP & VERSTEEGH, 1989 revealed a tangential orientation of crystallite c-axes in the early stages of wall crystallisation; this tangential orientation became more and more oblique with crystallisation progress as the crystallites move closer together (JANOFSKE, 1996, pers. comm.; KARWATH, unpubl. data). Consequently, this species is not a member of the subfamily Orthopithonelloideae, and should be installed into the subfamily Fuettererelloideae as well.

So far, all these data leave *Sphaerodinella arctica* (GILBERT & CLARK) KEUPP & VERSTEEGH, 1989 as the only species of *Sphaerodinella*. Specimens of this species were recently examined with a LM and a strictly radial orientation of the crystallographic c-axes was observed (JANOFSKE, pers. comm.).

Thus, the systematic positions of *Sphaerodinella* species, among others, are confused and there still are unsolved taxonomic problems of relating them with the "proper" subfamilies.

- **Calcareous dinoflagellates:** In the sediments, the calcareous dinocysts together with the vegetative-coccoid *Th. heimii*-shells make up the "calcareous dinoflagellate species assemblage". Descriptions of calcareous dinoflagellates are given on species level. For basic information purposes, they are primarily described from the sediments and discussed in detail, additional remarks on living specimens are given for the plankton samples.

2.3. PLANKTIC DISTRIBUTION PATTERNS

Plankton investigations within this study are focused on the shelled phytoplankton organisms with emphasis on shelled vegetative dinoflagellates and their cysts.

The planktic distribution pattern of the dinoflagellate species, presented here, was executed on presence-or-absence (binary) data, modified after DODGE & PRIDDLE (1987) and DODGE & HARLAND (1991). The abundance of species could only be estimated and is given in relative terms such as "rare" (not more than 5 specimens occurring in 1 or 2 samples each), "frequent" (up to 15 specimens reported from more than 3 samples respectively), or "abundant" (more than 15 specimens present in more than 5 samples respectively).

TAYLOR (1987b) summarizes previously offered general aspects of marine vegetative-thecate dinoflagellate distributions. The prevalent and extensive plankton surveys of WOOD (1968), DODGE (1982), BALECH (1988), and STEIDINGER & TANGEN (1996) have been selected to achieve a maximum in consistency while comparing previously presented data with the planktic distribution data of the present study.

Furthermore, an attempt has been made to correlate the distribution pattern of selected planktic dinoflagellate species with various oceanographic parameters. Non-ubiquitous species which occurred in more than three samples were selected and their presence was plotted for the site positions in a) temperature-, b) salinity-, and c) productivity-maps. Temperature and salinity were routinely noted with the plankton sample parameters. The phytoplankton productivity map, i.e. chlorophyll pigment concentrations recorded via satellite, has been adapted from BERGER (1989). The resulting biogeographic distribution maps show the influence of the surface circulation pattern and other oceanographic parameters of the tropical Atlantic.

3. OCEANOGRAPHIC PARAMETERS

The tropical oceans act as a regulating and transporting medium of heat for the earth's climate. Interhemispheric heat transfer by surface waters characterises the Atlantic Ocean. Vertical and horizontal advection of warmth at the equator is controlled in part by surface winds forced by insolation.

The modern circulation of the surface waters in the tropical Atlantic is driven by seasonal variations in the trade wind system. The asymmetry of the continents and the Atlantic Ocean shape the tropospheric structure such that the southern hemisphere trade winds extend into the northern hemisphere for much of the year.

Seasonal changes of the winds are associated with the meridional migrations of the Intertropical Convergence Zone (ITCZ) which fluctuates between 5°N and 10°-15°N in the East Atlantic; the ITCZ may be defined as the boundary between the southeast (SE) and northeast (NE) trade winds (RICHARDSON & PHILANDER, 1987), i.e. the doldrums. The mean annual position of the ITCZ in the northern hemisphere, near 8°N, is associated with a net flow of warm near-surface waters from the southern to the northern hemisphere.

Much of the seasonal variability in the upper ocean is associated with the meridional motion of the ITCZ as it follows the periodical cycle of the thermal equator; the most remarkable examples are the seasonal cycle within the equatorial current system and the seasonal reversal of some currents (HOUGHTON, 1991).

High-frequency wind fluctuations may stir the surface waters. The depth of this stirring or mixed layer is defined by the depth in which the influences of surface heat exchange and surface wind stress forcing are most intense (HASTENRATH & MERLE, 1987). In the Gulf of Guinea the mixed layer may be shallow, but it will increase its depth towards the west as the thermocline deepens in that direction (RICHARDSON & PHILANDER, 1987).

During boreal summer (June-September), the confluence between weak NE trades and strong cross-equatorial airstreams from the southern hemisphere is displaced far northwards and a pronounced pattern of wind stress curl dominates over the equatorial North Atlantic (HASTENRATH & LAMB, 1977). The SE trade winds are at their seasonal maximum intensity, they invade the northern hemisphere and push the ITCZ northwards according to the asymmetry of the Atlantic Ocean and the bordering continents. In August, the thermal equator and the ITCZ are furthest from the equator in their northernmost position, between ~5°N in the west and ~15°N in the east (PETERSON & STRAMMA, 1991). The NE trades are at their seasonal minimum intensity.

During boreal winter (December-March), the NE trade winds are at their strongest, and the thermal equator is at its southernmost position, near the equator in the west and near 5°N in the east. The intensity of the SE trades are at a seasonal minimum. The ITCZ is displaced to the south and at its southernmost position from November to April (HASTENRATH & LAMB, 1977).

In times of maximum NE trades, the winds bring a significant supply of aeolian dust to the Gulf of Guinea which precipitates within the ITCZ and may influence oceanic sedimentation north of the equator (MATTHEWSON et al., 1995).

During March and April, at the end of boreal winter, the surface wind field is least asymmetric with respect to the equator. The ITCZ is close to the equator, winds at the ITCZ are relaxed and surface currents are relatively weak and westwards everywhere except to the north of the equator in the Gulf of Guinea (RICHARDSON & PHILANDER, 1987). Cruise M 23/3 started from Brazil and four days were spent offshore South America in an area of weak SE trade wind intensity; the ITCZ was only slightly evident and it was passed between ~0°N/12°W and ~10°N/20°W; north of 11°N the region of NE trade winds, with frequently changing strength, was entered (WEFER. et al., 1994).

3.1. SURFACE CURRENTS

The modern sea surface circulation of the tropical Atlantic Ocean is driven by seasonal variations of the trade winds. Fig.7 shows schematically the upper-level circulation of the tropical Atlantic.

The important oceanographic currents for this study are the Canary Current (CC) and the equatorial current system with its system of gyres and the equatorial current and counter current system.

- **Offshore NW Africa:** The oceanography of the eastern ocean boundary, with its seasonal variation of temperature, salinity, and upwelling, was summarized by MITTELSTAEDT (1991).

The Canary Current (CC) and coastal upwelling are the two principal components of the modern surface circulation in this area (CHAPMAN et al., 1996). Both are driven by seasonal variations in the position and intensity of the NE trade winds.

Fig.7: Tropical Atlantic Sea Surface Currents

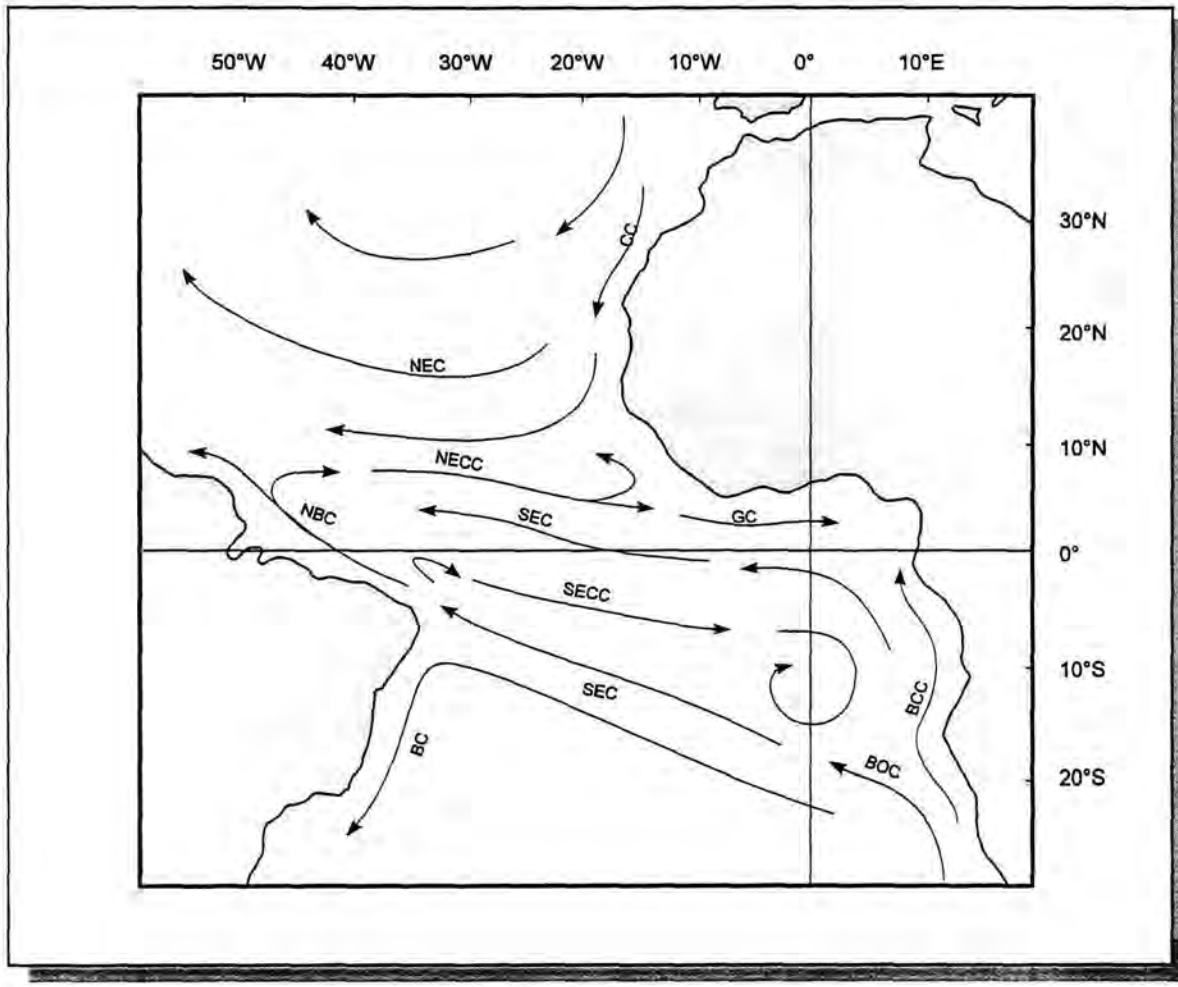

Fig. 7: Schematic representation of large-scale, upper-level current system of the tropical Atlantic (after PETERSON & STRAMMA, 1991; MITTELSTAEDT, 1991).

NEC:	North Equatorial Current	NECC:	North Equatorial Counter Current
SEC:	South Equatorial Current	SECC:	South Equatorial Counter Current
CC:	Canary Current	GC:	Guinea Current
NBC:	North Brazilian Coastal Current	BCC:	Benguela Coastal Current
BC:	Brazil Current	BOC:	Benguela Oceanic Current

The CC is part of the eastern boundary current of the NAST. South of 33°N it flows south-westward along the NW African continent and transports cooler water from higher to lower latitudes. It becomes detached from the continental margin between 25°N and 20°N and branches further south to feed the North Equatorial Current (NEC) and the Guinea Current (GC). During boreal summer the NE trades are at their seasonal minimum intensity, resulting in a weak NEC and little upwelling off NW Africa. The strong NE winds during boreal winter drive the NEC to its maximum. This is accompanied by greatly enhanced wind driven coastal upwelling and a pronounced southward advection of cold water in the CC along the NW African coast. This cold water may be entrained into the North Atlantic Subtropical Gyre (NAST). The relatively large seasonal cycle off NW Africa at 15°-20°N reflects seasonal movements of a front

separating cold CC waters from warmer tropical waters.

- **Equatorial Atlantic:** The current system south of 15°N comprises an intricate pattern of westward flowing currents and seasonal eastward flowing countercurrents. PETERSON & STRAMMA (1991) described the upper-level general circulation with its large-scale variability and interannual warmings.

During boreal summer, the strong SE trade winds drive the South Equatorial Current (SEC) to its maximum velocity (PHILANDER & PACANOWSKI, 1986; PETERSON & STRAMMA, 1991). The SEC is a multi-banded north-westward flowing structure originating from the eastern South Atlantic. North of 30°S, the Benguela Oceanic Current (BOC) turns offshore and toward the northwest, as it feeds the eastward flowing, relatively warm surface waters of the South Atlantic Subtropical Gyre (SAST); BOC and SAST blend gradually and become the southern branch of the SEC, which may be described as the main westward current of the SAST.

The SEC flows with maximum velocity along the equator from 2°N to 4°S. Between this fast but narrow northern branch and the broad southern branch of the SEC flows the South Equatorial Counter Current (SECC) in an eastward direction along the 5°S latitude (REID, 1964a,b; MOLINARI, 1982; PETERSON & STRAMMA, 1991). The SECC extends from the coast of Brazil to the north Angola Basin, where it turns towards the south.

At the eastern rise of South America at 10°S, the SEC bifurcates into the north-westward flowing North Brazilian Coastal Current (NBC) and into the south-westward flowing Brazil Current (BC) (STRAMMA et al., 1990). The NBC flows along the South American Coast in a generally north-westward direction. The NBC increases between 5°S and 2.5°S, as it is fed from the westward directed northern branch of the SEC; and it decreases across ~10°N as it, in turn, is feeding the North Equatorial Counter Current (NECC) (PHILANDER & PACANOWSKI, 1986).

The NECC forms a band of eastward flow between 3°N and 10°N and has its greatest eastward advection during boreal summer (MITTELSTAEDT, 1991). The NECC comprises the northern boundary of the westward flowing SEC (PETERSON & STRAMMA, 1991). The NECC loses some of its water to the northward Ekman drift, but most of it is lost to convergence (PHILANDER & PACANOWSKI, 1986). Between July and October, when the local westward winds are most intense, there is intense convergence along ~8°N latitude, and water flows back south at the depth of the thermocline.

Because of the strong westward advection of the SEC, the eastward flowing Equatorial Under Current (EUC), is poorly developed (PETERSON & STRAMMA, 1991). The weak EUC is found directly beneath the sea surface along the equator

As the NECC approaches the African continent, it branches out into a northward flowing part that blends into the NEC, and an eastward flowing part that enters into the Gulf of Guinea and merges into the Guinea Current (GC) (MITTELSTAEDT, 1991; PETERSON & STRAMMA, 1991).

In the western tropical Atlantic, all this strong westward advection leads to a sloping sea surface, as the surface water masses are piled up.

During boreal winter, weak SE trades in the western Atlantic result in a seasonal decrease in westward advection of the SEC. At the equator, the velocity is even less intense owing to the eastward flowing EUC which has its maximum flow during this time.

The EUC is a narrow jet of relatively saline and well oxygenated subthermocline water fed by the NBC across ~3°N (PETERSON & STRAMMA, 1991). Observations by DÜING et al. (1975) showed a condensed EUC with a meandering core between 0°50`N and 0°50`S, its intensity weakening towards the east before it terminates ~150 km from the African coast at 1°20`S (PETERSON & STRAMMA, 1991).

The advection of the EUC, although it is fed from the north as it flows eastward, decreases from 30°W to 10°W because of equatorial divergence. The ascending water feeds the westward flow of the SEC, which occupies the surface layers in the area to the south of 3°N, and sustains the divergent Ekman drift, especially into the southern hemisphere, where it is swept westward toward the NBC (PHILANDER & PACANOWSKI, 1986).

During boreal winter, the NECC is pushed south to the equator and its flow is weak and irregular (MITTELSTAEDT, 1991). NECC flow decreases even more as water is lost to convergence; this water flows southward and feeds into the EUC (PHILANDER & PACANOWSKI, 1986). The EUC in turn loses it because of weak equatorial divergence (PHILANDER & PACANOWSKI, 1986; HASTENRATH & MERLE, 1987).

Fig.8: April Sea Surface Temperature

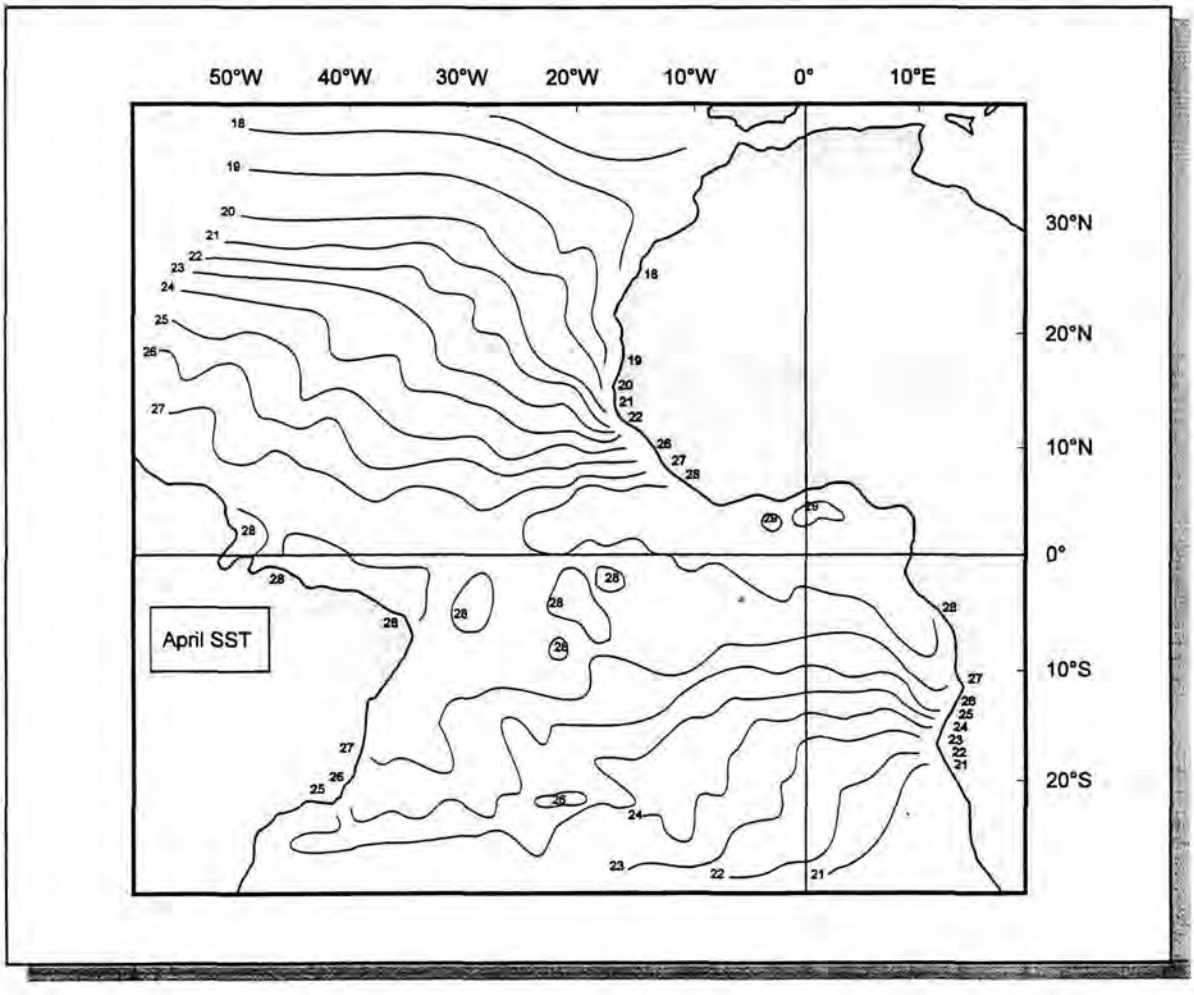

Fig. 8: April sea surface temperature map of the tropical Atlantic (after HASTENRATH & LAMB, 1977). Isotherms (in °C) correspond with the actually recorded temperatures during cruise M 23/3.

3.2. SEA SURFACE TEMPERATURE

Sea Surface Temperature (SST) is the oceanographic parameter with the most direct influence on the overlying atmosphere (HOUGHTON, 1991). Modern SST of the tropical Atlantic, in turn, is controlled by both atmospheric and upper ocean processes, i.e. by the wind driven surface currents and divergence.

The plankton samples were taken in March and April, and a representative SST distribution map after HASTENRATH & LAMB (1977), is given in Fig.8. The isotherms correspond with the actually recorded temperatures during cruise M 23/3. Any SST ranges of plankton organisms will be recorded temperature ranges.

Temperature references for the sediment cores will be mean annual temperatures (Fig.9) according to LEVITUS (1982). The warmest mean annual (MA) SST (>27°C) is found in the western equatorial Atlantic. This reflects the radiative heating of surface waters advected westward in the NEC and SEC, and the general northward cross-equatorial heat transport in the Atlantic.

The relatively cool MA SST off NW Africa (<21°C) and in the eastern equatorial Atlantic just south of the equator (<25°C) are caused by seasonal divergence and advection of cool subthermocline waters into these areas.

Fig.9: Mean Annual Sea Surface Temperature

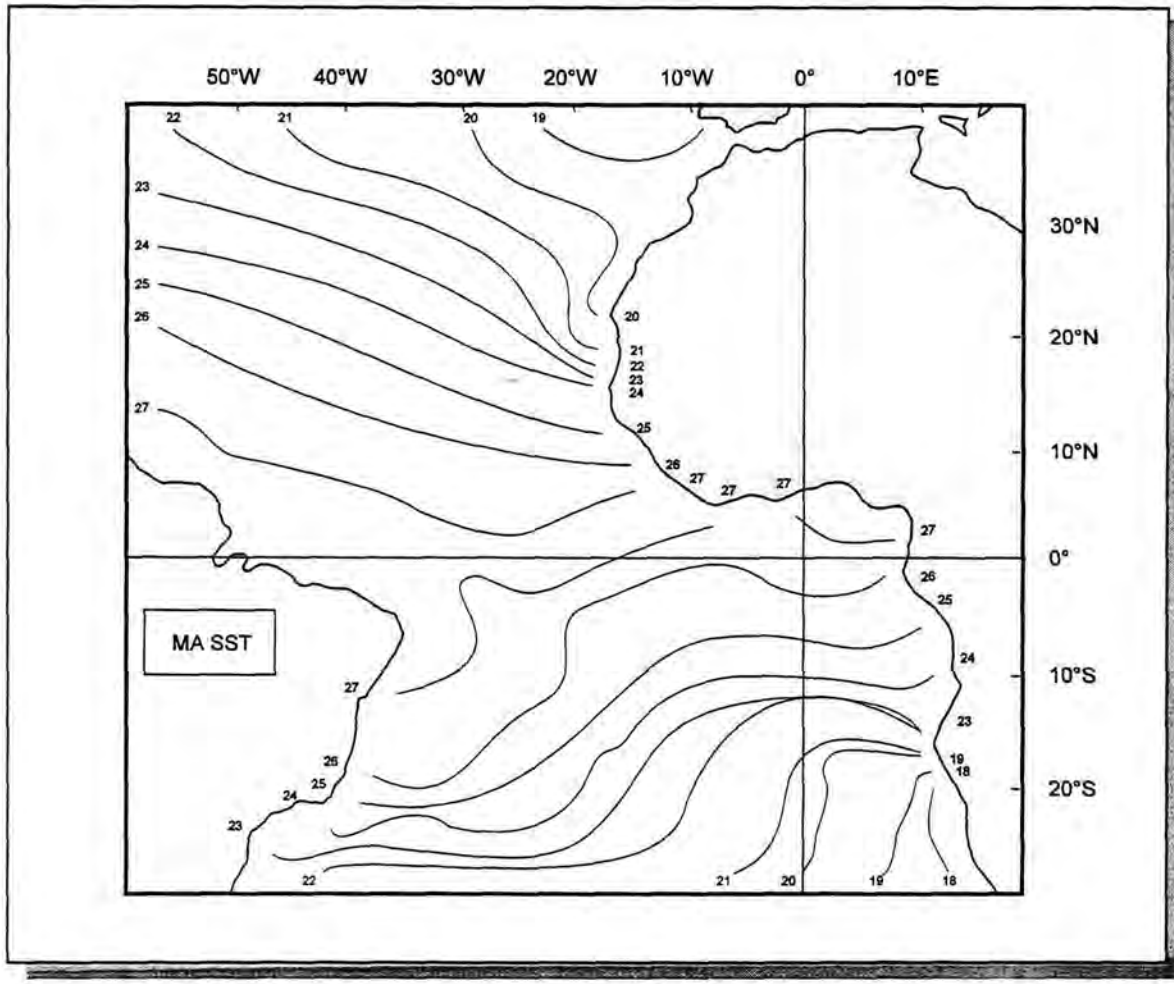

Fig. 9: Mean annual sea surface temperature map of the tropical Atlantic (isotherms in °C, after LEVITUS, 1982).

The annual variation of SST, i.e. the SST range, is commonly expressed as seasonality.

- **Offshore NW Africa:** The annual changes in SST on the NW African shelf vary with the latitude, increasing towards the south (MITTELSTAEDT, 1991). Seasonality is no more than 2-3°C north of 30°N, with a minimum SST of 15°C (cold season temperature, or Tc), and a maximum of 18°C (warm season temperature, or Tw). But seasonality increases to 10-13°C south of 20°N, with Tc ~15°C and Tw ~29°C. NE trades that blow parallel to the coast drive the southward advection of cool water in the CC and local "coastal" upwelling, which chills surface waters as much as 600 km offshore. The advection of warm surface water with the seasonal strengthening and northward extension of the NECC further enlarge the annual SST amplitude.

- **Equatorial Atlantic:** The mixed layer of the equatorial Atlantic may be divided into a western part with relatively low SST variations (1-3°C) and an eastern part with high seasonality (6-8°C) (HASTENRATH & LAMB, 1977; MIX et al., 1986b; PETERSON & STRAMMA, 1991).

Fig.10: Sea Surface Salinity during Cruise M23/3

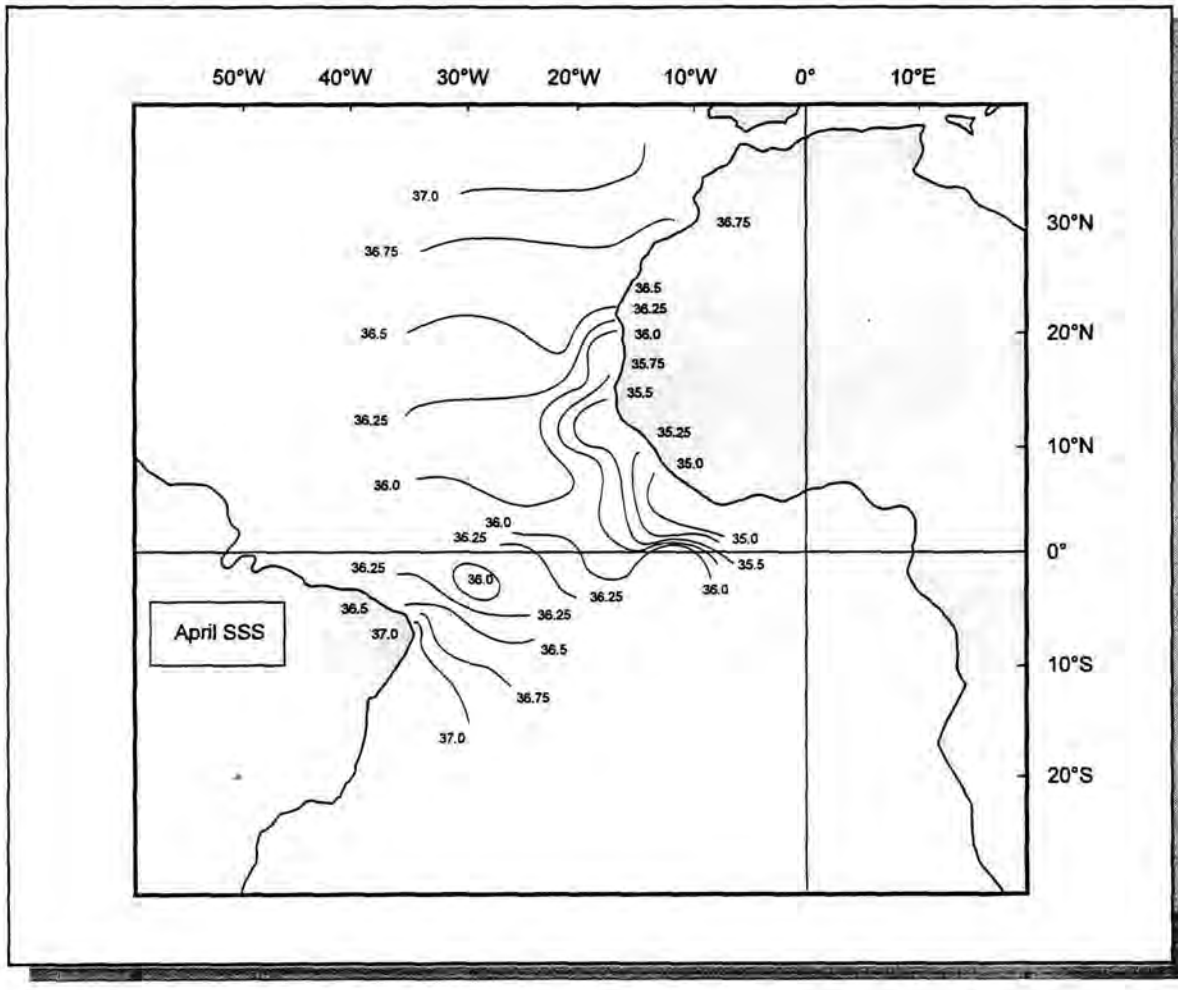

Fig. 10: Sea surface salinity map (isolines in ‰). The schematic map was modified after MITTELSTAEDT (1991) and DESSIER & DONGUY (1994) to correspond with the actually recorded salinities during cruise M 23/3.

The western part acts as the Atlantic's warm water reservoir and was quite stable trough time (MCINTYRE et al., 1989). The temperature variations in the subsurface are mainly caused by seasonal vertical movements of the thermocline within the photic zone.

Cool temperatures south of the equator in the Gulf of Guinea reflect a combination of advection of cool eastern boundary current waters and Ekman divergence south of the equator responding to meridional winds and of thermocline adjustments responding to remote (western Atlantic) wind forcing (HOUGHTON, 1991). This leads to a shoaling of the thermocline and a local SST minimum in the Gulf of Guinea.

3.3. SEA SURFACE SALINITY

The Sea Surface Salinity (SSS) in the modern tropical Atlantic is generally higher than in the Pacific Ocean. In fully oceanic areas, which are well off the continental shelf or coastal boundaries, the spatial and temporal variations in SSS are caused by evaporation and precipitation, and/or by advection and vertical mixing of water masses. The high salinity of the tropical Atlantic is the result of the net excess of evaporation over precipitation, which in turn is related to the movements of the ITCZ. More water evaporates than enters from river run-off and/or is added as precipitation.

Fig.11: Mean Annual Sea Surface Salinity

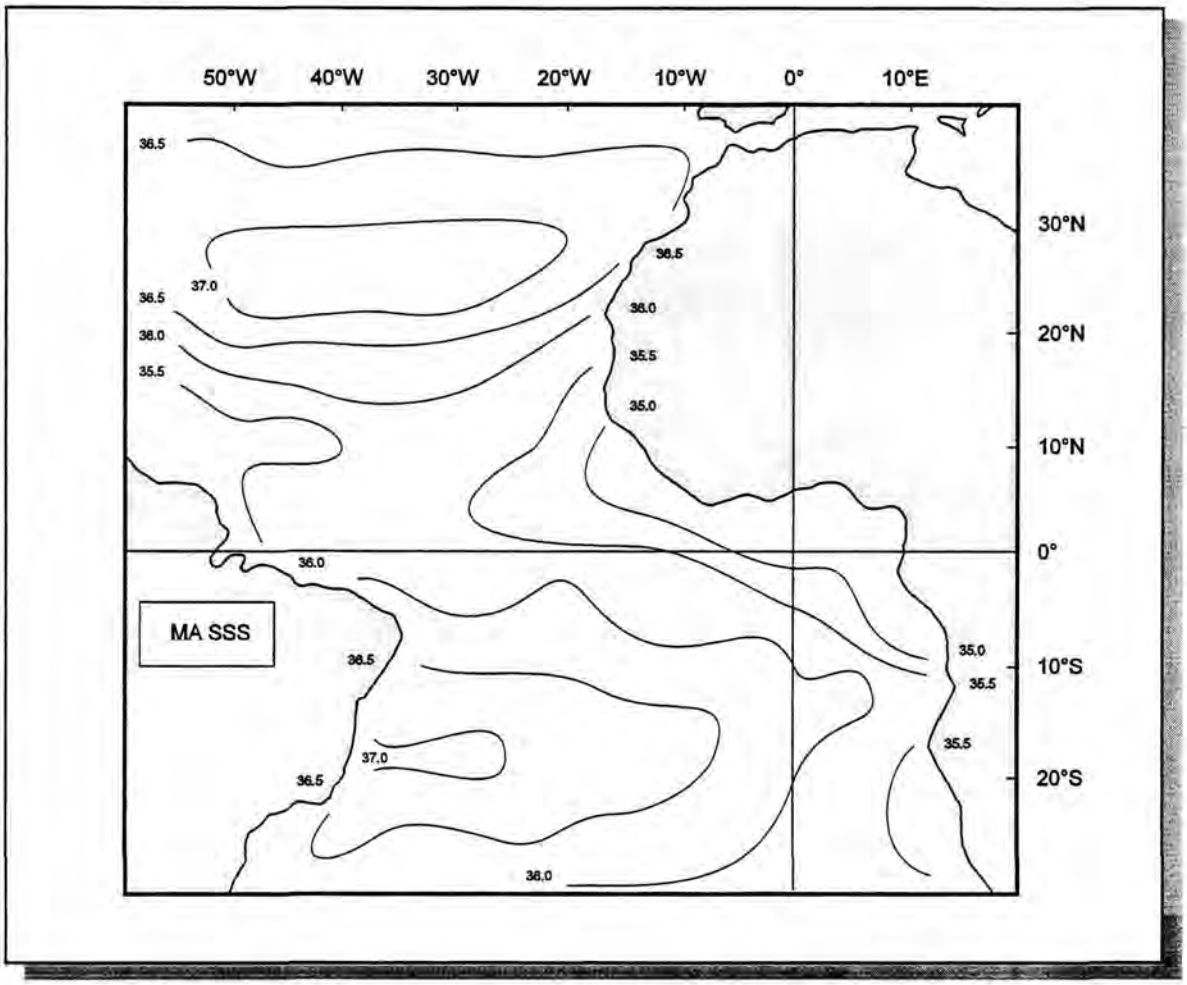

Fig. 11: Mean annual sea surface salinity map of the tropical Atlantic (isolines in ‰, after LEVITUS, 1986).

The recorded SSS during cruise M 23/3 is generally ~1‰ higher than presented by common oceanographic salinity maps of the tropical Atlantic (e.g. DÜING et al., 1980; and other maps older than 1986). LEVITUS (1989) observed a significant increase in SSS in the Atlantic from the year 1955 onwards; especially in the eastern tropical Atlantic there is a clear increase in SSS (DESSIER & DONGUY, 1994). A schematic map of salinity isotherm distribution (Fig.10) was adapted from MITTELSTAEDT (1991) and, slightly altered, from DESSIER & DONGUY (1994). This map corresponds with the actually recorded salinities during cruise M 23/3 in March and April 1993. The planktic SSS ranges of dinoflagellates will be these recorded ranges.

The sediment data are reflecting the influence of the MA SSS. The salinity references for the sediment cores are given in Fig.11 according to LEVITUS (1986). Both offshore NW Africa and the Gulf of Guinea are regions of maximum annual SSS variations (DESSIER & DONGUY, 1994).

- **Offshore NW Africa:** The distribution of the SSS along the coast shows a different pattern from that of the SST (MITTELSTAEDT, 1991). North of 20°N, temperature decreases and salinity increases as the more saline but cool North Atlantic Central Water (NACW) ascends to the surface. South of 20°N, temperature increases and salinity decreases with decreasing latitude as less saline South

Atlantic Central Water (SACW) upwells along the coast.

- **Equatorial Atlantic:** South of Cape Vert, the low MA SSS values are caused by the high precipitation rate of the tropics. After the rainy season the surface waters are diluted with freshwater run-off from the rivers Niger and Congo; SSS has a high seasonality and ranges from 33.0‰ to 35.75‰ (DESSIER & DONGUY, 1994). During cruise M 23/3 in March and April, the ITCZ was located between ~0°/12°W and ~10°N/20°W, and just south of the equator a zone of precipitation was present and some strong showers were associated with changing winds (WEFER et al., 1994).

3.4. PRODUCTIVITY AND BIOGEOGRAPHY

Any attempt to interpret variations in the distribution of dinoflagellate species inevitably involves considerations of nutrient supply and grazing. Precise data are not available for this study neither for nutrient levels nor for rates of grazing and regeneration. Given the available data, it is very difficult to produce an estimate of dinoflagellate dependence on nutrients, even in a purely relative sense. Anyway, the total productivity of a water mass is difficult to estimate because of great variations in cell numbers and division rates, as well as the patchiness of plankton distribution.

Productivity of a water mass may be interpreted as "primary productivity", i.e. concentration patterns of chlorophyll and its derivatives and the rate of carbon fixation in the surface water photic zone, and as "export production" accumulating in sediment traps and on the sea floor (BERGER et al., 1989; BERGER & WEFER, 1996). The geographical setting of high primary productivity areas in the tropical Atlantic is revealed by satellite images (BERGER, 1989; BERGER et al., 1989; LONGHURST et al., 1995; BERGER & WEFER, 1996). It will be assumed that the extent of productivity (given in Fig.12, after BERGER, 1989) roughly resembles the amount of the main nutrient supply.

In the eastern tropical Atlantic, seasonal divergence/upwelling events lead to a complex mixing of subpolar, transitional, and subtropical surface waters, which bring cool water and nutrients into the photic zone. This in turn makes the eastern tropics a region with high surface productivity and steep thermal gradients.

Variations in the strength of the trade winds control the surface currents that cause the spatial and temporal variations in divergence/upwelling and convergence/ downwelling intensity. Upwelling brings cool and nutrient rich waters into the photic zone, which in turn significantly enhances primary productivity and causes steep thermal gradients.

On the basis of the interaction of phytoplankton communities with surface water hydrodynamics, the investigated area may be related to different biogeographic "zones" or "provinces" (TAYLOR, 1987b; LONGHURST, 1993; DODGE, 1994; DODGE & MARSHALL, 1994; LONGHURST et al., 1995; PLATT et al., 1995; SATHYENDRANATH et al., 1995; JICKELLS et al., 1996). LONGHURST et al. (1995) offer an estimate of net primary productivity together with biogeochemical "provinces" which are given as zones in Fig.13.

- **Canary Isles:** The ocean area of the Canary Isles is located within the North Atlantic Subtropical Gyre (NAST) province of LONGHURST et al. (1995). North of 30°N, the NAST is divided by the mid-Atlantic Ridge into an eastern and a western basin. The ocean sector around the Canary Isles lies within the Westerlies domain, belongs to the eastern NAST, and is characterised by the lowest SST and the highest SSS values of the investigated area.

- **Offshore NW Africa:** The North Atlantic Tropical Gyre (NATR) is positioned between 10°N and 30°N and is adjacent to the Canary Current Coastal (CNRY) province east of 20°W (LONGHURST et al., 1995). In the CNRY province, the Coriolis force and the prevailing trade winds cause an alongshore and offshore blowing wind that drives the coastal surface water offshore and causes the inshore upwelling of cool and nutrient rich subsurface water, seasonally shifting from 11°N to 43°N.

DODGE (1994) and DODGE & MARSHALL (1994) made no clear distinction between the upwelling area offshore NW Africa and the oligotrophic Sargasso Sea in the central North Atlantic but included these "contrasting areas" into Zone 3, their warm-temperate or subtropical zone. The CNRY north of 8°N is predominantly affected by the CC and by coastal upwelling, with a decrease in SST and an increase in SSS from south to north.

This coastal upwelling is a dominant feature along the NW African coast. There are three major regimes of upwelling with different seasonality (MITTELSTAEDT, 1991):

- North of 25°N, there is a weak coastal upwelling during August/September/ October and the flow of the CC is relatively suppressed.

Fig.12: Tropical Atlantic Productivity ("Dahlem" Map)

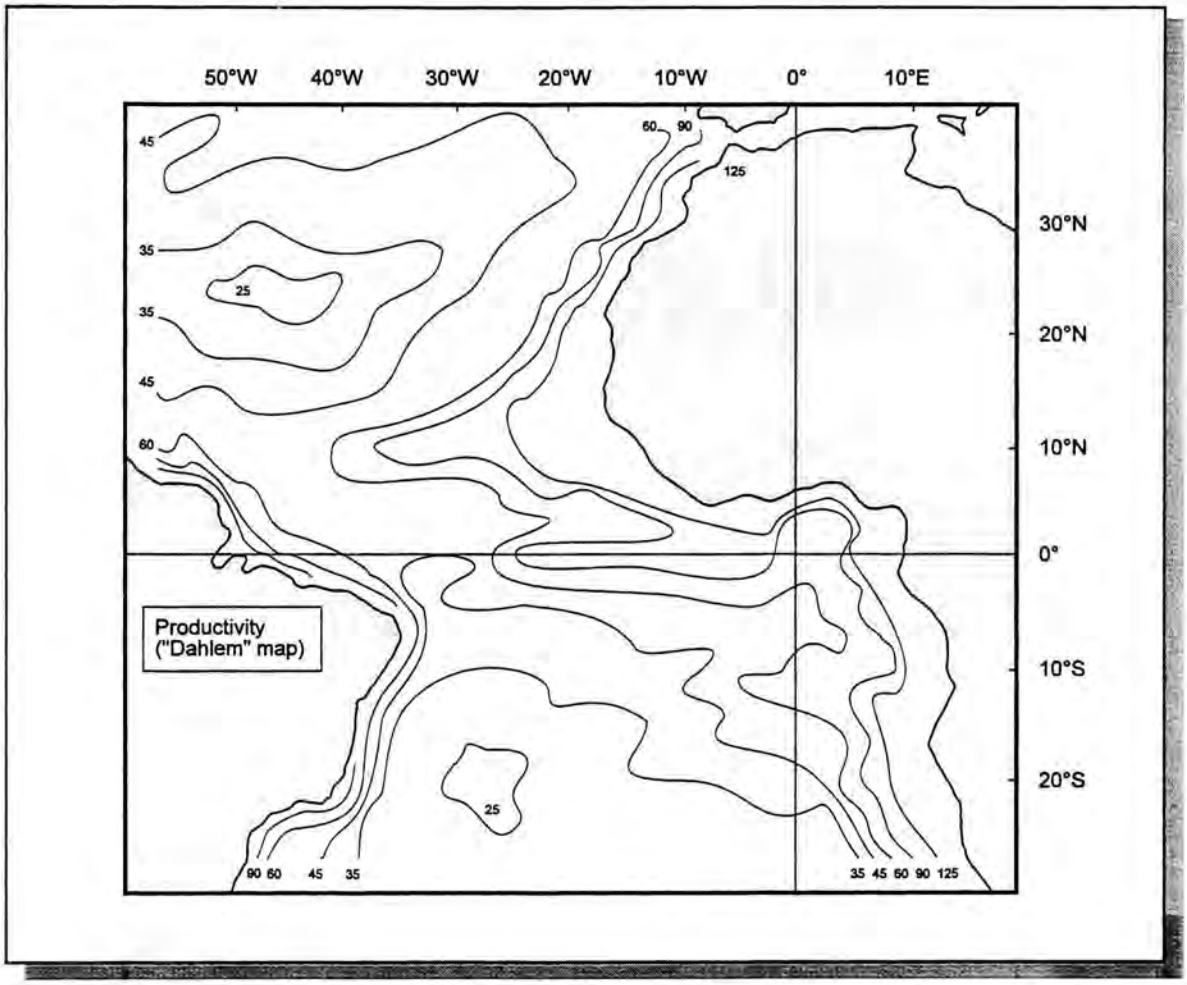

Fig. 12: Total annual productivity map of the tropical Atlantic ("Dahlem" map, isolines in gC/m²·a, after BERGER, 1989).

- Between 25°N and 20°N, there is the area where the strongest and most productive upwelling occurs year-round with a maximum both in spring and autumn.
- South of Cape Blanc (20°N), the seasonal variability in coastal upwelling is remarkable. The upwelling happens only during winter and spring. This upwelling is more intense, but its duration depends on the latitude, becoming briefer to the south. The CC shows a greater southward advection of cold water.

The main area directly affected by upwelling is located between 14°N and 25°N within a narrow band of 20-30 km along the coast (THIEDE & JÜNGER, 1992). But the influence of upwelling with its relatively low SST can be observed as far as 200-300 km offshore, along the continental margin (MITTELSTAEDT, 1991).

Further offshore along the shelf break, a "secondary upwelling" (MITTELSTAEDT, 1991) may appear, the sediment sample site off Cape Blanc, GeoB 1602-7, is located below this zone. Seasonal variations lead to significant changes in the hydrographic properties of the surface waters, and are accompanied by fluctuations in the local production of phytoplankton and zooplankton.

Fig.13: Tropical Atlantic Biogeographic Zones

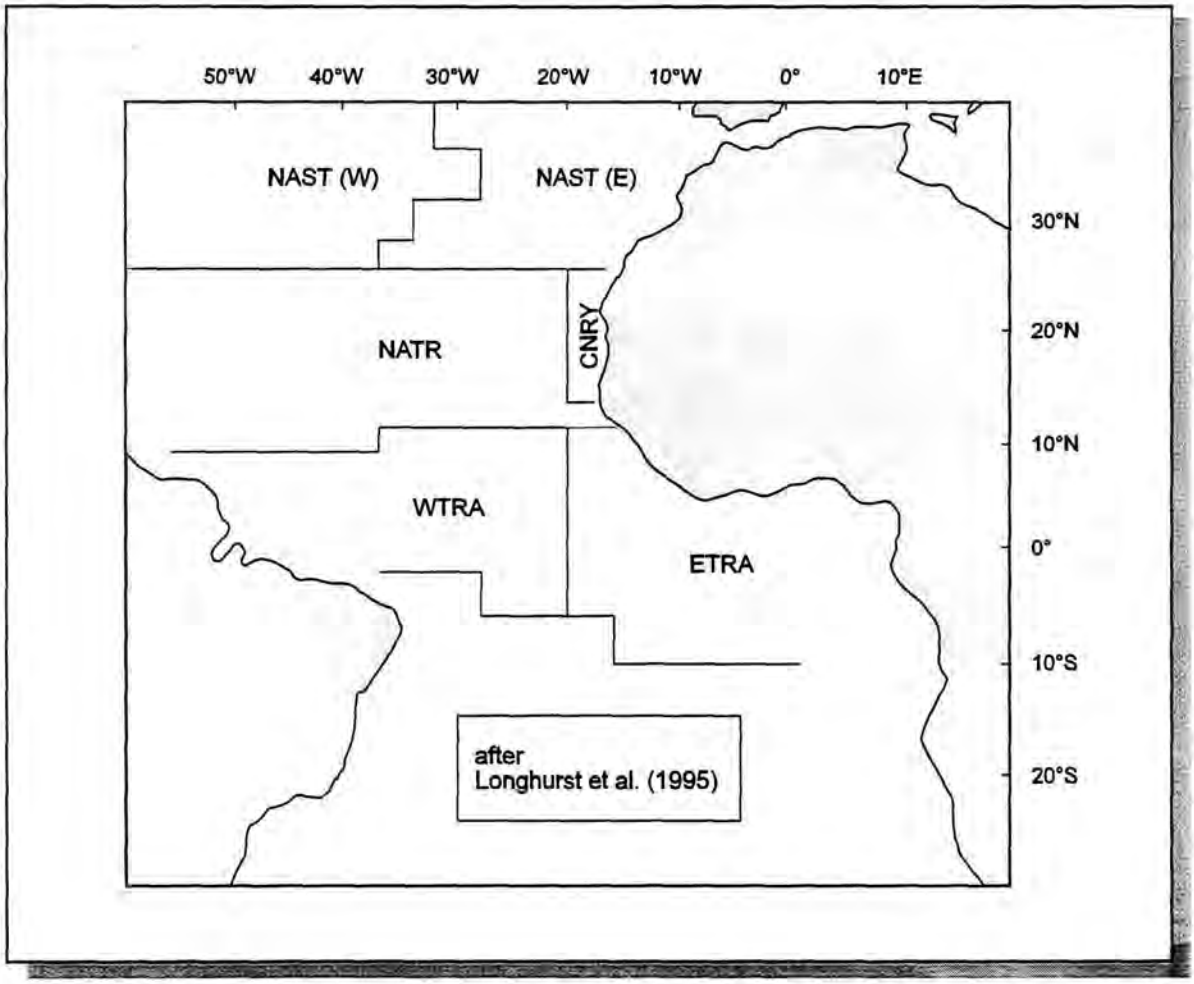

Fig. 13: Map of the tropical Atlantic biogeographic zones (after LONGHURST et al., 1995).

NAST (W):	North Atlantic Subtropical Gyre (western part)
NAST (E):	North Atlantic Subtropical Gyre (eastern part)
NATR:	North Atlantic Tropical Gyre
CNRY:	Canary Current Coastal
WTRA:	Western Tropical Atlantic
ETRA:	Eastern Tropical Atlantic

Sediment trap data collected from off Cape Blanc (WEFER & FISCHER, 1993; FISCHER & WEFER, 1996; HEAD et al., 1996; JICKELLS et al., 1996) documented high carbonate fluxes with a complex pattern of seasonal production peaks in boreal winter, spring, and summer months. Highest total and calcium carbonate fluxes were recorded during boreal summer with carbonate fluxes amounting to 25-60% of the total fluxes. Along the entire upwelling area off NW Africa, modern productivity is high and rates are more than 125 gC/m²·a (BERGER, 1989; LONGHURST et al., 1995). The long-term stability of this coastal upwelling regime and its depositional environment was shown by RUDDIMAN et al. (1989) and THIEDE & JÜNGER (1992). This regime existed for a relatively long time during the Neogene and Quaternary, producing its typical sediment facies of pelagic calcareous oozes.

The upwelling is mainly caused by two different subsurface water masses that ascend into the surface layer along the NW

African coast. North of Cape Blanc, the major contributor to the upwelled water is the more saline North Atlantic Central Water (NACW). South of Cape Blanc the nutrient richer and low salinity South Atlantic Central Water (SACW) is upwelled, which flows northward in 200-600 m water depth (FÜTTERER, 1983).

- **Equatorial Atlantic:** South of 10°N the equatorial Atlantic may be divided along the 20°W longitude into two different biogeographical provinces (LONGHURST et al., 1995): the Western Tropical Atlantic (WTRA) located west of the Mid-Atlantic Ridge, and the Eastern Tropical Atlantic (ETRA) positioned east of the 20°W longitude. DODGE (1994) and DODGE & MARSHALL (1994) include the entire low-nutrient equatorial Atlantic in Zone 4, their tropical zone. This zone coincides with the tropical-temperate macrozone of TAYLOR (1987b) which is defined within the 22°C isotherm.

During divergence/upwelling events, plankton organisms are more abundant and have a high diversity (CHAPMAN et al., 1996). Equatorial upwelling is strongest during boreal summer (HASTENRATH & MERLE, 1987; HOUGHTON, 1989, 1991; PHILANDER & PACANOWSKI, 1986; PETERSON & STRAMMA, 1991; LONGHURST, 1993). The easterly winds lead to divergence above and convergence below the thermocline, and at some distance from the equator to the opposite pattern of vertical motion.

The SEC has its maximum intensity with a strong westward advection; at the same time the NECC has its greatest eastward advection, which leads to intense convergence and downwelling in the contact zone along the 8°N latitude. The same pattern of eastward SEC and westward counter current flow happens just south of the equator as well, contact between the SEC and the SECC here causes convergence and downwelling. The downwelled water flows in a south-eastward and north-eastward direction at the depth of the thermocline, thus leading to divergence and upwelling of cold, nutrient rich waters, a shallow thermocline that can be well above the photic zone, and a steep temperature gradient with low SST in the eastern equatorial Atlantic. The intense SEC transports warm surface water to the west, thus causing a deep thermocline, that extends well below the photic zone, and a deep but nutrient depleted mixed layer in the western equatorial Atlantic. Generally, the thermocline dips downward from east to west, with depressions in downwelling areas and doming in upwelling areas.

Upwelling in the Gulf of Guinea is considered to be strong during June and July, it is associated with high phytoplankton biomass, high production, and low SST between 3°N and 7°S (LONGHURST, 1993).

At their northern Guinea Basin trap site WEFER & FISCHER (1993) recorded total flux maxima in March and August-September with carbonate flux amounting to 26-81% in the upper trap; in the lower trap the total flux maximum occurred in March and carbonate flux adding up to 41-76% of the total. The region with maximum equatorial upwelling is centred on 10°W between 0° and 4°S (VERARDO & MCINTYRE, 1994).

Upwelling brings cool and nutrient rich waters into the photic zone, which in turn enhances primary productivity significantly and causes steep thermal gradients. Productivity of the equatorial Atlantic ranges from ~45 $gC/m^2 \cdot a$ in the west to >90 $gC/m^2 \cdot a$ in the east (BERGER, 1989).

3.5. DEEP WATER MASSES

Today, in the tropical Atlantic Ocean, heat transport is northward in both hemispheres and increases near the equator, where there is always a flux of heat into the ocean (PHILANDER & PACANOWSKI, 1986). Trade wind induced surface currents advect this heat to the Arctic and sub-Arctic regions. During the cold boreal autumn and winter seasons, the relatively warm and salty North Atlantic surface waters are exposed to the colder atmosphere in the Norwegian-Greenland and Iceland seas. The water is cooled by complex interactive processes and becomes dense. Finally, owing to its saltiness, it will convect and sink toward the bottom. Additionally, a small amount of deep water is formed in the Arctic from sea-ice formation, which extracts fresh water from the surface waters and leaves the remaining water enriched in salt (JANSEN, 1992). This brine may become so dense that it starts deep convective overturning.

This newly formed deep water is well oxygenated and ventilated, but has a low nutrient content. It flows southward across the sills of the Greenland-Scotland ridge and, after mixing with intermediate waters, forms the North Atlantic Bottom Water (NABW) (JANSEN, 1992). Thus, the net inflow of surface water, which transports heat across the equator from the southern to the northern hemisphere, is compensated by a net export of deep waters out of the North Atlantic. The

deep thermohaline ocean circulation responds slowly to global climatic changes, alterations occur on time scales of 1,000 rather than 100 years (JANSEN, 1992).

Today, the principal trajectory of flow for deep water masses is southward along the Atlantic basin, west of the Mid Atlantic Ridge (MAR). The NADW may be divided in the Upper-NADW (maximum salinity, depth 1,500-2,00 m) and the Lower-NADW (maximum oxygen, depth ~3,000 m). Within about 100 years, the NADW has travelled the entire length of the Atlantic as a deep water mass, where it mixes with circum-Antarctic deep and intermediate waters, which in turn were produced by freezing processes around Antarctica (JANSEN, 1992).

The Antarctic Intermediate Water (AAIW, minimum salinity, depth 750-1,000 m) is located above the Upper-NADW. Below 3,500-4,000 m the cold (<2°C) abyssal geostrophic Antarctic Bottom Water (AABW), is supplied from the south to the north. The AABW has lower contents of oxygen and nutrient than the NADW. The interface between the southward flowing NADW and northward flowing AABW occurs at about 4,000 m at the equatorial Atlantic. There, the primary flow paths of the deep water masses is west to east along the equator and through low-latitude fracture zones. These structural sills act as "gateways" (VERARDO & MCINTYRE, 1994). The approximate depth of the Romanche Fracture Zone sill is ~3,750 m, this is the principal conduit for deep water flow into the eastern Atlantic (CURRY & LOHMANN, 1990). The NADW is overlain by the South Atlantic Intermediate Water (SAIW), which has less oxygen but is nutrient-enriched (SARNTHEIN et al., 1994).

Extending from Gibraltar, the cold, saline NADW is joined by the warmer but saltier and nutrient-depleted Mediterranean Outflow Water (MOW). These waters flow southward above 1,500-2,000 m (SARNTHEIN et al., 1994). The MOW is mainly restricted to the eastern Atlantic margin.

Therefore, the water entering the equatorial Atlantic today at ~3,600 m depth is composed of a mixture of well oxygenated and nutrient-rich NADW and less oxygenated and nutrient-poor AABW, the present ratio is considered to be 4:1 (CURRY & LOHMANN, 1990; BROECKER et al., 1991) or 3:1 (BEVERIDGE et al., 1995); with isolated maxima in NADW composition occurring within the equatorial region. Deep water with approximately these characteristics fills the eastern Atlantic from the sill depth to below 5,000 m (CURRY & LOHMANN, 1990). The western Atlantic basin is more rapidly ventilated than the eastern margin.

In the tropical Atlantic east of the MAR, the Sierra Leone Rise climbs to a depth of about 1,500 m and has well-sedimented flanks with biogenic carbonate and opal throughout the depth range of 2,500-5,000 m. West of the MAR, the conjugate submarine rise is the Ceara Rise, which is well-sedimented throughout the depth range of 2,800-4,700 m (CURRY & LOHMANN, 1990).

In the eastern Atlantic where a smaller fraction of AABW has entered the basin, the dissolution rate of calcium carbonate is significantly lower than in the western basin. Today, the Carbonate Compensation Depth (CCD) and lysocline are deeper in the eastern basin (lysocline ~4,800 m; THUNELL, 1982) than in the western Atlantic (lysocline ~4,000-4,300 m BROECKER & TAKAHASHI, 1978; THUNELL, 1982). Therefore, the sediment surface samples of this study were obtained from a sea floor that lies well above the lysocline.

South of the equator, the ocean surface layers (above 50 m) have a southward Ekman transport, just as the waters of the deep ocean (below 1,500 m) move southward, while the intermediate waters move northward (PHILANDER & PACANOWSKI, 1986). In the equatorial Atlantic, upwelling brings some of the intermediate northward flowing waters into the surface layers (PHILANDER & PACANOWSKI, 1986).

At a mooring site in the Guinea Basin, at 905 m water depth, two pronounced shifts in current directions were observed by WEFER & FISCHER (1993). The current direction changed rather abruptly from 90° to 270° and back again.

4. THE ORGANISMS RECORDED

4.1. SHELLED PHYTOPLANKTON COMPOSITION

The plankton filters of cruise M 23/3 were closely investigated for phytoplankton organisms which were counted directly from the SEM screen. Unfortunately, it was not possible to calculate the absolute specimen density on the filters, owing to clogging with organic mucus. The clogging was extremely high on samples 22-S20 and 22-S21, causing a very low species diversity. Only the shelled phytoplankton organisms were counted. The athecate or "naked" dinoflagellates of the order Gymnodiniales, together with other "non-shelled" algae, collapsed and were smashed on the filters, thus very probably contributing to the clogging mucus. Just as the very small coccospheres (<5 µm) were not included into the plankton samples. They are too small and were washed through the filter pores.

The relative composition of the shelled phytoplankton has been plotted as a cumulative curve (Fig.14). The following organisms were recorded: dinoflagellates of various life stages, coccolithophorids and diatoms. In some samples of the equatorial Atlantic, a small amount of silicoflagellates was observed.

During cruise M 23/3, plankton samples were obtained from various biogeographical "zones" and "provinces" (TAYLOR, 1987b; LONGHURST, 1993; DODGE, 1994; DODGE & MARSHALL, 1994; LONGHURST et al., 1995; PLATT et al., 1995; SATHYENDRANATH et al., 1995; JICKELLS et al., 1996). According to LONGHURST et al. (1995), the subsequent zones were investigated: Along the equator, the Western Tropical Atlantic (WTRA) and Eastern Tropical Atlantic (ETRA) were passed, beyond that the ETRA was studied from 0°/12°W to 10°N/20°W. Afterwards, the Canary Current Coastal (CNRY) was crossed up north to 25°N/18°W and the Canary Isles which are located in the eastern part of the North Atlantic Subtropical Gyre [NAST (E)].

The terminology of LONGHURST et al. (1995) will not be further used in this study, but instead the following terms will be applied: Equatorial Atlantic (samples 22-S08 to 22-S18), Offshore NW Africa (samples 22-S20 to 22-S34), and Canary Isles (samples 22-S35 and 22-S37). Each biogeographic area is characterized by a well defined combination of oceanographic parameters (Table 1, Table 2).

- **Equatorial Atlantic:** South of 10°N, the low productivity of the oligotrophic equatorial Atlantic is indicated by high sample volumes (up to 140 litres), a domination of coccolithophorids, and small amounts of diatoms. The proportional amount of diatoms reached only 8% in the western equatorial Atlantic, and further decreased to 2% in the eastern part. Coccospheres were accounting for up to 70%, thecate dinoflagellates add up to 25%-50% of the shelled phytoplankton. The proportional amount of the vegetative-coccoid *Th. heimii* and the calcareous dinocysts averages 2-5% each.
- **Offshore NW Africa:** North of 10°N, the influence of upwelling may be observed along the continental margin between 15°N and 25°N. Samples 22-S27 to 22-S34 are characterized by low sample volume and higher amounts of diatoms. The relative specimen densities of the shelled and other phytoplankton organisms increased up to tenfold, which in turn caused heavy clogging of the plankton filters, and in three samples only 10-28 litres of sea water were filtered. The diatoms add up to 10-38% and the amount of coccospheres decreased to 25%-50% of the shelled phytoplankton. The relative amount of thecate dinoflagellates varied between 23% and 40%. The coccoid *Th. heimii* (7%) and the calcareous dinocysts (15%) reach a maximum at 11.5°N/21°W (sample 22-S23). Generally, diatoms tend to dominate phytoplankton communities under high nutrient conditions (LANGE et al., 1994; FISCHER & WEFER, 1996; JICKELLS et al., 1996; TREPPKE et al., 1996). Here, the quantity of nutrients caused only a small increase in diatom content but was not high enough for a true "diatom bloom".
- **Canary Isles:** The samples from the Canary Isles increase in volume with small amounts of diatoms and high quantities of coccolithophorids. Thus showing reduced productivity and more or less oligotrophic characteristics again. Here, the relative specimen density decreased by half, and about 84 litres were pumped through the filters. The diatoms decreased to 8% and the amount of coccospheres increased to 57%. The thecate dinoflagellates accounted for 35% and the relative amount of vegetative-coccoid *Th. heimii*-shells reached their maximum of 12%.

Fig14: M23/3 Shelled Phytoplankton Composition

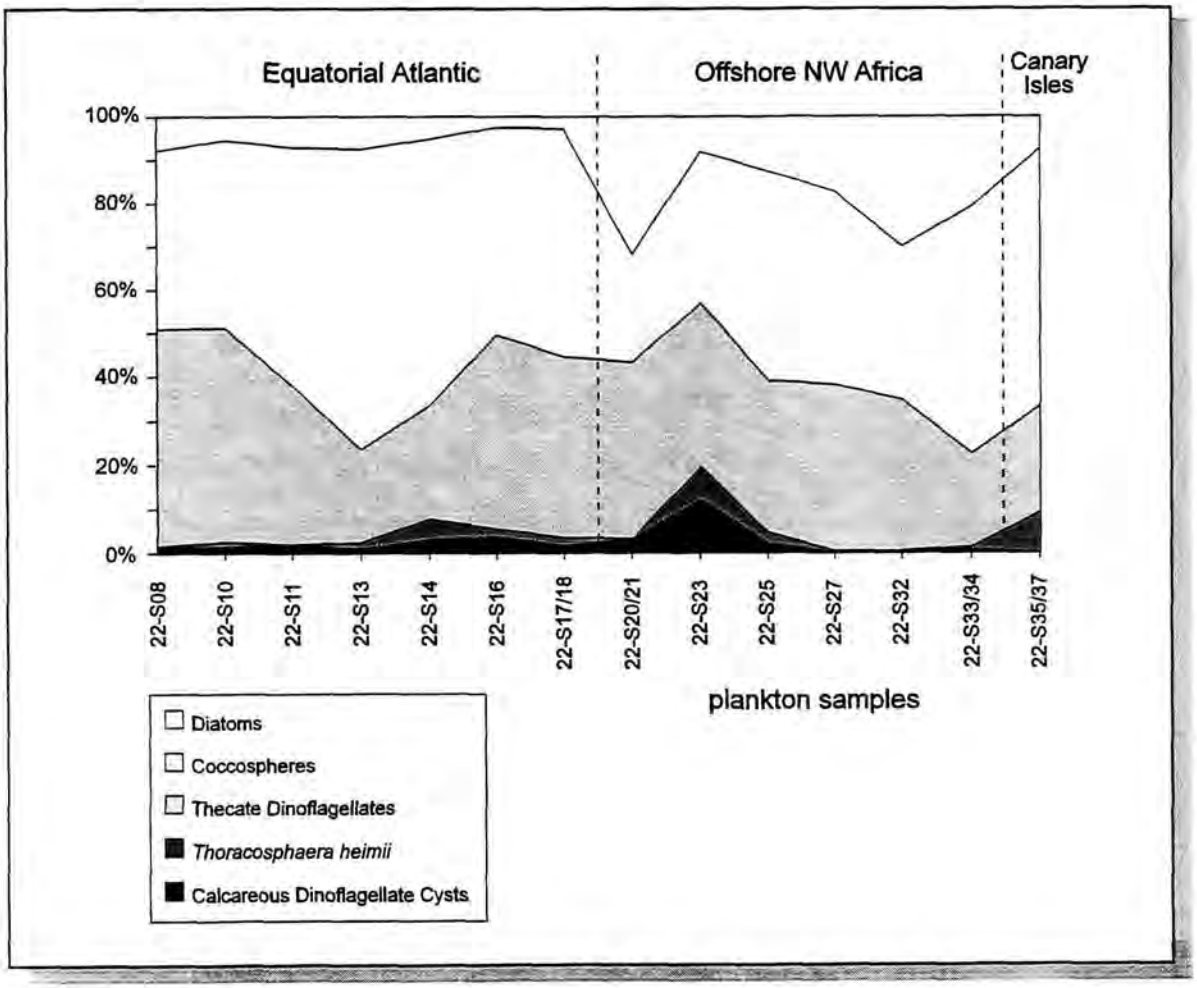

Fig. 14: Relative shelled phytoplankton composition in the tropical Atlantic during cruise M 23/3 (plotted as a cumulative curve).

Thus, in the tropical Atlantic Ocean dinoflagellates of various life stages obviously are major contributors to the primary productivity of shelled phytoplankton organisms (23-58%). Dinoflagellate productivity, in turn, is dominated by vegetative-thecate dinoflagellates (23%-50%).

During earlier plankton surveys in the tropical and South Atlantic (LOHMANN, 1912; HENTSCHEL 1936), shelled phytoplankton populations showed an amount of 2-67% dinoflagellates (mean relative amount: ~38%). The data of the present study confirm the shelled phytoplankton composition data of HENTSCHEL (1936), who recorded a relative dinoflagellate amount of 29% offshore Cape Blanc and 59% in the Guinea Basin (Fig.15).

But, this huge amount of vegetative-thecate dinoflagellates does not contribute to the export production. Usually, the thecae are destroyed by bacterial activity even in the upper water column. On the other hand, *Th. heimii* is equipped with a mineralized test and should be readily preserved in the sediments. In their tropical Atlantic sediment trap studies, DALE & DALE (1992) observed only fragments of thecae in the lower water column but recorded a huge flux of several thousands of *Th. heimii*-shells and dinocysts.

Besides the vegetative-coccoid *Th. heimii*, only dinosporin and calcareous dinocysts withstand the bacterial decay and are embedded into sediments.

Fig15: Tropical Atlantic Shelled Phytoplankton Composition

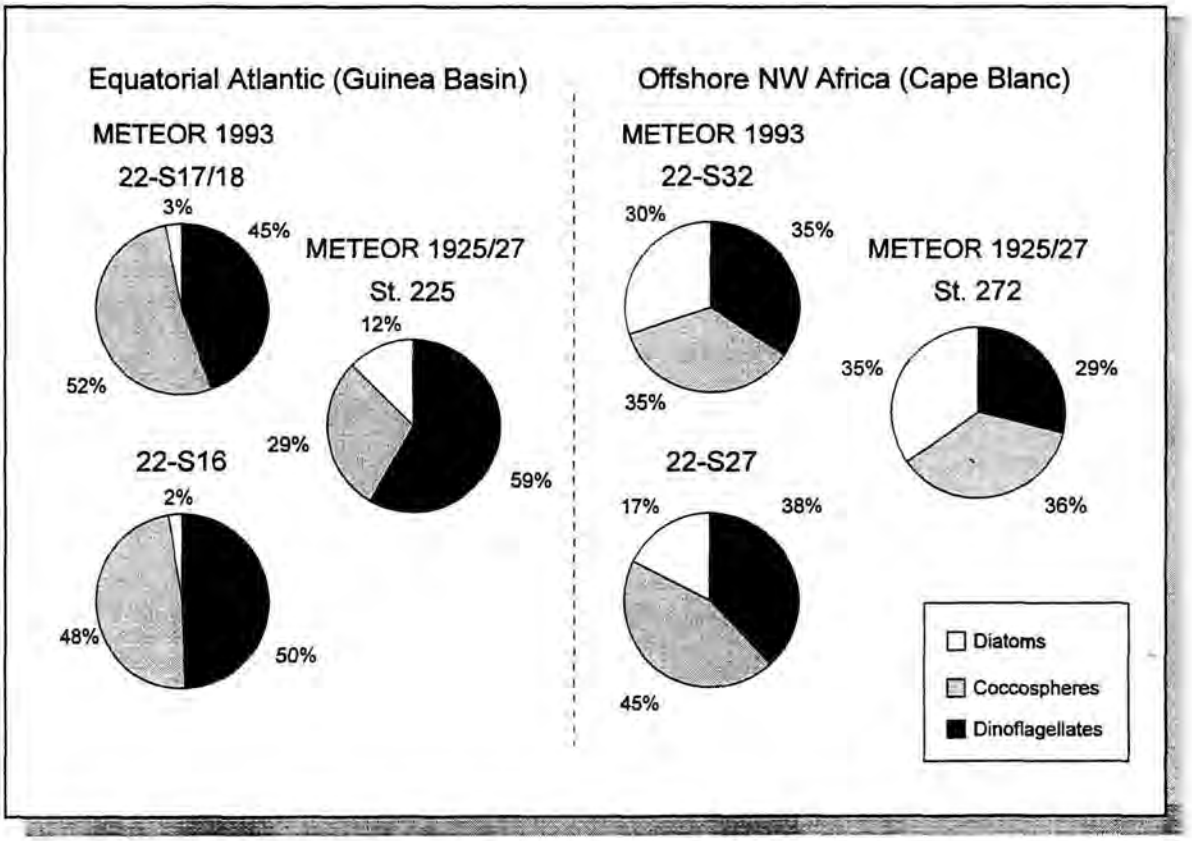

Fig. 15: Relative shelled phytoplankton composition in the equatorial Atlantic and offshore NW Africa during METEOR cruises in 1993 and 1925/27. Data for St. 225 (Guinea Basin) and St. 272 (Off Cape Blanc) adapted from HENTSCHEL (1936).

DALE & DALE (1992) emphasized that calcareous cysts heavily dominate the dinoflagellate cyst assemblages in tropical fully oceanic waters and that dinosporin cysts are insignificant contributors to dinoflagellate export production. This is confirmed within the current study: only calcareous forms were observed, no dinosporin cysts were recorded.

Comparing the phytoplankton data of this study with sediment trap data of previous studies (WEFER & FISCHER, 1993; LANGE et al., 1994; FISCHER & WEFER, 1996; HEAD et al., 1996; JICKELLS et al., 1996; TREPPKE et al., 1996) is extremely difficult.

Sediment trap studies were carried out offshore NW Africa and in the Guinea Basin. WEFER & FISCHER (1993), FISCHER & WEFER (1996), HEAD et al. (1996), and JICKELLS et al. (1996) recorded total flux rates, carbonate flux, and the biogenic opal flux, but made no distinction between phytoplankton and zooplankton organisms. Several sediment flux maxima were recorded (WEFER & FISCHER, 1993). One of these maxima was observed during spring (March, April) for both sites. The plankton data of cruise M 23/3 should, therefore, reflect an enhanced productivity in comparison to the mean annual data of the trap studies.

In the area offshore Cape Blanc, the following fluxes were recorded (WEFER & FISCHER, 1993; FISCHER & WEFER, 1996; JICKELLS et al., 1996): Biogenic calcium carbonate content varies between 25-83% of the total flux rate; the recorded calcareous organisms were coccolithophorids, planktic foraminifera, and pteropods. Biogenic opal content was 4-24% of the total, and the contributing organisms were diatoms and radiolarians.

The trap site in the Guinea Basin was located at ~2°N/~11°W and, according to WEFER & FISCHER (1993) and FISCHER & WEFER (1996), the carbonate flux was higher than offshore NW Africa. The organisms were mostly

coccolithophorids and planktic foraminifera. The biogenic opal flux varied from 3% to 20% of the total, and was composed of diatoms, radiolarians, and silicoflagellates. One seasonal diatom flux maximum was observed in spring (LANGE et al., 1994; TREPPKE et al., 1996).

The highest total flux rates and the highest organic carbon export fluxes were recorded offshore NW Africa and relatively moderate rates in the northern Guinea Basin (WEFER & FISCHER, 1993; FISCHER & WEFER, 1996; HEAD et al., 1996; JICKELLS et al., 1996). At all sites, carbonate was the dominant contributor to the sea floor. But, no information on the flux rates of *Th. heimii*-shells and calcareous dinocysts was provided.

Identification of various calcareous dinocysts may be difficult and the average plankton worker may have problems of distinguishing them from invertebrate eggs, from foraminiferal proloculi, and from coccospheres. There exist only a few studies of their ecology, biogeography, and biostratigraphy (FÜTTERER, 1976, 1977; DALE & DALE, 1992) as against other groups of microfossils or nannofossils. Even after the clonal culture studies of TANGEN et al. (1982) and INOUYE & PIENAAR (1983), *Th. heimii* was still sometimes described as a member of the coccolithophorids. However, large amounts (up to 20%) of *Th. heimii*-shells and calcareous dinocysts are observed in sediment cores of the tropical Atlantic (WEFER et a., 1994; KARWATH, 1995; HÖLL et al., subm.).

Even now, after this first rough plankton survey, the following biological and ecological situation may be suggested for the investigated area:

- *Th. heimii*-shells, together with calcareous dinocysts, account for a comparatively small amount of the shelled phytoplankton.
- They are the only contributors to dinoflagellate export production. Therefore, they represent the total amount of all dinoflagellates (25-58% of the shelled phytoplankton population) which is preserved in the sediments.
- These organisms are, after the coccospheres, the second most important contributors to carbonate primary productivity (up to 20% of the shelled phytoplankton).

4.2. SHELLED VEGETATIVE DINOFLAGELLATES

4.2.1. VEGETATIVE-THECATE DINOFLAGELLATES

CLASS DINOPHYCEAE
PASCHER, 1914

ORDER PROROCENTRALES
LEMMERMANN, 1910

- **Description** (DODGE, 1982; LOEBLICH III, 1982; SOURNIA, 1986; BALECH, 1988; FENSOME et al., 1993; STEIDINGER & TANGEN, 1996): "Armoured". Bivalvate cells with desmokont flagellar insertion; anterior periflagellar area; no cingulum nor sulcus.

FAMILY PROROCENTRACEAE
STEIN, 1883

- **Description** (SOURNIA, 1986; BALECH, 1988; FENSOME et al., 1993; STEIDINGER & TANGEN, 1996): Cells with thecal plates. Flagella inserted apically, wavy flagellum homologues to transverse flagellum of other dinoflagellates. No cingulum nor sulcus.

-**Remarks:** These dinoflagellates are characterised by a laterally compressed thecate cell with two dissimilar, apically inserted flagella. The theca consists more or less of two large lateral plates or valves.

MESOPORUS
LILLICK, 1937

- **Description** (WOOD, 1968; DODGE, 1982; SOURNIA, 1986; BALECH, 1988; STEIDINGER & TANGEN, 1996): Cells small, round to ovoid, compressed laterally. Bivalvate, similar to *Prorocentrum* but with a characteristic conical depression (the "pore") in centre of each main valve or thecal plate. Theca covered with small spines (small "pimples"). Chloroplasts present, **autotrophic.** Produces **no cysts.**

- **Remarks:** Various species belonging to *Mesoporos* have been described but they very probably are variants of the type species *M. perforatus*, which was recorded here. This is a small organism and easily confused with *Prorocentrum balticum* (LOHMANN) LOEBLICH, 1970, specially while looking at it with a LM (DODGE, 1982; BALECH, 1988).

Distribution data are presented in Table 4; temperature and salinity ranges are plotted in Fig.16.

PROROCENTRUM
EHRENBERG, 1834

- **Description** (WOOD, 1968; DODGE, 1982; BALECH, 1988; STEIDINGER & TANGEN, 1996): Cells small to medium-sized, covered by two opposing porulate valves or thecal plates, varying from spheroid to pyrifom in lateral view. Cells with two anterior dissimilar flagella emerging out of flagellar pore complex. Anterior end bluntly pointed and may bear a spine or projection, posterior half normally acute. Plate ornamentations vary from pores to areolae to tiny spines ("pimples"). Cells with chloroplasts, **autotrophic. Not known to produce cysts.**

- **Remarks:** The theca consists of two large plates, or valves, which merge at a sagittal suture. The following characteristics are used for species identification: size, shape, presence and shape of apical processes, surface markings.

8 *Prorocentrum* species have been recorded in the present survey and their distribution data are displayed in Table 5. Temperature and salinity ranges are plotted in Fig.16.

Table 4: *Mesoporos* distribution data.

SPECIES	WOOD (1968)	DODGE (1982, 1985, 1993)	STEIDINGER & TANGEN (1996)	THIS STUDY
M. perforatus (GRAN) LILLICK, 1937 Pl.1, Fig.1	Benguela Current, Brazil (N coast), Straits of Florida	Adriatic Sea, E Atlantic, British Isles, off Norway	neritic and oceanic, in cold temperate to tropical waters	**SST: 18-29°C SSS: 35.0-36.8‰** abundant throughout the investigated region

Table 5: *Prorocentrum* distribution data.

SPECIES	WOOD (1968)	DODGE (1982, 1985, 1993)	BALECH (1988)	STEIDINGER & TANGEN (1996)	THIS STUDY
P. balticum (LOHMANN) LOEBLICH, 1970 Pl.1, Fig.2		E Atlantic, North Sea, off W Scotland	**SST: 6.3- 10.8°C SSS: 33.6-34.6‰** neritic and oceanic	cosmopolitan	**SST: 18-29°C SSS: 35.0-36.8‰** frequent throughout the investigated area
P. compressum (BAILEY) ABÉ ex DODGE, 1975 Pl.1, Fig.3		neritic and oceanic, Atlantic, Gulf Stream	**SST: -1.8-19°C SSS: 33.2-35.9‰** most frequent off Patagonica	neritic and oceanic, in cold temperate to tropical waters	**SST: 20-29°C SSS: 35.0-36.8‰** rare in the equatorial Atlantic, frequent offshore NW Africa south of 20°N
P. gracile SCHÜTT, 1895 Pl.1, Fig.4	Atlantic, Brazil (N coast)	Atlantic, Mediterranean, Pacific	**SST: >17°C SSS: >36.0‰** warm water species	neritic and estuarine, in cold temperate to tropical waters	**SST: 19-29°C SSS: 35.0-36.7‰** frequent throughout the prospected region
P. lebourae SCHILLER, 1928 Pl.1, Fig.6	Adriatic Sea, Caribbean, Gulf Stream				**SST: 19-29°C SSS: 35.0-36.7‰** abundant in the equatorial Atlantic, frequent off NW Africa
P. micans EHRENBERG, 1833 Pl.1, Fig.7	cosmopolitan	neritic, cosmopolitan	**SST: 5.5-23°C SSS: 33.60-36.24‰** neritic and oceanic	**tolerating SSS: >39.0‰** neritic, estuarine, and oceanic, in cold temperate to tropical waters	**SST: 19-20°C SSS: 36.3-36.5‰** rare off NW Africa
P. nanum SCHILLER, 1918 Pl.1, Fig.8		neritic, Adriatic Sea Atlantic	**SST: -1.76-19°C SSS: 33.147-35.926‰** most frequent off Patagonica		**SST: 21-22°C SSS: 36.0-36.1‰** rare off NW Africa
P. rostratum STEIN, 1883 Pl.1, Fig.5	warm water species, Straits of Florida	E Atlantic	warm water species, Caribbean, Indian O., Mediterranean	neritic, warm water species; worldwide distribution	**SST: 19-22°C SSS: 35.9-36.7‰** frequent off NW Africa
P. sphaeroideum SCHILLER, 1928 Pl.1, Fig.9+10	Straits of Florida				**SST: 19-29°C SSS: 35.0-36.7‰** rare in the equatorial Atlantic, frequent off NW Africa

ORDER DINOPHYSIALES
KOFOID, 1926

- **DESCRIPTION** (LOEBLICH III, 1982; SOURNIA, 1986; FENSOME et al., 1993; STEIDINGER & TANGEN, 1996): Cells laterally flattened with desmokont flagellar orientation and premedian cingulum. Cingulum and sulcus often with wide lists supported by ribs.

FAMILY AMPHISOLENIACEAE
LINDEMANN, 1928

- **Description** (FENSOME et al., 1993; STEIDINGER & TANGEN, 1996): Motile cell is at least four times as long as broad. Epitheca is much reduced, hypotheca accounting for the majority of the cell. Ventral pore on ventral epitheca, flagellar pore is situated posterior to cingulum at anterior end of "mid-body". Hypotheca may be drawn out into one or more projections or prongs.

Fig.16: Prorocentrales Temperature and Salinity Ranges

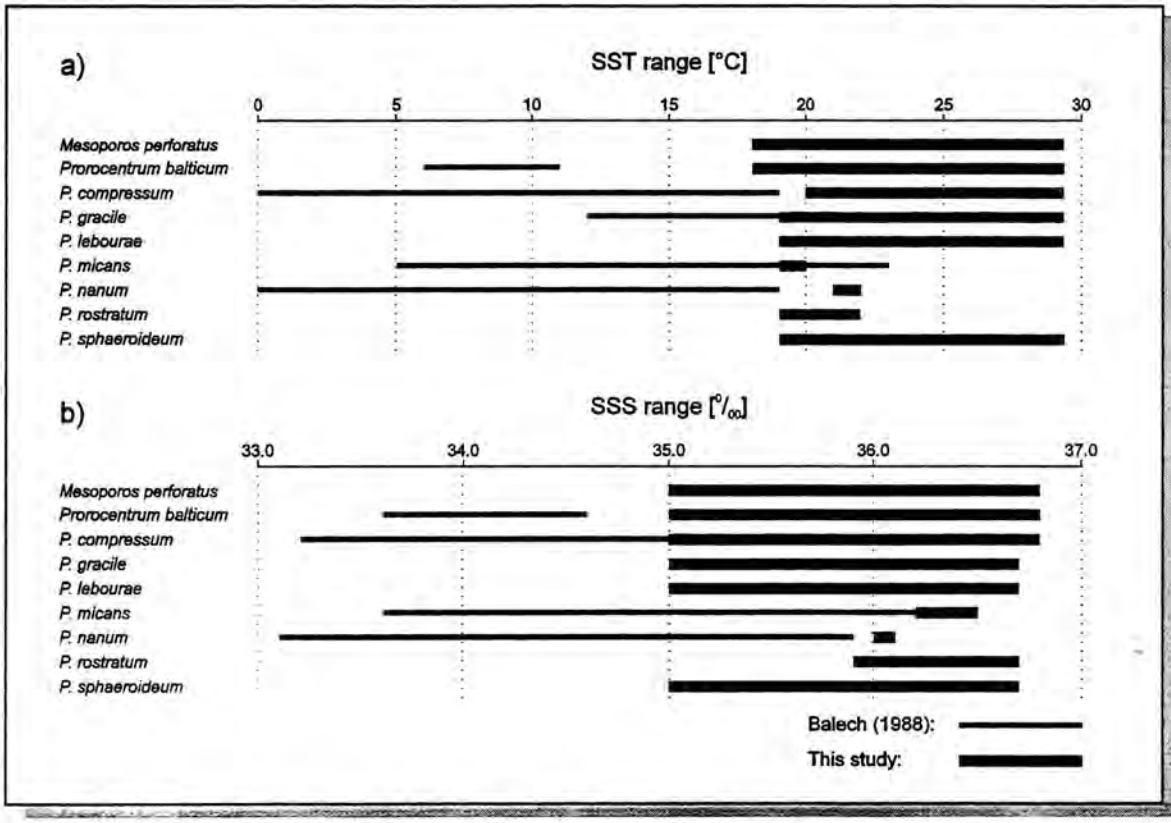

Fig. 16: Bar graphs of temperature (a) and salinity (b) ranges of the recorded Prorocentrales.

AMPHISOLENIA
STEIN, 1883

- **Description** (WOOD, 1968; TAYLOR, 1976; DODGE, 1982; SOURNIA, 1986; BALECH, 1988; STEIDINGER & TANGEN, 1996): Cells large, up to 1,500 µm in length, needle-shaped with reduced, cap-like epitheca and extremely elongated hypotheca. Cingulum circular, positioned much anteriorly and has lists.

- **Remarks:** In spite of the odd shape, the thecal plates are organised more or less the same way as in *Dinophysis*. The anterior part of the cells including the cingulum is often described as the "head". The hypotheca consists of a thin "neck" with a "shoulder", a swollen midbody and one or more posterior processes or "feet". The sulcus is positioned at the "neck" and "shoulder" with sulcal lists only present in the upper part of the hypotheca. Chloroplasts are present, most species are associated with **external, symbiotic cyanobacteria** in the cingular area.

During the present study only one specimen of *Amphisolenia* was encountered. Distribution data are presented in Table 7 and temperature and salinity ranges are plotted in Fig.17.

Table 7: *Amphisolenia* distribution data.

SPECIES	WOOD (1968)	DODGE (1982, 1985)	BALECH (1988)	STEIDINGER & TANGEN (1996)	THIS STUDY
A. globifera STEIN, 1883 Pl.4, Fig.4+5	common in tropical waters, Benguela Current, Brazil (N coast), Caribbean	tropical Atlantic, Mediterranean	**SST: 16.3-17.3°C SSS: 36.9‰**	eupelagic, in warm temperate to tropical waters	**SST: 24°C SSS: 36.59‰** one specimen offshore Cape Blanc

FAMILY DINOPHYSIACEAE
STEIN, 1883

- **Description** (FENSOME et al., 1993; STEIDINGER & TANGEN, 1996): Cells rounded, ovoid to reniform, never more than three times as long as broad. Ventral pore on ventral epitheca. Flagellar pore immediately posterior to cingulum.

DINOPHYSIS
EHRENBERG, 1839

- **Description** (WOOD, 1968; TAYLOR, 1976; DODGE, 1982; BALECH, 1988; FENSOME et al., 1993; STEIDINGER & TANGEN, 1996): Cells medium to large, usually compressed laterally. Epitheca small or rudimentary; hypotheca generally represents three-quarters or more. Cingulum moderately wide with lists.

The main characteristics used for species identification are cell size and shape, thecal ornamentation and morphology (lists, spines).

- **Remarks:** *Phalacroma* STEIN, 1883 is now generally considered to be synonymous with *Dinophysis* (FENSOME et al., 1993). Dinoflagellates formerly identified as species of *Phalacroma* were described as being non-photosynthetic and heterotrophic, whereas in cells of *Dinophysis* species chloroplasts were observed and this genus was considered to be autotrophic (TAYLOR, 1987a; HALLEGRAEFF & LUCAS, 1988).

Several authors (REGUERA et al., 1990, 1995; MACKENZIE, 1992; MOITA & SAMPAYO, 1993) suggest that some *Dinophysis*-species may represent a gamete or another distinct life cycle stage of another *Dinophysis*-species.

The food of the heterotrophic species is mostly unidentifiable, HALLEGRAEFF & LUCAS (1988) described *D. cuneus* containing algal cells, bacteria, and virus-like particles. HANSEN (1991) observed a *D. rotundata*-cell feeding on a tintinnid with a "feeding tube" emerging from the flagellar pore area.

REGUERA et al. (1995) described small *D. dens*-like cells inside bigger *D. acuta* EHRENBERG 1840 thecae (*D. acuta* being "pregnant" with *D. dens*) and *D. acuta* / *D.* cf. *dens* couplets connected at the ventral edges with a tube emerging from the flagellar pore area of both cells (the tube representing a "fertilisation tube"). Thus, the question rises whether, in *Dinophysis*, the very same tube can be used both as a "fertilisation tube" and a "feeding tube".

In the present study no such "thecate/gamete" pairs were found.

The appearance of various hypothetical life stages of *D. caudata* including *D. caudata* var. *tripos* are associated with different growth phases. During this study, pairs of *D. caudata* var. *tripos*-cells (Pl.2, Fig.4) were observed in several samples offshore NW Africa. As reported by HALLEGRAEFF & LUCAS (1988) and REGUERA et al. (1995) they are products of asexual reproduction by binary fission. The two cells seen after longitudinal division are of identical shape and size. They are still joined by the margins of their hypothecae through a dorsal megacytic bridge, even though either member of the pair has developed an entire new theca including both sulcal lists.

13 species have been recorded in the investigated region and the distribution data are displayed in Table 8. Their temperature and salinity ranges are given in Fig.17.

ORNITHOCERCUS
STEIN, 1883

- **Description** (WOOD, 1968; TAYLOR, 1976; SOURNIA, 1986; BALECH, 1988; STEIDINGER & TANGEN, 1996): Rounded cell body small to medium sized, compressed laterally. Epitheca small and disk-like, hypotheca bowl-shaped. Cingulum generally wide and oblique, surrounded by hugely enlarged lists. Sulcus with extensive sail-like left list. Shape and ornamentation of cingular and sulcal list and rib systems characterise the species.

Fig.17: Dinophysiales Temperature and Salinity Ranges

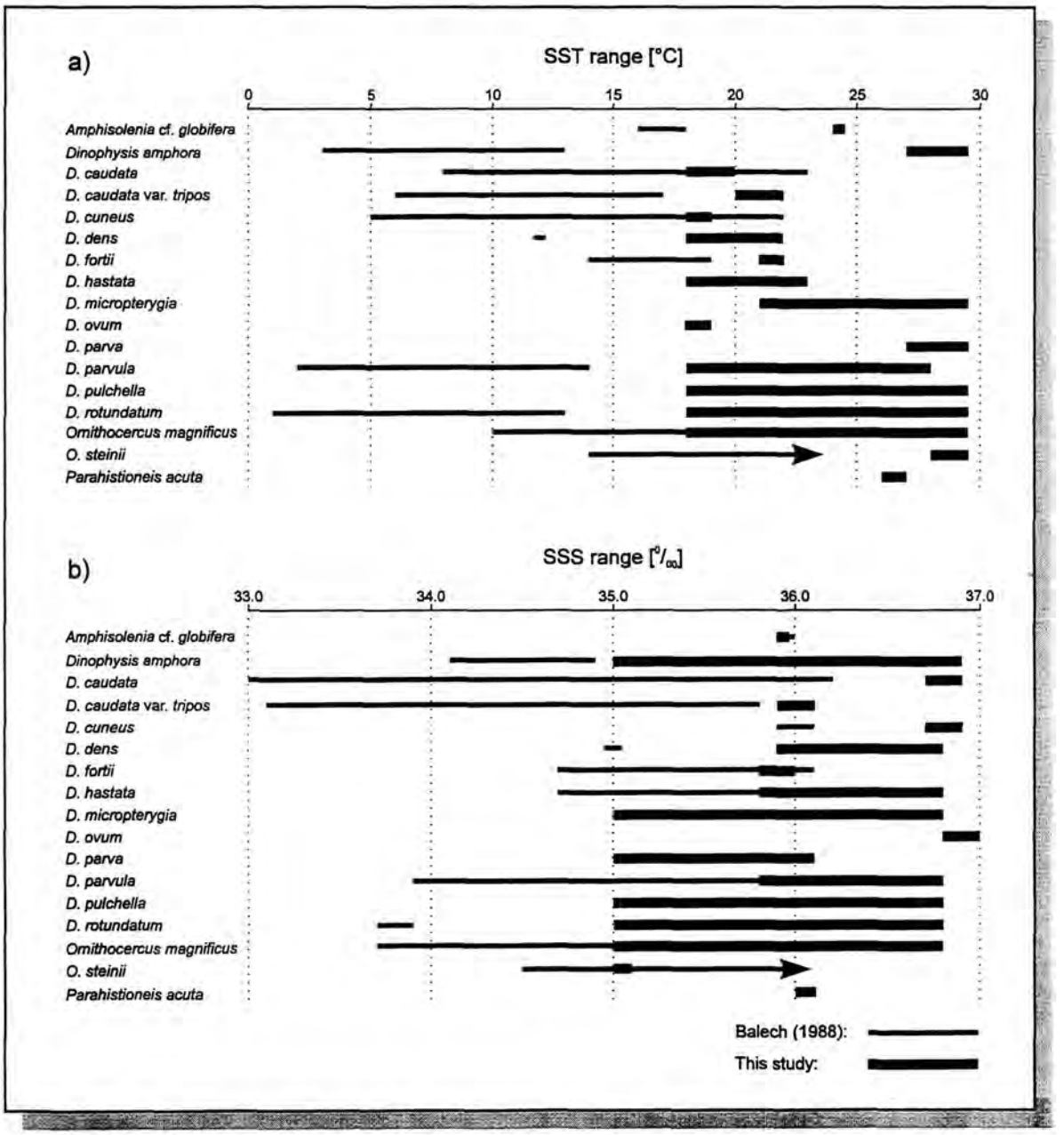

Fig. 17: Bar graphs of temperature (a) and salinity (b) ranges of the recorded Dinophysiales.

- **Remarks:** *Ornithocercus* is a large and impressively ornamented dinoflagellate genus and obviously of dinophysoid lineage: *Dinophysis* transforms into *Ornithocercus* by increasing list elaboration and by the acquisition of **external, symbiotic cyanobacteria** in the cingular area (HALLEGRAEFF & LUCAS, 1988).

(For further information see remarks on *Parahistioneis.*)

Two species have been recorded in the prospected area, but never abundant (Table 9), their temperature and salinity ranges are plotted in Fig.17.

Table 8: *Dinophysis* distribution data:

SPECIES	WOOD (1968)	DODGE (1982, 1985, 1993)	BALECH (1988)	HALLEGRAEFF & LUCAS (1988)	STEIDINGER & TANGEN (1996)	THIS STUDY
D. amphora BALECH, 1971			**SST: 3.4-12.4°C** **SSS: 34.1-34.9‰** oceanic			**SST: 27-29°C** **SSS: 35.0-35.8‰** rare in the equatorial Atlantic
D. caudata SAVILLE-KENT, 1881	neritic to estuarine, in subtropical to tropical waters	NE Atlantic, British Isles	**SST: 8.5-23°C** **SSS: 28.8-36.2‰** neritic to oceanic	coastal, in temperate to tropical waters,	neritic to estuarine, in warm temperate to tropical waters	**SST: 18-20°C** **SSS: 36.7-36.9‰** rare offshore NW Africa and at the Canary Isles
D. caudata* var. *tripos (GOURRET) GAIL, 1950	Caribbean, Straits of Florida	Atlantic (Gulf Stream)	**SST: 6.4-16.2°C** **SSS: 33.1-35.8‰** oceanic, in cold to warm waters	Tasman Sea	neritic, estuarine and oceanic, in warm temperate to tropical waters, rare in cold waters	**SST: 20-22°C** **SSS: 35.9-36.1‰** rare off NW Africa
D. cuneus (SCHÜTT) ABÉ, 1967	tropical to subtropical, Benguela Current, Straits of Florida	E Atlantic	**SST: 15-22°C** **SSS: 35.9-36.1‰** oceanic, in cold waters Brazil Current	coastal to oceanic, in temperate to tropical waters, NW shelf of Australia	oceanic, in warm temperate to tropical waters; worldwide distribution	**SST: 18-19°C** **SSS: 36.7-36.9‰** rare at the Canary Isles
D. dens PAVILLARD, 1915		NE Atlantic, rare W British Isles, Danish Strait, Mediterranean, off Norway	**SST: ~12°C** **SSS: ~34.9‰** oceanic, in cold to temperate waters		warm to cold water species; worldwide distribution	**SST: 18-22°C** **SSS: 35.9-36.8‰** rare off NW Africa
D. fortii PAVILLARD, 1923	neritic, in warm waters		**SST: 14.9-18.1°C** **SSS: 34.7-36.1‰** neritic to oceanic, Brazil Current	coastal, in temperate to subtropical waters	neritic to oceanic, in cold temperate to tropical waters	**SST: 21-22°C** **SSS: 35.8-36.0‰** rare off NW Africa
D. hastata STEIN, 1883	neritic, in warm waters, Brazil (N coast), Caribbean, Straits of Florida	Atlantic (Gulf Stream), British Isles, off Norway, off NW Spain	**SST: 18.6-22.7°C** **SSS: 34.7-36.2‰** oceanic, in cold waters	coastal to oceanic, in temperate to tropical waters, Indian Ocean	neritic, in warm temperate to tropical waters, rare in cold waters	**SST: 20-22°C** **SSS: 35.9-36.8‰** rare off NW Africa north of 10°N

Table 8: *Dinophysis* distribution data (continued).

SPECIES	WOOD (1968)	DODGE (1982, 1985, 1993)	BALECH (1988)	HALLEGRAEFF & LUCAS (1988)	STEIDINGER & TANGEN (1996)	THIS STUDY
D. micropterygia DANGEARD, 1927	in warm Atlantic waters, Caribbean	E Atlantic		coastal, in temperate waters		**SST: 21-29°C** **SSS: 35.0-36.8‰** frequent in the equatorial Atlantic south of 15°N
D. ovum SCHÜTT, 1895	in subtropical waters, Benguela Current, Brazil (N coast), Caribbean, Sargasso Sea	Atlantic, British Isles, Indian O., Mediterranean, Pacific		coastal to oceanic, in temperate to tropical waters		**SST: 18-19°C** **SSS: 36.8-37.0‰** rare at the Canary Isles
D. parva SCHILLER, 1928	Adriatic Sea, Caribbean, Coral Sea, Straits of Florida	E Atlantic				**SST: 27-29°C** **SSS: 35.0-36.1‰** rare in the equatorial Atlantic
D. parvula (SCHÜTT) BALECH, 1967	in warm waters, Benguela Current, Straits of Florida		**SST: 2.5-13.9°C** **SSS: 33.9-37.7‰** oceanic, in cold to warm waters	coastal to oceanic, in temperate to tropical waters, Tasman Sea		**SST: 18-28°C** **SSS: 35.8-36.8‰** rare in the equatorial Atlantic and off NW Africa
D. pulchella (LEBOUR) BALECH, 1967	Antarctic convergence, Australia, Brazil (N coast)	neritic to oceanic, in temperate to tropical waters, E Atlantic		coastal, in temperate to subtropical waters		**SST: 18-29°C** **SSS: 35.0-36.8‰** frequent throughout the investigated area
D. rotundatum CLAPARÈDE & LACHMANN, 1859	Atlantic, Benguela Current, Brazil (N coast), Straits of Florida	neritic to oceanic, in temperate to tropical waters, Atlantic, Indian O. and Pacific.	**SST: 1.5-12.4°C** **SSS: 33.7-33.9‰** oceanic, in cold waters	coastal to oceanic, in temperate to tropical waters	cosmopolitan	**SST: 18-29°C** **SSS: 35.0-36.8‰** abundant in the equatorial Atlantic, frequent off NW Africa

Table 9: *Ornithocercus* distribution data.

SPECIES	WOOD (1968)	DODGE (1985)	BALECH (1988)	HALLEGRAEFF (1988)	STEIDINGER & TANGEN (1996)	THIS STUDY
O. magnificus STEIN, 1883 Pl.4, Fig.1	warm water species	E Atlantic	**SST: 10.7-24°C SSS: 33.7-36.1‰** oceanic	NW shelf of Australia	oceanic, in warm temperate to tropical waters	**SST: 18-29°C SSS: 35.0-36.8‰** frequent in the equatorial Atlantic and at the Canary Isles
O. steinii SCHÜTT, 1900 Pl.4, Fig.2	in subtropical to tropical waters	E Mediterranean	**SST: >14.5°C SSS: >34.6‰** oceanic, Brazil Current	Gulf of Carpentaria	oceanic, in warm temperate to tropical waters	**SST: 28-29°C SSS: 35.0-35.1‰** one specimen in the eastern equatorial Atlantic

PARAHISTIONEIS
KOFOID & SKOGSBERG, 1928

- **Description** (WOOD, 1968; TAYLOR, 1976; BALECH, 1988; STEIDINGER & TANGEN, 1996): Cells with small to large sub circular body with ornate list and rib systems and large cingular chamber. Posterior cingular list often cup-shaped, largest portion of cingulum being posterior with ribs. Anterior cingular area funnel-shaped with lists. Left sulcal list extensive and sail-like.

- **Remarks:** This is a dinophysoid genus which is intermediate in list development between *Ornithocercus* and *Histioneis* and strongly resembles *Ornithocercus* in shape (HALLEGRAEFF & LUCAS, 1988). And, like *Ornithocercus*, it is equipped with **cyanobacterial episymbionts**.

Ornithocercus magnificus, *O. steinii*, and *Parahistioneis acuta* are large tropical dinoflagellates, their morphology is distinctly different from other species common in subtropical and temperate waters. The main differences are the possession of large spines or horns as well as wing-like structures. Their exaggerated ornamentation may function as a flotation device, increase nutrient uptake in oligotrophic waters through greater cell surface area for absorption, or may be a kind of defence mechanism against grazing by small zooplankton organisms. The symbiotic associations may benefit both partners through mutual exchange of organic or inorganic nutrients, and thus enable these organisms to thrive on a "starvation diet".

Only one specimen was found during cruise M 23/3 (see distribution data in Table 10, SST and SSS ranges in Fig.17).

Table 10: *Parahistioneis* distribution data.

SPECIES	WOOD (1968)	THIS STUDY
P. acuta KOFOID & SKOGSBERG, 1928 Pl.4, Fig.3	tropical Atlantic, Indian Ocean, Straits of Florida	**SST: 26-27°C SSS: 36.0-36.1‰** one specimen in the equatorial Atlantic

Fig.18: Temperature and Salinity Ranges of *Ceratium* Species

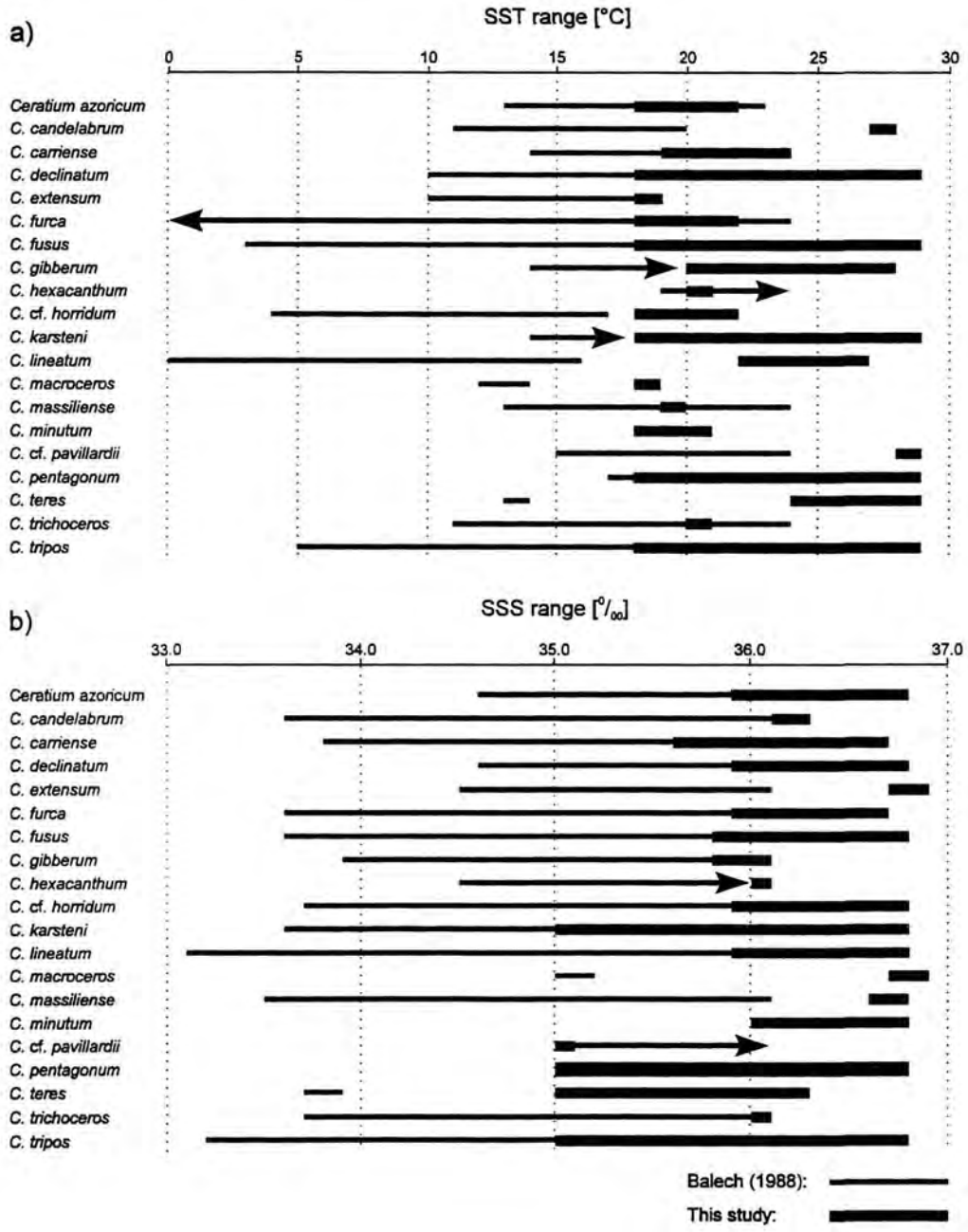

Fig. 18: Bar graphs of temperature (a) and salinity (b) ranges of the recorded *Ceratium* species.

Table 11: *Ceratium* distribution data.

SPECIES	WOOD (1968)	DODGE (1982, 1993)	BALECH (1988)	DODGE & MARSHALL (1994)	STEIDINGER & TANGEN (1996)	THIS STUDY
C. azoricum CLEVE, 1900	rare in subtropical and tropical waters	in subtropical to tropical waters, NE Atlantic	**SST: 13.7-23°C** **SSS: 34.6-36.1‰**	**MA SST: 10-28°C** intermediate species		**SST: 18-22°C** **SSS: 35.9-36.8‰** abundant offshore NW Africa
C. candelabrum (EHRENBERG) STEIN, 1883	oceanic, in warm, temperate waters	oceanic, in warm waters, NE Atlantic	**SST: 11-20°C** **SSS: 33.6-36.1‰** neritic and oceanic,	**MA SST: 5-28°C** temperate-tropical species	oceanic, in warm temperate to tropical waters, worldwide distribution	**SST: 27-28°C** **SSS: 36.1-36.3‰** frequent in the equatorial Atlantic
C. carriense GOURRET, 1883	endemic in tropical oceanic waters	in tropical waters	**SST: 14.6-24°C** **SSS: 33.8-36.1‰**	**MA SST: 5-28°C** temperate-tropical species	oceanic, in warm temperate to tropical waters, worldwide distribution	**SST: 18-24°C** **SSS: 35.6-36.7‰** frequent off NW Africa north of 10°N
C. declinatum KARSTEN, 1907	inter-oceanic, in tropical waters		**SST: 10.6-23°C** **SSS: 34.6-36.1‰** oceanic	**MA SST: 14-28°C** warm-temperate to tropical species	oceanic, in temperate to tropical waters, worldwide distribution	**SST: 18-29°C** **SSS: 35.9-36.8‰** frequent in the equatorial Atlantic and at the Canary Isles
C. extensum (GOURRET) CLEVE, 1901	oceanic, rare in tropical waters	E Atlantic	**SST: 10.6-19°C** **SSS: 34.6-36.1‰** oceanic, worldwide distribution	**MA SST: 5-28°C** temperate-tropical species		**SST: 18-19°C** **SSS: 36.7-36.9‰** rare at the Canary Isles
C. furca (EHRENBERG) CLAPARÈDE & LACHMANN, 1858	ubiquitous, not in antarctic waters	NE Atlantic	**SST: <24°C** **SSS: 33.6-36.1‰** neritic and oceanic, in eutrophic waters	**MA SST: 2-30°C** coastal, neritic, and oceanic, ubiquitous	coastal, estuarine, and oceanic, in cold temperate to tropical waters	**SST: 18-22°C** **SSS: 35.9-36.7‰** frequent off NW Africa north of 10°N
C. fusus (EHRENBERG) DUJARDIN, 1841	ubiquitous, not in sub-antarctic and antarctic waters	cosmopolitan	**SST: 3.4-24°C** **SSS: 33.6-36.1‰** ubiquitous	**MA SST: 2-30°C** coastal, neritic, and oceanic, ubiquitous	coastal, estuarine, and oceanic, in cold temperate to tropical waters	**SST: 18-29°C** **SSS: 35.8-36.8‰** frequent throughout the prospected area

Table 11: *Ceratium* distribution data (continued).

SPECIES	WOOD (1968)	DODGE (1982, 1993)	BALECH (1988)	DODGE & MARSHALL (1994)	STEIDINGER & TANGEN (1996)	THIS STUDY
C. gibberum GOURRET, 1883	oceanic, in tropical waters, never abundant	NE Atlantic	**SST: >14°C SSS: 33.9-36.1‰** oceanic	**MA SST: 5-28°C** temperate-tropical species	coastal and oceanic, in warm temperate to tropical waters	**SST: 20-28°C SSS: 35.8-36.1‰** rare in the equatorial Atlantic south of 15°N
C. hexacanthum GOURRET, 1883	in subtropical to tropical waters, Benguela Current,, Brazil (north coast), Caribbean	in warm waters, Atlantic (Gulf Stream)	**SST: >19°C SSS:>34.5‰** oceanic	**MA SST: 7-28°C** intermediate species	coastal and oceanic, in cold temperate to tropical waters, common in warm waters	**SST: 20.1°C SSS: 36.03‰** in one sample off Cape Blanc
C. horridum GRAN, 1902	in cool waters, Atlantic, Indian O., Pacific	in cool waters, British Isles, NE Atlantic	**SST: 4.6-16.8°C SSS: 33.7-36.1‰**	**MA SST: 2-30°C** coastal, neritic, and oceanic, ubiquitous	coastal and oceanic, in cold to warm temperate waters, as well as tropical waters	**SST: 18-21°C SSS: 35.9-36.8‰** rare off NW Africa north of 20°N
C. karsteni PAVILLARD, 1907	frequent but not abundant in oceanic waters, subtropical to tropical species		**SST: >14°C SSS: 33.6-36.1‰**	**MA SST: 14-28°C** warm-temperate to tropical species		**SST: 18-29°C SSS: 35.0-36.8‰** frequent in the equatorial Atlantic and off NW Africa
C. lineatum (EHRENBERG) CLEVE, 1899	in cold to temperate waters	in cool and temperate waters, NE Atlantic	**SST: -1.7-15.7°C SSS: 33.1-36.1‰** coastal to oceanic	**MA SST: 3-20°C** intermediate species	neritic and oceanic, in cold temperate to tropical waters	**SST: 22-27°C SSS: 35.9-36.8‰** frequent in the equatorial Atlantic and off NW Africa
C. macroceros (EHRENBERG) VANHOFFEN, 1897	inter-oceanic, in cool waters	in cool and temperate waters, NE Atlantic	**SST: 12-14°C SSS: ~35‰** oceanic	**MA SST: 2-30°C** coastal, neritic, and oceanic, ubiquitous	coastal and oceanic, in cold temperate to tropical waters, worldwide distribution	**SST: 18-19°C SSS: 36.7-36.9‰** rare at the Canary Isles
C. massiliense (GOURRET) JÖRGENSEN, 1911	inter-oceanic, in warm waters	in tropical waters	**SST: 11-24°C SSS: 33.6-36.1‰** neritic and oceanic	**MA SST: 5-28°C** temperate-tropical species	coastal and oceanic, in warm temperate to tropical waters	**SST: 19-20°C SSS: 36.6-36.8‰** rare off NW Africa

Table 11: *Ceratium* distribution data (continued).

SPECIES	WOOD (1968)	DODGE (1982, 1993)	BALECH (1988)	DODGE & MARSHALL (1994)	STEIDINGER & TANGEN (1996)	THIS STUDY
C. minutum JÖRGENSEN, 1920	Benguela Current, Brazil (north coast), Straits of Florida	in warm and temperate waters, NE Atlantic		**MA SST: 15°C** intermediate species		**SST: 18-21°C** **SSS: 36.0-36.8‰** frequent off NW Africa
C. pavillardii JÖRGENSEN, 1911	inter-oceanic, in warm waters		**SST: 15-24°C** **SSS: >35‰**	**MA SST: 14-28°C** warm-temperate to tropical species		**SST: 28-29°C** **SSS: 35.0-35.1‰** rare in the eastern equatorial Atlantic
C. pentagonum GOURRET, 1883	eupelagic in all oceans	NE Atlantic	**SST: >17°C** **SSS: >35‰**	**MA SST: 5-28°C** temperate-tropical species	oceanic, in warm temperate to tropical waters, worldwide distribution	**SST: 18-28°C** **SSS: 35.0-36.8‰** frequent throughout the investigated area
C. teres KOFOID, 1907	oceanic, in subtropical and tropical waters		**SST: 13.7°C** **SSS: 33.8‰** oceanic, abundant in tropical waters with SST >20°C	**MA SST: 5-28°C** temperate-tropical species	oceanic, in warm temperate to tropical waters, but rare	**SST: 24-29°C** **SSS: 35.0-36.3‰** frequent the equatorial Atlantic south of 15°N
C. trichoceros (EHRENBERG) KOFOID, 1908	neritic and oceanic, in subtropical and tropical waters	in tropical waters	**SST: 11.4-24°C** **SSS: 33.7-36.1‰** oceanic	**MA SST: 14-28°C** warm-temperate to tropical species	coastal and oceanic, in warm temperate to tropical waters, worldwide distribution	**SST: 20.1°C** **SSS: 36.03‰** in one sample off NW Africa
C. tripos (O.F. MÜLLER) NITZSCH, 1817	cosmopolitan	cosmopolitan	**SST: 5.9-20°C** **SSS: 33.2-36.1‰** neritic and oceanic	**MA SST: 2-30°C** coastal, neritic, and oceanic, ubiquitous	coastal and oceanic, in cold temperate to tropical waters, worldwide distribution	**SST: 18-29°C** **SSS: 35.0-36.8‰** frequent in the tropical E Atlantic

- **Remark:** Temperature data of DODGE & MARSHALL (1994) are mean annual sea surface temperatures (MA SST).

ORDER GONYAULACALES
TAYLOR, 1980

- **Description** (TAYLOR, 1980, 1987; DODGE, 1982, 1989b; LOEBLICH III, 1982; SOURNIA, 1986; FENSOME et al., 1993; STEIDINGER & TANGEN, 1996): Armoured dinokont cells with asymmetrical plate pattern, apical pore complex typically lacks the X plate of the peridinoids. Gonyaulacoid plate tabulation usually: 3-4', variable anterior intercalary tabulation, 5-7" but typically 6", 5-6c but typically 6c, 5-6‴ but typically 6‴, 1-3⁗ but typically 2⁗, and 0-1p but typically 0p. The 1' is usually asymmetrical.

FAMILY CERATIACEAE
WILEY & HICKSON, 1909

- **Description** (SOURNIA, 1986; FENSOME et al., 1993; STEIDINGER & TANGEN, 1996): Cells with at least three horns, one or two horns are formed by postcingular plates. First antapical plate is in contact with six or seven adjacent plates, including distal most postcingular. Plate formula: (Po), 4', 6", 5c, 2+s, 6‴, 2⁗.

CERATIUM
SCHRANK 1793

- **Description** (WOOD, 1968; TAYLOR, 1976; DODGE, 1982; SOURNIA, 1986; BALECH, 1988; FENSOME et al., 1993; STEIDINGER & TANGEN, 1996): Cells small to large (over 1,000 µm). Gonyaulacoid body usually flattened dorso-ventrally and drawn out into 2-4 hollow horns. Surface smooth with numerous trichocyst pores to highly reticulate. Plate formula: Po, cp, 4', 6", 5c, 2+s, 6‴, 2⁗. Cingulum slightly descending to the right. Ventral area depressed and wide, consists of three hyaline plates: 6"+5c+6⁗. Trough-like sulcus to the left of ventral area. Apical plates form the apical horn; postcingular and antapical plates form the antapical or hypothecal horns.

- **Remarks:** The presence of 2-4 horns, a single apical horn and 2-3 antapical horns, is characteristic of this genus. *Ceratium* cells are equipped with **chloroplasts**, sometimes with food vacuoles owing to phagocytic activity.

Species differentiation is based on cell outline including horn curvature and direction (i.e. shape and width of body, total length of cell, shape and size of horns, relation of left to right antapical horns, epitheca in relation to hypotheca), and plate ornamentation (STEIDINGER & TANGEN, 1996).

The genus *Ceratium* is widely distributed with species abundant in **fresh and marine waters**. Although sexual reproduction may occur, **no cysts** are known from the marine taxa. Only the freshwater species produce resting cysts.

20 species of *Ceratium* were recorded during cruise M23/3. Distribution data are presented in Table 11. The temperature and salinity ranges for the different species are plotted in Fig.18.

FAMILY CERATOCORYACEAE
LINDEMANN, 1928

- **Description:** (see description of genus)

CERATOCORYS
STEIN, 1883

- **Description** (WOOD, 1968; TAYLOR, 1976; LOEBLICH III, 1982; DODGE, 1985; SOURNIA, 1986; BALECH, 1988; FENSOME et al., 1993; CARBONELL-MOORE, 1996a; STEIDINGER & TANGEN, 1996): Armoured cell medium-sized, shape is angular to round with 2-8 characteristic short- to long-winged spines or horns (some species resembling a gladiator's helmet). Body is more or less spherical and may be compressed laterally. Hypotheca exceeds epitheca which is flattened. Heavy theca with prominent areolae. Plate formula: Po, 3', 1a, 5", 6c, 10s, 5‴, 1⁗. Cingulum premedian and displaced, cingular lists supported by prominent spines.

- **Remarks:** Dinoflagellates of this genus are observed to contain chloroplasts and are considered to be **autotrophic** (LATZ & LEE, 1995). Cells of *C. horrida* are usually rounded (diameter ~70 µm) and are characterised by six distinctive long ridged spines or horns, each one body size in length. This bizarre shape is supposed to protect against grazing by small zooplankton organisms, additionally, the larger cell surface enhances the nutrient uptake in oligotrophic waters.

Recently, spontaneous bioluminescence has been reported in *C. horrida* (LATZ & LEE, 1995), with *C. horrida* displaying similar rhythms as *Lingulodinium polyedra* in flashing and glowing. This bioluminescence may be regarded as a "burglar alarm" to signal the presence of a grazer, or as an additional defence mechanism by interrupting the normal course of predator feeding behaviour (BUSKEY et al., 1983; ABRAHAMS & TOWNSEND, 1993).

One species was frequently observed in the investigated area. Distribution data are given in Table 12; temperature and salinity ranges are plotted in Fig.19.

Fig.19: Gonyaulacales Temperature and Salinity Ranges

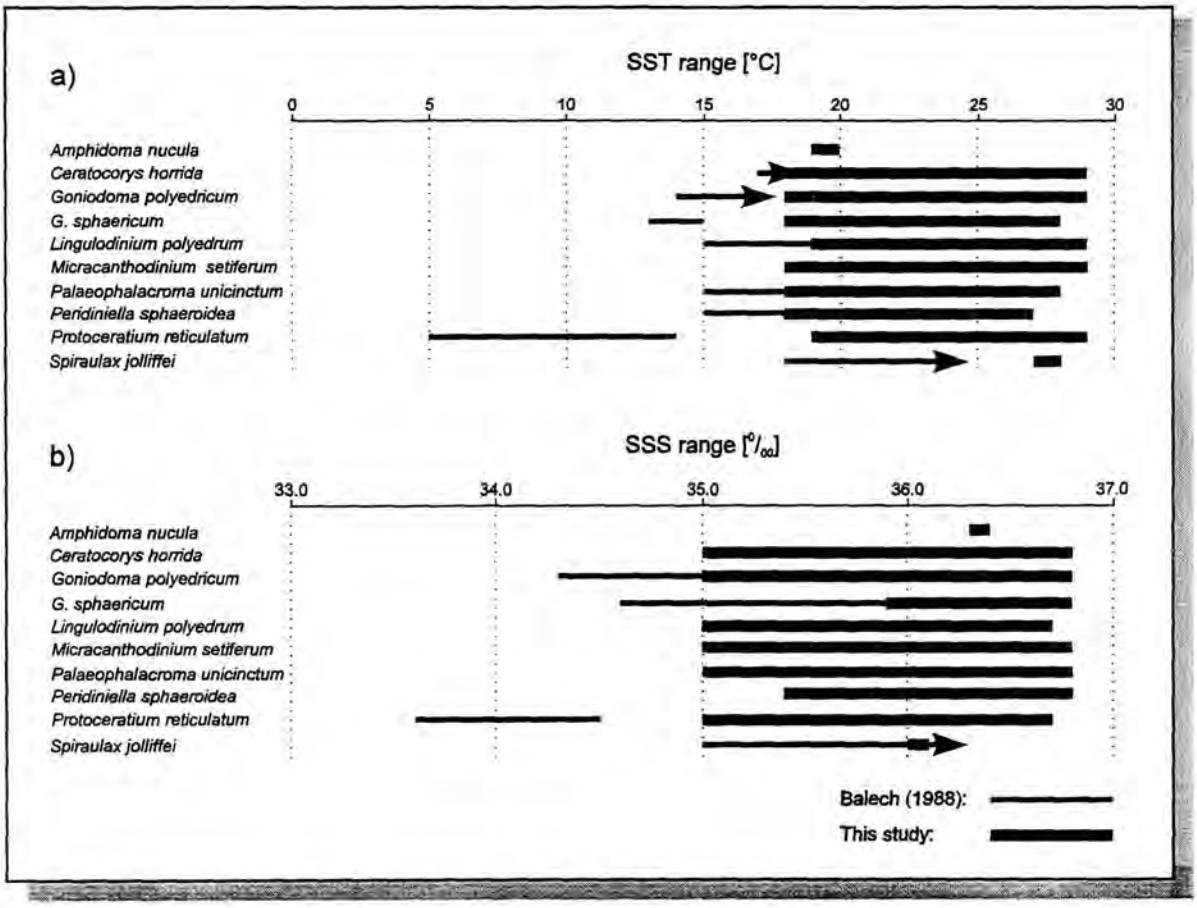

Fig. 19: Bar graphs of temperature (a) and salinity (b) ranges of the recorded Gonyaulacales.

Table 12: *Ceratocorys* distribution data.

SPECIES	WOOD (1968)	DODGE (1985)	BALECH (1988)	CARBONELL-MOORE (1996a)	STEIDINGER & TANGEN (1996)	THIS STUDY
C. horrida STEIN, 1883 Pl.9, Fig.1+2	oceanic, in tropical waters	tropical E Atlantic	**SST: >17°C SSS: >35.5°/oo** oceanic	subtropical to tropical, commonly found	neritic and oceanic, in warm temperate to tropical waters, worldwide distribution	**SST: 18-29°C SSS: 35.0-36.8°/oo** frequent in the equatorial Atlantic and at the Canary Isles (Fig.29)

FAMILY CLADOPYXIDACEAE
STEIN, 1883

- **Description** (SOURNIA, 1986; BALECH, 1988; FENSOME et al., 1993; DODGE, 1995; STEIDINGER & TANGEN, 1996): Cells globular with strongly developed thecal processes or spines, on each thecal plate one process. Plate formula: Po, 3-4', 3-4a, 7", 6-7c, 5-6s, 6"', 2"".

MICRACANTHODINIUM
DEFLANDRE, 1937

- **Description** (WOOD, 1968; TAYLOR, 1976; DODGE, 1982, 1995; LOEBLICH III, 1982; SOURNIA, 1986): Cell small-sized and spherical to ovoid. Surface covered with small "pimples", on each plate one long and slender spine. Cingulum median, incised, and displaced. Sulcus is small and present on hypotheca only.

-**Remarks:** Previously, cells of *Micracanthodinium* were rarely observed in plankton samples and were probably confused with specimens of *Palaeophalacroma unicinctum* owing to its similar shape and size; recently the presence of thecal plates on cells of *Micracanthodinium* was reported with plate formula: Po, 4', 7", 7c, ?s, 6"', 2"" (DODGE, 1995).

One species was recorded in the investigated area with distribution data given in Table 13, temperature and salinity ranges are given in Fig.19.

Table 13: *Micracanthodinium* distribution data.

SPECIES	WOOD (1968)	DODGE (1982)	DODGE (1995)	THIS STUDY
M. setiferum (LOHMANN) DEFLANDRE, 1937 PL.9, Fig.3+4	Adriatic Sea, Gulf of Naples	Adriatic, North Atlantic, Baltic Sea	a warm water species, E Atlantic, Mediterranean	**SST: 18-29°C** **SSS: 35.0-36.8‰** frequent in the equatorial Atlantic south of 12°N and at the Canary Isles

Table 14: *Palaeophalacroma* distribution data.

SPECIES	DODGE (1982, 1985, 1993)	BALECH (1988)	STEIDINGER & TANGEN (1996)	THIS STUDY
P. unicinctum SCHILLER, 1928 Pl.9, Fig.5+6	Adriatic Sea, Atlantic	**SST: 16-22.8°C** **SSS: 35.5-36.2‰**	in warm temperate to tropical oceans	**SST: 18-29°C** **SSS: 35.0-36.8‰** abundant throughout the investigated area

Table 15: *Amphidoma* distribution data.

SPECIES	DODGE (1985)	STEIDINGER & TANGEN (1996)	THIS STUDY
A. nucula STEIN, 1883 Pl.10, Fig.1+2	E Atlantic	in subtropical to tropical waters, Atlantic	**SST: 19.3°C** **SSS: 36.37‰** frequent off Cape Blanc

PALAEOPHALACROMA
SCHILLER, 1928

- **Description** (TAYLOR, 1976; DODGE, 1982, 1995; LOEBLICH III, 1982; SOURNIA, 1986; STEIDINGER & TANGEN, 1996): Cells small, sub spherical. Cingulum premedian, descending, only anterior list present. Sulcus not excavated. Theca smooth with pores; plate formula: Po, 4', 3a, 7", 6c, 6s, 6‴, 2⁗. Chloroplasts usually present.

Only one of the two *Palaeophalacroma* species was found (Table 14). Temperature and salinity ranges are given in Fig.19.

FAMILY GONYAULACACEAE
LINDEMANN, 1928

- **Description** (SOURNIA, 1986; BALECH, 1988; FENSOME et al., 1993; STEIDINGER & TANGEN, 1996): Cells with mid ventral sulcus, may be straight, oblique from upper right to lower left, or sigmoidal. No dorsoventral compression. Antapex more or less symmetric. Plate formula: Po, 3-4', 0-4a, 6(7)", 6c, 6-8s, 6‴, 1p, 1⁗.

AMPHIDOMA
STEIN, 1883

- **Description** (DODGE, 1982; SOURNIA, 1986; STEIDINGER & TANGEN, 1996): Cells small to medium-sized, more or less biconical or drawn out, typically with descending cingulum and small hollow antapical projection. Short sulcus is restricted to hypotheca. Plate formula: Po, X(?), 6', 6", 6c, 4s(?), 6‴, 2⁗. Apical pore complex distinctive. No anterior intercalaries. Chloroplasts present, **autotrophic**.

Only one species of *Amphidoma* could be identified in the investigated area. Distribution data are presented in Table 15 with temperature and salinity ranges in Fig.19.

GONIODOMA
STEIN, 1883

- **Description** (WOOD, 1968; TAYLOR, 1976; DODGE, 1981, 1982; SOURNIA, 1986; BALECH, 1988; STEIDINGER & TANGEN, 1996): Cells polygonal or rounded. Cingulum median with lists, slightly descending. The basic plate formula is Po, cp, 4', 6", 6c, 6s, 6‴, 2⁗. Cells with chloroplasts, **autotrophic. Not known to produce cysts.**

- **Remarks:** The thecae are composed of regularly punctulate plates, and ridges that follow the plate sutures may be present. An apical pore is present, but no apical or antapical horns. A taxonomic characteristic of this genus is the arrangement of three plates at the antapex and around the apical pore.

Both species of *Goniodoma* were recorded and distribution data are given in Table 16 with temperature and salinity ranges in Fig.19.

Table 16: *Goniodoma* distribution data.

SPECIES	WOOD (1968)	DODGE (1982, 1985, 1993)	BALECH (1988)	STEIDINGER & TANGEN (1996)	THIS STUDY
G. polyedricum (POUCHET) JORGENSEN, 1899 PL.11, Fig.1,3,5	ubiquitous in subtropical and tropical waters	oceanic, in tropical waters, NE Atlantic, Caribbean, Indian O., Mediterranean	**SST: >14°C SSS: 34.8-36.1‰** coastal, neritic, and oceanic	oceanic, ubiquitous in subtropical and tropical waters	**SST: 18-29°C SSS: 35.0-36.8‰** abundant throughout the investigated area
G. sphaericum MURRAY & WHITTING, 1899 PL.11, FIG.2,4,6,7	Atlantic, Caribbean, Indian O., Mediterranean	Atlantic, Caribbean, China Sea	**SST: 13.3-15°C SSS: 34.6-35.9‰** oceanic	worldwide distribution	**SST: 18-28°C SSS: 35.9-36.8‰** frequent off NW Africa

Table 17: *Gonyaulax* distribution data.

SPECIES	WOOD (1968)	DODGE (1982, 1985, 1993, 1994)	BALECH (1988)	STEIDINGER & TANGEN (1996)	THIS STUDY
G. digitalis (POUCHET) KOFOID, 1911	estuarine, Caribbean, Straits of Florida	oceanic, NE Atlantic, British Isles, North Sea, widespread	**SST: 2.2-18°C** **SSS: 33.6-35.7‰** frequent in the investigated area		**SST: 18-28°C** **SSS: 35.5-36.8‰** frequent throughout the investigated region
G. fragilis (SCHÜTT) KOFOID, 1911	Atlantic, Brazil (north coast), Caribbean, Mediterranean, Pacific	in waters of low latitudes		oceanic and coastal, in warm temperate to tropical waters	**SST: 19-27°C** **SSS: 35.5-36.7‰** rare in the equatorial Atlantic and off NW Africa
G. hyalina OSTENFELD & SCHMIDT, 1901		in warm waters			**SST: 20.1°C** **SSS: 36.03‰** in one sample off NW Africa
G. milneri (MURRAY & WHITTING) KOFOID, 1911	in tropical waters, Atlantic, Caribbean		**SST: 17.3°C** **SSS: 35.9‰**		**SST: 19.3°C** **SSS: 36.37‰** in one sample off NW Africa
G. monospina RAMPI, 1951		in waters of low latitudes, E Atlantic			**SST: 18-29°C** **SSS: 35.0-36.8‰** frequent throughout the investigated region
G. polygramma STEIN, 1883	cosmopolitan	in warm waters, E Atlantic, Florida, off Scotland, off South Africa	**SST: 8.7-20°C** **SSS: 33.7-36.1‰**	neritic and oceanic, in cold temperate to tropical waters, worldwide distribution	**SST: 18-29°C** **SSS: 35.0-36.8‰** abundant throughout the prospected region
G. spinifera (CLAPARÈDE & LACHMANN) DIESING, 1866	neritic and estuarine, interoceanic, Bahama Banks, Brazil (north coast), Santaren Channel, Straits of Florida, West Channel	NE Atlantic, British Isles, North Sea, widespread	**SST: 2.2-15.6°C** **SSS: 33.2-35.7‰**	neritic, estuarine, oceanic, cosmopolitan	**SST: 18-29°C** **SSS: 35.0-36.8‰** frequent throughout the prospected area
G. striata MANGIN, 1926		in waters of low latitudes, E Atlantic	**SST: 4.7-9.6°C** in subantarctic waters		**SST: 18-28°C** **SSS: 35.8-36.8‰** frequent throughout the study area
G. turbynei MURRAY & WHITTING, 1899	in tropical waters, Atlantic, Caribbean, Pacific, Straits of Florida	in waters of low latitudes, NE Atlantic	**SST: 2-22.4°C** **SSS: 33.2-36.1‰**		**SST: 18-29°C** **SSS: 35.0-36.8‰** abundant throughout the investigated area

Fig.20: Temperature and Salinity Ranges of *Gonyaulax* Species

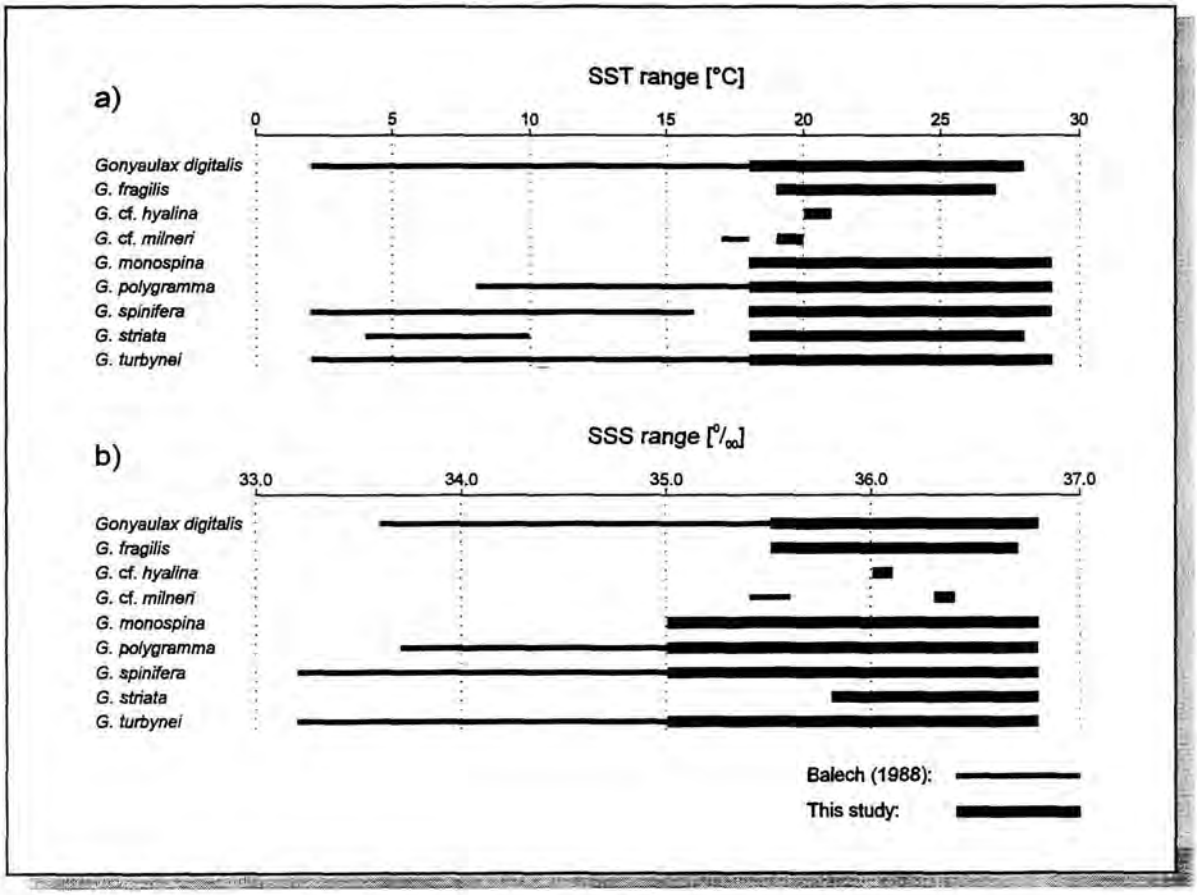

Fig.20: Bar graphs of temperature (a) and salinity (b) ranges of the recorded *Gonyaulax* species.

Table 18: *Lingulodinium* distribution data.

SPECIES	WOOD (1968)	DODGE (1982, 1985, 1994)	BALECH (1988)	STEIDINGER & TANGEN (1996)	THIS STUDY
L. polyedrum (STEIN) DODGE, 1989 Pl.10, Fig.3+4	in warm waters, Benguela Current, Brazil (north coast), Caribbean	neritic, in temperate to tropical waters, off Scotland	**SST: 15.5-18.1°C SSS: 35.5-36.1‰**	neritic, in warm temperate to tropical waters	**SST: 19-29°C SSS: 35.0-36.7‰** frequent throughout the investigated area

GONYAULAX
DIESING, 1866

- **Description** (WOOD, 1968; TAYLOR, 1976; DODGE, 1982, 1989a; SOURNIA, 1986; BALECH, 1988; FENSOME et al., 1993; STEIDINGER & TANGEN, 1996): Cells ovoid to biconical to fusiform. Cingulum descending (left-handed), displaced by a variable amount, the two ends often overlapping. Sulcus straight to sinuous, enters epitheca only slightly. Plate formula: Po, 3', 2a, 6", 6c, 7s, 6"', 2"". 1' may be sigmoid and narrow to rhomboidal. Apical pore complex with oval pore plate or elongate oval pore plate. Apical horn and antapical spines may be present. Chloroplasts present, **autotrophic**. Some species form **dinosporin cysts**

- **Remarks:** Identification of some *Gonyaulax* species may be exceedingly difficult for a plankton worker, e.g. *G. spinifera* has been confused with *G. digitalis* and other species owing to morphological variations and transitional stages of the thecae, i.e. *G. spinifera* complex. Thecal plates are normally thick and strongly ornamented with ridges, reticulations, and thickened rings. They are shared after division or shed before cell divides.

According to DODGE (1988) cell division in some species of *Gonyaulax* occurs along a predetermined oblique division plane, running from the anterior right side of the cell to the posterior left. The two daughter cells retain two completely different parts of the parental theca and subsequently synthesise the missing plates. This process takes several hours and thecae of recently divided cells are clearly discernible from other "older" specimens.

9 species of *Gonyaulax* have been recorded during this study (Table 17), their temperature and salinity ranges are presented in Fig.20.

LINGULODINIUM
WALL, 1967 *emend.* DODGE, 1989

- **Description** (WOOD, 1968; DODGE, 1989a; FENSOME et al., 1993; STEIDINGER & TANGEN, 1996): Motile cells polyhedral with no antapical spines or apical horns. Girdle descending without overhang, more or less median. Sulcus straight. Plate formula: Po, 3', 3a, 6", 6c, 7s, 6"', 1p, 2"". Thecal plates thick with ridges along the sutures and circular depressions over the surface of plates. Apical pore complex typically of *Gonyaulax*. Cells with chloroplasts, **autotrophic**. Forming **dinosporin cysts**.

- **Remarks:** *L. polyedrum* is also known as *Gonyaulax polyedra* STEIN, 1883; DODGE (1989a) removed this species from the genus *Gonyaulax* owing to the epithecal tabulation pattern. He assigned the thecate stage to its cyst genus *Lingulodinium* in combination with the earliest specific name, *polyedrum*. Thus, *Lingulodinium polyedrum* is the name of the thecate stage, and *Lingulodinium machaerophorum* is the name of the cyst stage. This is a very unusual combination in dinoflagellate taxonomy: the theca having the same generic name as the cyst.

Distribution data are presented in Table 18, temperature and salinity ranges are plotted in Fig.19.

Table 19: *Peridiniella* distribution data.

SPECIES	WOOD (1968)	DODGE (1985)	BALECH (1988)	THIS STUDY
P. sphaeroidea KOFOID & MICHENER, 1911 PL.10, Fig.5+6	off California, Straits of Florida	E Atlantic	**SST: 16-18°C SSS: 35.5-36.1‰** oceanic	**SST: 18-27°C SSS: 35.4-36.8‰** rare in the equatorial Atlantic and off NW Africa

Table 20: *Protoceratium* distribution data.

SPECIES	WOOD (1968)	DODGE (1982, 1985, 1993, 1994)	BALECH (1988)	STEIDINGER & TANGEN (1996)	THIS STUDY
P. reticulatum (CLAPARÈDE & LACHMAN) BÜTSCHLI, 1885 Pl.10, Fig.7+8	nertic to estuarine, Benguela Current, Caribbean	neritic, NE Atlantic, British Isles, North Sea, off South Africa, widespread, may occur in high numbers	**SST: 6.9-13.5°C SSS: 33.6-34.6‰**	nertic to estuarine, cold temperate to subtropical waters	**SST: 19-29°C SSS: 35.0-36.7‰** rare in the eastern equatorial Atlantic and off NW Africa

Table 21: *Spiraulax* distribution data.

SPECIES	WOOD (1968)	BALECH (1988)	CARBONELL-MOORE (1996b)	STEIDINGER & TANGEN (1996)	THIS STUDY
Sp. jolliffei (MURRAY & WHITTING) KOFOID, 1911, *emend.* CARBONELL-MOORE, 1996 PL.12, FIG.1	oceanic, *in tropical waters*, Brazil (north coast), Straits of Florida, Santaren Channel	**SST: >18°C SSS: >35.0‰** oceanic, frequent but not abundant	in subtropical to tropical waters, Atlantic, Pacific	oceanic, *in subtropical to* tropical waters, widely distributed	**SST: 27.5°C SSS: 36.07‰** in one sample in the equatorial Atlantic

PERIDINIELLA
KOFOID & MICHENER, 1911

- **Description** (DODGE, 1985; BALECH, 1988; STEIDINGER & TANGEN, 1996): Cells small-sized. Cingulum descending, displaced one width. Epitheca with *Protoperidinium*- and hypotheca with *Gonyaulax*-type plate pattern. Plate formula: Po, x, 4', 3 or 4a, 7", 6c, 6 or 7s, 6‴, 2⁗.

- **Remarks:** *Peridiniella* is closely related to *Gonyaulax* and resembles it in shape. The small theca is strongly reticulated enclosing a characteristic cluster of small poroids.

This is a rarely found genus of **tropical oligotrophic waters**. Chloroplasts are present and the genus is considered to be **autotrophic**.

Only two species of *Peridiniella* are known and one was found with distribution data in Table 19 and temperature and salinity ranges in Fig.19.

PROTOCERATIUM
BERGH, 1882

- **Description** (WOOD, 1968; TAYLOR, 1976; DODGE, 1982, 1989a; BALECH, 1988; STEIDINGER & TANGEN, 1996): Cells small-sized, ovoid to broadly biconical to polyhedral. Cingulum slightly descending. Plate formula: Po, 3', 1a, 6", 6c, s, 6‴, 1p, 1⁗ (DODGE, 1989a). Chloroplasts present, **autotrophic**. It **produces dinosporin cysts**.

- **Remarks:** *P. reticulatum* is also known as *Gonyaulax grindleyi* REINECKE, 1967. In his revision of the Gonyaulacaceae DODGE (1989a) made *Protoceratium* a synonym to *Gonyaulax*.

Thecal plates are thick and heavily reticulated with areolations. No apical horn is present, the apical pore complex differentiates this genus from *Gonyaulax* and *Alexandrium*. Po is round and has a crescent-shaped pore.

During this study one species has been found and distribution data are presented in Table 20. Temperature and salinity ranges are given in Fig.19.

SPIRAULAX
KOFOID, 1911 *emend.* CARBONELL-MOORE, 1996b

Description (WOOD, 1968; DODGE, 1985, 1989; SOURNIA, 1986; BALECH, 1988; CARBONELL-MOORE, 1996b; STEIDINGER & TANGEN, 1996): Cells large, broadly fusiform with pointed ends. Cingulum narrow and displaced. Prominent antapical spine. Plate formula: Po, 3', 2a, 6", 6c, 6s, 6‴, 1p, 1⁗. Cells with chloroplasts.

Table 22: *Oxytoxum* distribution data.

SPECIES	WOOD (1968)	DODGE (1982, 1985, 1993)	DODGE & SAUNDERS (1985)	BALECH (1988)	STEIDINGER & TANGEN (1996)	THIS STUDY
O. challengeroides KOFOID, 1907	tropical Pacific, Straits of Florida		E Atlantic, off Spain			**SST: 26-28°C** **SSS: 35.8-36.3‰** frequent in the equatorial Atlantic
O. constrictum (STEIN) BÜTSCHLI, 1885	Benguela Current, Caribbean, Coral Sea, Mediterranean, Santaren Channel, Straits of Florida	E Atlantic	E Atlantic	**SST: 18.3°C** **SSS: 36.1‰**	in warm temperate to tropical waters, worldwide distribution	**SST: 20-28°C** **SSS: 35.8-36.4‰** rare in the equatorial Atlantic and off NW Africa
O. crassum SCHILLER, 1937	Adriatic Sea, Straits of Florida	E Atlantic	E Atlantic, North Atlantic, Indian O.			**SST: 24-29°C** **SSS: 35.0-36.3‰** frequent in the equatorial Atlantic south of 15°N
O. elongatum WOOD, 1963	Caribbean, Coral Sea, off New Ireland, Vitiaz Strait	E Atlantic	E Atlantic			**SST: 28-29°C** **SSS: 35.0-35.1‰** rare in the eastern equatorial Atlantic
O. laticeps SCHILLER, 1937	Adriatic Sea, Caribbean, Coral Sea, Indian O., Straits of Florida	Adriatic Sea, E Atlantic, Indian O., tropical Pacific	E Atlantic, English Channel			**SST: 19-29°C** **SSS: 35.0-36.7‰** frequent throughout the investigated area

Table 22: *Oxytoxum* distribution data (continued).

SPECIES	WOOD (1968)	DODGE (1982, 1985, 1993)	DODGE & SAUNDERS (1985)	BALECH (1988)	STEIDINGER & TANGEN (1996)	THIS STUDY
O. ovale SCHILLER, 1937		E Atlantic	E Atlantic			**SST: 24-29°C** **SSS: 35.0-36.1‰** frequent in the equatorial Atlantic south of 15°N
O. reticulatum (STEIN) SCHÜTT, 1895		Atlantic, Mediterranean	E Atlantic	oceanic, warm water species		**SST: 20-29°C** **SSS: 35.0-35.9‰** rare in the eastern equatorial Atlantic
O. sceptrum (STEIN) SCHRÖDER, 1906	Caribbean, Indian O., Pacific, Straits of Florida	E Atlantic	E Atlantic, E Mediterranean	**SST: 16.5°C** **SSS: 33.4‰**		**SST: 20-29°C** **SSS: 35.0-36.1‰** frequent in the E Atlantic south of 20°N
O. scolapax STEIN, 1883	interoceanic, in warm waters	in warm waters, E Atlantic	E Atlantic, E Mediterranean, Galway Bay	**SST: 6.1-21°C** **SSS: 33.4-36.1‰** oceanic	in warm temperate to tropical waters, mostly recorded in the Atlantic	**SST: 18-28°C** **SSS: 35.0-36.8‰** abundant throughout the investigated area
O. stropholatum DODGE & SAUNDERS, 1985		E Atlantic	E Atlantic			**SST: 19-29°C** **SSS: 35.0-36.7‰** frequent throughout the study area
O. tesselatum (STEIN) SCHÜTT, 1895	Brazil (north coast), Caribbean, Straits of Florida	E Atlantic	E Atlantic	**SST: >16°C** **SSS: 35.0-36.1‰**	in warm temperate to tropical waters, mostly recorded in the Atlantic	**SST: 19-29°C** **SSS: 35.0-36.4‰** frequent throughout the prospected region

Fig.21: Temperature and Salinity Ranges of *Oxytoxum* Species

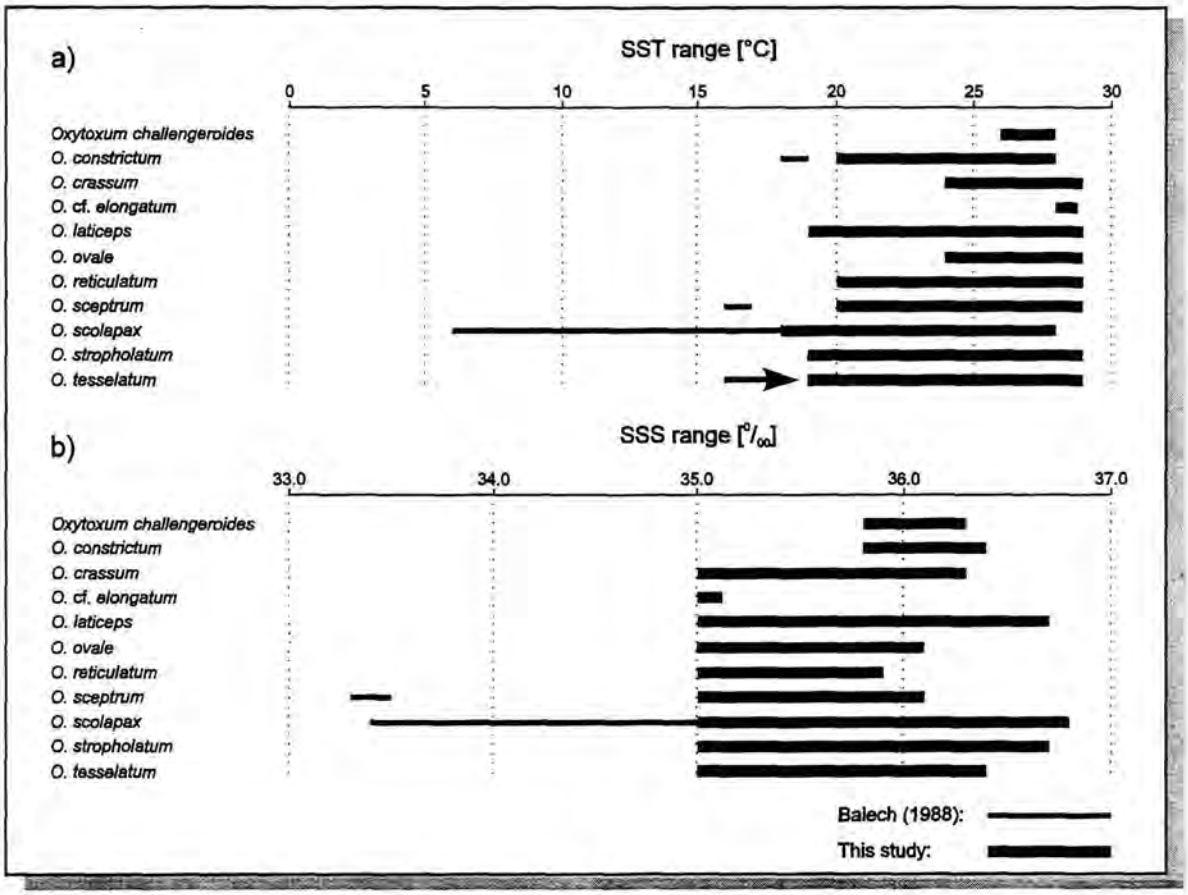

Fig.21: Bar graphs of temperature (a) and salinity (b) ranges of the recorded *Oxytoxum* species.

- **Remarks:** *Sp. jolliffei* is also known as *Gonyaulax jolliffei* MURRAY & WHITTING, 1899 as well as *Spiraulax kofoidii* GRAHAM, 1942. It closely resembles *Gonyaulax fusiformis* GRAHAM, 1942 and *G. birostris* STEIN, 1883 in shape, and identification of the three species may be a problem for a plankton worker (CARBONELL-MOORE, 1996b).

One species was found in only one sample of cruise M23/3 (Table 21, Fig.19).

FAMILY OXYTOXACEAE
LINDEMANN, 1928

- **Description** (DODGE & SAUNDERS, 1985; SOURNIA, 1986; BALECH, 1988; FENSOME et al., 1993; STEIDINGER & TANGEN, 1996): Cells longer than broad, oval to biconical to fusiform in dorsoventral view, circular in anterior or posterior view. Apex and antapex may be rounded or pointed. Cingulum may be median or may be close to the apex. Epitheca may be smaller or as large as hypotheca. Plate formula: (Po), 2-3', 1-3a, 3-7", 5-6c, ?s, 5‴, 0-2p, 1⁗.

OXYTOXUM
STEIN, 1883

- **Description** (WOOD, 1968; DODGE, 1982; DODGE & SAUNDERS, 1985; SOURNIA, 1986; BALECH, 1988; STEIDINGER & TANGEN, 1996): Cells small to large, biconical to elongate needle-shaped. Epitheca smaller than hypotheca. Cingulum descending, anterior to

median. Chloroplasts present, **autotrophic**. **No cyst stages**.

-Remarks: Several species of the genus *Oxytoxum* are also known as species of *Corythodinium* LOEBLICH & LOEBLICH III, 1966 and *Pavillardinium* DE TONI, 1936, which are now considered to be synonyms of *Oxytoxum* (DODGE & SAUNDERS, 1985; FENSOME et al., 1993).

The genus shows a great variability of morphology, but DODGE & SAUNDERS (1985) suggested the following general plate pattern: Po, 5', 6", 5c, 4s, 5"', 1"". Cells may be as small as 10-15 µm or as large as 100 µm. The apical and antapical terminations show a great morphological variability, they may be rounded and domed or drawn out into a spine. Thecal plate ornamentation varies and may be used for species identification.

11 species have been found with distribution data displayed in Table 22, their temperature and salinity ranges are plotted in Fig.21.

ORDER PERIDINIALES
HAECKEL, 1894

- **Description** (LOEBLICH III, 1982; SOURNIA, 1986; FENSOME et al., 1993; STEIDINGER & TANGEN, 1996): Armoured dinokont cells with symmetrical plate pattern, apical pore complex typically with X plate. Peridinoid plate tabulation usually: 3-6' but typically only 3 or 4', 1-3a, 6-7", 4-6c, 5"', 1-2"" but typically 2"". The 1' is usually symmetrical.

FAMILY CALCIODINELLACEAE
DEFLANDRE, 1949 *emend.* BUJAK & DAVIS, 1983

- **Original diagnosis** (BUJAK & DAVIS, 1983, p.127): "Peridininean dinoflagellates with an ortho-hexa tabulation of 4', 3a, 7", 4-6c, 5"', 2"" plus a transitional cingular-sulcal plate that is sometimes designated as an additional cingular plate. Variations to this basic tabulation formula occasionally occur, giving a general formula of 4', 2-3a, 4-7", 4-6c, 0-1p, 5"', 2"". Cysts, when formed, are calcareous with an apically located archaeopyle that includes plates of the intercalary or apical series or both."

PENTAPHARSODINIUM
INDELICATO & LOEBLICH III, 1986
emend. MONTRESOR et al., 1993

- **Description** (INDELICATO & LOEBLICH III, 1986; BALECH, 1990; LEWIS, 1991; MONTRESOR et al., 1993; STEIDINGER & TANGEN, 1996): Cells small, with plate formula: Po, X, 4', 3a, 7", 5c (4c+t), 4s, 5"', 2"".

- **Remarks:** This is an **autotrophic** peridinioid dinoflagellate genus. The plate surfaces are ornamented with various kinds of pores and knobs, which are species criteria. This is a cyst forming genus, **dinosporin and calcareous cysts** are known; it is a genus of **marine waters**.

Absolutely positive identification of *Pentapharsodinium* species is not possible in the present study. The thecae of *P.* cf. *thyrrhenicum* show the hypothecal plate pattern (BALECH, 1990) and the same plate ornamentation (MONTRESOR et al., 1993) as *P. thyrrhenicum*. Distribution data are presented in Table 23 with temperature and salinity ranges in Fig.22.

SCRIPPSIELLA
BALECH, 1959

- **Description** (DODGE, 1982; INDELICATO & LOEBLICH III, 1986; BALECH, 1988; GAO et al., 1989; GAO & DODGE, 1991; LEWIS, 1991; STEIDINGER & TANGEN, 1996): Cells small, with plate formula: Po, X, 4', 3a, 7", 6c (5c+t), 4s, 5"', 2"".

- **Remarks:** The vegetative cells of this genus are small and broadly tear-shaped, with a conical epitheca (that may have an apical process) and a rounded hypotheca. The cingulum is more or less median and slightly excavated; the sulcus is mainly developed on the hypotheca. The cells are covered with relatively thin plates that may have pores. Species of *Scrippsiella* are equipped with chloroplasts and are therefore considered to be **autotrophs**. They can produce **dinosporin and calcareous cysts**.

Superficially, the outer cell morphologies of *Ensiculifera, Pentapharsodinium, Peridinium, Protoperidinium* and *Scrippsiella* are very similar. The genera differ mainly in the size of the first apical plate and in the number of sulcal and cingular plates. In the past, this caused various taxonomic problems which were solved i.a. by BALECH (1974).

INDELICATO & LOEBLICH III (1986) separated the genus *Pentapharsodinium* from *Peridinium* EHRENBERG, 1830 by attributing great importance to the postcingular and cingular plates. *Pentapharsodinuim* is considered to have a transitional plate in addition to 4 cingular plates (4c+t). Regarding the cingular plates as shown in MONTRESOR et al. (1993) the suture of the third and fourth cingular plates is at the mid-dorsal side of the theca, whereas *Peridinium*, which is a freshwater genus, has 5 cingular plates (5c)

Fig.22: Peridiniales Temperature and Salinity Ranges

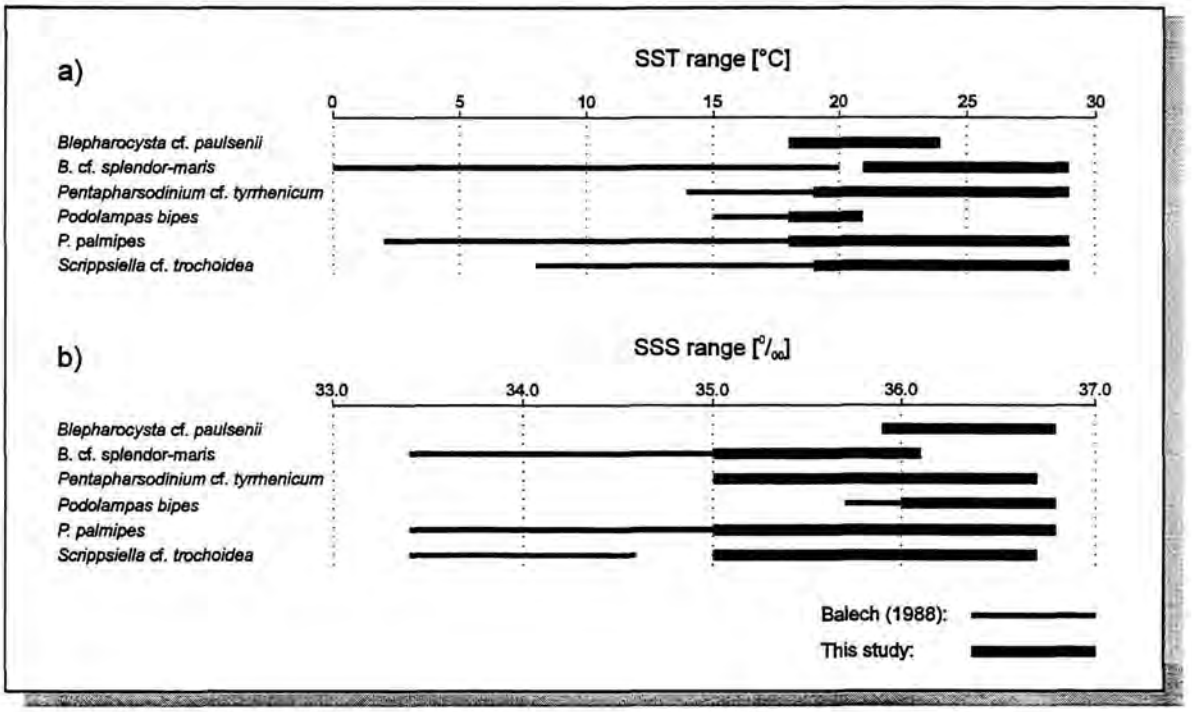

Fig.22: Bar graphs of temperature (a) and salinity (b) ranges of the recorded Peridiniales.

Table 23: *Pentapharsodinium* distribution data.

SPECIES	BALECH (1990)	MONTRESOR et al. (1993)	MONTRESOR et al. (1994)	THIS STUDY
P. tyrrhenicum (BALECH) MONTRESOR, 1993	Mediterranean (Thyrrhenian Sea)	marine, Mediterranean	**SST: 14-28°C SSS: 37.8-38.2 PSU** (PSU: Practical Salinity Units) marine, Mediterranean (Gulf of Naples)	**SST: 19-29°C SSS: 35.0-36.7‰** rare in the equatorial Atlantic and offshore NW Africa

Table 24: *Scrippsiella* distribution data.

SPECIES	WALL & DALE (1968b)	WOOD (1968)	DODGE (1982, 1985, 1993)	BALECH (1988)	STEIDINGER & TANGEN (1996)	THIS STUDY
S. trochoidea (STEIN) LOEBLICH III, 1976 Pl.4, Fig.6+7	Caribbean, off Woods Hole	neritic, in European waters	around the British Isles, Atlantic, West Indies	**SST: 8.7-21°C SSS: 33.4-34.6‰** nertic	neritic and estuarine	**SST: 19-29°C SSS: 35.0-36.7‰** frequent in the equatorial Atlantic and offshore NW Africa (Fig.16)

and two sutures can be seen on the dorsal side. *Scrippsiella* is equipped with 6 cingular plates (5c+t) which also show two cingular plate sutures on the dorsal side. Absolutely positive species identification of *Pentapharsodinium* and *Scrippsiella* is therefore extremely difficult, and, while using an SEM, only possible when a single specimen can be turned around to look both at the ventral and the dorsal side.

Distribution data are presented in Table 24 with temperature and salinity ranges plotted in Fig.22.

FAMILY PODOLAMPADACEAE
LINDEMANN, 1928

- **Description** (SOURNIA, 1986; BALECH, 1988; FENSOME et al., 1993; CARBONELL-MOORE, 1994b; STEIDINGER & TANGEN, 1996): Cells globular, slightly compressed dorsoventrally or laterally. Cingulum not apparent, series of three plates are posterior to equator. Plate formula: Po, Pt, X, 3', 1a, 5", 3c, 4-5s, 4-5"', 1''''. Genera are distinguished on the basis of apical pore types, cell compression and/or cell bilateral asymmetry.

- **Remark:** This family has been generally considered to be a group of rarely found **oceanic warm water** species (BALECH, 1963; DODGE, 1982). CARBONELL-MOORE (1994a) gives a summary of previously accomplished distribution data and compares them with her own observations, and thus shows that this "scarcity" is mostly the result of inadequate sampling methods. The Podolampadaceans may be regarded as "...a diverse group with a wide range in both vertical and latitudinal distribution, and in temperature tolerance, achieving maximum species diversity in the tropics..." (CARBONELL-MOORE, 1994a, p.23).

BLEPHAROCYSTA
EHRENBERG, 1873

- **Description** (WOOD, 1968; TAYLOR, 1976; DODGE, 1982; SOURNIA, 1986; BALECH, 1988; FENSOME et al., 1993; CARBONELL-MOORE, 1994b; STEIDINGER & TANGEN, 1996): Cells medium-sized, spherical to oval shape without apical attenuation or processes. Homologous cingular area not excavated and without cingular lists, sulcus with lists. Plate formula presented by CARBONELL-MOORE (1994b): Po, Pt, X, 3', 1a, 5", 3c, 4-5s, 4-5"', 1''''.

-**Remarks:** The organisms are covered with smooth plates that may be perforated by pores. These plate pore patterns and the general cell shape together with shape and position of the sulcal "wings" may help to identify at least four species.

The cells do not have a cingular groove. Apical and antapical plates are very small with larger "equatorial" and "postequatorial" plates in between, which probably represent precingulars and cingulars (i.e. "homologous cingular area").

Cells of this genus are easily overlooked or mistaken for invertebrate eggs by plankton workers using standard LM examination techniques (BALECH, 1988; CARBONELL-MOORE, 1992). SEM observations of the plankton filters in the present study have been still not adequate for absolutely positive species identification.

Two "species" of *Blepharocysta* have been recorded in the prospected area. Their distribution data are given in Table 25 with temperature and salinity ranges plotted in Fig.22.

PODOLAMPAS
STEIN, 1883

- **Description** (WOOD, 1968; TAYLOR, 1976; DODGE, 1982, 1985; SOURNIA, 1986; BALECH, 1988; FENSOME et al., 1993; CARBONELL-MOORE, 1994b; STEIDINGER & TANGEN, 1996): Cells large, pear- to top-shaped. Epitheca tapering to a distinct apical horn which ends in an apical pore. Hypotheca with one to three prominent antapical spines which may have lists. Homologous cingular area not excavated with three plates and without lists. Plate formula: Po, cp, X, 3', 1a, 5", 3c, 4-6s, 5"', 1''''. Postcingular plates with prominent double pore tract.

- **Remarks:** *Podolampas* is an unusually shaped peridinioid dinoflagellate genus; like *Blepharocysta*, it lacks the cingular and sulcal depressions. The surface of the theca is smooth for both genera. *Podolampas* has only a left sulcal list, but two strong antapical spines are present, the "wings" of the left spine merge with the sulcal list. In comparison, *Blepharocysta* is equipped with both left and right sulcal lists.

Podolampas is typical of **warmer waters**. Two species have been identified in the present study within quite different temperature and salinity ranges (Fig.22). Their distribution data are presented in Table 26.

Table 25: *Blepharocysta* distribution data.

SPECIES	WOOD (1968)	DODGE (1982, 1993)	BALECH (1988)	CARBONELL-MOORE (1994a)	STEIDINGER & TANGEN (1996)	THIS STUDY
B. paulsenii SCHILLER, 1937 PL.20, Fig.1+2		Atlantic, Mediterranean		neritic to oceanic, in warm temperate to tropical waters		**SST: 18-24°C SSS: 35.9-36.8‰** rare off NW Africa north of 10°N
B. splendor-maris (EHRENBERG) EHRENBERG, 1859	neritic, in temperate to tropical waters	Atlantic, Gulf Stream	**SST: -1.7-20°C SSS: 33.4-36.0‰**	neritic to oceanic, in cold to tropical waters	coastal to oceanic, warm water species	**SST: 21-29°C SSS: 35.0-36.1‰** rare in the equatorial Atlantic south of 15°N

Table 26: *Podolampas* distribution data.

SPECIES	WOOD (1968)	DODGE (1982, 1985, 1993)	BALECH (1988)	CARBONELL-MOORE (1994a)	STEIDINGER & TANGEN (1996)	THIS STUDY
P. bipes STEIN, 1883 Pl.20, Fig.3	tropical, interoceanic species	NE Atlantic, Mediterranean	**SST: 15.5-20°C SSS: 35.7-36.1‰** oceanic	**SST: 10.2-28.6°C SSS: 27.6-37‰** neritic to oceanic, in warm temperate to tropical waters	oceanic, warm temperate to tropical waters	**SST: 18-21°C SSS: 36.0-36.8‰** rare off NW Africa
P. palmipes STEIN, 1883 PL.20, Fig.4	tropical, interoceanic species	warm water species, Atlantic, Pacific	**SST: 2.4-22.8°C SSS: 33.4-36.2‰**	**SST: 2.4-28°C SSS: 33.4-36.7‰** neritic to oceanic, in cold to tropical waters	oceanic, warm temperate to tropical waters	**SST: 18-29°C SSS: 35.0-36.8‰** frequent throughout the investigated region

FAMILY PROTOPERIDINIACEAE
BUJAK & DAVIES, 1983

- **Original diagnosis** (BUJAK & DAVIES, 1983, p.137): "Peridiniinean dinoflagellates with a tabulation of 3-4', 1-3a, 6-7", 3c, 5"', 1-2"", sometimes with transitional cingular-sulcal plate. Cysts when formed have a sporopollenin wall and are acapsulate."

- **Remarks:** Most members of this family belong to the extant genus *Protoperidinium*. FENSOME et al. (1993) considered the Congruentidiaceae SCHILLER, 1935 to be the oldest validly published and legitimate family name for these dinoflagellates.

PROTOPERIDINIUM
BERGH, 1882

- **Description** (WALL & DALE, 1968b; WOOD, 1968; TAYLOR, 1976; ABÉ, 1981; DODGE, 1982; SOURNIA, 1986; BALECH, 1988; FENSOME et al., 1993; STEIDINGER & TANGEN, 1996): Cells small to large, shape is variable, apical and antapical horns or antapical spines may be present. Cingulum more or less equatorial with or without lists, may be displaced, descending or ascending. Typical plate formula: Po, X, 4', 2-3a, 7", (3+t)c, 6s, 5"', 2"". Surface marked with areolae, spines, or poroids. Most species without chloroplasts, **heterotrophic**.

Table 27: *Protoperidinium* distribution data.

SPECIES	WOOD (1968)	DODGE (1982, 1985, 1993, 1994)	BALECH (1988)	STEIDINGER & TANGEN (1996)	THIS STUDY
P. brevipes (PAULSEN) BALECH, 1974	neritic and estuarine, in cold subarctic to tropical waters, Antarctic, North and Baltic Sea, Straits of Florida	neritic, in temperate to tropical waters, E Atlantic, British Isles	**SST: -1.5-16.5°C** **SSS: 33.4-35.6‰** subarctic species	in cold coastal water	**SST: 28-29°C** **SSS: 35.0-35.1‰** rare in the eastern equatorial Atlantic
P. cerasus (PAULSEN) BALECH, 1973	neritic and estuarine, Benguela Current, Brazil (N coast), Caribbean	NE Atlantic, British Isles (North Sea), Caribbean			**SST: 24-28°C** **SSS: 35.5-35.9‰** rare in the equatorial Atlantic south of 12°N
P. crassipes (KOFOID) BALECH, 1974	neritic to estuarine, in all oceans	North Sea	**SST: 14.5-18°C** **SSS: 34.6-36.0‰** neritic and oceanic	coastal to estuarine, in temperate to tropical waters	**SST: 24-27°C** **SSS: 35.5-36.1‰** rare in the equatorial Atlantic
P. curvipes (OSTENFELD) BALECH, 1974	neritic to estuarine, widely distributed	NE Atlantic	**SST: 5.5-8.5°C** **SSS: 33.3-34.2‰** neritic		**SST: 21.7°C** **SSS: 35.9‰** in one sample offshore NW Africa
P. depressum (BAILEY) BALECH, 1974	eurythermal and euryhaline, cosmopolitan	NE Atlantic, North Sea, most common and widespread	**SST: 5.9-19°C** **SSS: 33.6-36.1‰**	estuarine to oceanic, in temperate to tropical waters	**SST: 19-20°C** **SSS: 35.6-35.7‰** rare off NW Africa
P. diabolum (CLEVE) BALECH, 1974	warm water species	Atlantic, Off Brazil, British Isles, Caribbean, Mediterranean			**SST: 19-20°C** **SSS: 35.6-35.7‰** in two samples off NW Africa
P. divergens (EHRENBERG) BALECH, 1974	interoceanic, euryhaline	neritic, NE Atlantic, British Isles, North Sea, most common and widespread	**SST: 11.5-20°C** **SSS: 33.4-36.0‰** in temperate to warm waters	coastal, in temperate to tropical waters	**SST: 18-28°C** **SSS: 35.5-36.8‰** frequent throughout the investigated area
P. elegans (CLEVE) BALECH, 1974			oceanic	coastal to oceanic, in tropical waters	**SST: 27.4°C** **SSS: 35.83‰** in one sample in the equatorial Atlantic

Table 27: *Protoperidinium* distribution data (continued).

SPECIES	WOOD (1968)	DODGE (1982, 1985, 1993, 1994)	BALECH (1988)	STEIDINGER & TANGEN (1996)	THIS STUDY
P. globulus (STEIN) BALECH, 1974	interoceanic, warm water species	Atlantic, Indian O., Mediterranean, Pacific			**SST: 18-28°C** **SSS: 35.7-36.8‰** frequent throughout the prospected region
P. hamatum BALECH, 1979a			**SST: >14.5°C** **SSS: 34.6-36.1‰** oceanic		**SST: 20.1°C** **SSS: 36.03‰** in one sample off NW Africa
P. minutum (KOFOID) LOEBLICH III, 1969	in temperate estuaries and inshore areas, Atlantic, Pacific	in the middle latitudes, Atlantic, British Isles, Pacific, widespread		coastal, in cold temperate to warm waters	**SST: 19-20°C** **SSS: 35.6-35.7‰** rare off Cape Blanc
P. oceanicum (VANHÖFFEN) BALECH, 1974	neritic and oceanic, Caribbean, Straits of Florida	oceanic, in subarctic to tropical waters, Atlantic, Mediterranean, Indian O., most common and widespread	**SST: 3-20°C** **SSS: 33.6-36.1‰** neritic and oceanic, in subarctic to tropical waters	coastal and oceanic, in temperate to tropical waters	**SST: 19-21°C** **SSS: 35.9-36.7‰** rare off NW Africa
P. ovatum POUCHET, 1883	interoceanic, euryhaline, Straits of Florida	Atlantic, British Isles, Indian O., Mediterranean, may occur in high numbers	**SST: 6.5-18°C** **SSS: 33.5-35.5‰**		**SST: 27.5°C** **SSS: 36.07‰** in one sample in the equatorial Atlantic
P. oviforme (DANGEARD) BALECH, 1974			**SST: 13.7-20°C** **SSS: 34.6-36.1‰** neritic		**SST: 18-24°C** **SSS: 35.9-36.8‰** frequent off NW Africa north of 13°N
P. ovum (SCHILLER) BALECH, 1974	in subtropical and tropical waters, Atlantic, Mediterranean, Pacific	E Atlantic	**SST: 7.2-18.1°C**		**SST: 19-20°C** **SSS: 36.6-36.7‰** off Cape Blanc
P. parviventer BALECH, 1978			**SST: 10.6-19°C** **SSS: 34.6-36.1‰** oceanic, in temperate to warm waters		**SST: 18-27°C** **SSS: 35.5-36.8‰** frequent in the eastern equatorial Atlantic and offshore NW Africa

Table 27: *Protoperidinium* distribution data (continued).

SPECIES	WOOD (1968)	DODGE (1982, 1985, 1993, 1994)	BALECH (1988)	STEIDINGER & TANGEN (1996)	THIS STUDY
P. pentagonum (GRAN) BALECH, 1974	neritic to estuarine, widely distributed	neritic, NE Atlantic, British Isles (North Sea), Caribbean	**SST: 9-22°C** **SSS: 33.7-36.1‰** neritic and oceanic,	coastal to estuarine, in temperate to tropical waters	**SST: 26-29°C** **SSS: 35.7-36.3‰** rare in the equatorial Atlantic and off NW Africa
P. punctulatum (PAULSEN) BALECH, 1974		neritic and oceanic, British Isles	**SST: 6.3-18.3°C** **SSS: 32.2-36.1‰** neritic		**SST: 19-20°C** **SSS: 36.6-36.7‰** rare off Cape Blanc
P. quarnerense (SCHRÖDER) BALECH, 1974	interoceanic, warm water species		**SST: 11.3-20°C** **SSS: 33.4-36.1‰**	oceanic, in warm temperate to tropical waters	**SST: 18-22°C** **SSS: 35.9-36.8‰** frequent off NW Africa
P. rectum (KOFOID) BALECH, 1974			**SST: 14.9-18.1°C** **SSS: 34.6-36.1‰** oceanic		**SST: 18-21°C** **SSS: 36.0-36.8‰** frequent off NW Africa
P. simulum (PAULSEN) BALECH, 1974			**SST: 5.5-19°C** **SSS: 33.2-36.1‰** neritic and oceanic, in warm waters		**SST: 20-22°C** **SSS: 36.0-36.8‰** rare off NW Africa
P. steinii (JORGENSEN) BALECH, 1974	warm water species, Atlantic, Pacific	neritic and oceanic, Atlantic, Baltic, Caribbean, Indian O., Pacific			**SST: 21-29°C** **SSS: 35.0-36.1‰** frequent in the eastern equatorial Atlantic south of 15°N
P. subcurvipes (LEBOUR) BALECH, 1974		NE Atlantic, British Isles, off Spitzbergen			**SST: 18-29°C** **SSS: 35.0-36.8‰** frequent throughout the investigated area
P. tenuissimum (KOFOID) BALECH, 1974	oceanic, in tropical waters, Atlantic, Indian O., Pacific				**SST: 21.7°C** **SSS: 35.9‰** in one sample off NW Africa
P. tuba (SCHILLER) BALECH, 1974	Adriatic Sea, Straits of Florida	NE Atlantic			**SST: 21-29°C** **SSS: 35.0-36.1‰** frequent in the equatorial Atlantic south of 18°N

Fig.23: Temperature and Salinity Ranges of *Protoperidinium* Species

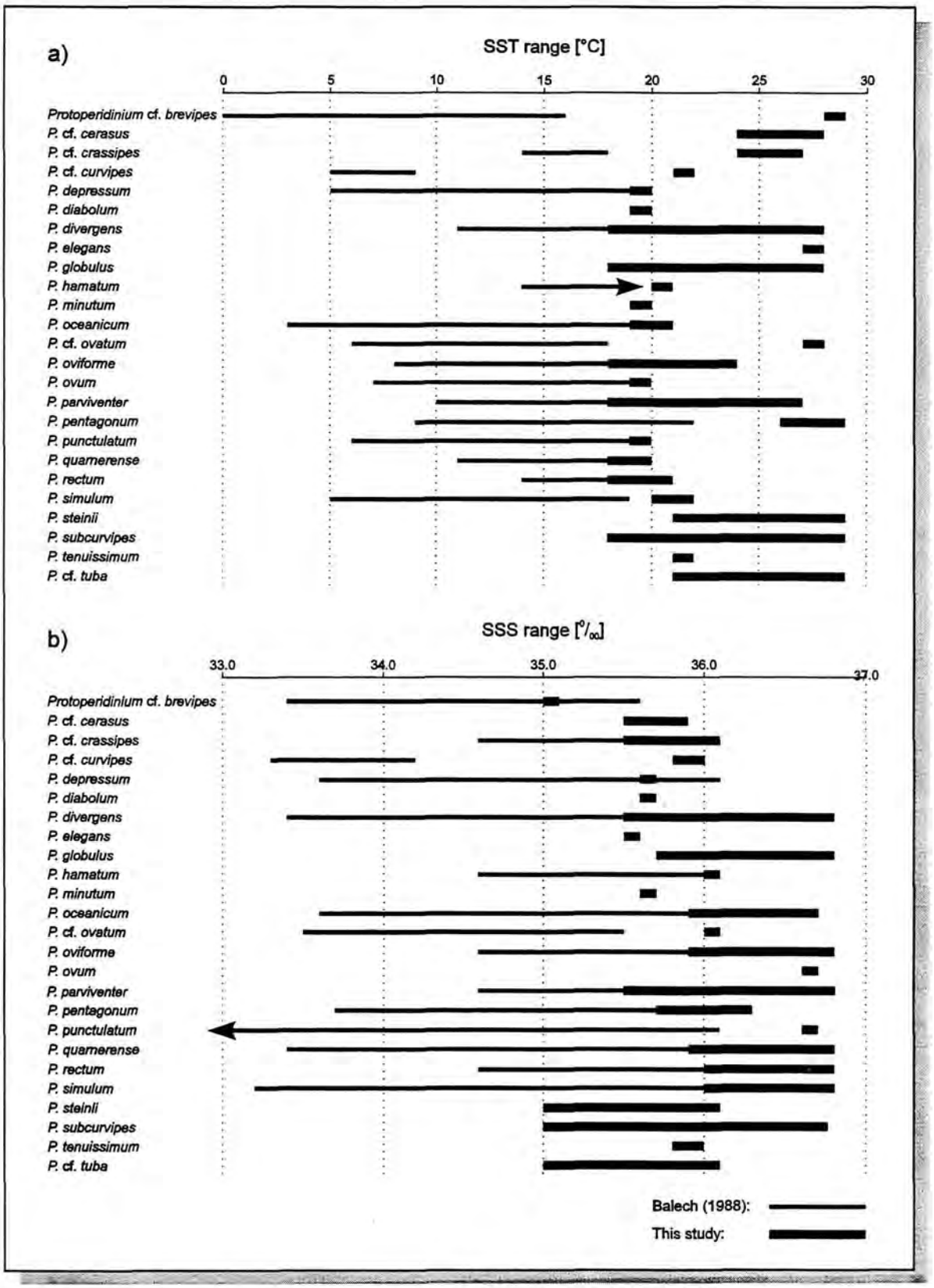

Fig.23: Bar graphs of temperature (a) and salinity (b) ranges of the recorded *Protoperidinium* species.

- **Remarks:** The plate formula are numerous in this genus but well defined for the different species. The morphology of the species is variable: the bodies are rotund to polygonal, often flattened or curved laterally. Epitheca and hypotheca are usually of the same size. The sulcus is generally present on the hypotheca and has lists. There has been much confusion between several *Protoperidinium* species, e.g. *P. curtipes/ crassipes, P. divergens / curtipes / depressum, P. ovatum / quarnerense / globulus / cerasus, P. oviforme / rectum, P. subcurvipes / curvipes*. They are sometimes difficult to distinguish and may differ only in one minor taxonomic characteristic.

Taxonomic characteristics are: cell size and shape, body contour, shape of 1' and 2a, shape and position of plates, cingulum displacement, presence of horns or spines, type of apical pore complex, and ornamentation of thecal plates.

Most species of *Protoperidinium* are non-photo-synthetic and heterotrophic. They are predators and feed on other plankton organisms, e.g. diatoms. Some taxa are known to produce **dinosporin cysts**.

Protoperidinium is a **marine** genus with **world wide distribution**. This genus has the highest species diversity in the prospected area. 25 taxa have been recorded, their temperature and salinity ranges are listed in Fig.18.

4.2.1.1. SPECIES ASSOCIATIONS

The examinations of the plankton samples have revealed 114 species of vegetative-thecate dinoflagellates belonging to 26 genera. These dinoflagellates show a high overall abundance (25%-50% of the shelled phytoplankton) and are considered to play an important role in the tropical Atlantic ecosystem.

- The most widespread species is *Gonyaulax polygramma* which is present in 94% of the samples. *Palaeophalacroma unicinctum* is the second most common species, it has been recorded from 89% of the samples. Three species are present in 78% of the sites, *Gonyaulax turbynei*, *Podolampas palmipes*, and *Prorocentrum balticum*; while one, *G. spinifera*, is recorded in 72% of the samples. *Mesoporos perforatus* has appeared in 67%, and *Dinophysis rotundatum* is present in 61% of the sites. Quite an amount of species have been recorded in 56% of the samples: *Ceratium fusus*, *C. pentagonum*, *Goniodoma polyedricum*, *Micracanthodinium setiferum*, *Oxytoxum laticeps*, *O. scolapax*, *O. stropholatum*, and *Prorocentrum gracile*. 6 species are present in 50% of the sites: *Gonyaulax digitalis*, *G. monospina*, *Oxytoxum crassum*, *Prorocentrum lebourae*, *Protoperidinium divergens*, and *P. globulus*. All these species cover extensive temperature and salinity ranges, some of them have been recorded within the entire temperature and salinity ranges; therefore all but one species are considered to be ubiquitous in the investigated area. The exception is *Oxytoxum crassum* which has exclusively been recorded from the equatorial Atlantic.
- Further 10 species have been recorded from 44% of the sites: *Blepharocysta* cf. *splendor-maris*, *Ceratium tripos*, *Dinophysis pulchella*, *Goniodoma sphaericum*, *Gonyaulax striata*, *Lingulodinium polyedrum*, *Oxytoxum sceptrum*, *O. tesselatum*, *Prorocentrum compressum*, and *P. sphaeroideum*. Within this group, the majority of the species are considered to be ubiquitous as well. There are two exceptions: *Ceratium tripos* and *Goniodoma sphaericum* have mostly been recorded from the waters offshore NW Africa but nevertheless within wide temperature and salinity ranges.
- The following 11 species are present in 30-40% of the samples: *Ceratium azoricum*, *C. declinatum*, *C. karsteni*, *C. lineatum*, *C. minutum*, *C. teres*, *Ceratocorys horrida*, *Dinophysis micropterygia*, *Protoperidinium parviventer*, *P. quarnerense*, *P steinii*, and *Scrippsiella* cf. *trochoidea*; while 16 species have been recorded from 20-30% of the sites: *Ceratium carriense*, *C. furca*, *C. gibberum*, *C.* cf. *horridum*, *Dinophysis caudata*, *D. parva*, *Gonyaulax fragilis*, *Ornithocercus magnificus*, *Oxytoxum ovale*, *Pentapharsodinium* cf. *thyrrhenicum*, *Peridiniella sphaeroidea*, *Prorocentrum rostratum*, *Protoceratium reticulatum*, *Protoperidinium oviforme*, *P. subcurvipes*, and *P.* cf. *tuba*. All these species show distinct distribution patterns. According to their temperature and salinity ranges, these species are considered to be members of the following species associations: Equatorial Atlantic (oligotrophic waters with high SST and low salinity values), off NW Africa (with low SST and high SSS and nutrients), Canary Isles (oligotrophic waters with lowest temperatures and highest salinity values) or ubiquitous (covering wide temperature and salinity ranges).
- 15 species have appeared in 3 samples, that is 17% of the sites: *Blepharocysta* cf. *paulsenii*, *Ceratium candelabrum*, *Dinophysis amphora*, *D. dens*, *D. fortii*, *D. hastata*, *D. parvula*, *Oxytoxum challengeroides*, *O reticulatum*, *Podolampas bipes*, *Prorocentrum micans*, *Protoperidinium oceanicum*, *P. pentagonum*, *P. rectum*, and *P. simulum*. *Dinophysis parvula* may be regarded as ubiquitous within an extended temperature range. The other species are restricted to certain temperature and salinity ranges and are grouped within the corresponding species associations.
- The remaining 37 species have been recorded from less than 2 samples, they are considered to be rare in the investigated area. However, owing to the sampling method and the use of a 250µm mesh sieve, some species, e.g. *Amphisolenia globifera*, have scarcely been found or have not been included at all in the plankton samples.

On the basis of the dinoflagellate distribution patterns presented here, the species may be grouped in relation to their temperature, salinity, and biogeographic ranges. Different species associations (Table 28) are defined for the biogeographic zones of previous authors (TAYLOR, 1987b; DODGE, 1994; DODGE & MARSHALL, 1994; LONGHURST et al., 1995) which have basically been confirmed.

Table 28: On the basis of data presented in this study, vegetative-thecate dinoflagellate species associations are defined for the biogeographic areas.

EQUATORIAL ATLANTIC	OFF NW AFRICA	CANARY ISLES	UBIQUITOUS
Ceratium candelabrum	*Amphidoma nucula*	*Ceratium declinatum*	*Blepharocysta* cf. *splendor-maris*
C. declinatum	*Amphisolenia* cf. *globifera*	*C. extensum*	*Ceratium fusus*
C. gibberum	*Blepharocysta* cf. *paulsenii*	*C. macroceros*	*C. lineatum*
C. cf. *pavillardii*	*Ceratium azoricum*	*Ceratocorys horrida*	*C. karsteni*
C. teres	*C. carriense*	*Dinophysis cuneus*	*C. pentagonum*
Ceratocorys horrida	*C. furca*	*D. ovum*	*Dinophysis parvula*
Dinophysis amphora	*C.* cf. *horridum*	*Ornithocercus magnificus*	*D. pulchella*
D. micropterygia	*C. minutum*		*D. rotundatum*
D. parva	*C. tripos*		*Goniodoma polyedricum*
Ornithocercus magnificus	*Dinophysis caudata*		*Gonyaulax digitalis*
O. steinii	*D. caudata* var. *tripos*		*G.* cf. *fragilis*
Oxytoxum challengeroides	*D. dens*		*G. monospina*
O. crassum	*D. fortii*		*G. polygramma*
O. ovale	*D. hastata*		*G. spinifera*
Parahistioneis acuta	*Goniodoma sphaericum*		*G. striata*
Protoperidinium cf. *brevipes*	*Podolampas bipes*		*G. turbynei*
P. cf. *cerasus*	*Prorocentrum micans*		*Lingulodinium polyedrum*
P. cf. *crassipes*	*P. nanum*		*Mesoporos perforatus*
P. elegans	*P. rostratum*		*Micracanthodinium setiferum*
P. cf. *ovatum*	*Protoperidinium* cf. *curvipes*		*Oxytoxum laticeps*
P. pentagonum	*P. depressum*		*O. reticulatum*
P. cf. *tuba*	*P. diabolum*		*O.* cf. *sceptrum*
Spiraulax jolliffei	*P. hamatum*		*O. scolapax*
	P. minutum		*O. stropholatum*
	P. oceanicum		*O. tesselatum*
	P. oviforme		*Palaeophalacroma unicinctum*
	P. ovum		*Peridiniella sphaeroidea*
	P. cf. *punctulatum*		*Podolampas palmipes*
	P. quarnerense		*Prorocentrum balticum*
	P. rectum		*P. compressum*
	P. simulum		*P. gracile*
	P. tenuissimum		*P. lebourae*
			P. sphaeroideum
			Protoceratium reticulatum
			Protoperidinium divergens
			P. globulus
			P. parviventer
			P. steinii
			P. subcurvipes
			Scrippsiella cf. *trochoidea*

4.2.1.1.1. EQUATORIAL ATLANTIC

The equatorial Atlantic is considered to represent one biogeographic zone and the species association may be interpreted as being characteristic of very warm and less saline waters with relatively low nutrient contents.

The species association of the equatorial Atlantic comprises 23 species, and the following species are considered to be characteristic: ***Ceratium gibberum, C. teres, Dinophysis micropterygia, D. parva, Oxytoxum crassum* (most widespread), *O. ovale,*** and ***Pentapharsodinium* cf. *tyrrhenicum***. These species are probably stenothermal and can tolerate only minor shifts in SST. One exception is *Pentapharsodinium tyrrhenicum*, so far this species has only been recorded in the Mediterranean Sea (MONTRESOR et al., 1993; MONTRESOR et al., 1994; BALECH, 1990) and should be able to endure SST <20°C.

➳

Fig.24: The distribution pattern of selected *Ceratium* species is plotted in the temperature map (a), the salinity map (b), and the productivity map (c).

Fig.24: M23/3 Distribution of Selected *Ceratium* Species

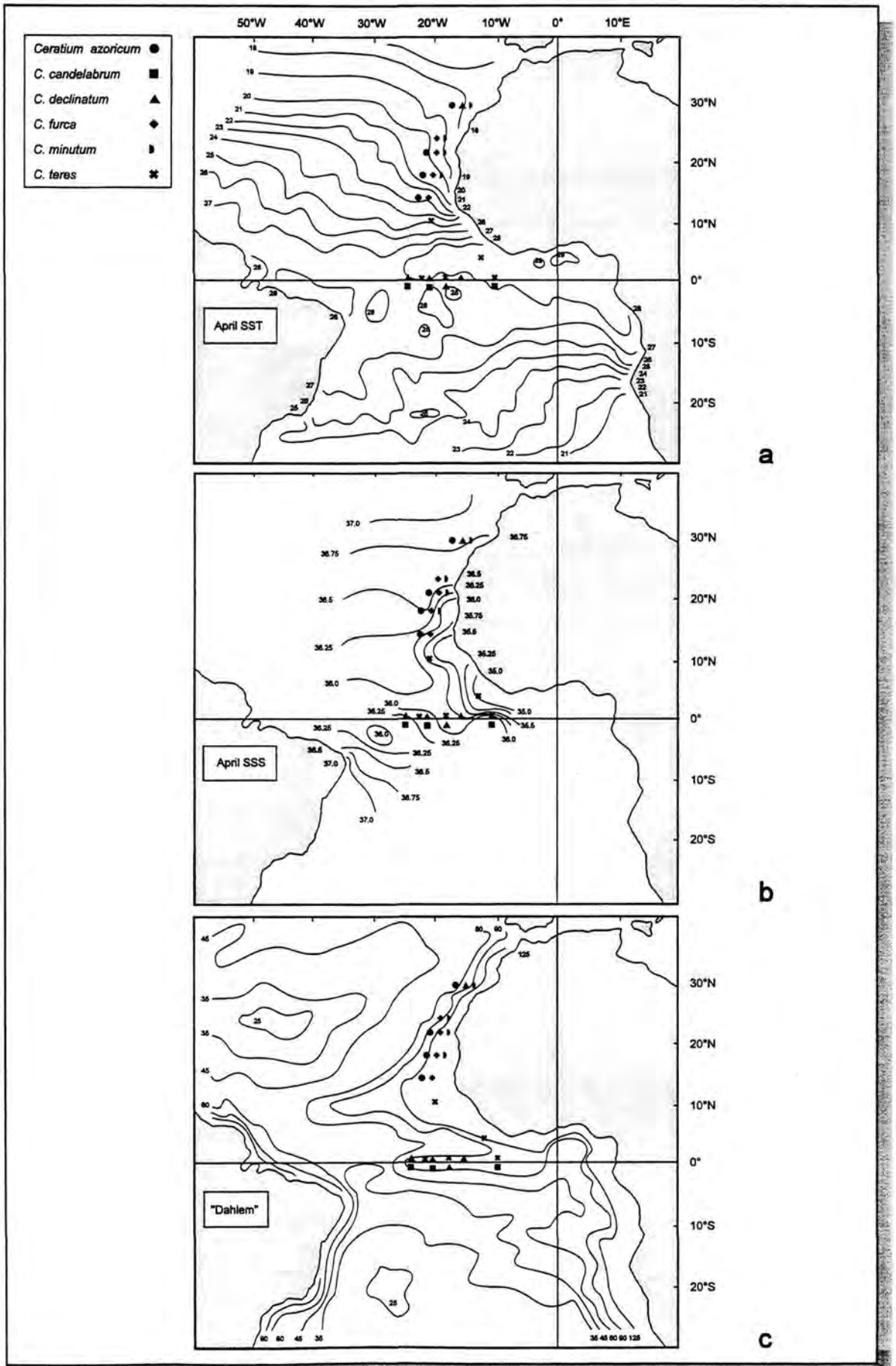

- ***Ceratium*** has, after *Protoperidinium*, the second most species diversity in the investigated region. Several marine species may be used as indicators for distinctive water masses and major ocean currents. In their analysis DODGE & MARSHALL (1994) defined six different groups of *Ceratium* species for four biogeographic zones with the highest species diversity occurring in tropical waters.

  The temperate-tropical species association of DODGE & MARSHALL (1994) consists i.a. of *Ceratium candelabrum*, *C. gibberum*, *C. massiliense*, and *C. teres*.; and the associations of the warm-temperate to tropical group included i.a. *C. declinatum* and *C. trichoceros*. The various temperature ranges of the species were given as MA SST, and the definitions of their biogeographic zones correspond mainly with MA SST isotherms. These definitions could not be fully confirmed within this study. Only *C. candelabrum*, *C. declinatum*, *C. gibberum*, and *C. teres* have been recorded from the very warm waters with low salinity and nutrient contents of the equatorial Atlantic (Fig.24).

- ***Ceratocorys*** species have frequently been recorded from tropical oligotrophic waters. During the current study *Ceratocorys horrida* has frequently been recorded from the equatorial Atlantic and shows more or less the same distribution pattern as ***Ornithocercus magnificus***. Both species are considered to be tropical "oceanic" dinoflagellate species which are relatively independent of temperature and salinity and negatively correlated to the nutrient contents of the investigated waters (see Chapter 4.2.1.2., Fig.25).

- ***Dinophysis*** is a marine genus that is common in neritic and oceanic, tropical and temperate waters throughout the world. This is a mixothrophic genus and the presence or absence of chloroplasts in the different species is considered to be reflected in their distribution patterns. HALLEGRAEFF & LUCAS (1988) categorised photosynthetic, neritic "*Dinophysis*"-species and heterotrophic, oceanic "*Phalacroma*"-species. This distribution pattern could not be confirmed in the present study. According to FENSOME et al. (1993) *Phalacroma* STEIN, 1883 is a taxonomic synonym of *Dinophysis*. Here, the species reported from more oligotrophic waters, from the equatorial Atlantic and from offshore Canary Isles, include both hetero- and autotrophic *Dinophysis* taxa.

- ***Oxytoxum*** is a marine genus and is found predominantly in tropical to subtropical waters. Little is known about the distribution patterns of *Oxytoxum*, besides being a warm water genus. It has no toxic or bioluminescent species and therefore is no primary research objective (DODGE & SAUNDERS, 1985). Three species have exclusively been found in the equatorial Atlantic (*Oxytoxum challengeroides, O. crassum, O. ovale*, Fig.27).

- ***Pentapharsodinium tyrrhenicum*** was, so far, exclusively reported from the Tyrrhenian Sea (BALECH, 1990) and its coastal areas (MONTRESOR et al., 1993; MONTRESOR et al., 1994), where high percentages of its calcareous cysts contributed to a diverse assemblage of calcareous dinocysts.

- ***Protoperidinium*** species are not abundant in the warm oligotrophic waters of the equatorial Atlantic. *Protoperidinium pentagonum* and *P. ovatum* are usually regarded as neritic forms, but may be widespread and sometimes numerous in the E Atlantic (WALL et al., 1977; DODGE, 1994).

4.2.1.1.2. OFF NW AFRICA

The present plankton survey has been carried out east of 21°W longitude in the relatively cool and high salinity waters of the CNRY (LONGHURST et al., 1995). The CNRY is affected by the CC and by substantial coastal upwelling between 15°N and 25°N (TAYLOR, 1987b; MITTELSTAEDT, 1991). Looking at the 32 dinoflagellate species found offshore NW Africa, the distribution pattern seems to be closely related to the local current system, with cool and high salinity waters, and considerable nutrient supply from the upwelling area.

Ceratium tripos and ***Goniodoma sphaericum*** are most widespread offshore NW Africa. These two and the following species are suggested to be characteristic of this area:

Ceratium azoricum, C. furca, C. cf. horridum, C. minutum, Dinophysis caudata

---

➤

Fig.25: The distribution pattern of selected "oceanic" species is plotted in the temperature map (a), the salinity map (b), and the productivity map (c).

Fig.25: M23/3 Distribution of Selected "Oceanic" Species

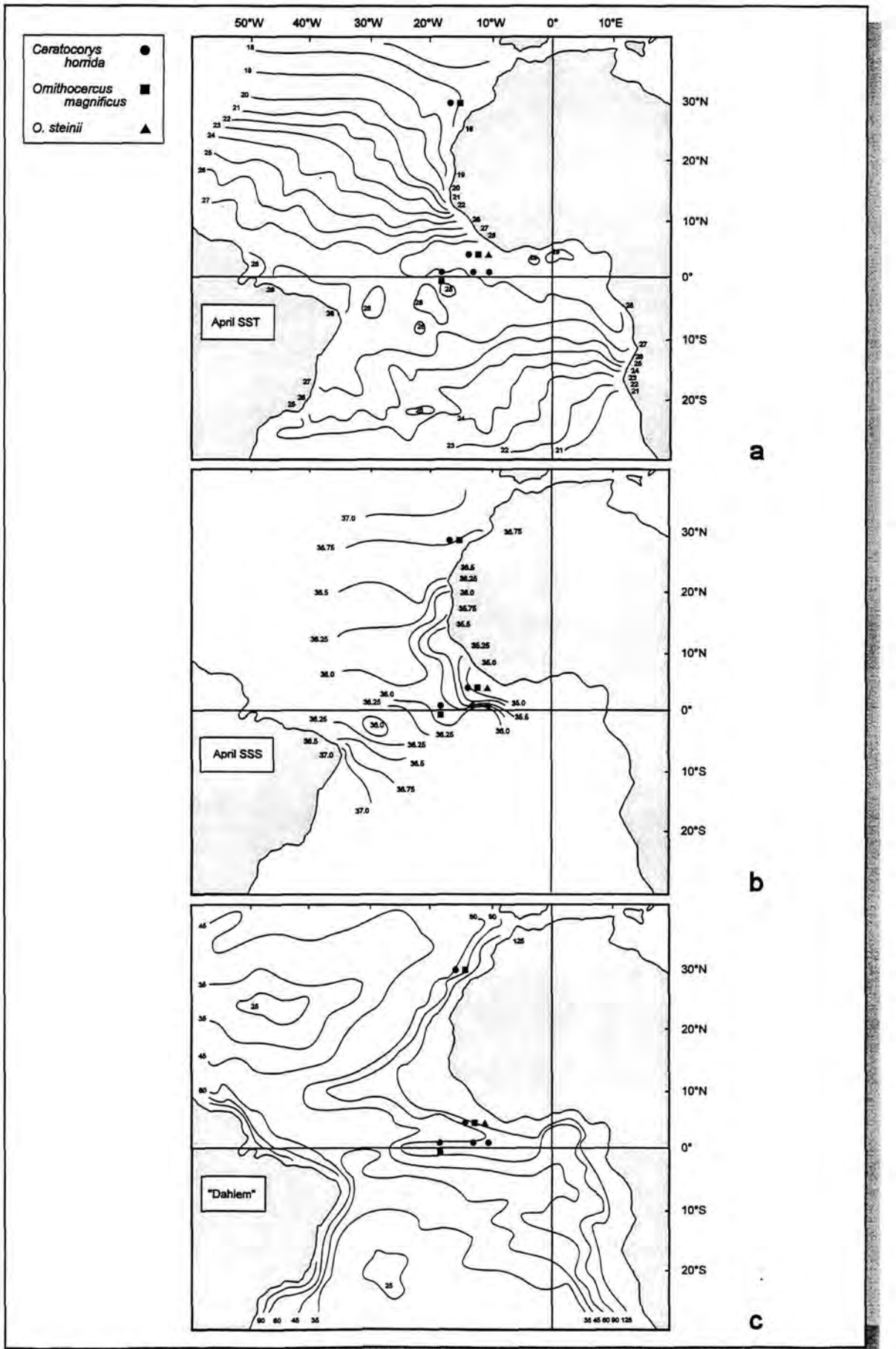

(including *D. caudata* var. *tripos*), *Prorocentrum rostratum*, and ***Protoperidinium oviforme***. 12 other species of *Protoperidinium* have been found in the waters of the CC, but usually only in one or two samples and in small numbers. Some species, e.g. *Ceratium azoricum*, *Prorocentrum rostratum*, *Goniodoma sphaericum*, have been found abundantly. These species very probably can not endure very high temperatures >27°C, even though high salinity and nutrient contents are accepted.

- ***Amphisolenia*** cells are characterized by extremely elongated bodies. Very probably, these very long dinoflagellates (length 100-1,500 µm) are rarely found in the samples owing to the use of a 250 µm mesh sieve for separating the larger zooplankton organisms. Fossils are not known.

- ***Ceratium*** is consistently the most important genus of thecate dinoflagellates in the seas around the British Isles (HOLLIGAN et al., 1980; DODGE, 1989b) where *Ceratium furca*, *C. fusus*, *C. lineatum*, *C. minutum*, and *C. tripos* form a significant part of the phytoplankton. *C. azoricum*, *C. hexacanthum*, *C. minutum*, and *C. lineatum* are considered to be intermediate species (Fig.24) characteristic of waters with moderate temperature (DODGE & MARSHALL, 1994).

  In the plankton samples of this study, specimens of various *Ceratium* species have sometimes been found in great numbers, e.g. cells of *C. azoricum* and *C. furca*. These two species together with *C. carriense*, *C. minutum* and *C. tripos* have exclusively been found off NW Africa.

- ***Dinophysis*** species associations, in the nutrient rich waters off NW Africa, consist exclusively of autotrophic taxa, even though the high food supply causes an increase in species diversity of heterotrophic genera (e.g. *Protoperidinium*). *Dinophysis caudata* and its variant *D. caudata* var. *tripos* tend to be restricted to the area influenced by upwelling. *Dinophysis*-cells are seldom abundant, the exception are seasonal blooms (10^3 to 10^4 cells/litre) of toxic species, e.g. *D. fortii*, which have caused diarrhetic shellfish poisoning in humans (HALLEGRAEFF & LUCAS, 1988). But, these blooms cannot be traced in the dinoflagellate fossil record; *Dinophysis* are not capable of cyst production.

- ***Goniodoma*** planktic distribution patterns confirm the data from BALECH (1988) where *Goniodoma sphaericum* seems to prefer slightly cooler and more saline waters than *G. polyedricum* (Fig.26), even though high nutrient contents are accepted by both species. *G. sphaericum* is commonly regarded as a rare species, which could not be confirmed within this study. Although the distribution of *G. sphaericum* is more or less restricted to the CNRY, specimens have frequently been recorded.

- ***Podolampas bipes*** is one of the most common species of *Podolampas*. CARBONELL-MOORE (1994a) gives the temperature and salinity ranges of previous studies. In this study, *P. bipes* is suggested to be associated with the cool, higher saline, and nutrient rich waters of the CC.

- ***Protoperidinium*** species are usually suggested to prefer similar environmental conditions (DODGE, 1994). In the present study, the majority of species have been found offshore NW Africa in relatively cool and high salinity waters. *P. punctulatum* is mainly considered to be a neritic form, whereas *P. oceanicum* is widespread and sometimes numerous in the E Atlantic (WALL et al., 1977; DODGE, 1994).

  One major factor controlling species diversity and specimen densities of *Protoperidinium*-thecae is food supply. The heterotrophic cells have been observed to be selective grazers, i.a. feeding on diatoms (JACOBSON & ANDERSON, 1986). Offshore NW Africa the diatoms are widespread and abundant, they add up to 38% of the shelled phytoplankton community. In the equatorial Atlantic, the amount of diatoms is generally lower (8-2%, decreasing from the western to the eastern part) and only some *Protoperidinium* species are found in these warm oligotrophic waters.

  Thus, the higher food supply offshore NW Africa may be related to the higher species diversity of *Protoperidinium* (Fig.28).

➤➤

Fig.26: The distribution pattern of selected *Goniodoma* species is plotted in the temperature map (a), the salinity map (b), and the productivity map (c).

Fig.26: M23/3 Distribution of *Goniodoma* Species

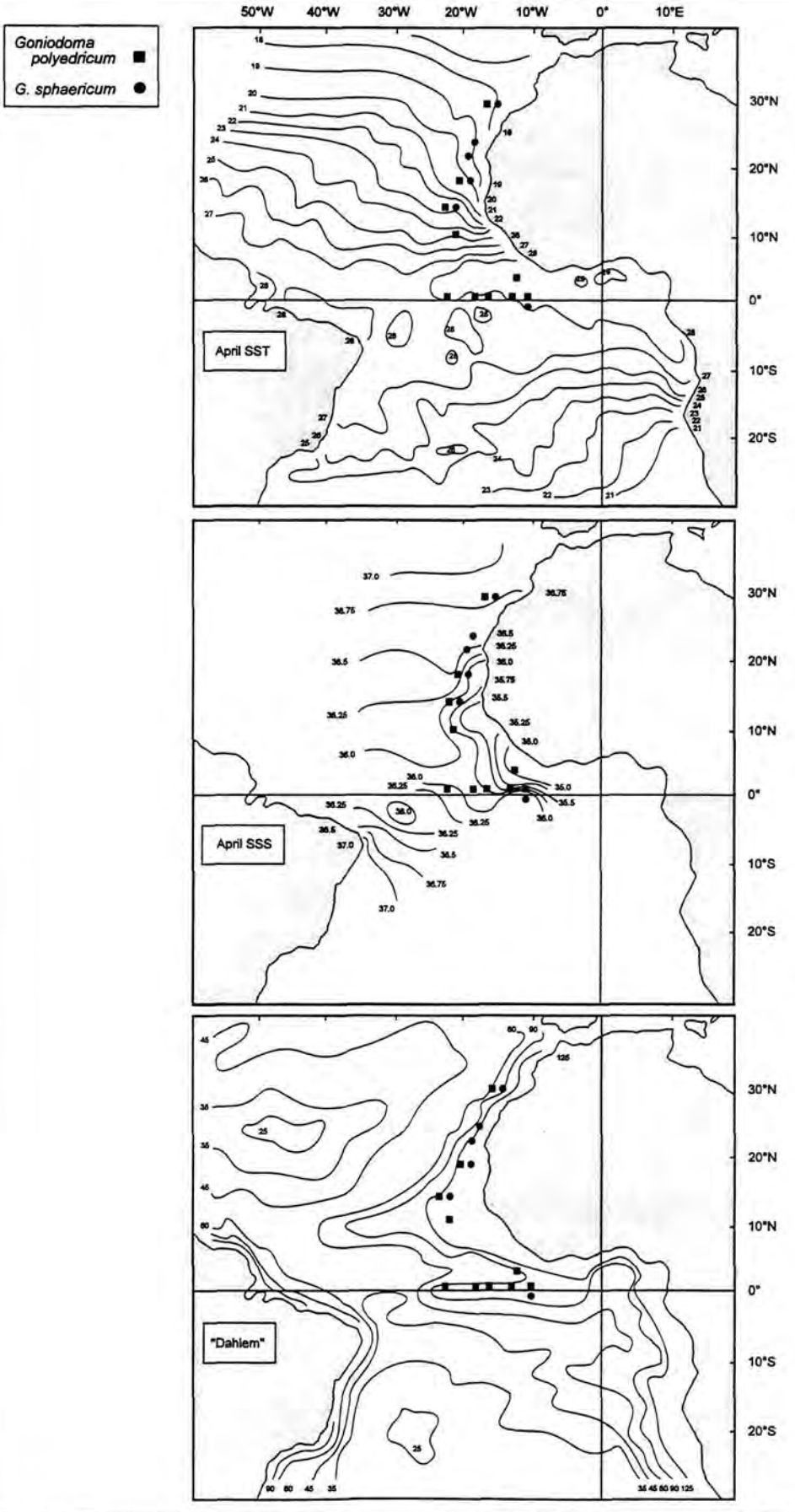

And, the absence of food, linked to very high specimen densities may induce cyst formation. *Protoperidinium* is one major cyst producing genus forming the P-cysts. However, no cysts have been found in the plankton samples, even though cyst production may be related to cool water conditions (DODGE & HARLAND, 1991).

4.2.1.1.3. CANARY ISLES

The NAST is located north of 30°N (LONGHURST et al., 1995). The mid-Atlantic Ridge subdivides this zone into an eastern and a western basin. The ocean sector around the Canary Isles is influenced by the biological properties of the NAST (E) with high SSS, low SST and mesotrophic to oligotrophic waters. Three species (***Ceratium declinatum, Ceratocorys horrida, Ornithocercus magnificus***), which are generally found in very warm equatorial waters, have been recorded in these waters as well. According to the present sea surface currents, no transport from warm water bodies into this area could have happened.

- ***Ceratocorys*** *horrida*-cells normally occur in waters with SST above 19°C (LATZ & LEE, 1995). This study reports their presence in cool waters (18.6°C) offshore the Canary Isles as well (Fig.25). Owing to the present sea surface current system, no transport from warm water bodies into this sector could have happened. Therefore, the Canary Isles may either be regarded as the NE margin of the *C. horrida*-distribution area in the Atlantic Ocean, or the presumed temperature range of LATZ & LEE (1995) is questionable. Suggesting a higher tolerance of SST below 19°C, further surveys will have to establish a more solid basis of *C. horrida* temperature ranges.
- ***Ornithocercus*** *magnificus*, together with ***Ceratocorys*** *horrida*, are suggested to be characteristic species in oligotrophic waters with much wider temperature ranges than generally presumed (Fig.25). DODGE & MARSHALL (1994) described ***Ceratium*** *declinatum* as a warm-temperate to tropical species within a temperature range of 14-28°C but gave no evidence on nutrient requirements. Further studies will have to establish if this is another index species for oligotrophic waters.

4.2.1.1.4. UBIQUITOUS SPECIES

A large amount of species, 40 species, are considered to be ubiquitous in the tropical Atlantic. They are most widespread, most abundant, do not show any restriction to a biogeographic zone, and cover nearly the entire temperature and salinity ranges.

- ***Blepharocysta*** species may be found throughout the upper water column. However, its maximum abundance has been reported from between 100m and 150m water depth (CARBONELL-MOORE, 1994a). *Blepharocysta splendor-maris* is considered to be the most common species of *Blepharocysta* (CARBONELL-MOORE, 1994a).
- ***Ceratium*** is a one of the most widely distributed genera of modern dino-flagellates. It has a notable biogeographical range with species abundant in tropical to polar waters, in neritic and oceanic waters, as well as in freshwater environments. DODGE & MARSHALL (1994) described *Ceratium furca*, *C. fusus*, *C. horridum*, *C. macroceros*, and *C. tripos* as ubiquitous species. However, only *C. fusus*, *C. lineatum*, *C. karsteni*, and *C. pentagonum* have frequently been recorded all over the present study area, and are therefore regarded as ubiquitous in the low to mid latitudinal Atlantic Ocean.
- ***Goniodoma*** is generally regarded as a tropical and oligotrophic genus. *Goniodoma polyedricum* is considered to be eurythermal and euryhaline within the recorded temperature and salinity ranges. It is assumed to be ubiquitous in the tropical Atlantic (Fig.26), i.a. it is abundant in the waters of the CC and the SEC.
- ***Gonyaulax*** is a widely distributed marine genus. *Gonyaulax polygramma* is the most widespread species in the investigated area. Most of the other gonyaulacoids have been reported from more than 44% of the samples and are generally frequent to abundant.

➤➤

Fig.27: The distribution pattern of selected *Oxytoxum* species is plotted in the temperature map (a), the salinity map (b), and the productivity map (c).

Fig.27: M23/3 Distribution of Selected *Oxytoxum* Species

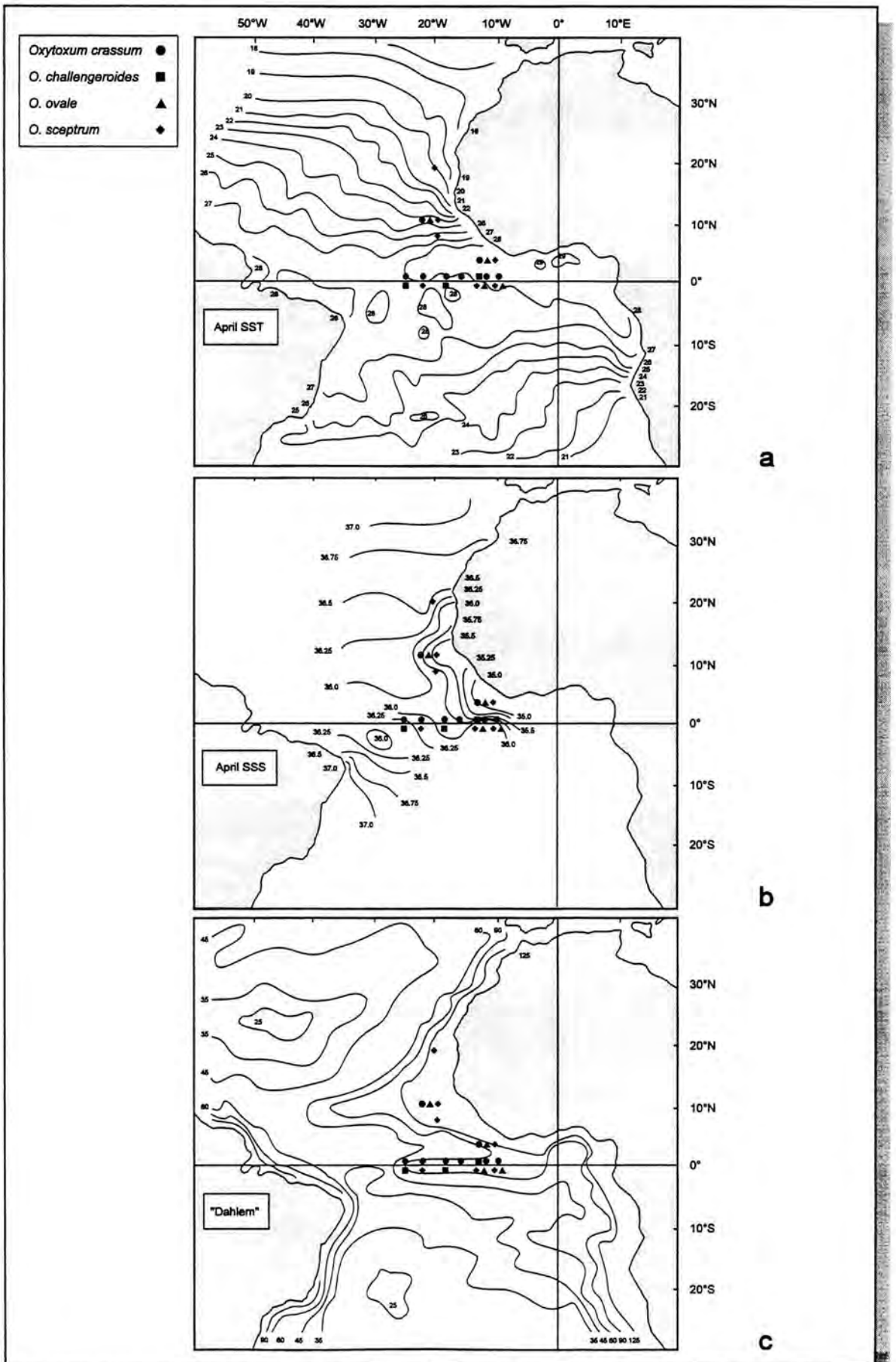

Previously, *G. polygramma* and *G. hyalina* have mainly been recorded from the warmer waters of the North Atlantic Drift (DODGE, 1994). *G. polygramma* is very prevalent, and at times forms high concentrations in the temperate oceanic zone defined by DODGE (1994b). Additionally, BALECH (1988) described *G. polygramma* from the West Atlantic south of 41°S and as common in waters with SST values below 20°C.

Former plankton workers (DODGE & HARLAND, 1991; AMADI et al., 1992; DODGE, 1993, 1994) described *G. digitalis* and *G. spinifera* as fairly common and widespread in the Atlantic north of 20° N, where *G. spinifera* is known to have caused red tides in coastal waters. According to BALECH (1988) they are frequent in the South Atlantic as well; he found *G. spinifera* in waters with SST below 14°C, but *G. digitalis* was abundant throughout his investigated area.

BALECH (1988) described *G. turbynei* as a eurythermal species and *G. striata* as a species of subantarctic waters in the SW Atlantic. In the lower latitudes, DODGE (1994) found these species together with *G. monospina*, but only in small numbers.

Owing to the present study, the tropical Atlantic, with its SST values up to 29°C, may be added to the distribution area of all these *Gonyaulax* species, suggesting a tolerance of higher SST values. They may be regarded as ubiquitous in the entire Atlantic Ocean and largely independent of temperature and salinity. So far, no connection between distribution and nutrient content of the waters could be made. Typical species associations for the different parts of the prospected waters could not be identified.

Only two species (*G.* cf. *hyalina*, *G.* cf. *milneri*) cannot be included in this pattern, either has been found in only one sample, respectively.

- ***Lingulodinium*** *polyedrum* is widely distributed but usually considered to be neritic (BALECH, 1988; DODGE, 1994; STEIDINGER & TANGEN, 1996) even though HARLAND (1983) associated the sedimentary distribution data of its cysts with the SEC, suggesting a great tolerance in temperature and salinity ranges. In this study, *L. polyedrum* is considered a eurythermal, eurysaline species and ubiquitous in the prospected region confirming the temperature and salinity independence of the cysts.

- ***Mesoporos*** *perforatus* has abundantly been recorded in the present study, sometimes in high numbers. Therefore it is regarded as eurythermal and eurysaline as well as ubiquitous in the tropical Atlantic.

- ***Micracanthodinium*** *setiferum* was described by DODGE (1995) as a warm water species in both neritic and oceanic areas with SST above 20°C. This could not be fully confirmed within this study. It has also been recorded in the cool waters (18.6°C) around the Canary Isles.

- ***Oxytoxum*** species have frequently been recorded in the current study (Fig.27), but never as abundantly as e.g. *Prorocentrum lebourae* or *Gonyaulax turbynei*. Species diversity is high in the waters of the equatorial Atlantic and half as high off NW Africa. Five species may be regarded as ubiquitous (*Oxytoxum laticeps, O. reticulatum, O. sceptrum, O. scolapax, O. stropholatum, O. tesselatum*).

- ***Palaeophalacroma*** *unicinctum* is the second most abundant species in the investigated waters, covering the entire SST and SSS range, and it is clearly ubiquitous.

- ***Podolampas*** *palmipes* tolerates large SST and SSS variations with wide temperature (up to 29°C) and salinity ranges (below 36.8‰). It is considered to be ubiquitous in the study area. Other *Podolampas* species, besides *P. bipes*, have not been recorded, very probably owing to a too shallow sampling depth. CARBONELL-MOORE (1994a) reported a maximum abundance of *Podolampas* species between the sea surface and 40m water depth.

- ***Prorocentrum*** is commonly considered to be an all marine genus with a world wide distribution. Most of the reported *Prorocentrum* species seem to be more or less eurythermal and euryhaline, within extensive temperature and salinity ranges.

➤

Fig.28: The distribution pattern of selected *Protoperidinium* species is plotted in the temperature map (a), the salinity map (b), and the productivity map (c).

Fig.28: M23/3 Distribution of Selected *Protoperidinium* Species

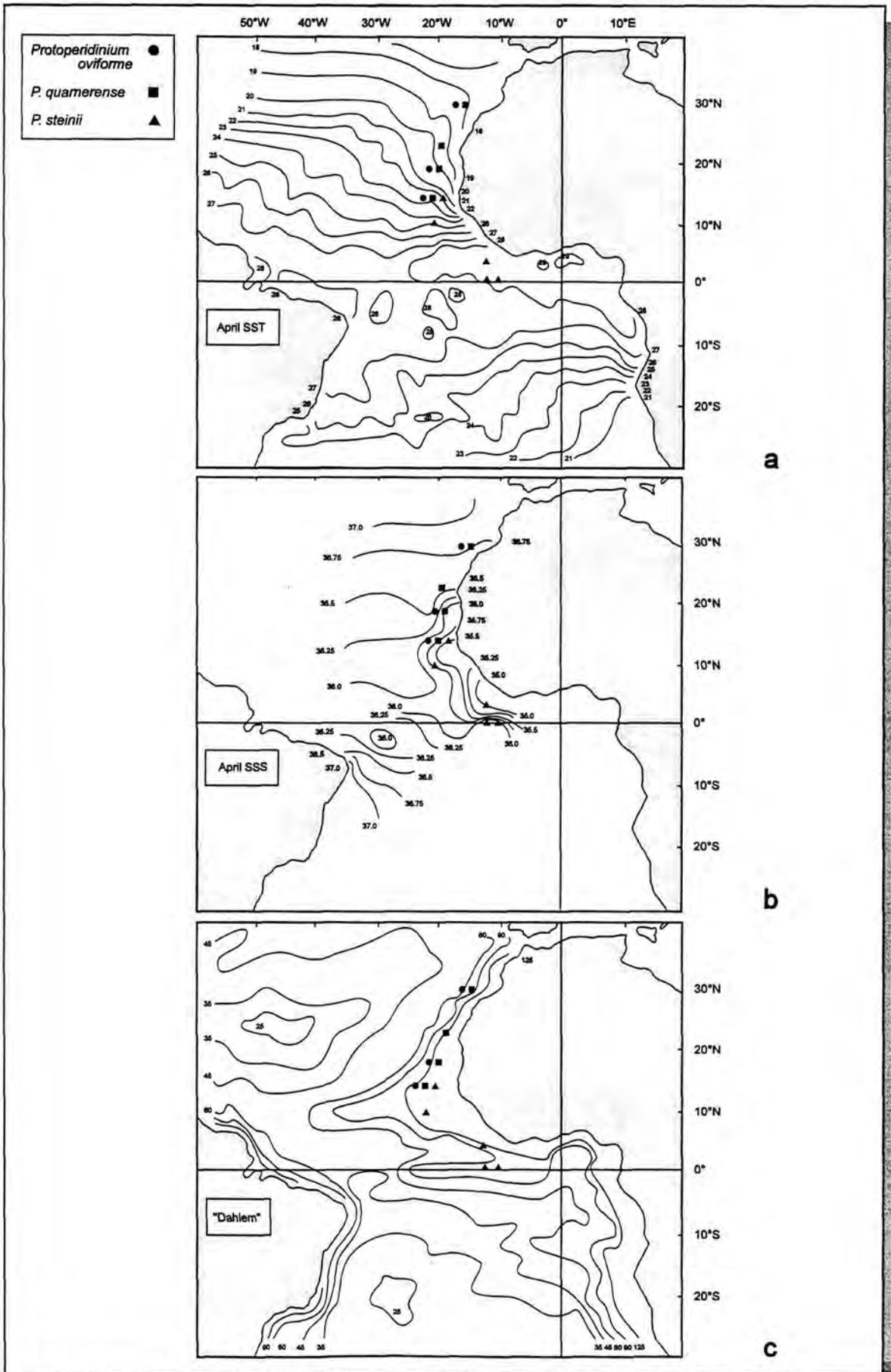

They are, therefore, considered to be ubiquitous in the tropical Atlantic, even though the relative specimen densities of the different taxa are variable. Three species have been found exclusively offshore NW Africa and very probably they tolerate only relatively low temperatures, even though high salinity and nutrient contents are accepted. Here, *Prorocentrum rostratum* has been recorded abundantly and may be regarded as an index species of the CC.

- ***Protoceratium*** *reticulatum* and its cysts are usually considered to have a widespread distribution (DODGE, 1994). BALECH (1988) associated this species with low salinity waters. In neritic situations they may be present in high numbers and have been the cause of red water blooms offshore Africa (REINECKE, 1967). In this study, *P. reticulatum*-cells have only been rarely found

- ***Protoperidinium*** cf. *ovatum* has been reported in small numbers from one sample of the equatorial Atlantic. *P. pentagonum* is a rare species in the equatorial Atlantic south of 10°N. *P. depressum*, *P. oceanicum*, and *P.* cf. *punctulatum* have been found only in one sample offshore NW Africa. A lateral transport by local currents from coastal waters into the oceanic sample area may be probable, and their main distribution areas may be located in a more inshore or higher latitudinal area. Of the above mentioned species, only *P. divergens* has been found repeatedly and in considerable numbers in the prospected area. *P. divergens* is widespread and sometimes numerous in the E Atlantic (DODGE, 1994) and may be regarded as ubiquitous in the lower and in the higher latitudinal Atlantic.
  So far, information about the distribution of *P. parviventer* was given by BALECH (1988) who described this species from offshore Brazil, Uruguay, and Argentine and as living in more temperate waters (11-19°C). According to the data of this study *P. parviventer* can tolerate much higher SST (up to 27°C). The distribution area can be spread well beyond the equator and up north to the Canary Isles, and therefore, it is regarded as being ubiquitous, at least in the tropical Atlantic.

- ***Scrippsiella*** is an autotrophic and marine genus covering wide temperature and salinity ranges. Previous plankton workers described *Scrippsiella trochoidea* as being a neritic species and abundant in the middle latitudes (i.a. WALL & DALE, 1968a,b; DODGE, 1982), it was seldom reported from oceanic waters. Only recently thecae and cysts of *S. trochoidea* have been recorded in considerable numbers from tropical oligotrophic waters of the Atlantic and Pacific Ocean (DALE & DALE, 1992).

  In the plankton samples of the current study, *Scrippsiella*-like thecae have been observed frequently, sometimes being abundant. Identification has not been possible, the thecae with their thin and delicate plates were mostly shrunken and had collapsed on the filters. Nevertheless, on various filters thecae resembling *S. trochoidea*-thecae have been found, sometimes together with the calcareous cysts *Rhabdothorax erinaceus*. The presence of thecae and cysts could not be associated with any specific temperature or salinity range (Fig.36, Fig.37). A negative correlation to nutrient contents as suggested by Fig.37c would contradict any previously achieved data on the abundance in coastal waters. Therefore, *S. trochoidea* is suggested to be a ubiquitous species in the low and middle latitudinal Atlantic Ocean.

Water currents play an important role in the distribution of dinoflagellates (DALE & DALE, 1992). From the shelf or coastal environment, dinoflagellate species with a more neritic character may be transported offshore into oceanic waters. In the East Atlantic, the Coriolis force and the prevailing trade winds cause winds blowing alongshore and offshore which drive the coastal surface water offshore and causes the inshore upwelling of cool and nutrient-rich subsurface water. The CC then transports the water masses towards the south-west feeding into the NEC and into the equatorial current system. But the dinoflagellates will not survive for long when transported into areas where they cannot divide. Therefore, some distinctive distribution patterns will be maintained in spite of the constant movement of surface waters that might otherwise result in a general mixing of the species (DODGE & MARSHALL, 1994). Some vegetative-thecate dinoflagellate species may be excellent biomarkers for distinctive surface water masses.

Fig.29: Thecate Dinoflagellate Nutritional Modes

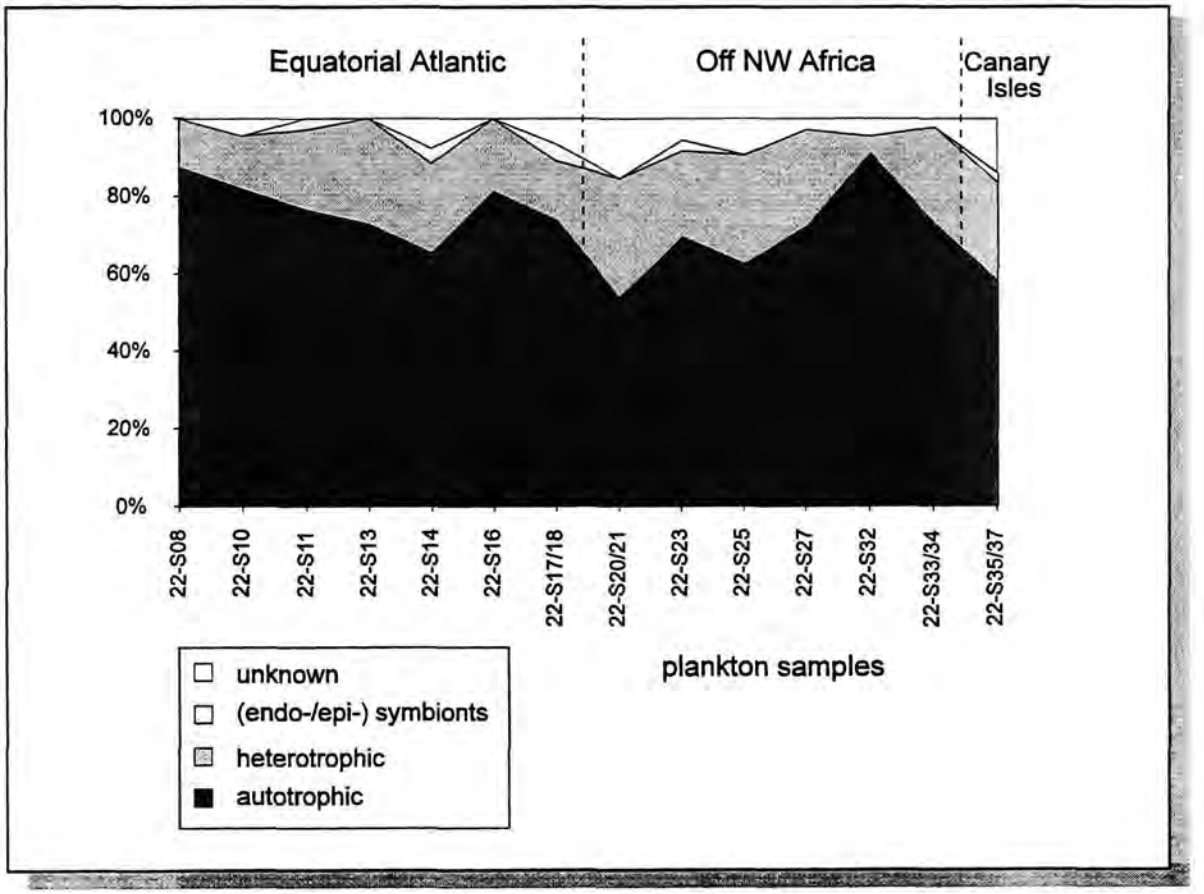

Fig. 29: The relative amount of the nutritional types is plotted as a cumulative curve for thecate dinoflagellate species.

4.2.1.2. NUTRITION

Dinoflagellates vary greatly in their nutrition. They can be regarded either as plants or as animals according to their modes of nutrition; they possess both photosynthetic and non-photosynthetic members. According to GAINES & ELBRÄCHTER (1987) approximately half of the known species of vegetative dinoflagellates are autotrophs which use only inorganic compounds for metabolism, growth and reproduction (for photosynthesis); the other half is considered to be heterotrophs which use organic compounds for growth or increased survival.

Most vegetative-thecate species are equipped with chloroplasts and are therefore considered to be autotrophs (TAYLOR, 1987; STEIDINGER & TANGEN, 1996). In this study, species are classified as **autotrophic**, as **heterotrophic**, and as **symbiotic** (LESSARD & SWIFT, 1986; BALECH, 1988; HALLEGRAEFF & LUCAS, 1988; GORDON *et al.*, 1994). The number of species for the modes of nutrition and their relations are plotted in Fig.29.

4.2.1.2.1. AUTOTROPHIC SPECIES

Autotrophic dinoflagellates have a unique photosynthetic pigment system, which gives them a golden-brown colour. In addition to chlorophyll *a* and c_2, they usually have the xanthophyll peridinin as their major light harvesting carotenoid (PRÉZELIN, 1987). Other plastid pigments are ß-carotene and small amounts of diadinoxanthin, diatoxanthin, and dinoxanthin (FENSOME et al., 1993). The major food storage product is typically starch, together with unsaturated fatty acids in small lipid droplets.

In the present study, nearly all of the most abundant species of vegetative-thecate dinoflagellates are autotrophs. Here, they are most numerous in species and dominate the plankton samples. The non-thecate, naked dinoflagellates of the order Gymnodiniales have not been included in this study. They are generally considered to be heterotrophic and would have changed the situation completely.

The autotrophic taxa amount to **55-90%** of the assemblages throughout the investigated area. These include the gonyaulacoid species and the well-represented *Ceratium* taxa, species of *Goniodoma*, *Oxytoxum*, *Pentapharsodinium*, *Prorocentrum*, and *Scrippsiella*, as well as some *Dinophysis* taxa (see Appendix A). The relative amount of autotrophic species is high in the western part of the equatorial Atlantic (75-90%). Nevertheless, the number of photosynthetic taxa is higher in the east-equatorial Atlantic (34-17 species) than in the west (16-26 species). Their proportional amount in the dinoflagellate association offshore NW Africa rises with the latitudes from 55% in the south to 90% in the area influenced by upwelling , and then gradually decreases to the north and the Canary Isles. The numbers of taxa increase from only 7 to 32 in the north. The autotrophic species (25) amount to approx. 60% at the Canary Isles.

The autotrophic genus *Ceratium* forms an important component of the phytoplankton, and blooms may occur at minimal nutrient levels of the surrounding water masses (DODGE & MARSHALL, 1994). In the present study, this genus has the highest species diversity of the autotrophs. Occasionally, specimens of this genus were recorded in high numbers.

4.2.1.2.2. HETEROTROPHIC SPECIES

The proportional amount of heterotrophic species in the plankton samples is generally less, only **4-30%**, and includes mainly *Protoperidinium* and a few *Dinophysis* species. In the equatorial Atlantic, the numbers of heterotrophic taxa vary between 3 and 7 increasing to the east; they amount to 7-30%. Off NW Africa, the amount stays more or less the same, and the number of taxa successively rises with the latitudes from 4 to 11. Sample 22-S32 may be regarded as the exception of the rule. This pattern may be followed north to the Canary Isles.

Most heterotrophic dinoflagellates lack chlorophyll (LESSARD & SWIFT, 1986). Occasionally, a food object containing chlorophyll can be seen inside a heterotrophic dinoflagellate. The feeding mechanisms, preferences, and rates of heterotrophic dinoflagellates are not well known. Most graze on other phytoplankton organisms or on bacteria. The genus *Dinophysis* includes both autotrophic and heterotrophic species; the heterotrophic taxa feed on a multitude of organisms. Specimens were recorded to contain algal cells, bacteria, or tintinnid remains (HALLEGRAEFF & LUCAS, 1988; HANSEN, 1991). *Podolampas palmipes* is known to be a heterotrophic species and has been observed to contain chlorophyll food objects. On the other hand, *Podolampas bipes* has either been reported totally lacking chlorophyll or filled with spherical chlorophyll bodies, it still has to be determined whether these were food objects or not (LESSARD & SWIFT, 1986). In the nutrient rich waters off NW Africa, the high food supply may cause an increase in species diversity of the heterotrophic genus *Protoperidinium*. These predators feed almost exclusively on diatoms, sometimes much larger than themselves, by means of a pseudopodal mechanism (JACOBSON & ANDERSON, 1986).

4.2.1.2.3. SYMBIOTIC SPECIES

A small number of species in the plankton samples are reported to have epi- or endosymbionts, they amount to only a few percent (**max. 3%**).

Ornithocercus and *Parahistioneis* are usually considered to be genera of tropical waters. They are primarily heterotrophic dinoflagellates devoid of photosynthetic pigments, but often host clusters of cyanobacteria. These symbiotic genera are characteristic of tropical and subtropical oceanic waters that coincide with nitrogen limitations (GORDON et al., 1994).

In the investigated area, distribution patterns of *Ornithocercus magnificus*, *O. steinii*, and *Parahistioneis acuta*, together with *Ceratocorys horrida*, are independent of temperature and salinity. But their presence in the oligotrophic waters of the equatorial Atlantic and the Canary Isles, and the corresponding absence in the nutrient rich waters offshore NW Africa, suggest a negative correlation to nutrient supply. In the tropical Atlantic, they may be regarded as tropical and "oceanic" species and may be used as indicator species for oligotrophic conditions in surface waters (Fig.25).

Table 29: A list of the planktic vegetative-thecate dinoflagellate species capable of cyst production and the names of the respective cyst species.

VEGETATIVE-THECATE STAGE	Cysts recorded	CYST STAGE
a) CALCIODINELLACEAE:		
Pentapharsodinium tyrrhenicum BALECH, 1990	-	Calcareous cysts
Scrippsiella trochoidea (STEIN) LOEBLICH III, 1976	+	***Rhabdothorax erinaceus*** KAMPTNER, 1937
b) GONYAULACACEAE:		
Gonyaulax digitalis (POUCHET) KOFOID, 1911	-	***Spiniferites bentori*** (ROSSIGNOL) WALL & DALE, 1970
Gonyaulax spinifera (CLAPARÈDE & LACHMANN) DIESING, 1866	-	***Gonyaulax spinifera*-cysts group**
Lingulodinium polyedrum (STEIN) DODGE, 1989	-	***Lingulodinium machaerophorum*** (DEFLANDRE & COOKSON) WALL, 1967
Protoceratium reticulatum (CLAPARÈDE & LACHMAN) BÜTSCHLI, 1885	-	***Operculodinium centrocarpum*** (DEFLANDRE & COOKSON) WALL, 1967
c) PROTOPERIDINIACEAE:		
Protoperidinium divergens (EHRENBERG) BALECH, 1974	-	***Peridinium ponticum*** WALL & DALE, 1973
P. minutum (KOFOID) LOEBLICH III, 1969	-	Dinosporin cysts
P. oceanicum (VANHÖFFEN) BALECH, 1974	-	Dinosporin cysts
P. pentagonum (GRAN) BALECH, 1974	-	***Trinovantedinium capitatum*** REID, 1977
P. punctulatum (PAULSEN) BALECH, 1974	-	***Brigantedinium* sp.** ("round-brown" cysts)

4.2.1.3. CYST PRODUCTION CAPABILITY

Of the recorded vegetative-thecate dinoflagellate species, only 11 species, which is **9.65%** of all recorded thecate species, are able to produce cysts (Appendix A). Two species of the family Calciodinellaceae, four species of the family Gonyaulacaceae, and five species of the family Peridiniaceae are capable of cyst formation.

So far, the majority of species are not known to produce cysts and are therefore not included in the dinoflagellate fossil record. Despite this, their cells have frequently been found throughout the prospected region sometimes accounting for quite an amount of the total thecate dinoflagellates, e.g. plankton samples 22-S08 and 22-S10 caught a *Prorocentrum lebourae*-"bloom" with its thecae accounting for 30% of the thecate dinoflagellates.

These numbers confirm the data of previous studies (DALE, 1976, 1983; DODGE & HARLAND, 1991; DALE & DALE, 1992). The dinoflagellate cyst assemblage in the fully marine open ocean of the tropical Atlantic is overwhelmingly dominated by calcareous forms, with dinosporin cysts adding a negligible part. Dinosporin cysts have not been recorded. The relative amount of calcareous cysts is 100% of the whole planktic dinocyst assemblage.

During the present survey, calcareous cysts have been found abundantly in the plankton.

Two vegetative-thecate peridinioid dinoflagellate species have been observed that are known to form calcareous cysts: *Pentapharsodinium* cf. *tyrrhenicum* and *Scrippsiella* cf. *trochoidea* (WALL & DALE, 1968,b; FÜTTERER, 1977; MONTRESOR et al., 1993). Here, the cysts of *S. trochoidea* have been recorded in several plankton samples. The cyst was previously described as *Rhabdothorax erinaceus* (KAMPTNER, 1937, 1958).

Two other species of calcareous cysts ("*Sphaerodinella*" *albatrosiana*, "*Sph.*" *tuberosa*) have frequently to abundantly been found in the equatorial Atlantic. The corresponding vegetative stages have recently been identified in clonal cultures as belonging to the genus *Scrippsiella* (MONTRESOR et al., 1997; JANOFSKE, pers. comm.). Another recorded calcareous cyst species, *Orthopithonella granifera*, has been recorded throughout the prospected region of the tropical Atlantic. Its cyst-theca relationship is still unknown.

4.2.2. VEGETATIVE-COCCOID DINOFLAGELLATES

CLASS DINOPHYCEAE
PASCHER, 1914

ORDER THORACOSPHAERALES
TANGEN in TANGEN et al. (1982)

- **Original diagnosis** (TANGEN et al., 1982, p.210): "Marine planktic dinophytes, autotrophic; predominant stage during vegetative life phase coccoid. Coccoid cell spherical, cell wall composed of calcium carbonate elements. Asexual reproduction by formation of aplanospores or planospores or by binary fission of a weakly calcified cell. Spores unarmoured; planospores biflagellate, with transverse and longitudinal grooves. Nucleus spherical, in all life stages with continually condensed chromosomes."

FAMILY THORACOSPHAERACEAE
SCHILLER, 1930
emend. TANGEN in TANGEN et al. (1982)

- **Original description** (TANGEN et al., 1982, p.210): "Coccoid cell small, calcareous cell wall continuous, spherical, outer surface granular. An aperture in the cell wall formed in connection with spore formation. Calcareous shell formed after gradual growth of numerous crystals near the cell surface. Planospores with undulating transverse flagellum and whiplike longitudinal flagellum, coccoid cells, planospores and aplanospores with chloroplasts."

THORACOSPHAERA
KAMPTNER, 1927

- **Original diagnosis** (KAMPTNER, 1927, p.180-181): "Testa sphaeroidea, diametro 10-20 µ. Vertex flagelliferus pro maxima parte speciminum sine coccolithis. Coccolithi diametro 1-2 µ, alti 1-2 µ, dense cohaerentes sine ullis interstitiis, lateribus invicem polygonaliter applanatis, foramine centrali."

-**Type species:** *Thoracosphaera heimii* (LOHMANN) KAMPTNER, 1944

Thoracosphaera heimii
(LOHMANN) KAMPTNER, 1944

(Pl.20, Fig.5-8; Pl.21, Fig.1-8)

- **Description** (KAMPTNER, 1927, 1944, 1967; FÜTTERER, 1976, 1977; TANGEN et al., 1982; INOUYE & PIENAAR, 1983; SOURNIA, 1986; STEIDINGER & TANGEN, 1996): Cells spherical with calcitic shell wall approximately 1-1.5 µm thick, shell diameter ~10-18 µm (considerable size variations: 9-27 µm). Outer shell surface shows small polygonal, granular crystallites of various numbers forming an irregular "rosette" around +/- rectangular central pseudo-pore. Empty shells with sub-circular aperture 3-7 µm wide with irregularly serrated margin, some shells have no discernible aperture.

- **Stratigraphic range:** ?Triassic (JAFAR, 1979) to Recent.

DISCUSSION:

- **Planktic specimens** (Pl.20, Fig.5-8): Shells lacking an aperture are considered to be shells with cell content. LM examinations of embedded plankton filters show "clear" specimens with no visible cell content. The appearances of calcareous shells were consistent with the descriptions of KAMPTNER (1927, 1967). All life stages are equipped with chloroplasts (TANGEN et al., 1982).

Living cells in the plankton samples as seen with the SEM are covered with a continuous outer organic phragma forming a "skin" on the calcareous shell surface and obscuring the arrangement of crystals (Pl.20, Fig.6-7). This and various stages of calcification of the shell lead to several morphological varieties of the same species. Empty shells are quite rare in the water column, but when present, the inner shell surface is covered by an inner organic phragma as well. The calcite deposition is considered to occur in the space between the inner and the outer shell phragma (INOUYE & PIENAAR, 1983). The polygonal calcite crystals are loosely compacted aggregates embedded in an organic matrix (TANGEN et al., 1982). One specimen without an outer organic phragma shows tiny crystallites which are arranged around square pseudo-pores (Pl.20, Fig.8). The crystallites get smaller to the periphery of the "rosettes" and do not merge laterally with neighbouring "rosettes". This may be interpreted either as an early stage of calcification or the onset of solution affecting the shell of a dead organism or an empty shell. Mature cells are suggested to have a rigid, continuous shell.

- **Ultrastructure** (Pl.21, Fig.1-8): The skeletal elements on the distal shell surface are composed of many "blocky" crystallites. They are arranged around a rectangular "pore-like" structure (Pl.21, Fig.2, 4). FÜTTERER (1977) suggested that, between the outer and inner shell surface, the poroids branch into tiny, probably irregular, conduits to build the pseudo-pores on the outer surface. A cross section of the shell wall shows that it is composed of "spongious" crystals and is not perforated by the "pores" (Pl.21, Fig.8).

Fig.30: M23/3 *Thoracosphaera heimii* Temperature and Salinity Ranges

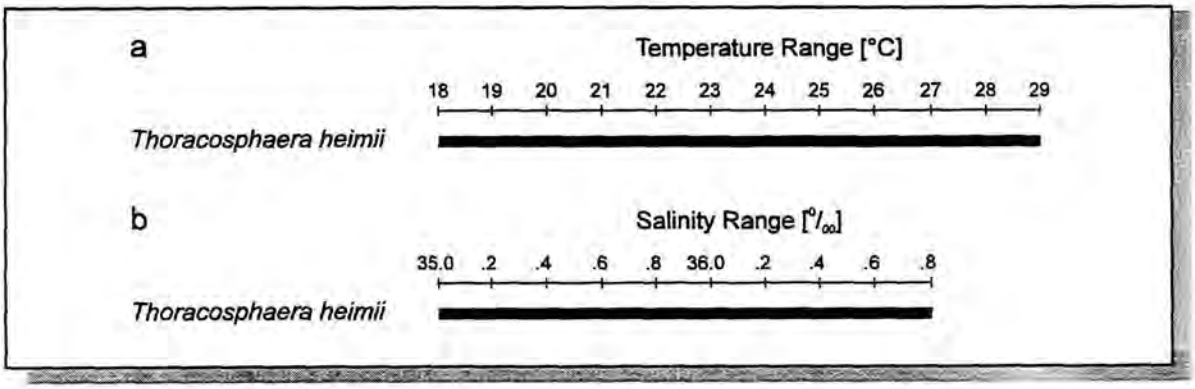

Fig. 30: Bar graphs of temperature (a) and salinity (b) ranges of *Thoracosphaera heimii*.

Table 30: *Thoracosphaera heimii* distribution data.

A Recent distribution in the plankton

SPECIES	TANGEN et al. (1982)	INOUYE & PIENAAR (1983)	DALE & DALE (1992)	STEIDINGER & TANGEN (1996)	THIS STUDY
Th. heimii (LOHMANN) KAMPTNER, 1944	in temperate to tropical waters, cosmopolitan	offshore SW Africa	Sediment trap data: **Söhm Abyssal Plain:** **MA SST: 22°C** **MA SSS: 36.5°/oo** low flux rates: ?313-?768 spec. m²/day (Thoracosphaerida)	oceanic, in temperate to tropical waters, widely distributed	**SST: 18-29°C** **SSS: 35.0-36.8°/oo** abundant throughout the investigated area, 2-12% of the shelled phytoplankton, max. at Canary Isles

B Sub-Recent distribution in the sediments

SPECIES	KAMPTNER (1927, 1967)	FÜTTERER (1976, 1977)	KARWATH (1995)	THIS STUDY
Th. heimii (LOHMANN) KAMPTNER, 1944	**S Atlantic** **Mid Atlantic Ridge:** **MA SST: 22-23°C** **MA SSS: ~36.5°/oo** in temperate to tropical waters, worldwide distribution	most abundant in low latitude sediments of the eastern N Atlantic	**Offshore Recife, Brazil:** **MA SST: 26°C** **MA SSS: 36.0-36.5°/oo** GeoB 2204-2: 68% = 1,911,000 spec./g	**Off Cape Blanc:** **MA SST: 21°C** **MA SSS: 36.0-36.5°/oo** GeoB 1602-7: 85% = 1,472 spec./cm² **Guinea Basin:** **MA SST: 26-27°C** **MA SSS: 34.5-35.0°/oo** GeoB 1606-7: 18% = 625 spec./cm² GeoB 1607-8: 31% = 862 spec./cm²

Fig.31: The distribution pattern of *Thoracosphaera heimii* is plotted in the temperature map (a), the salinity map (b), and the productivity map (c).

Fig.31: M23/3 Distribution of *Thoracosphaera heimii*

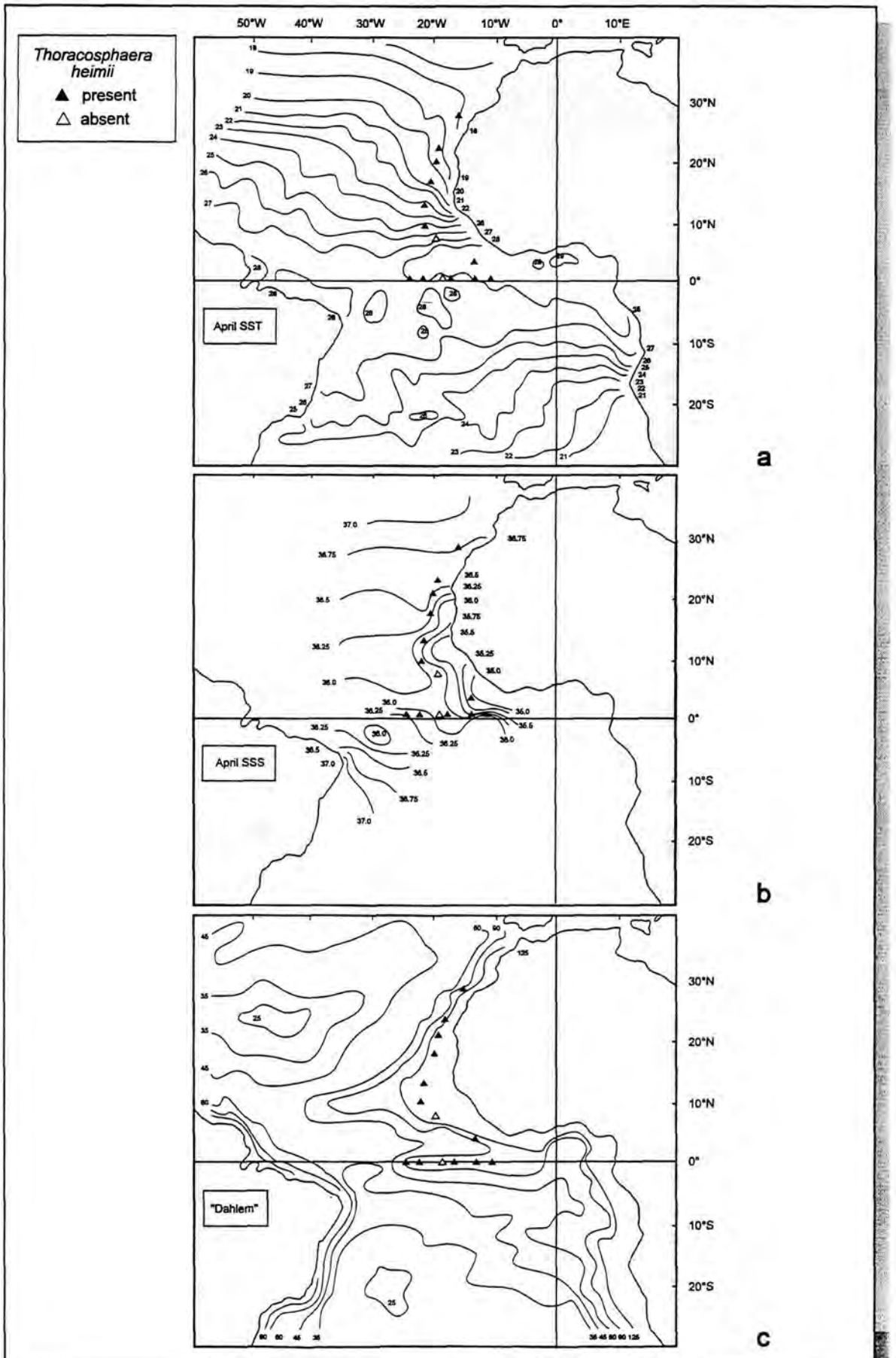

The proximal shell base is smooth with vermiculate-like crystal surfaces and poroids (Pl.21, Fig.8). Disintegrated shells which are split and spread out show polygonal fragments (Pl.21, Fig.7). On the distal surface, these fragments are composed of crystals arranged "rosette-like" around a pseudo-pore.

The proximal shell base is smooth with vermiculate-like crystal surfaces and poroids (Pl.21, Fig.8). Disintegrated shells which are split and spread out show polygonal fragments (Pl.21, Fig.7). On the distal surface, these fragments are composed of crystals arranged "rosette-like" around a pseudo-pore.

- **Aperture** (Pl.21, Fig.5-6): Empty specimens have a characteristic aperture. The crystals around the aperture form an irregularly serrated margin built by distally bent crystallites. TANGEN et al. (1982) suggested that the aperture is formed by ring-shaped dissolution of the calcite from the inner shell surface. INOUYE & PIENAAR (1983) reported that pressure applied by the organism from the inside causes the aperture to open and the cell emerges through this opening. The distally bent crystals around the aperture may show how the organism struggled to leave its shell.

4.2.2.1. DISTRIBUTION PATTERNS

From the bottom sediments of the low latitudes, *Th. heimii* has been frequently recorded from the Palaeocene onwards (KAMPTNER, 1927, 1963, 1967; FÜTTERER, 1976, 1977; KARWATH, 1995). In the modern temperate to tropical, fully oceanic waters, it is a ubiquitous species (Table 30) and sometimes abundant (GOULD & FRYXELL, 1988). Fluxes of more than 30,000 spec./m²·day were recorded in sediment trap studies (STEINMETZ, 1991; DALE & DALE, 1992).

- **Plankton:** The vegetative-coccoid *Th. heimii*-shells add up to 1-12% of the shelled phytoplankton (Fig.14), they were found in each plankton sample but three (22-S11, 22-S20, 22-S21) and show no restriction in temperature or salinity range. For the sampled water masses no exact data on nutrient contents are available, but the influence of coastal upwelling from offshore NW Africa was observed between ~15°N and ~25°N (see Chapter 4.1.).

In the equatorial Atlantic south of 8°N, in oceanic waters with relatively low nutrient contents, the proportional amount of the coccoid *Th. heimii* averages 2-5%. They reach a local maximum of 7% at 11.5°N/21°W (sample 22-S23), are only rarely found in the area influenced by upwelling, but the absolute maximum amount, 12% of the shelled phytoplankton, was observed at the Canary Isles. The Canary Isles ocean sector is located within the NAST (E) (LONGHURST et al., 1995) which shows oligotrophic characteristics. Therefore, the highest amount of *Th. heimii* in the plankton was recorded in an area predominated by oceanic influences.

Little is known about *Th. heimii* nutrient requirements. For their culture studies, TANGEN et al. (1982) used a medium very much enriched with nutrients to provide f/2 nutrient concentrations (with depleted Si, added Fe and other trace elements). This high nutrient content probably started the discussion of using *Th. heimii* as a palaeoproductivity indicator. On the other hand, in the Provasoli-Guillard National Center for Culture of Marine Phytoplankton (CCMP) (at the Bigalow Laboratory for Ocean Sciences, West Boothbay Harbor, Maine 04575) *Th. heimii* is generally grown in a medium with much lower nutrient contents, i.a. a modified f/20 medium.

Within the investigated waters, *Th. heimii* is considered to be a **ubiquitous** species (Fig.31) largely **independent of temperature and salinity** (Fig.30) and not requiring large amounts of nutrients.

- **Sediments:** The species assemblages of calcareous dinocysts and *Th. heimii*-shells in the sediments offshore NW Africa (off Cape Blanc) and in the Guinea Basin are clearly distinct. Their relative amounts vary significantly for the different regions.

The area offshore NW Africa is mainly affected by the CC and a complex system of seasonal winds causing the local upwelling regime. This results into a relatively low MA SST (~21°C, LEVITUS, 1982), high MA SSS (36.0-36.5‰, LEVITUS, 1986), and high productivity rates (>125gC/m² yr, BERGER, 1989). Whereas the Guinea Basin is influenced by the equatorial current system and shows a high MA SST (~27°C, LEVITUS, 1982), low MA SSS (35.0-35.5‰, LEVITUS, 1986) and slightly lower productivity rates (90-125gC/m² yr, BERGER, 1989).

The calcareous dinoflagellate species assemblage in the sediments off Cape Blanc is overwhelmingly dominated by *Th. heimii*-shells. At multicorer (MUC) site GeoB 1602-7 *Th. heimii* adds up to 85% and the calcareous cysts amount only to 15%. However, in the Guinea Basin the calcareous dinocysts are dominating the assemblage (GeoB 1606-7 MUC: 80%, GeoB 1607-8 MUC: 68%) and the relative amount of *Th. heimii* is 18% and 31% respectively.

Fig.32: Calcareous Dinoflagellate Species Assemblages
Relation *Th. heimii* / Calcareous Dinocysts

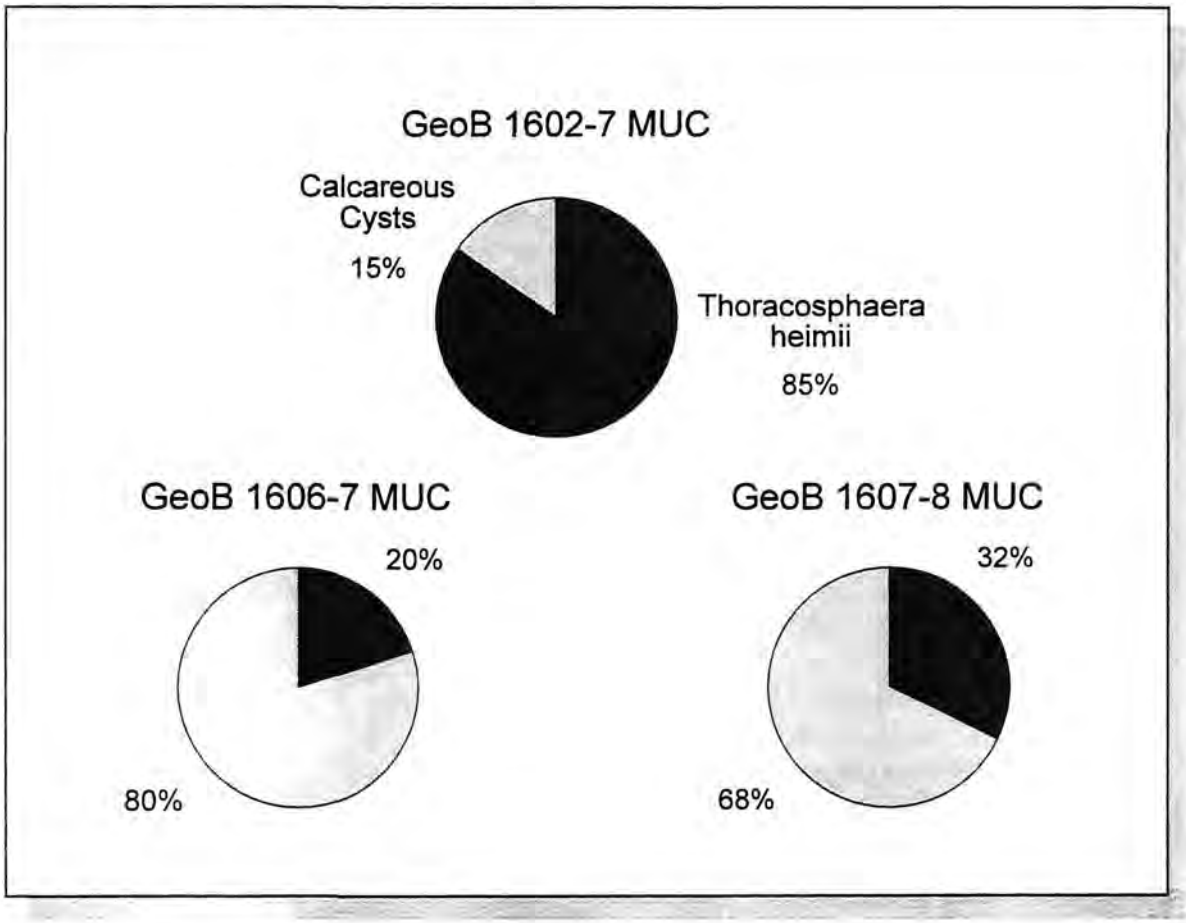

Fig. 32: The relative amounts of *Th. heimii*-shells and calcareous dinocysts are plotted for the uppermost sediment samples from offshore NW Africa (GeoB 1602-7 MUC) and from the Guinea Basin (GeoB 1606-7 MUC, GeoB 1607-8 MUC).

The semi-quantitative specimen densities off Cape Blanc are more than twice as high as in the Guinea Basin. Today, the productivity offshore NW Africa is generally considered to be at least twice as high as in the Guinea Basin. If the abundancy data of *Th. heimii* are directly transferred into productivity rates, they would agree with the general productivity data, but contrast with the data previously discussed from the plankton samples.

On the other hand, this *Th. heimii*-signal from the sediments off Cape Blanc may reflect a southward lateral transport of shells from the NAST with its high amount of planktic *Th. heimii*. The transport may have happened by various currents in the water column. At the surface the CC has a southward direction, the deep waters of the NADW and the MOW show a strong southward advection, only the SAIW flows in a northward direction.

Thus, the potential of *Th. heimii* as productivity indicator is questionable. And, further surveys and/or culture studies have to establish a more solid basis for their nutrient requirements.

4.3. DINOFLAGELLATE CYSTS: CALCAREOUS CYSTS

CLASS DINOPHYCEAE
PASCHER, 1914

ORDER PERIDINIALES
HAECKEL, 1894

- **Description** (LOEBLICH III, 1982; SOURNIA, 1986; FENSOME et al., 1993; STEIDINGER & TANGEN, 1996): Armoured dinokont cells with symmetrical plate pattern, apical pore complex typically with X plate. Plate tabulation usually: 3-6' but typically only 3 or 4', 1-3a, 6-7", 4-6c, 5‴, 1-2⁗ but typically 2⁗. The 1' is usually symmetrical.

SUBORDER PERIDINIINEAE
FOTT, 1959 *emend.* BUJAK & DAVIS, 1983

- **Original diagnosis** (BUJAK & DAVIS, 1983, p.124): "Peridinialean dinoflagellates characterized by the possession of an anterior intercalary plate series and a tabulation of 3-4', 1-4a, 4-7", 3-6c, 0-1p, 5‴, 1-2⁗. Most pre-Cenozoic taxa have a linteloid hexa second intercalary plate and bipesioid tabulation style. Modern thecae are cellulosic with some fossil representatives possibly being siliceous. Cysts have walls that are either sporopollenin, calcareous or possibly siliceous, and form an archaeopyle that generally comprises one or more anterior intercalary plates with or without contributions from adjacent plate series. Exceptions to this mode of archaeopyle formation occur in the families Calciodinellaceae, Peridinitaceae and Protoperidiniaceae."

FAMILY CALCIODINELLACEAE
DEFLANDRE, 1949
emend. BUJAK & DAVIS, 1983

- **Original diagnosis** (BUJAK & DAVIS, 1983, p.127): "Peridininean dinoflagellates with an ortho-hexa tabulation of 4', 3a, 7", 4-6c, 5‴, 2⁗ plus a transitional cingular-sulcal plate that is sometimes designated as an additional cingular plate. Variations to this basic tabulation formula occasionally occur, giving a general formula of 4', 2-3a, 4-7", 4-6c, 0-1p, 5‴, 2⁗. Cysts, when formed, are calcareous with an apically located archaeopyle that includes plates of the intercalary or apical series or both."

- **Type genus:** *Calciodinellum* DEFLANDRE, 1947.

SUBFAMILY FUETTERERELLOIDEAE
KOHRING, 1993

- **Original diagnosis** (KOHRING, 1993, p.87): "Dinoflagellate cysts with a calcareous outer wall, consisting of crystals with the c-axes parallel to the cysts surface."

CALCIODINELLUM
DEFLANDRE, 1947

- **Original diagnosis** (DEFLANDRE, 1947, p.201-202): "Microfossile à thèque calcaire mince, globuleuse, portant des crêtes disposées de manière à diviser, par une série équatoriale (correspondant à un sillon transversal) la coque à deux parties - épithèque et hypothèque - elles mêmes découpées en champs formant une tabulation analogue à celle de représentants du genre *Peridinium* EHR., soit 4', 6 ou 7", ? 0 ou 1-3a, 5‴, 2⁗."

Calciodinellum operosum
DEFLANDRE, 1947 *emend.* MONTRESOR et al., 1997

(Pl.22, Fig.1-6; Pl.23, Fig.1-4; Pl.24, Fig.1-8; Pl.25, Fig.1-5)

- **Original diagnosis for vegetative-thecate and cyst stage** (MONTRESOR et al., 1997): "Cellula, 20-28 µm longa (media ratio = 23.7 µm, SD = 2.6), 18-24 µm lata (media ratio = 21.1, SD = 2.2), colore quasi fusco, multos globosos chloroplastos continet. Epitheca, rotundo-conica, sine cornu apicali, paulo longior quam epitheca est. Cellulae superficieslevis videtur; sed parvi pori sine ullo ordine disposti, per microscopium electronicum (SEM) observantur. Formula laminarum: Po, X, 4', 3a, 7", 6C, (5C+T), 5S, 5‴, 2⁗. Pori lamina (po) porum apicalem circumdat. Lamina 1' ortho forma est. Lamina 2a, forma hexa, cum laminis 1a et 3a ad lineam collacata, in parte dorsali epithecae est. Laminae 1a et 3a, forma pentagonali, ad latera laminae 2a sunt. Cingulum e quineque laminis maioribus, eadem magnitudine, constat. Suturae inter laminas 3C et 4C et inter 4C et 5C, in parte dorsali cinguli equiliter dispostae, observantur. Prima lamina cingularis transitionis lamina (T) appellatur quia ceteris laminis cingularibusminor et iuxta sulcum est.

Cistis corpus rotundum est (diameter = 32-40 µm) et involvitur calcario tegimento quod e crystallis constat, quorum aliqua parva, aliqua in bacillorum speciem. Primi calcarii corii structura spongiosa-reticulata est. Crystalla in bacillorum speciem septa 8-12 µm alta faciunt, quae cistis para-laminas definiunt."

Fig. 33: *Calciodinellum operosum* Paratabulation

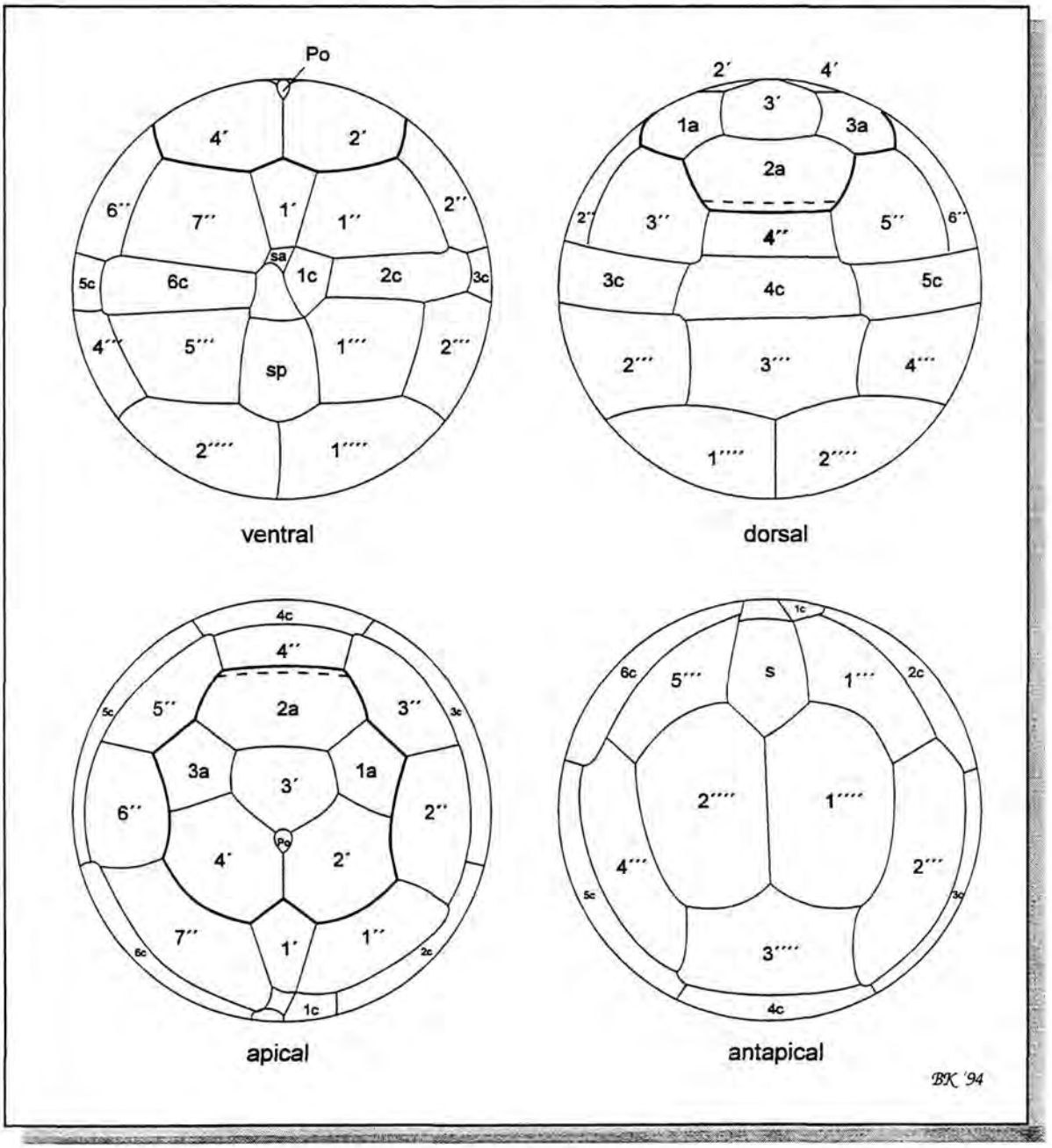

Fig. 33: *Calciodinellum operosum* paratabulation: **Po, 4', 3a, 7", 6c, 3?s, 5"', 2""**.

- **Description of cyst stage** (DEFLANDRE, 1947; WALL & DALE, 1968b; FÜTTERER, 1976, 1977; DALE & DALE, 1992; KOHRING, 1993; KEUPP & KOHRING, 1993; KARWATH, 1995; MONTRESOR et al., 1997): Spherical cysts with single-layered calcareous wall. Crystallites arranged around pores forming an overall reticulate pattern, their number (10-20) varies with pore-size (0.3-2.0 µm). Ortho-hexa paratabulation (Po, 4', 3a, 7", 6c, 3?s, 5'", 2""; Fig.33) defined by sutural calcareous ridges of various height on outer cyst wall. Diameter quite variable, from 22 µm to 36 µm, depending on height of ridges. FÜTTERER (1977) describes higher variations (20-45 µm).

Large polygonal **archaeopyle** (diameter: 17-27 µm) in apical position, formed by release of apical and intercalary paraplates, including the equivalent of apical pore plate.

Skeletal **ultrastructure** composed of small crystallites with flat proximal bases and pointed, pyramid-like distal surfaces. Tangential orientation of crystallite c-axes. Diameters of distal faces 0.2-1.7 µm, thickness of cyst wall 1.0-2.3 µm, which corresponds with crystal height.

The height of **crystallite ridges** varies greatly from only a tiny fraction of a micrometer to several micrometers with a maximum of 5.5 µm. The archaeopyle suture shows a compact "double-rim" of high crystallites.

- **Stratigraphic range:** Upper Eocene (KOHRING, 1993) to Recent.

DISCUSSION:

- **Thecate stage:** Recent incubation experiments with isolated *C. operosum* cysts from the Mediterranean produced *Scrippsiella*-like motile thecate dinoflagellates (MONTRESOR et al., 1997).

- **Planktic cysts:** No specimen of *C. operosum* with visible ridges was found in the plankton samples of this study.

- **Ultrastructure:** Specimens of *C. operosum* were only rarely found in the sediments and were absent in the plankton. Nevertheless, details of the skeletal ultrastructure show complete correspondence with the ultrastructure of "*Sph.*" *albatrosiana*.

- **Paratabulation** (Pl.22, Fig.1-8; Pl.23, Fig.1-8; Pl.24, Fig.1-8): The reflected tabulation pattern is almost identical with that of the living thecate genus *Scrippsiella* (WALL & DALE, 1968b).

Regarding the paratabulation ridges, a continuous morphological reduction or transition between well defined ridges (height > 1 µm, max. 5.5 µm) and a smooth surface, with ridges only a tiny fraction of a micrometer in height, were observed (Pl.24, Fig.1-8). MONTRESOR et al. (1997) recorded a wide range of morphotypes "from cysts identical to the cysts recorded in natural samples with well-developed paratabulation ridges to cysts in which the paratabulation was not visible and that were covered by irregularly shaped crystals" and they "observed cysts in which the paratabulation was only faintly marked by crystals that had an irregular knoblike shape".

The ridges start either with a slight growing of the crystals between two series of pores, or with two lines of crystals bordering one series of pores, whereas the longitudinal ridges rather tend to form two lines of crystals (Pl.24, Fig.1-2). The crystals of fully "mature" ridges may have a diameter of up to 1 µm terminating as "blocky" rhomboids (Pl.24, Fig.3-6), or the ridge crystallites are very long and flat with a "feathery" texture when seen in lateral view (Pl.24, Fig.7-8).

In connection with the crystallite ridges, a certain amount of enlarged pores was recorded. The most striking pore is located on the operculum and surrounded by crystallite ridges (Pl.23, Fig.1-8). FÜTTERER (1977) described this as an additional plate area between the 2', 4', and 3' paraplates. This pore is suggested to be the equivalent of an apical pore. In the sulcal area, beside the crystallite ridges, a whole pattern of larger pores was observed (Pl.22, Fig.1-8) that clearly distinguished an anterior and posterior sulcal paraplate. The sinistral and dextral sulcal paraplates are not easy to define, they more or less merge into one paraplate.

In the fossil record a second species of *Calciodinellum* was recorded from the upper Miocene (KOHRING, 1993: Pl.39, Fig.a-b; KEUPP & KOHRING, 1994). *Calciodinellum limbatum* (DEFLANDRE) KOHRING, 1993 was described as an equivalent to *C. operosum* with reduced ridges.

- **Operculum** (Pl.23, Fig.1-8): The archaeopyle has an apical and slightly dorsal position, it is large (diameter 17-27 µm) with a polygonal outline (Pl.25, Fig.1-4). Two thirds of the archaeopyle boundary show a clear suture.

The operculum consists of a combination of the apical and intercalary paraplates including the equivalent of the apical pore plate (Po + 2'-4' + 1a-3a) (Pl.23, Fig.1-8). The separation of the 2a-paraplate is mostly incomplete. It ruptures either within or directly after the most dorsal and posterior serie of pores with these parts of the paraplate remaining with the main cyst body.

"Sphaerodinella" albatrosiana
(KAMPTNER) KEUPP & VERSTEEGH, 1989

(Pl.22, Fig.7-8; Pl.23, Fig.5-8; Pl.25, Fig.6-9; Pl.26, Fig.1-12)

- **Description** (KAMPTNER, 1967; FÜTTERER, 1976, 1977; KEUPP & VERSTEEGH, 1989; DALE & DALE, 1992; KOHRING, 1993; KEUPP & KOHRING, 1993; KARWATH, 1995; JANOFSKE, 1996): Spherical poorly paratabulated cyst with single-layered calcareous wall. Crystallite ultrastructure the same as by *Calciodinellum operosum* but without any visible sutural crystallite ridges on distal cyst wall surface. Cyst diameter mostly less than *C. operosum*, averages 21-27 µm, greater size range (18-32 µm) has been reported (KAMPTNER, 1963; FÜTTERER, 1977).

Large polygonal apical **archaeopyle** is formed by detachment of paraplates Po + 2'-4' + 1a-3a. Diameter of archaeopyle: 14-21 µm, two thirds of archaeopyle boundary show suture composed of slightly higher than average crystallites (2.1-2.9 µm).

- **Stratigraphic range:** Upper Palaeocene (KOHRING, 1993) to Recent.

DISCUSSION:

- **Planktic cysts** (Pl.26, Fig.1-12): LM examinations of embedded plankton filters show golden-brown cysts with a red eyespot-like central feature and the operculi still attached. The overall appearance is roughly the same as "*Sph.*" *tuberosa*, but the wall crystallites generally are smaller (diameter <1 µm), and their reticulate arrangement can be seen on the outer cyst surface (KAMPTNER, 1963).

SEM examinations reveal that the cysts are "wrapped" in an outer organic wall layer or phragma (Pl.26, Fig.1-9). This organic layer covers the calcite crystallites and the pores like a sheet. These specimens are considered to be living cysts with cell content. Specimens found in the sediment are lacking this phragma.

One specimen was found with the operculum still attached, but obviously fell prey to a zooplankton organism (Pl.26, Fig.10). The cell content is gone and the calcareous cyst wall is perforated by a boring.

A crushed specimen on a plankton filter showed that the calcareous elements of the cyst wall are located between an inner and an outer organic wall layer or phragma (Pl.26, Fig.11-12). It is assumed that calcification happens between these two phragmas. The pores of the calcareous cyst wall are proximally completely covered by the inner organic layer and distally partly covered by the outer layer. A third organic layer is not discernible. GAO et al. (1989) described the formation of partly calcified cysts from *Scrippsiella* sp. There, the cell was surrounded by three membranes, with the organic layer of the cyst wall built between the inner and the middle membrane, and the calcareous elements formed between the middle and the outer membrane.

- **Ultrastructure:** The calcareous ultrastructure of the cyst wall shows numerous variations owing to different stages of initial calcification and to secondary factors like calcite overgrowth.

Calcification of the cyst wall is suggested to start from numerous nucleation sites arranged in a circular pattern. As calcification proceeds the skeletal elements form ring-like structures with central pores. At this stage these structures are only loosely attached and still fragile (Pl.26, Fig.1-6). With calcification complete the calcite crystals are interconnecting and the ring-like structures blend into an overall reticulate test pattern (Pl.26, Fig.7-9). But on the inner cyst surface, the initial ring-like arrangement of the skeletal elements is still discernible (Pl.25, Fig.5-6).

In some sediment samples of various core depths, specimens with an "overgrowth" of additional small rhombic crystals on the outer cyst wall was observed (Pl.25, Fig.8-9). How far this feature indicates another morphological variety of "*Sph.*" *albatrosiana* or simply a secondary crystallite overgrowth is uncertain, although longer projections were previously recorded on specimens from the Pliocene and were interpreted as an independent variety (FÜTTERER, 1977; VERSTEEGH, 1993).

The equivalent of an apical pore, defined by calcareous ridges, is fairly obvious on the operculi of *C. operosum*. In the present study, an identical enlarged pore were found on the operculi of "*Sph.*" *albatrosiana* (Pl.23, Fig.5-8; Pl.26, Fig.4-5). In both cases the pore is filled with calcite crystals building a very small longitudinal ridge. Additionally, in the sulcal area, a similar design of enlarged pores, such as seen on the cysts of *C. operosum*, was noticed (Pl.22, Fig.7-8).

- **Paratabulation:** According to MONTRESOR et al. (1997) "*Sph.*" *albatrosiana* may be regarded as a *C. operosum*-variety without visible paratabulation ridges.

- **Operculum** (Pl.23, Fig.5-8; Pl.26, Fig.1-2, 4-5): The archaeopyle and the operculum have a similar position and morphology such as seen with *C. operosum*, but without ridges. Two thirds of the archaeopyle boundary show a clear suture of a compact "double-rim" of crystallites (Pl.30, Fig.7; Pl.31, Fig.1-2, 4-5).

"Sphaerodinella" tuberosa
(KAMPTNER) KEUPP & VERSTEEGH, 1989

(Pl.27, Fig.1-8; Pl.28, Fig.1-8; Pl.29, Fig.1-8)

- **Description** (KAMPTNER, 1967; FÜTTERER, 1976, 1977; KEUPP & VERSTEEGH, 1989; DALE & DALE, 1992; KOHRING, 1993; KEUPP & KOHRING, 1993; KARWATH, 1995; JANOFSKE, 1996): Spherical to slightly ovoid, poorly paratabulated cysts, with single-layered calcareous walls constructed by rhomboidal crystals. Cyst diameters mainly 22-24 µm, but may vary between 19-39 µm.

Large apical **archaeopyle** (diameter 12-25 µm), formed by loss of plates homologous with apical and intercalary plate system. Two thirds of archaeopyle boundary show clearly serrated suture.

Skeletal **ultrastructure** composed of many interconnected rhombic crystallites. Tangential orientation of crystallite c-axes. Crystals of different specimens display various sizes (diameter 1.5-4.5 µm, height 2.3-3.5 µm). On outer cyst surface calcite rhomboids show three-sided pointed pyramids, small furrow or groove may run along the crystal edges, tips of pyramids are mostly flattened, a pseudo-pore is present on lower part of crystal faces. Inner cyst surface formed by polygonal even crystal bases with a small central poroid.

- **Stratigraphic range:** Middle Eocene (KOHRING, 1993) to Recent.

DISCUSSION:

KAMPTNER (1963) first described "*Sph.*" *tuberosa* as a species of the then coccolithophorid genus "*Thoracosphaera*". Later, FÜTTERER (1976, 1977) discussed the taxonomic position of the "Thoracosphaeroidea" and considered them to be calcareous dinocysts. TANGEN et al. (1982) and INOUYE & PIENAAR (1983) proved that the type species of the Thoracosphaeroidea, *Th. heimii*, is a vegetative-coccoid dinoflagellate and not a resting cyst. Therefore, the taxonomic position of all the other "*Thoracosphaera*" species, presumably real dinocysts, was uncertain; until KEUPP & VERSTEEGH (1989) established a new genus for calcareous dinocysts and included this species as "*Sphaerodinella*" *tuberosa*, thus creating new taxonomic uncertainties as noted above.

- **Thecate stage:** Very recently, clonal cultures were started with small *Scrippsiella*-like thecae (max. 35 µm) isolated from plankton samples offshore Chile (KARWATH, pers. comm.). 30% and more of the clonal thecae were observed to produce "*Sph.*" *tuberosa*-like cysts with encystment happening over a period of 2h. Hatching occurred after approx. 12 hours (JANOFSKE, pers. comm.).

- **Planktic cysts** (Pl.27, Fig.1-6): LM examinations of embedded plankton filters show dark-gray cysts. The wall crystals are sometimes "big" (diameter 3.3-4.4 µM; KAMPTNER, 1963) and their pyramid-like contour is easily recognized on the outer cyst surface.

Specimens found in the plankton are usually complete, with cell content and the operculi still attached, and are covered with an outer organic wall layer or phragma (Pl.27, Fig.1-6). These specimens are considered to be living cysts. During SEM examinations the outer phragma may obscure the ultrastructure such that only the outlines of the pyramid tips of the crystallites are discernible (Pl.27, Fig.2, 4, 6). A disintegrated cyst reveals the presence of an inner organic layer or phragma even though the outer layer was already decayed. Unfortunately, no specimen with a clear wall cross section was observed.

- **Ultrastructure** (Pl.27, Fig.7-8; Pl.28, Fig.1-8; Pl.29, Fig.1-8): During the present study a wide morphological range of the ultrastructural crystallites of "*Sph.*" *tuberosa* was observed. It is assumed that this morphological range is a natural predisposition.

The proximal bases of the crystallites show only a limited morphological range (Pl.29, Fig.2, 6-8). They generally have a smooth slightly convex surface with a small poroid in the center. The outline is triangular and resembles the spade of cards if crystal growth is not inhibited by neighboring crystals (Pl.29, Fig.8).

The distal faces of the crystals vary from a "buckle-like" framework (Pl.27, Fig.7-8; Pl.28, Fig.1-4), a more or less solid "blocky" contour (Pl.28, Fig.6-8) to a "cap-like" appearance (Pl.29, Fig.1-4). The "buckle"-crystals are loosely packed with the pseudo-pores on the lower crystal faces as big as 1 µm in diameter. The rhombic "blocks" are closely crammed and the pseudo-pores are not always visible. The distal sides of the "cap-like" crystallites do not display sharp crystal edges and have an "organic" look. These crystal lines of the "caps" may be interpreted as the rudimentary onsets of spines, and the morphological outline of the crystallites indicates similarities to some *Rhabdothorax erinaceus*-crystals (FÜTTERER, 1977). On the other hand, the proximal bases of the crystallites show the typical polygonal and sharp-edged contour of "*Sph.*" *tuberosa*.

A cross section of the archaeopyle rim reveals a "pseudo-double-layer" of crystallites. This effect is produced by inhibited crystal growth at the edges bordering the archaeopyle suture, which appears like a "shearing off" of crystallite edges (Pl.29, Fig.5-7).

- **Paratabulation:** So far, no modern paratabulated equivalent of "*Sph.*" *tuberosa* was observed, neither in the plankton (DALE & DALE, 1992; this study), nor in the sub-Recent sediments (FÜTTERER, 1976, 1977; KARWATH, 1995; HÖLL, pers. comm.; this study).

In the fossil record, several different paratabulation patterns were recorded for cysts with the same morphological crystallite ultrastructure as seen with "*Sph.*" *tuberosa*. Two species of the genus *Calcigonellum* (DEFLANDRE) *emend.* KEUPP, 1984 *emend.* KEUPP & VERSTEEGH, 1989 were described as prismatic stages (*sensu* KEUPP et al., 1991) and a paratabulated variety of "*Sph.*" *tuberosa* (KOHRING, 1993; KEUPP & KOHRING, 1994). Other varieties show the same paratabulation patterns as the two species of *Calciodinellum* (KOHRING, 1993; pl.11). All these paratabulated varieties display an apical pore equivalent as seen on *Calciodinellum operosum*.

- **Operculum** (Pl.27, Fig.1, 7-8; Pl.28, Fig.2-4, 7--8; Pl.29, Fig.5-6): The archaeopyle has an anterior position, it is large (diameter 12-25 µm) with a polygonal outline.

The operculum consists of a combination of the apical and intercalary paraplates (?Po+2'-4' + 1a-3a). Two thirds of its boundary exhibit a serrated suture.

RHABDOTHORAX
KAMPTNER, 1958

- **Original description** (KAMPTNER, 1958, p.88-90): "*Rhabdothorax* hat ein eiförmiges, zuweilen annähernd kugeliges Gehäuse. Die Coccolithen sind bei der typischen Spezies verhältnismäßig niedrig und undurchbohrt. Ihre Oberfläche fällt dachartig ab, und in der Mitte erhebt sich ein stabartiges Gebilde, dessen Ende verbreitert sein kann."

- **Type species:** *Rhabdothorax erinaceus* (KAMPTNER) KAMPTNER, 1958.

Rhabdothorax erinaceus
(KAMPTNER) KAMPTNER, 1958

(Pl.30, Fig.1-8; Pl.31, Fig.1-8)

- **Description** (KAMPTNER, 1937, 1958; WALL & DALE, 1968b; WALL et al., 1970; FÜTTERER, 1977; KEUPP & VERSTEEGH, 1989; DALE & DALE, 1992; KARWATH, 1995): Cell spherical to ovoid, covered with numerous, polygonal calcareous skeletal elements, each with a projection or spine in the center. Spines are either long and rod-like, triangular in cross-section with pointed arrowhead-shaped terminations, or short and blunt with a distal knob. Tangential orientation of crystallite c-axes. Diameter of central body is 22-34 µm and spine length is 1-6 µm, but may reach more than 10 µm. The large apical archaeopyle has a circular outline with diameter of 17-22 µm, some tests have no discernible archaeopyle.

Calcareous shell approximately 1-2 µm thick, diameter of interconnected crystals 3-6 µm with pores in between of sizes 0.5-1 µm. Inner surface of skeletal elements shows a smooth base with an irregular smooth-edged "star-like" outline and a small central poroid.

- **Remarks:** KAMPTNER (1958, p.88) gives a datum on the tangential crystallographic orientation of the crystallites ("....anisotrope Kristallite mit ihren optischen Achsen....genau quer zur Längsrichtung des Stabes orientiert sind").

Rh. erinaceus was originally, and erroneously, assigned to the coccolithophorid genus *Rhabdosphaera* HAECKEL, 1894 (KAMPTNER, 1937). Later KAMPTNER (1958) established the new genus *Rhabdothorax* (transferring the species "*Rhabdosphaera*" *erinaceus*) within the then coccolithophorid subfamily Thoracosphaeroideae KAMPTNER, 1928. Therefore, a general relation-ship of the genus *Rhabdothorax* with the genus *Thoracosphaera* was already established. Later, in culturing experiments, both were proven to belong to the dinophyceae (WALL & DALE, 1968b; TANGEN et al., 1982; INOUYE & PIENAAR, 1983).

- **Stratigraphic range:** ?Middle Eocene (KOHRING, 1993) to Recent.

DISCUSSION:

- **Thecate stage:** WALL & DALE (1968b) successfully germinated calcareous cysts that were later identified as *Rh. erinaceus*, and produced *Scrippsiella trochoidea*-thecae; thus "proving" and establishing one of the earliest calcareous cyst/theca-relationships. Later DALE & DALE (1992) presumed that modern tropical oceanic calcareous dinocysts are produced by different species within the thecate dinoflagellate genera *Scrippsiella* or *Ensiculifera*.

- **Planktic cysts** (Pl.30, Fig.1-8): One "perfect specimen" was found in the plankton samples with well developed crystal bases and long spines up to 6 µm (Pl.30, Fig.1-3). The crystal bases match and form a rigid and perfectly round central cyst body without any gaps in

between. Other planktic specimens have an ovoid shape, the spines are short, below 3 µm, and the bases not fully developed (Pl.30, Fig.4-8). They are not interconnected and only loosely attached on an inner organic wall layer or "membrane" such as described by WALL et al. (1970). These cysts can break quite easily. Slightly damaged specimens reveal the inner organic cell contents (Pl.30, Fig.5-6). These specimens with short spines and rudimentary crystal bases are suggested to represent an early stage of calcification of the cyst wall.

Cells of *Rh. erinaceus* obtained from plankton samples have no organic outer layer or phragma like the other planktic cysts described here, although both inner and outer phragmas have been reported from *Scrippsiella* clonal culture studies (WALL et al., 1970; GAO et al., 1989; GAO & DODGE, 1991).

- **Ultrastructure** (Pl.30, Fig.1-8; Pl.31, Fig.1-8): On the outer cyst surface the crystal bases display a triangular "clover leaf" outline with six lateral indentations which alternately link together or form pseudo-pores in the cyst body (Pl.30, Fig.2; Pl.31, Fig.2, 4). From the center of the "clover leaf" rises a triangular spine of various height tapering to a pointed pyramid-like tip (Pl.30, Fig.2-3; Pl.31, Fig.2, 4) or ending in a "knob" (Pl.30, Fig.4-8; Pl.31, Fig.7). Drawings of both a perpendicular and a lateral cross section of a crystallite were presented by KAMPTNER (1937). Later he submitted additional information on the crystallographic orientation of the calcitic spines, i.e. tangential orientation of c-axes (KAMPTNER, 1958).

The proximal crystal bases are plain and slightly convex with a small central poroid. The general outline resembles a star with blunt edges (Pl.31, Fig.8) if crystal growth is not inhibited by neighboring crystals.

SUBFAMILY ORTHOPITHONELLOIDEAE
KEUPP, 1987

-Original diagnosis (KEUPP, 1987, p.38): "Dinoflagellate cysts with a single or double-layered calcareous wall. The calcite crystals at least of the outer wall layer show a strong radial orientation."

TRIBE ORTHOPITHONELLEAE
KEUPP & VERSTEEGH, 1989:

-Original diagnosis (KEUPP & VERSTEEGH, 1989, p.208): "Dinoflagellaten-Kalkzysten mit Wänden aus radial orientierten Kalzitkristalliten. Die in ihrer Anlage nicht streng fixierte Archaeopyle ist in der Regel entsprechend den apikalen Platten-Homologen angelegt (2'+3'+4', meist jedoch nur 3')."

ORTHOPITHONELLA
KEUPP, 1984 *emend.* KEUPP & VERSTEEGH, 1989

- **Original description** (KEUPP & VERSTEEGH, 1989, p.210): "Kugelige, nicht bis rudimentär paratabulierte Zysten mit überwiegend einschichtigen Kalkwänden, deren blockige bis stengelige Kristalle c-Achsen-radial orientiert sind. Die in ihrer Anlage nicht streng fixierte Archaeopyle ist meist im Äquivalent der Apikalplatten 2'-4' angelegt."

Type species: *Orthopithonella gustafsoni* (BOLLI, 1974)

Orthopithonella granifera
(FÜTTERER) KEUPP & KOHRING, 1993

(Pl.32, Fig.1-8; Pl.33, Fig.1-8)

- **Description** (FÜTTERER, 1977; DALE & DALE, 1992; KOHRING, 1993; KEUPP & KOHRING, 1993; KARWATH, 1995; JANOFSKE, 1996): Dinoflagellate cyst with calcareous wall. Cysts spherical to slightly ovoid with diameters 12-25 µm.

Wall **ultrastructure** composed of small and tightly packed, "needle-like" or "fringe" crystals (c-axes perpendicular to cyst surface, i.e. radial orientation). Crystallite length 1.5-2 µm, diameter only a fragment of a micrometer.

Archaeopyle formed by detachment of a singular paraplate, diameter 4-9 µm with "flattened" rim or sutural area approximately 1 µm in width. Sub-circular operculum is composed of densely packed crystallites sometimes with a central knob-like feature.

- **Stratigraphic range:** Middle Oligocene (KEUPP & KOHRING, 1994) to Recent.

DISCUSSION:

- **Thecate stage:** So far no cyst-theca relationship could be established for this species. This is a "presumed" dinocyst owing to the presence of an archaeopyle. - **Planktic cysts** (Pl.32, Fig.1-4): SEM examinations reveal that the specimens in the plankton samples are covered by an outer organic wall layer or phragma. The calcite crystallites are concealed by this organic layer and the cyst surface has a granular "organic" appearance. (It shows many similarities with the thecal surface of *Protoperidinium globulus*, Pl.17, Fig.3.) Owing to this appearance in the SEM plankton workers can easily confuse planktic cysts of *O. granifera* with invertebrate zooplankton eggs. And, during LM examinations their calcareous tests are readily mistaken for foraminiferal proloculi both on embedded plankton filters and on sediment sample smear slides.

Table 31: Calcareous dinocyst distribution data. The relative species composition is given in percent. MA SST data from LEVITUS (1982), MA SSS data from LEVITUS (1986).

SPECIES	PLANKTON		SUB-RECENT SEDIMENTS			
	DALE & DALE (1992)	THIS STUDY	KAMPTNER (1967) WALL & DALE (1968b)	FÜTTERER (1976, 1977)	KARWATH (1995)	THIS STUDY
C. operosum DEFLANDRE, 1947 *emend.* MONTRESOR et al., 1997	Sediment trap data, **Söhm Abyssal Plain:** **MA SST: 22°C** **MA SSS: 36.6‰** low flux rates: 57 spec. m²/day **Demerara Abyssal Plain:** **MA SST: 26°C** **MA SSS: ~36.6‰** low flux rates: 112-184 spec. m²/day		**WALL & DALE (1968b):** Caribbean Yucatan Basin	rare to abundant, SE North Atlantic, Sierra Leone Rise		**Off Cape Blanc:** **MA SST: 21°C** **MA SSS: 36.0-36.6‰** GeoB 1602-7 MUC: 3% = 8 spec./cm² **Guinea Basin:** **MA SST: 27°C** **MA SSS: 36.0‰** GeoB 1606-7 MUC: 4% = 107 spec./cm²
"Sph." albatrosiana (KAMPTNER) KEUPP & VERSTEEGH, 1989	**Söhm Abyssal Plain:** **MA SST: 22°C** **MA SSS: 36.6‰** high flux rates: 2,304-8,448 spec. m²/day **Demerara Abyssal Plain:** **MA SST: 26°C** **MA SSS: ~36.6‰** very high flux rates: 5,353-13,750 spec. m²/day	**SST: 24-29°C** **SSS: 35.0-36.3‰** most abundant, in the equatorial Atlantic	**KAMPTNER (1967):** **Central S Atlantic, Mid Atlantic Ridge:** **MA SST: 22-23°C** **MA SSS: ~36.6‰** present	common to abundant, SE North Atlantic, Sierra Leone Rise	**Offshore Recife, Brazil:** **MA SST: 26°C** **MA SSS: 36.0-36.6‰** GeoB 2204-2 GC: 17% = 145,000 spec./g	**Off Cape Blanc:** **MA SST: 21°C** **MA SSS: 36.0-36.6‰** GeoB 1602-7 MUC: 56% = 146 spec./cm², **Guinea Basin:** **MA SST: 27°C** **MA SSS: 36.0‰** GeoB 1606-7 MUC: 74% = 1,821 spec./cm², GeoB 1607-8 MUC: 78% = 1,414 spec./cm²

Table 31: Calcareous dinocyst distribution data (continued).

SPECIES	PLANKTON		SUB-RECENT SEDIMENTS			
	DALE & DALE (1992)	THIS STUDY	KAMPTNER (1967) WALL & DALE (1968b)	FÜTTERER (1976, 1977)	KARWATH (1995)	THIS STUDY
"Sph." tuberosa (KAMPTNER) KEUPP & VERSTEEGH, 1989	**Söhm Abyssal Plain:** **MA SST: 22°C** **MA SSS: 36.5‰** moderate flux rates: 114-171 spec. m²/day **Demerara Abyssal Plain:** **MA SST: 26°C** **MA SSS: ~35.5‰** low flux rates: 63-78 spec. m²/day	**SST: 24-28°C** **SSS: 35.5-36.3‰** frequent, in the equatorial Atlantic south of 12°N	**KAMPTNER (1967):** **Central S Atlantic,** **Mid Atlantic Ridge:** **MA SST: 22-23°C** **MA SSS: ~36.5‰** present	rare to moderately frequent, SE North Atlantic, Sierra Leone Rise	**Offshore Recife, Brazil:** **MA SST: 26°C** **MA SSS: 36.0-36.5‰** GeoB 2204-2 GC: 83% = 730,000 spec./g	**Off Cape Blanc:** **MA SST: 21°C** **MA SSS: 36.0-36.5‰** GeoB 1602-7 MUC: 41% = 107 spec./cm² **Guinea Basin:** **MA SST: 27°C** **MA SSS: 35.0‰** GeoB 1606-7 MUC: 21% = 518 spec./cm², GeoB 1607-8 MUC: 21% = 379 spec./cm²
Rh. erinaceus (KAMPTNER) KAMPTNER, 1958	**Söhm Abyssal Plain:** **MA SST: 22°C** **MA SSS: 36.5‰** low flux rates: 28-85 spec. m²/day **Demerara Abyssal Plain:** **MA SST: 26°C** **MA SSS: ~35.5‰** low flux rates: 19-136 spec. m²/day	**SST: 19-29°C** **SSS: 35.0-36.7‰** frequent, in the equatorial Atlantic and offshore NW Africa	**WALL & DALE (1968b):** Bermuda, Gulf of Paria, Kingston, Miami, Woods Hole	present in small numbers, Sierra Leone Rise		**Guinea Basin:** **MA SST: 27°C** **MA SSS: 35.0‰** GeoB 1606-7 MUC: 1% = 18 spec./cm², GeoB 1607-8 MUC: 1% = 17 spec./cm²

Table 31: Calcareous dinocyst distribution data (continued).

	PLANKTON		SUB-RECENT SEDIMENTS			
SPECIES	DALE & DALE (1992)	THIS STUDY	KAMPTNER (1967) WALL & DALE (1968b)	FÜTTERER (1976, 1977)	KARWATH (1995)	THIS STUDY
O. granifera (FÜTTERER) KEUPP & KOHRING, 1993	Sediment trap data: **Söhm Abyssal Plain:** **MA SST: 22°C** **MA SSS: 36.5‰** low flux rates: ?313-?768 spec. m²/day (Thoracosphaerida)	**SST: 19-28°C** **SSS: 35.2-36.7‰** frequent, in the equatorial Atlantic south of 15°N, one site off Cape Blanc		rare to abundant, Sierra Leone Rise		**Off Cape Blanc:** **MA SST: 21°C** **MA SSS: 36.0-36.5‰** GeoB 1602-7 MUC: 15 spec./cm² **Guinea Basin:** **MA SST: 27°C** **MA SSS: 35.0‰** GeoB 1606-7 MUC: 393 spec./cm², GeoB 1607-8 MUC: 128 spec./cm²

Fig.34: M23/3 Temperature and Salinity Ranges of "Warm Water Cysts"

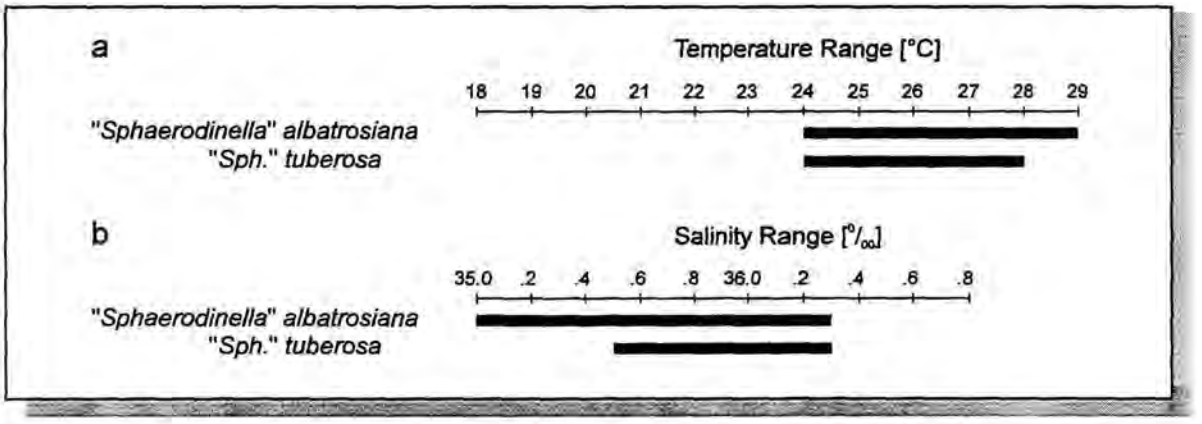

Fig. 34: Bar graphs of temperature (a) and salinity (b) ranges of "warm water cysts".

- **Planktic cysts** (Pl.32, Fig.1-4): SEM examinations reveal that the specimens in the plankton samples are covered by an outer organic wall layer or phragma. The calcite crystallites are concealed by this organic layer and the cyst surface has a granular "organic" appearance. (It shows many similarities with the thecal surface of *Protoperidinium globulus*, Pl.17, Fig.3.) Owing to this appearance in the SEM plankton workers can easily confuse planktic cysts of *O. granifera* with invertebrate zooplankton eggs. And, during LM examinations their calcareous tests are readily mistaken for foraminiferal proloculi both on embedded plankton filters and on sediment sample smear slides.

Complete specimens with operculi are considered to be living cysts with cell content. The outer phragma is partly decayed on specimens with open archaeopyle, revealing the distal surface of the needle-like crystals (Pl.32, Fig.1-3). The inner shell surfaces of these specimens are very smooth and covered with an inner organic layer. Specimens found in the sediment lack these phragmas.

- **Ultrastructure** (Pl.33, Fig.3-8): Originally FÜTTERER (1977) described *O. granifera* (i.e. "*Thoracosphaera*" *granifera* FÜTTERER, 1977) from SEM examinations, but he already observed that "...these crystallites.....do not have a specific orientation although a linear arrangement can be observed on the distal test surface..." (FÜTTERER, 1977, p.715). Interpreting crystal outline as being equivalent to crystallographic orientation KOHRING (1993) wrongly associated this species with the subfamily Obliquipithonelloideae.

Later KEUPP & KOHRING (1993) correctly described it as belonging to the subfamily Orthopithonelloideae. They gave a schematic illustration of a cyst wall cross section and crystallite orientation: minute rhombic crystallites are tightly packed on edge. In the present study, broken specimens were observed that fully confirm this morphological arrangement of the wall crystallites (Pl.33, Fig.7). And the LM examinations by JANOFSKE (1996) prove the radial orientation of crystallite c-axes for *O. granifera*.

Morphological variations and diagenetic effects may change the outer characteristics of *O. granifera*. Crystallite overgrowth (Pl.33, Fig.6) can cover the ultrastructure; partial solution of calcitic crystals (Pl.32, Fig.7-8) leads to segmentation of the distal cyst surface into irregular plate-like elements (FÜTTERER, 1977) The crystallites are generally minute, i.e. have a diameter <0.5 µm. But even for this small size they show a remarkable variety. The crystals may have a diameter as "big" as 0.4 µm (Pl.33, Fig.4), they may be loosely packed in single file, or sometimes blend laterally to form a small scale reticulate pattern with pseudo-pores.

»

Fig.35: The distribution pattern of calcareous "warm water cysts" is plotted in the temperature map (a), the salinity map (b), and the productivity map (c).

Fig.35: M23/3 Distribution of Calcareous "Warm Water Cysts"

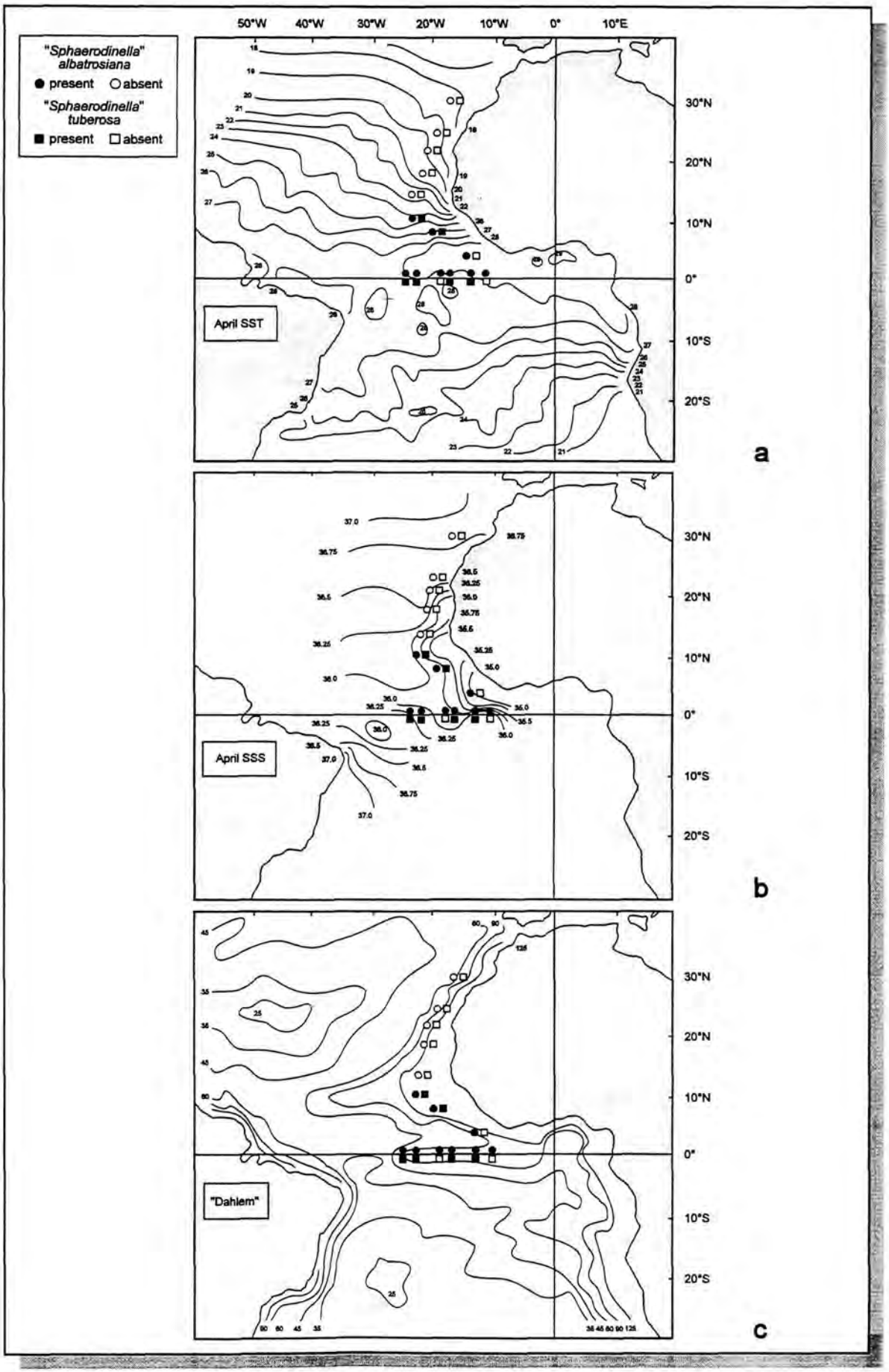

Fig.36: M23/3 Temperature and Salinity Ranges of *Scrippsiella trochoidea*

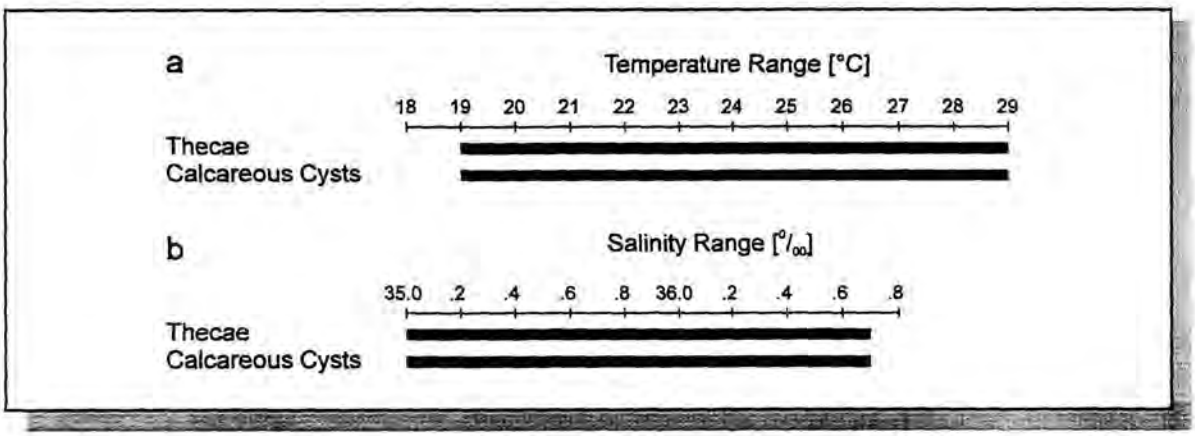

Fig. 36: Bar graphs of temperature (a) and salinity (b) ranges of *Scrippsiella trochoidea* thecae and cysts.

Very tiny crystallites may be smaller than 0.1 µm and are very difficult to examine even with a SEM (Pl.33, Fig.5). Combined they produce a delicate granular texture with poroids on the outer cyst surface.

The inner cyst surface of *O. granifera* shows some morphological similarities with the inner shell surface of *Thoracosphaera heimii*. It has a smooth base with vermiculate-like crystal surfaces and poroids, even though no polygonal wall fragmentation was observed (Pl.33, Fig.8).

- **Operculum** (Pl.32, Fig.5-8; Pl.33, Fig.1-2): The sub-circular operculum is the single conspicuous feature on the outer cyst surface. It is composed of tightly packed crystallites which have a solid appearance, even though no isolated operculum was observed neither in the plankton nor in the sediments (its absence in the sediment samples may be an effect of preparation technique, i.e. separation of particles <5 µm). A short "knobby" projection may be located in the center of the operculum. The height of this feature is generally below 1 µm, but it may be absent as well.

The archaeopyle is suggested to have an apical position and is formed by separation of an obviously single paraplate, presumably the 3' paraplate. In lateral view, a "flattened" area is visible that surrounds the archaeopyle rim-like (Pl.32, Fig.8; Pl.33, Fig.2).

4.3.1. DISTRIBUTION PATTERNS

In their sediment trap studies DALE & DALE (1992) observed an overwhelming domination of calcareous forms in the dinocyst assemblages of the tropical fully oceanic Atlantic. The present study confirms this domination. In the plankton as well as in the sediments only calcareous and no dinosporin cysts have been recorded.

For the first time, the distribution of calcareous dinocysts (Table 31) and their environmental requirements is investigated in the tropical Atlantic. In the present study, an attempt is made to link distribution patterns to various oceanographic parameters such as temperature, salinity, productivity, and currents. All MA SST and MA SSS data further referred to in this study are taken from LEVITUS (1982) and LEVITUS (1986) respectively; the productivity data have been adapted from the "Dahlem"-map of BERGER (1989).

»

Fig.37: The distribution pattern of *Scrippsiella trochoidea* is plotted in the temperature map (a), the salinity map (b), and the productivity map (c).

Fig.37: M23/3 Distribution of *Scrippsiella trochoidea*

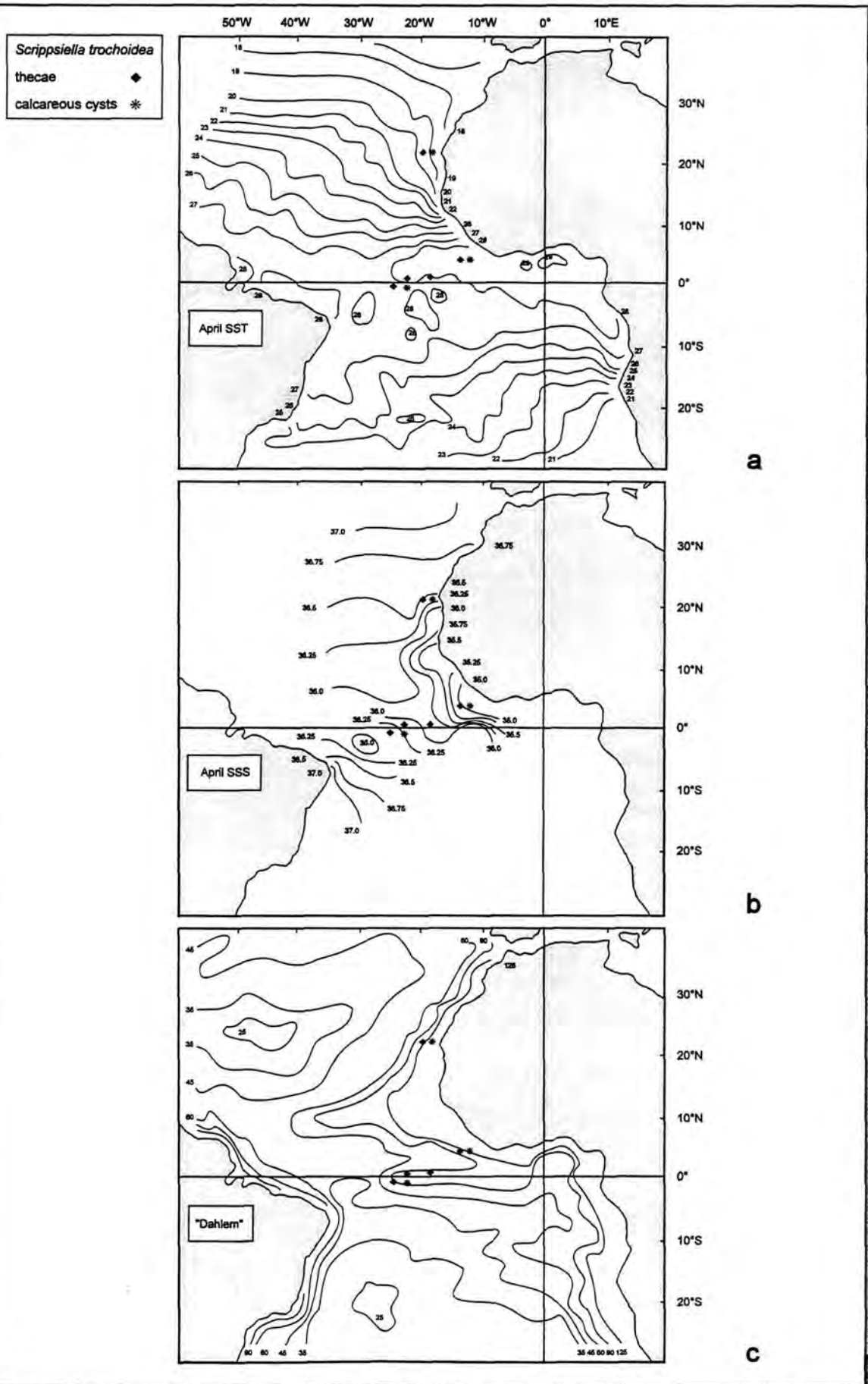

Fig.38: Calcareous Dinocyst Assemblages

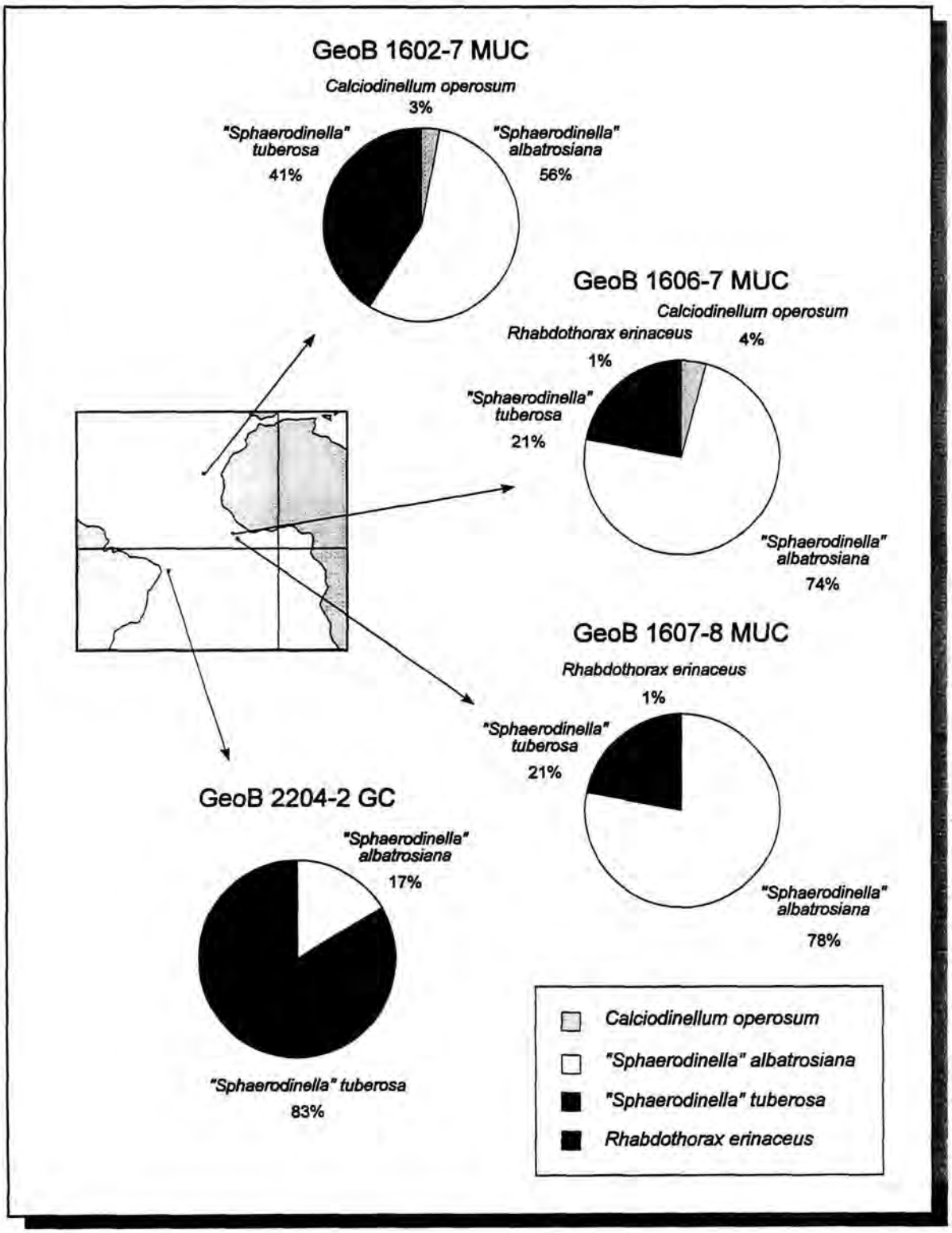

Fig. 38: Calcareous dinocyst assemblages in surface sediments offshore NW Africa (GeoB 1602-7 MUC) and in the eastern equatorial Atlantic (GeoB 1606-7 MUC, GeoB 1607-8 MUC).
Calcareous dinocyst assemblage in the uppermost sample of a gravity core from the western equatorial Atlantic (GeoB 2204-2 GC) adapted from KARWATH (1995).

Fig.39: M23/3 Temperature and Salinity Ranges of *Orthopithonella granifera*

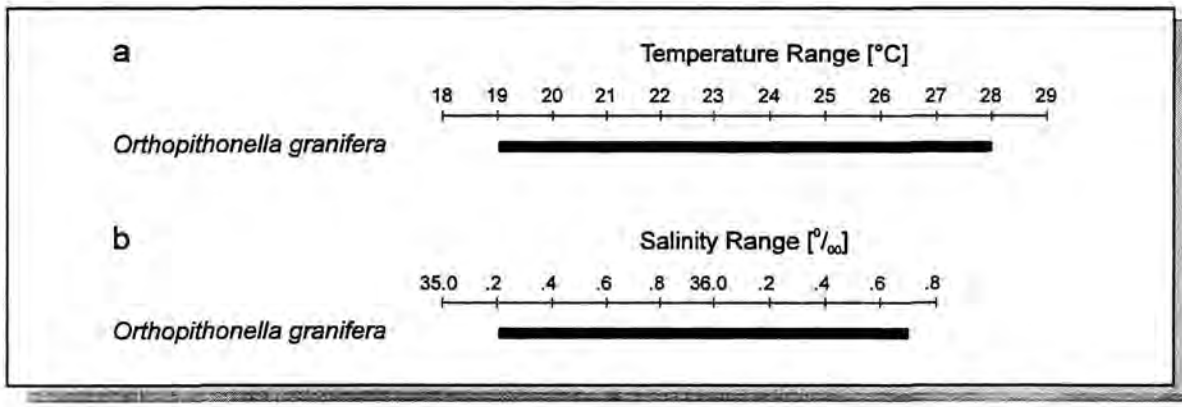

Fig. 39: Bar graphs of temperature (a) and salinity (b) ranges of *Orthopithonella granifera*.

- **Plankton:** "*Sphaerodinella*" *albatrosiana* is the most abundant calcareous dinocyst species in the equatorial East Atlantic Ocean (DALE & DALE, 1992; HÖLL, pers. comm.; JANOFSKE, pers. comm.; KARWATH, pers. comm.). In this study, the planktic distribution of "*Sph.*" *albatrosiana* is limited to the equatorial Atlantic and to waters warmer than 24°C (Fig.34). There, in every sample the cysts have been found abundantly (Fig.35) and sometimes in high numbers.

All specimens of "*Sph.*" *albatrosiana*, but one, are complete with the operculi still attached and covered with an outer organic phragma. These cysts are considered to be living cysts with cell content. A restriction to warm waters has been observed for "*Sph.*" *tuberosa* as well; it is not as abundant as "*Sph.*" *albatrosiana* (Fig.35) and shows a more scattered distribution, but displays a temperature range >24°C as well (Fig.34). It may be present in large numbers; thus "*Sph.*" *tuberosa* accounts for the high relative amount of calcareous dinocysts in sample 22-S23 (15%).

If the distribution of these calcareous cysts is positively temperature dependent, the distribution patterns should keep pace with the seasonal temperature shifts, and the temperature corresponding to the maxima of abundance should be more or less constant from month to month. Data from several plankton surveys (HÖLL, pers. comm.; JANOFSKE, pers. comm.; KARWATH, pers. comm.), including the present study, suggest a strong temperature dependence of **"*Sph.*" *albatrosiana* and "*Sph.*" *tuberosa***. Living specimens of these calcareous cysts are restricted to low-latitude waters and the geographical regions defined by the 24°C SST isotherm. They may be regarded as thermophytes or as **"warm water cysts"**. In waters colder than 24°C no such living calcareous "warm water cysts" have been recorded in the plankton.

For "*Sph.*" *tuberosa* a second limiting parameter for its planktic distribution has been observed: it shows a restriction to high salinity waters with SSS 35.5-36.3°/oo. In waters colder than 24°C and salinities below 35.5°/oo, no "*Sph.*" *tuberosa*-cysts have been recorded. The upper limit of this salinity range is very probably a secondary effect of the restricted SST range above 24°C. JANOFSKE (pers. comm.) recorded living specimens of "*Sph.*" *tuberosa* in waters with SSS up to 36.8°/oo; but observed the absence of this species in areas with SSS below 35.5°/oo as well.

On the other hand, "*Sph.*" *albatrosiana* seems to tolerate SSS well below 35.5°/oo. In low salinity waters of the equatorial East Atlantic, "*Sph.*" *albatrosiana* accounts for 3% of the shelled phytoplankton population. Other plankton surveys (JANOFSKE, pers. comm.; KARWATH, pers. comm.) have confirmed the correlation of "*Sph.*" *albatrosiana* distribution with wide SSS ranges.

DALE & DALE (1992) investigated sediment trap samples from the western tropical Atlantic (Table 31). One trap site was positioned above the Demarara Abyssal Plain (Station E) in an area of 26°C MA SST. Each year after snow-melt in the Andes and the rainy season, the ocean surface waters above Station E are diluted with freshwater run-off from the rivers Orinoco and Amazon; SSS has a high seasonality and extends from 35.0‰ to 36.5‰ (DESSIER & DONGUY, 1994). Another trap station (Station S) was located farther north moored in the Söhm Abyssal Plain in the western NAST. The MA SST is 23-24°C and the SSS is more or less stable and relatively high (36.75-37.0‰; DESSIER & DONGUY, 1994). DALE & DALE (1992) recorded "*Sph.*" *albatrosiana* maximum flux of ~13,800 cysts/m²·day in the lowermost trap of Station E. At Station S, they registered lower fluxes of 8,500 cysts/m²·day. "?Calcareous cysts sp." were described which were later identified as "*Sph.*" *tuberosa*. Low flux rates (63-78 cysts/m²·day) were recorded at Station E; but the fluxes of Station S were at least twice as high (114-171 cysts/m²·day).

This evidence suggests that, very probably, "*Sph.*" *albatrosiana* and "*Sph.*" *tuberosa* are characteristic and abundant species in the WTRA and ETRA biogeographic zones of LONGHURST et al. (1995), i. e. the equatorial Atlantic in this study. They are assumed to be frequent to abundant in the western part of the NATR and the north-eastern part of the South Atlantic Tropical Gyre (LONGHURST et al., 1995) as well. Both species may show similar distribution patterns regarding SST; but "*Sph.*" *tuberosa* will show a negative correlation to low SSS. This pattern may be determined not only in the plankton, but in the sediments as well.

It is remarkable that DALE & DALE (1992) recorded *Calciodinellum operosum* quite often in their sediment trap samples. At Station E, a considerable flux of *C. operosum* (112-184 cysts/m²·day) was observed, these flux rates exceed the rates of "*Sph.*" *tuberosa* by far. At Station S, *C. operosum* was found only in the uppermost trap and flux rates were lower (57 cysts/m²·day). Other plankton surveys (HÖLL, pers. comm.; JANOFSKE, pers. comm.; KARWATH, pers. comm.) have reported *C. operosum* only occasionally and in very low numbers but, nevertheless, with a SST range >24°C and SSS range of 35.5-36.0‰. Therefore, *C. operosum* may be another "warm water cyst" according to these distribution data and according to its close taxonomic relation to "*Sph.*" *albatrosiana*.

The distribution pattern of the vegetative-thecate species *Scrippsiella trochoidea* is obviously linked to the distribution of its calcareous cyst *Rhabdothorax erinaceus* (Table 31). Generally *S. trochoidea* is considered to be a neritic vegetative-thecate species in temperate waters. During the present study, it has been found in the equatorial Atlantic and off NW Africa in fully oceanic waters (Fig.37). In some samples cysts have been recorded as well. Both the thecae and the cysts have been found within extended temperature and salinity ranges (Fig.36).

According to the distribution of the thecae during this study, ***Rh. erinaceus*** is considered to be **ubiquitous**, **eurythermal**, **neritic** and **oceanic** as well. The cysts have been reported from coastal waters of high and low latitudes (WALL & DALE, 1968b; WALL et al., 1970) as well as from the plankton and sediments of tropical fully oceanic waters (FÜTTERER, 1977; DALE & DALE, 1992). But they have never been abundant.

DALE & DALE (1992) found *Rh. erinaceus* in relatively large numbers. In the trap station in the Söhm Abyssal Plain, flux rates of 28-85 cysts/m²·day were recorded. The flux rates in the Demerara Abyssal Plain were even higher (19-136 cysts/m²·day). In both trap stations, the highest flux rates were not recorded for the lowermost trap, but for an intermediate trap; thus indicating a lateral transport of an unknown amount of cysts within the water column.

Large variations in cyst shape and spinal lengths of *Rh. erinaceus* were confirmed for both plankton and sediment samples, and is assumed to be well within a natural range (KAMPTNER, 1937), even though no connection to oceanographic parameters could be made in the present study. Specimens of all morphologic variations have been found in warm and cooler waters as well as in high and low salinity areas.

Information on the present distribution of the "presumed" dinocyst *Orthopithonella granifera* is very limited (Table 31, Fig.39). As mentioned above, they are not easily recognized, neither by plankton workers nor palaeontologists working on nannoplankton.

»

Fig.40: The distribution pattern of *Orthopithonella granifera* is plotted in the temperature map (a), the salinity map (b), and the productivity map (c).

Fig.40: M23/3 Distribution of *Orthopithonella granifera*

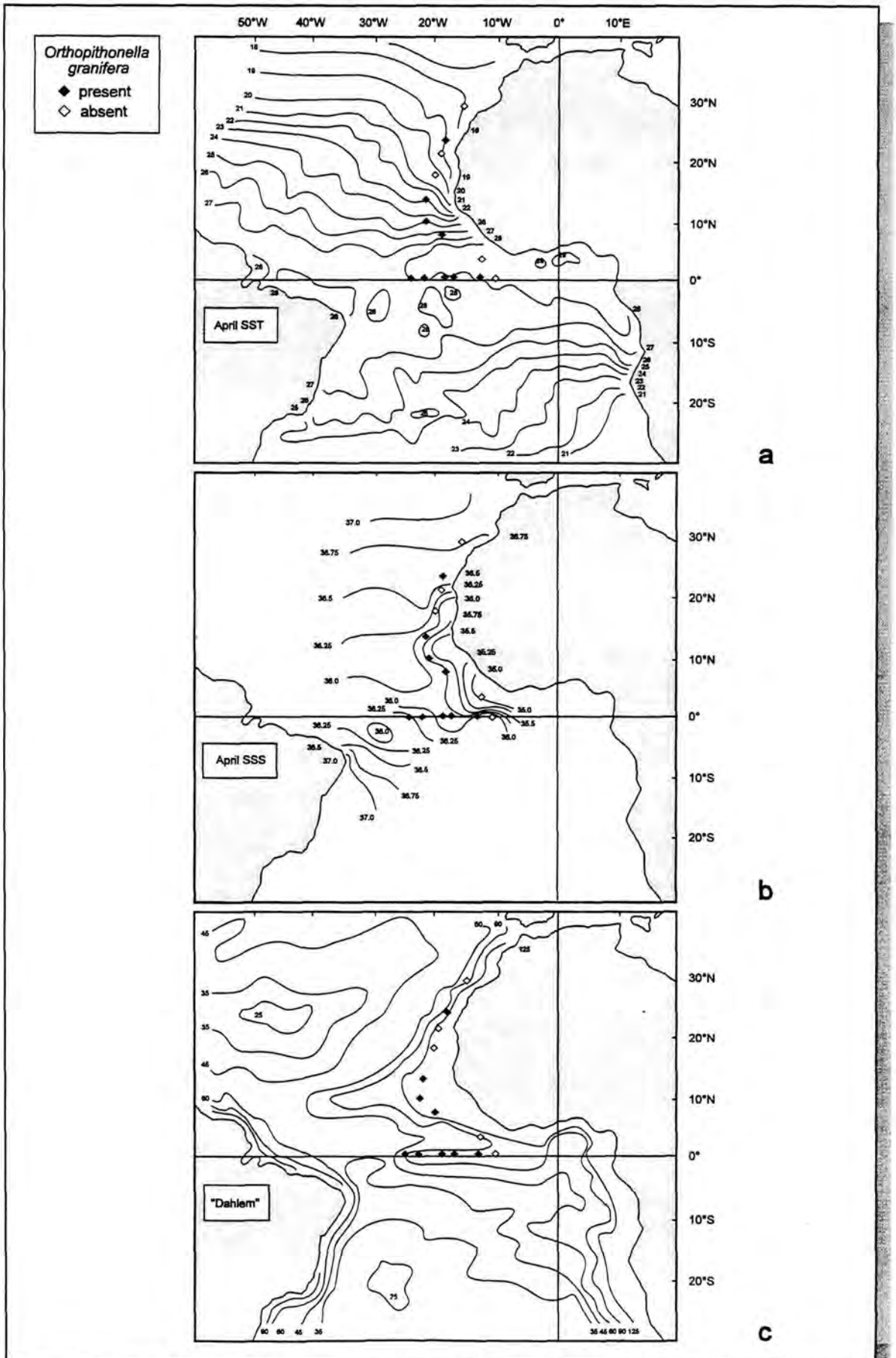

FÜTTERER (1977) originally reported *O. granifera* as being rare to abundant from the lower Pliocene onward. In their study DALE & DALE (1992) included this species together with *Thoracosphaera heimii* and counted them as small thoracosphaerids. They recorded fluxes of more than 35,000 thoracosphaerids/m²·day from the Panama Basin, but presented no data on the actual fluxes of *Th. heimii* or *O. granifera*.

In this study *O. granifera* has been recorded only in small numbers (Fig.40) and is not as abundant as *Th. heimii*. It has mostly been found in the equatorial Atlantic south of 15°N, both in the plankton and in the sediment samples. All this does not provide sufficient data to define *O. granifera*'s environmental requirements, or to suggest any biogeographical ranges, besides the sites discussed here. Future studies will have to establish, whether *O. granifera* may be regarded as a ubiquitous species, whether it is restricted to certain geographical areas with particular temperature and salinity ranges, or whether it requires distinctive nutrients for its metabolism.

- **Sediments:** The species assemblages of calcareous dinocysts in the sediments offshore NW Africa (off Cape Blanc) and in the eastern equatorial Atlantic (Guinea Basin) are clearly distinct (Table 31, Fig.38).

In the MUC samples of the Guinea Basin, the situation is completely different. Here, the specimen densities of "*Sph.*" *albatrosiana*-cysts are more than ten times as high as offshore NW Africa (1,414-1,821 spec./cm²). They add up to 74% and 78%. The specimen densities of "*Sph.*" *tuberosa* are three to five times as high as off Cape Blanc (379-518 spec./cm²). Nevertheless, they amount to only 21%. *C. operosum* is still a rare species in these sediments, it is absent in core GeoB 1607-8, but core GeoB 1606-7 shows a relatively high specimen density of 107 spec./cm² (4%) which is approx. fourteen times as high as off NW Africa. However, it may be assumed that the domination of "*Sph.*" *albatrosiana*-cysts and the low amount of "*Sph.*" *tuberosa*-cysts in the sediments of the Guinea Basin reflect the interaction of high SST and low SSS conditions in the eastern equatorial Atlantic.

Additional dinocyst data (Table 31, Fig.38) are available from a gravity core recovered from the continental shelf offshore Recife (Brazil). The western South Atlantic off Recife is influenced by the SEC which bifurcates into the northwestward flowing NBC and the southward flowing BC (PETERSON & STRAMMA, 1991). This area shows a very high MA SST (>27°C) with low seasonality (2°C, HASTENRATH & LAMB, 1977) and high SSS year-round (36.25-36.75‰, DESSIER & DONGUY, 1994). The calcareous dinocyst species assemblage of GeoB 2204-2 GL is heavily dominated by "*Sph.*" *tuberosa*-cysts (83%) (KARWATH, 1995), and therefore may reflect the controlling power of high SSS over high SST conditions in the western equatorial Atlantic surface waters.

While comparing the dinocyst assemblages offshore Cape Blanc with the assemblages of the eastern and western equatorial Atlantic, it may be assumed that at least the "warm water cysts" do not require high nutrient conditions. Specimen densities in the eastern equatorial Atlantic are three to fourteen times as high as offshore NW Africa, and thus may even indicate a negative correlation to enhanced nutrients in upwelling areas (HÖLL, pers. comm.).

Rh. erinaceus has only rarely been recorded in the sediments of the Guinea Basin, it amounts to 1% with 17 spec./cm² and 18 spec./cm². Most specimens of *Rh. erinaceus* found in sediment trap samples (DALE & DALE, 1992) or in the sediments (FÜTTERER, 1977; this study) have fully developed bases and long, but sometimes broken, spines. The skeletal elements are well connected and form a central body, which is rigid enough to withstand the sedimentation process. In case of weak or early calcification, the elements are only loosely packed and slightly attached on the organic part of the cyst wall. After the organism has decayed, the calcareous elements fall apart and are not embedded in the sediments. Thus, an unknown amount of *Rh. erinaceus*-cysts is lost during sedimentation processes, and the cyst data from the sediments give only rudimentary evidence on planktic abundances, which can be quite frequent.

An unknown amount of cysts may have been transported back and forth along the equator within the equatorial current system. Sediment trap studies (DALE & DALE, 1992; WEFER & FISCHER, 1993; LANGE et al., 1994; FISCHER & WEFER, 1996; TREPPKE et al., 1996) reported maximum flux rates not from the uppermost trap but from intermediate or the lowermost traps. These discrepancies may be the result of lateral transport in the water column.

Therefore, planktic distribution patterns observed during various plankton surveys (HÖLL, pers. comm.; JANOFSKE, pers. comm.; KARWATH, pers. comm.; this study), sediment flux rates (DALE & DALE, 1992), and abundances of calcareous dinocysts recorded in the sediments of the current study and by KARWATH (1995), are believed to be controlled by the interaction of SST and SSS (i.e. area of maximum planktic abundance), by nutrient availability, and by lateral transport. While examining cyst data from sediments, the appropriateness to draw any direct conclusions on the living vegetative-thecate biomass can be questioned.

5. DINOFLAGELLATE PRESERVATION IN LATE QUATERNARY SEDIMENTS

Palaeo-oceanographic reconstructions suggest that the atmospheric and oceanographic circulations in the tropical Atlantic have changed severely on glacial-interglacial time scales. In the palaeo-climatic history of the tropical East Atlantic, variations in the south- and northward flowing eastern boundary currents fundamentally affect the tropical Atlantic circulation and regional patterns of climatic change. It is generally believed that the large-scale glacial cycles are basically continuous linear responses to orbitally driven changes in the earth's radiation budget (IMBRIE et al., 1989, 1992a,b;). WEFER et al. (1996b) and various other studies demonstrated a strong response of SST, SSS, thermocline levelling, and surface water productivity in the tropical East Atlantic to precession-forced insolation changes in both hemispheres.

Reconstructions of glacial-interglacial oceanographic parameters and productivity may be extracted from proxies or indicators. Various plankton organisms are generally used as indicators for different parameters. All proxies/indicators have to be calibrated by comparing Recent oceanographic conditions with data from surface sediments.

Most shelled phytoplankton organisms are equipped with a rigid shell that commonly withstands the sedimentation process. They are preserved in the sediments and may be used as indicators for palaeo-oceanographic parameters and primary productivity. Unfortunately, most dinoflagellates decay in the upper water column and are not preserved in the sediments, even though they may account for a major part of the phytoplankton (see Chapter 4.1.). However, vegetative-coccoid dinoflagellates (*Thoracosphaera heimii*-shells) and dinocysts amount to only a small part of the phytoplankton but are frequently embedded into sediments. In tropical oceans the dinocyst assemblages are dominated by calcareous cysts. Dinosporin cysts are extremely rare and "tropical assemblages" of dinosporin cysts may be reported only after these cysts were extracted from a large bulk of sediment. In late Quaternary sediments of the equatorial Atlantic, HARLAND (pers. comm.) recorded the maximum total amount of 350 dinosporin cysts in 100 g (one hundred grams!) of sediment.

However, previous investigations of Holocene and Pleistocene sediments reported calcareous dinoflagellates, i.e. *Th. heimii*-shells and calcareous dinocysts, in considerable amounts (WALL & DALE, 1968b; WALL et al., 1970; FÜTTERER, 1977). Recent studies have emphasized the role these species play in the phytoplankton populations of tropical oceans.

In their sediment trap studies DALE & DALE (1992) recorded flux rates up to nearly 36,000 spec./m²·day of thoracosphaerids and more than 8,500 calcareous cysts/m²·day, together with trifling amounts of thecal remains and dinosporin cysts. To date, these flux rates have been confirmed by sediment data from the western and eastern equatorial Atlantic.

Gravity cores recovered from offshore Brazil showed overall amounts of calcareous dinoflagellates up to 20% (WEFER et al., 1994). In one of these cores KARWATH (1995) recorded an assemblage of calcareous dinoflagellates heavily dominated by *Th. heimii*-shells (68%), with "*Sphaerodinella*" *tuberosa* (26%) as the most abundant cyst species, and "*Sph.*" *albatrosiana* accounting for only 5%. Sediment surface samples from offshore NW Africa (off Cape Blanc) are dominated by *Th. heimii* (85%) as well and show only small amounts of "*Sph.*" *albatrosiana* (8%) and "*Sph.*" *tuberosa* (6%) (this study). This massive domination is not found in surface sediments of the Guinea Basin where *Th. heimii*-shells amount to 18-31%, with "*Sph.*" *albatrosiana* (50-52%) being the most abundant cyst species, and "*Sph.*" *tuberosa* accounting for only 13-15% of the calcareous dinoflagellate assemblage (this study). The other calcareous dinocysts (*Calciodinellum operosum*, *Orthopithonella granifera* and *Rhabdothorax erinaceus*) amount to only a few percent each (KARWATH, 1995; this study).

In the present study, relationships have been defined for calcareous dinoflagellate distribution patterns and the corresponding oceanographic parameters such as SST, SSS, productivity, and lateral transport within the water column (Chapters 4.2.2. and 4.3.).

From the present state of knowledge it may be assumed that "*Sph.*" *albatrosiana* and "*Sph.*" *tuberosa* both depend on SST warmer than 24°C and may be regarded as "warm water cysts"; the latter species shows a second restriction to waters with SSS higher than 35.5‰. A morphological transition between "smooth" "*Sph.*" *albatrosiana*-cysts and paratabulated *C. operosum*-cysts has been observed, and it is presumed that these two "species" are close systematic relations or even variations of the same species. Owing to its relation to "*Sph.*" *albatrosiana*,

C. operosum is considered to be a "warm water cyst" as well, even though it has not been found in the plankton samples of this study. The environmental requirements of *O. granifera* are very poorly known and, so far, relationships to oceanographic parameters have not been observed.

Observations on the planktic distribution of *Th. heimii* point to a negative correlation with waters influenced by upwelling; but on the other hand, sediment data from offshore Cape Blanc have revealed an overwhelming domination of *Th. heimii*-shells which are at least twice as abundant as in the Guinea Basin suggesting a productivity twice as high. This contradicting evidence raises doubt as to the utility of *Th. heimii* as a general indicator for dinoflagellate productivity, or may be simply the result of lateral transport.

During the last deglaciation, which lasted approximately 10,000 years, the northern hemisphere was transformed from maximum chilly glacial climate to maximum heated interglacial climate (JANSEN, 1992). The enormous ice sheets over North America and Europe melted and disappeared during this short time interval. Huge amounts of melt-water were injected into the North Atlantic (FAIRBANKS, 1989), which led to increasing water stratification and decreasing SST and SSS (DUPLESSY et al., 1992). Both effects led to reduced evaporation, enlarged precipitation, and lower polewards advection of saline subtropical water. At this time interval, including the Younger Dryas cold phase (BERGER, 1990), the ocean circulation patterns were significantly different from the present and from that of the Last Glacial Maximum (LGM) (JANSEN, 1992).

So far, there exist many reconstructions of glacial-interglacial variations of tropical Atlantic oceanography. There is abundant evidence for increased biological productivity during glacial times (i.a. SARNTHEIN et al., 1988; MIX, 1989; SCHNEIDER, 1991; MÜLLER et al., 1994; SIKES & KEIGWIN, 1994; CHAPMAN et al., 1996; SCHNEIDER et al., 1996). Mean annual SST oscillation, variations in SST seasonality, fluctuations in the surface current system, and changes of thermocline depth are documented (i.a. MIX et al., 1986a, b; MCINTYRE et al., 1989; RAVELO et al., 1990; KEMLE-VON MÜCKE, 1994; SIKES & KEIGWIN, 1994, 1996; BILLUPS & SPERO, 1996; MIX & MOREY, 1996; PFLAUMANN et al., 1996). Large variations in the salinity of the North Atlantic were linked to modifications in the strength of the thermohaline circulation and thus to changes of NADW production (i.a. FAIRBANKS, 1989; JANSEN & VEUM, 1990; BICKERT, 1992; SARNTHEIN et al., 1994; SIKES & KEIGWIN, 1996; ANDRIÉ, 1996; DUPLESSY et al., 1996; RHEIN et al., 1996).

- SST reconstructions have been achieved by various methods. Stable isotope analyses and planktic foraminiferal assemblage estimates from deep-sea sediments provide information about variations of mean annual temperature and seasonality.

The transfer technique for palaeo-temperature estimates (CLIMATE: LONG-RANGE INVESTIGATION, MAPPING, AND PREDICTION [CLIMAP], 1981) is based on factor analysis of species abundance data, usually distribution data of planktic foraminifera, and is widely used (MOLFINO et al., 1982; MIX et al., 1986a; IMBRIE et al., 1989a; MCINTYRE et al., 1989; MEINECKE, 1992). Seasonal regression equations yield calculations of warm season (Tw) and cold season (Tc) SST (MIX et al, 1986a, b; MCINTYRE et al., 1989). The standard errors of these palaeo-temperature equations are 1.2°C and 1.3°C for the warm and cold seasons, respectively (MOLFINO et al., 1982).

The modern analogue technique (MAT) is based on the degree of dissimilarity between fossil and modern faunal assemblages in a specified SST range (MCINTYRE et al., 1989; MEINECKE, 1992).

The stable isotope composition of calcareous foraminifera tests have been extensively applied in palaeo-oceanography. The biota of living foraminiferal species assemblages are controlled by oceanographic parameters. Planktic foraminifera live in and across the thermocline. They actively respond to changes in the hydrographic properties of the surrounding waters and calcification happens in isotopic equilibrium with these waters (FAIRBANKS et al., 1980, 1982). Recent observations (KEMLE-VON MÜCKE, 1994) on various foraminifera species have shown that the calcification process of the miscellaneous species happens at distinctive but different water depths.

Recently, a biomarker-based method has been developed for reconstructing past SST from marine sediments (BRASSEL et al., 1986). This method is based on the unsaturation ratio of alkenones which are biosynthesized by a restricted group of prymnesiophyte algae. The U^{k}_{37} index is considered to register the temperature during the season of maximum coccolith growth, i.e. predominantly records winter and spring mixed layer SST conditions. An alternative to other SST recontructions is provided by this

method, and by now is used routinely (MÜLLER et al., 1994; SIKES & KEIGWIN, 1994, 1996; SCHNEIDER et al, 1995, 1996; ZAO et al., 1995; CHAPMAN et al., 1996; SIKES & KEIGWIN, 1996).

The study of SIKES & KEIGWIN (1994) directly compared alkenone and transfer function temperature estimates in the equatorial Atlantic; both methods showed a similar glacial to interglacial SST increase (~1.6°C). CHAPMAN et al. (1996) suggested that the dual use of faunal and alkenone SST reconstructions may give further evidence of mixed layer and productivity changes.

- **SSS reconstructions** have been accomplished together with glacial-interglacial SST estimations by means of micropalaeontological and stable-isotope records (BROECKER, 1989; DUPLESSY et al., 1992, 1996; Sikes & Keigwin, 1996). Obviously, MA SSS during the LGM was considerably higher than today; DUPLESSY et al. (1996) estimated a positive salinity anomaly of 1‰ and suggested a MA SSS of ~38‰ for the tropical Atlantic.

Low salinities and/or high temperatures result in reduced $\delta^{18}O$ records of foraminiferal tests. The $\delta^{18}O$-based SST signals during deglaciation have a considerable ice-volume effect (FAIRBANKS, 1989). And, decreased SSS generally reflect a thinner surface mixed layer with thermal fluctuations.

SIKES & KEIGWIN (1994) suggested that isotope-based SST estimates may reflect not only temperature variations but surface salinity and subsurface thermocline changes as well. They confirmed the conclusion of RAVELO et al. (1990) that foraminiferal methods do not always lead to the best palaeo-SST estimates. Thus, besides SST distributions, oceanographic conditions within or below the thermocline are reflected by foraminiferal estimates. So far, no proxy is available that would respond directly to palaeo-salinity shifts.

- **Surface water productivity** changed on glacial-interglacial time scales because of variations in trade wind velocity (SARNTHEIN et al., 1982). Increasing trade wind velocity should simultaneously elevate the thermocline in the east and depress the thermocline in the western tropical Atlantic, heightening productivity in the east and reducing it in the west (VERARDO & MCINTYRE, 1994).

Global changes in productivity may have happened according to mean changes in the ocean's nutrient concentration or because of changes in the mixing rate between the nutrient-rich deep water masses and nutrient-poor but oxygenated photic surface layer (CURRY & LOHMANN, 1990).

- **Intercore stratigraphic correlation** of gravity or piston cores is routinely established by stable isotope records of planktic foraminifera. Age models for cores are produced by identifying isotopic events in each $\delta^{18}O$ isotopic record. The resulting record is then correlated to the SPECMAP oxygen isotope stacked record of IMBRIE et al. (1984). To generate final linear sedimentation-rate/age-models, the chronology of MARTINSON et al. (1987) is usually applied. Furthermore, a radiocarbon chronology may be established by using accelerator-mass-spectrometer (MAS) dating for key stratigraphic events or for all core samples.

Special problems have occurred with the dating of the MUC samples of the present study. The estimated sedimentation rate offshore NW Africa, i.e. for core GeoB 1602-7 off Cape Blanc, is ~3 cm/ka (ANDERSON, 1996). For the northwestern Guinea Basin, where cores GeoB 1606-7 and GeoB 1607-8 were obtained, WEFER et al. (1993) estimated a mean sedimentation rate of ~2 cm/ka for a neighbouring gravity core covering the last 370 ka.

But any direct interpolations of ages and sedimentation rates for the surface sediments are problematic, because the surface sediments are not compressed and still fully waterlogged, and the deglaciation time intervals are so densely packed that bioturbation must be considered a notable influence. Furthermore, the conversion of ^{14}C- or $\delta^{18}O$-ages into calendar years ("true age") is non-linear. In this study, to get any age references at all, the sedimentation rates are taken at face value. But, even very subtle sedimentation variations will lead to significant changes of age assignments and thus can gravely alter the interpretation of glacial-interglacial deep sea sediments.

Fig.41: The specimen densities of calcareous dinoflagellates on SEM stubs are plotted for core GeoB 1602-7 MUC (off Cape Blanc).

Fig.41: GeoB 1602-7 MUC Specimen Densities

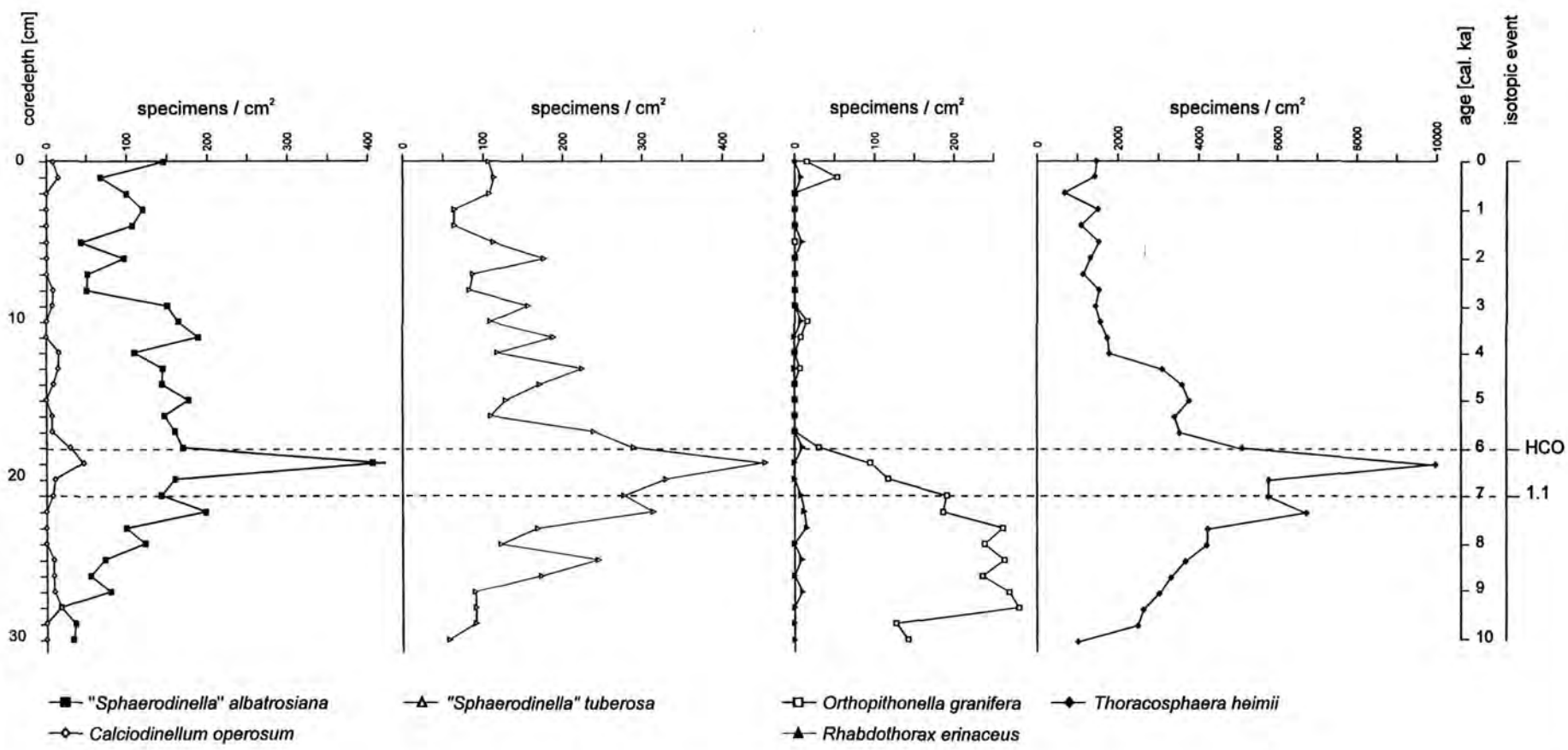

The isotope stages are defined as follows: Stage 1 (interglacial): 0-12.0 ^{14}C thousand years before present (^{14}C ka BP), Stage 2 (glacial): older than 12.0 ^{14}C ka BP. The radiocarbon ages are converted to calendar years using the calibration of BARD et al. (1993), and the corresponding calendar age would be 14.0-28.0 calendar ka BP for Stage 2. The following time intervals are applied to discuss the current sediment data, and age references are expressed as calendar years (ka BP):

- During the interval **0-8.0 ka BP**, the **Modern Ocean** circulation and sedimentation processes were achieved. The interval corresponds with the Warming Phase 2 of CHAPMAN et al. (1996). The Holocene Climatic Optimum (HCO) occurred 6.0 ka ago.
- **Isotopic Event 1.1** happened **7.0 ka BP** and represents the climatic changes between early and middle Holocene.
- **Deglaciation** happened during the interval **8.0-14.0 ka BP**, which agrees with Warming Phase 1 of CHAPMAN et al. (1996); and was "interrupted" by the Younger Dryas cooling event, which is represented by interval 12.0-13.0 ka BP.
- **Isotopic Event 2.0** occurred **14.0 ka ago**.
- The **Glacial Ocean** circulation is represented in interval **14-28 ka BP**. The Last Glacial Maximum (LGM) 21.5-23.5 ka BP is not included in the multicorer sediment samples. Nevertheless, a short overview of the oceanography during LGM is given in the current study.

The sediments of GeoB 1602-7 MUC (Fig.41, Fig.42) from offshore Cape Blanc represent the last 10.0 ka. The cores from the Guinea Basin cover the last 15 ka bp (GeoB 1606-7 MUC, Fig.43, Fig.44) and 17.0 ka bp (GeoB 1607-8 MUC, Fig.45, Fig.46) respectively, including Isotopic Event 2.0 and the Younger Dryas chronozone.

For the interpretation of calcareous dinoflagellate abundances in the sub-Recent sediments it has been assumed that the ecology of glacial-interglacial species assemblages has not changed and that the planktic distributions were then restricted by the same environmental parameters as they are today. However, the composition of the plankton assemblage entering the sedimentary record is modified significantly owing to breakage during sedimentation, selective dissolution, lateral transport, and other factors (see Chapters 4.2.2. and 4.3.). In addition, immense fluctuations in biological, physical, and chemical processes in the surface waters occur on much shorter time scales than are relevant for the fossil record.

5.1. GLACIAL OCEAN (28-14 ka BP)

It is now considered proven that the circulation of the ocean during the LGM was very different from the present. CHAPMAN et al. (1996) suggested that the glacial surface hydrography of the eastern tropical Atlantic resembled conditions that presently exist in the mid-latitudinal North Atlantic.

During the last glacial period and the deglacial, the planktic foraminiferal SST estimates offshore NW Africa yield colder SST conditions, reflecting enhanced surface advection by the CC, and intensified regional upwelling resulted in higher surface productivity (MIX et al., 1986a, b; MCINTYRE et al., 1989; RAVELO et al., 1990; CHAPMAN et al., 1996). A strong front between 15-20°N separated the cold CC (<18°C) from the warm equatorial waters (MIX et al., 1986a). The season of maximum NE trade wind intensity, which was generally stronger than today, may have expanded from late spring into summer, thus altering the pattern of mixing of nutrient-rich waters and other hydrographic properties (SARNTHEIN et al., 1981; HOOGHIEMSTRA, 1988). These interactions could produce high-productivity summer conditions comparable to the spring bloom in the modern ocean (CHAPMAN et al., 1996).

Sediments of the equatorial Atlantic reflect a glacial cooling of the sea surface associated with enhanced upwelling and productivity, together with a strong advection of eastern boundary currents which may have penetrated further into the lower latitudes than today, but apparently not into the Guinea Basin (JANSEN et al., 1996; MIX & MOREY, 1996; SCHNEIDER et al., 1995, 1996; WEFER et al., 1996b).

5.1.1. LAST GLACIAL MAXIMUM (23.3-21.5 ka BP)

The reconstruction of SST during peak glacial time conducted by the CLIMAP-Project (1981) suggested that, except in the equatorial divergence zone, little change occurred between glacial and interglacial time in the tropics. Their glacial SST estimates in the eastern part of the tropical Atlantic were cooler by only about 2°C relative to modern values. The annual thermal equator was located in the northern hemisphere, between 0° and 10°N, as it is today.

At the LGM enhanced trade wind fields such as suggested by MULITZA (1994) and WEFER et al. (1996a,b) may indicate an increase in equatorial upwelling, resulting in a shallower thermocline (KEMLE-VON MÜCKE, 1994) and in an increase in productivity of as much as four times over present day (SIKES & KEIGWIN, 1994). Estimated productivity rates of the LGM are highest along the equator, about 120 $gC/m^2 \cdot a$, and not in the eastern boundary currents as it is today (MIX, 1989; MEINECKE, 1992).

Probably, the production and flow of oxygenated NADW was drastically diminished (by about 40%, DUPLESSY et al., 1996), and in the deep North Atlantic the less ventilated AABW-layer was thicker and more widespread than today; this would have resulted in a higher NADW-AABW boundary and a general northward transport of water masses in the lower water column (BICKERT, 1992; SARNTHEIN et al., 1994; BERGER & WEFER, 1996). The reduction in NADW formation led to a nutrient-rich glacial deep ocean, but simultaneously the well ventilated intermediate waters, which today show a strong nutrient maximum, became depleted in nutrients (JANSEN, 1992; BERGER & WEFER, 1996).

The North Atlantic benthic $\delta^{18}O$ record indicates that glacial deep waters were ~3°C colder than at present; and the planktic record indicates a glacial-to-Holocene SST increase of ~7°C (JANSEN & VEUM, 1990).

5.1.2. GLACIAL OCEAN (17-14 ka BP)

RESULTS:

- **In the Guinea Basin** in sub-Recent sediments which are older than Isotopic Event 2.0, the calcareous dinoflagellate assemblage is dominated by *"Sph." albatrosiana* which amounts to 50% at 17.0 ka ago decreasing slightly to 40% in younger sediments (Fig.44, Fig.46). During this time interval the relative amount increased for *Th. heimii* (10-30%) and *"Sph." tuberosa* (10-20%%, and the amount of *O. granifera* was reduced from 10% to below 5%.

The lowermost two samples of core GeoB 1606-7 represent Isotope Stage 2, and display decreasing specimen densities for all species (Fig.43).

In GeoB 1607-8 MUC (Fig.45) *"Sph." albatrosiana*, *"Sph." tuberosa*, and *Th. heimii* show a synchronous increase in specimen densities during 17.0-15.5 ka BP, followed by a simultaneous decrease from 15.5 ka BP to 14.5 ka BP, and another subsequent rise until 14.0 ka BP. *C. operosum* shows the same pattern of rise and fall, but with a slight positive time lag of 0.5 ka; the maximum abundance for *C. operosum* has been observed at 15.5 ka BP. The maximum specimen density of *O. granifera* occurs at 17.0 ka BP decreasing stepwise until 14.0 ka BP, interrupted by a small peak at 15.5 ka BP. Only in the lowermost sample *Rh. erinaceus* has been found in very small numbers.

DISCUSSION:

For Isotopic Event 2.0 SST estimates of various methods suggested MA SST as low as 23-24°C (MIX et al., 1986a) and as high as 26-27.5°C (SIKES & KEIGWIN, 1994). CLIMAP (1981) suggested that SST in the eastern part of the tropical Atlantic were cooler by only about 2°C relative to modern values.

A decrease in equatorial upwelling since the LGM may have caused a deepening of the thermocline and the mixed layer. The SST reconstructions proclaimed a high seasonality during the LGM in the eastern equatorial Atlantic (CLIMAP, 1981; MIX et al., 1986b; MCINTYRE et al., 1989). From 17.0 ka BP to 14.0 ka BP seasonality decreased from 3-6°C to 3-2.5°C (MCINTYRE et al., 1989; SIKES & KEIGWIN, 1994). So far, it is still unknown if and how the calcareous dinoflagellates react to different annual temperature variations. But it is remarkable that, with decreasing seasonality, the "warm water cysts" show an overall increase in abundances and that *Th. heimii* exhibits the same pattern.

According to reconstructions of DUPLESSY et al. (1990) the SSS offshore NW Africa was about 36.5-38.0‰ in the LGM, diminishing to salinities below 34.0‰ during 4.5 ka, followed by an even more extensive increase to salinities of about 38.0‰ until Isotopic Event 2.0. The abundance of *"Sph." tuberosa* in core GeoB 1607-8 closely resembles this pattern.

5.2. DEGLACIATION (14-8 ka BP)

The disintegration of the large northern hemisphere ice sheets happened in two major steps, and the transfer of melt-water was more or less concentrated in those intervals of most rapid sea-level rise.

Fig.42: GeoB 1602-7 MUC Relative Amount of Species

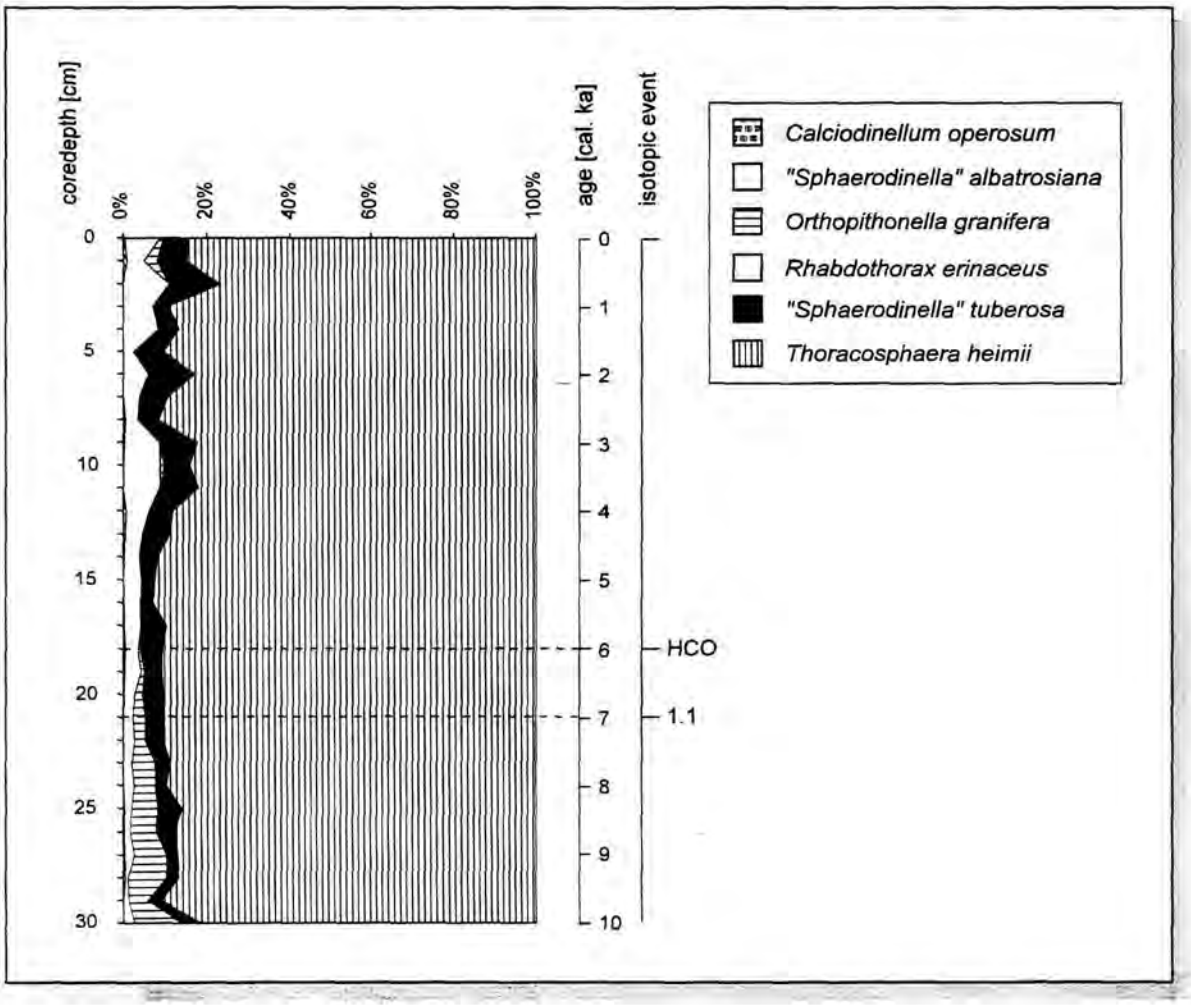

Fig. 42: Relative amount of recorded calcareous dinoflagellate species is plotted as cumulative curve for sediment core GeoB 1602-7 MUC (off Cape Blanc).

According to FAIRBANKS (1989), the glacial sea level was approximately 121 m below the present; deglaciation happened in two major steps from ~14.0-13.0 ka BP and ~12.0-8.0 ka BP separated by a mid-deglacial pause with little or no ice volume loss, the Younger Dryas. The rate of melt-water transfer of these steps was about five times higher than during the period in between. During the first phase of deglaciation, the sea level increased gradually and ended with an exceedingly rapid sea level rise of 24 m in less than 1.0 ka. This first most intense melt-water pulse (mwp-IA) happened between ~14.2 ka BP and 13.7 ka BP (FAIRBANKS, 1989; JANSEN & VEUM, 1990; CLARK et al., 1996; SIKES & KEIGWIN, 1996).

The beginning of the Younger Dryas chronozone (13.0-12.0 ka BP) was marked by a minimum rate of sea level rise; the last half of the Younger Dryas was characterized by reactivated sea level rise, followed by a second intense melt-water pulse (mwp-IB) from ~11 to ~10 ka BP (FAIRBANKS, 1989; JANSEN & VEUM, 1990; CLARK et al., 1996; SIKES & KEIGWIN, 1996). The rapid melting of the northern hemisphere ice sheets must have inserted large amounts of low-$\delta^{18}O$ melt water into the North Atlantic during boreal summer (FAIRBANKS, 1989; BARD et al., 1990; SIKES & KEIGWIN, 1994, 1996; CLARK et al., 1996). The benthic and planktic $\delta^{18}O$ records show the two major deglacial

steps in significant $\delta^{18}O$ decrease. It is uncertain to what extent these $\delta^{18}O$ anomalies have been caused by reduced SSS or increasing SST conditions.

During deglaciation, the warm seasons of the tropics may have been more strongly influenced by monsoons than today (MCINTYRE et al., 1989), or a strong divergence may have occurred at a different time of the year (MOLFINO & MCINTYRE, 1990). In their model of an ice age cycle MIX & MOREY (1996) associated diminished trade winds and equatorial upwelling with high SST during their ice melting phase. A stable freshwater layer in low latitudes would reduce the downward penetration of solar heating in summer and could actually result in increased SST, especially at a time of enhanced summer insolation (STREET-PERROTT & PERROTT, 1990). In the central and eastern equatorial Atlantic, the thermal equator may have been located south of the geographic equator (MIX et al., 1986a), though oceanographic conditions in the Gulf of Guinea may have been relatively stable compared to present time conditions (MIX & MOREY, 1996; JANSEN et al., 1996

MATTHEWSON et al. (1995) reported a dramatic decrease of carbonate content in sediments offshore NW Africa from 16.0 to 14.0 ka BP.

The production of oxygenated deep water masses through vertical overturn happened both at the LGM and in the first, slow deglacial phase, and only the first major deglacial melt-water pulse was able to turn off the formation of oxygenated deep water as the North Atlantic was covered by melt-water lenses (SARNTHEIN et al., 1994). Therefore, below 2,000 m, the deep water masses of the Atlantic Ocean were weakly differentiated, owing to the lack of influx of more ventilated deep and intermediate waters from the north. Only poorly ventilated deep water from the southern hemisphere flowed northward. The incursion of AABW was much enlarged below 4,000-4,500 m but decreased rapidly to upper water levels (3,500 m). Deep waters became better oxygenated in the Younger Dryas period, when the total deglacial melt-water release was markedly reduced.

Deglaciation Step 1 and the Younger Dryas chronozone lasted for about 1,000 years each. This is a very short time span represented only by three samples within the multicores. Even slight discrepancies in sedimentation rates can alter the age settings and thus seriously affect interpretation.

5.2.1. DEGLACIATION STEP 1 (14.0-13.0 ka BP)

RESULTS:

- **In the Guinea Basin**, for all but one of the calcareous dinoflagellate species, an interval of specimen density increase has been observed (Fig.43, Fig.45). In core GeoB 1607-8 the maximum abundances of *Th. heimii*, *"Sph." albatrosiana*, and *"Sph." tuberosa* have occurred in this interval. In core GeoB 1607-8 the specimen density of *O. granifera* has decreased from 14.0 ka BP to 13.5 ka BP. *Rh. erinaceus* has not been recorded.

The relative amounts of the assemblages do not change significantly during this time (Fig.44, Fig.46).

DISCUSSION:

During this first phase of deglaciation, the total sea-level rise was 44 m and a huge amount of low-$\delta^{18}O$ melt-water was discharged into the Gulf of Mexico (FAIRBANKS, 1989; BERGER, 1990; JANSEN & VEUM, 1990; CLARK et al., 1996; SIKES & KEIGWIN, 1996).

For Isotopic Event 2.0 in the eastern equatorial Atlantic reconstructions have shown mean annual SST as low 23-24°C (MIX et al., 1986a) and as high as 28.8°C (SIKES & KEIGWIN, 1994), the seasonality estimates have yielded the same high discrepancies (2-3°C, MCINTYRE et al., 1989; 6-7°C, BILLUPS & SPERO, 1996). The "warm water cysts" display a significant abundancy rise for both cores in the Guinea Basin and thus suggest SST conditions similar to the present ones.

In GeoB 1607-8 MUC *"Sph." tuberosa* shows its maximum abundance synchronous with the highest salinity estimates of DUPLESSY et al. (1990) shortly after Isotopic Event 2.0. From 14.0 ka BP to 13.0 ka BP they estimated a SSS decline of more than 3‰.

5.2.2. YOUNGER DRYAS EVENT (13.0-12.0 ka BP)

During the last deglaciation, after the temperature of northern Europe had increased almost to present-day warmth, the glacial meltdown was interrupted by the Younger Dryas Event and a sharp return to almost full glacial temperatures in the North Atlantic and Europe.

The Younger Dryas chronozone in sub-Recent marine sediments is characterized by both reduced deglaciation rates and minimal glacial melt-water discharge (FAIRBANKS, 1989; JANSEN & VEUM, 1990; CLARK et al., 1996). It is distinguished as an event primarily by its temporal position between two episodes of lower surface salinity (FAIRBANKS, 1989). A relatively open and ice-free North Atlantic Ocean resulted in deep-water convection (JANSEN & VEUM, 1990).

BERGER (1990) extensively discussed various likely causes for the Younger Dryas "cold spell". He considered three main causes for this abrupt climatic change: 1) the positive feedback loop of the climatic system could have been put into reverse (albedo, CO_2, ocean circulation), 2) disturbance from internal threshold feedback (collapse of ice-sheets after melting of shelf ice), and 3) outside disturbance or system-external forcing (volcanism, solar output, supernova, cosmic dust). Rerouting the melt-water outflow from the Mississippi to the St. Lawrence River provides another possibility for climate disruption. The stable isotope record shows a major anomaly in the Gulf of Mexico during the first half of deglaciation, which has been interpreted as melt-water input from the Laurentide Ice Sheet (BERGER, 1990).

In the North Atlantic, sharp negative salinity anomalies were associated with the Younger Dryas cold events. Melt-water discharge was small and the deep-water density did not change greatly, but the surface density decreased significantly and therefore greatly enhanced the stratification of the North Atlantic and reduced the production of NADW (DUPLESSY et al., 1992). The NADW was flowing southward from the Norwegian-Greenland Sea to the equator at a depth between 2,300 m and 3,700-4,000 m. Its boundary to the AABW lay at about the same depth as today (SARNTHEIN et al., 1994). Carbon isotope data indicate a sharp increase in oxygenation, and the formation of extremely cold deep waters during this cold phase. After the Younger Dryas, SST rose quickly again during the next deglacial step (JANSEN, 1992).

RESULTS:

For *Th. heimii*, this chronozone represents the maximum abundance in GeoB 1607-8 MUC (Fig.45), but in GeoB 1606-7 MUC only a small peak is observed (Fig.43). In GeoB 1606-7 "*Sph.*" *albatrosiana* displays high abundance in the middle of the Younger Dryas rapidly decreasing to the end of this interval; in core GeoB 1607-8 there is a slight decrease throughout the zone. "*Sph.*" *tuberosa* shows a gradual decease in GeoB 1606-7 and a shallow minimum in GeoB 1607-8. *O. granifera* shows high abundance in GeoB 1606-7 and only a slight peak in GeoB 1607-8. For *C. operosum* a shallow peak is observed in GeoB 1607-8, and a slight decrease in GeoB 1606-7. *Rh. erinaceus* was absent in both cores.

The relative amounts of the calcareous dinoflagellate assemblage do not change significantly in both cores (Fig.44, Fig.46).

DISCUSSION:

The Younger Dryas cold conditions were established at 13.0 ka BP, and lasted for about 1.0 ka. A change of the melt-water flow path may have reduced Mississippi run-off significantly, and thus caused minimal release of melt-water into low-latitude waters (BERGER, 1990; JANSEN & VEUM, 1990) and a small salinity increase of 1‰ (DUPLESSY et al., 1992). MA SST and seasonality reconstructions for the eastern equatorial Atlantic differ slightly from present temperature conditions. According to MIX et al. (1986a, b) and MCINTYRE et al. (1989) the mean annual SST was 26°C and seasonality was 2-4°C.

The "*Sph.*" *tuberosa*-signal from either core shows a decline which may indicate a more significant SST decrease neutralizing a minor SSS increase. The prevalent reduction of "*Sph.*" *albatrosiana* abundance may be interpreted as a reaction to lower SST as well.

Equatorial productivity may have been higher (MOLFINO & MCINTYRE, 1990) or lower (MIX et al., 1986a) than today. For *Th. heimii* a very high abundance peak has been observed in GeoB 1607-8, but the increase in GeoB 1606-7 is quite small.

➳

Fig.43: The specimen densities of calcareous dinoflagellates on SEM stubs are plotted for core GeoB 1606-7 MUC (Guinea Basin).

Fig.43: GeoB 1606-7 MUC Specimen Densities

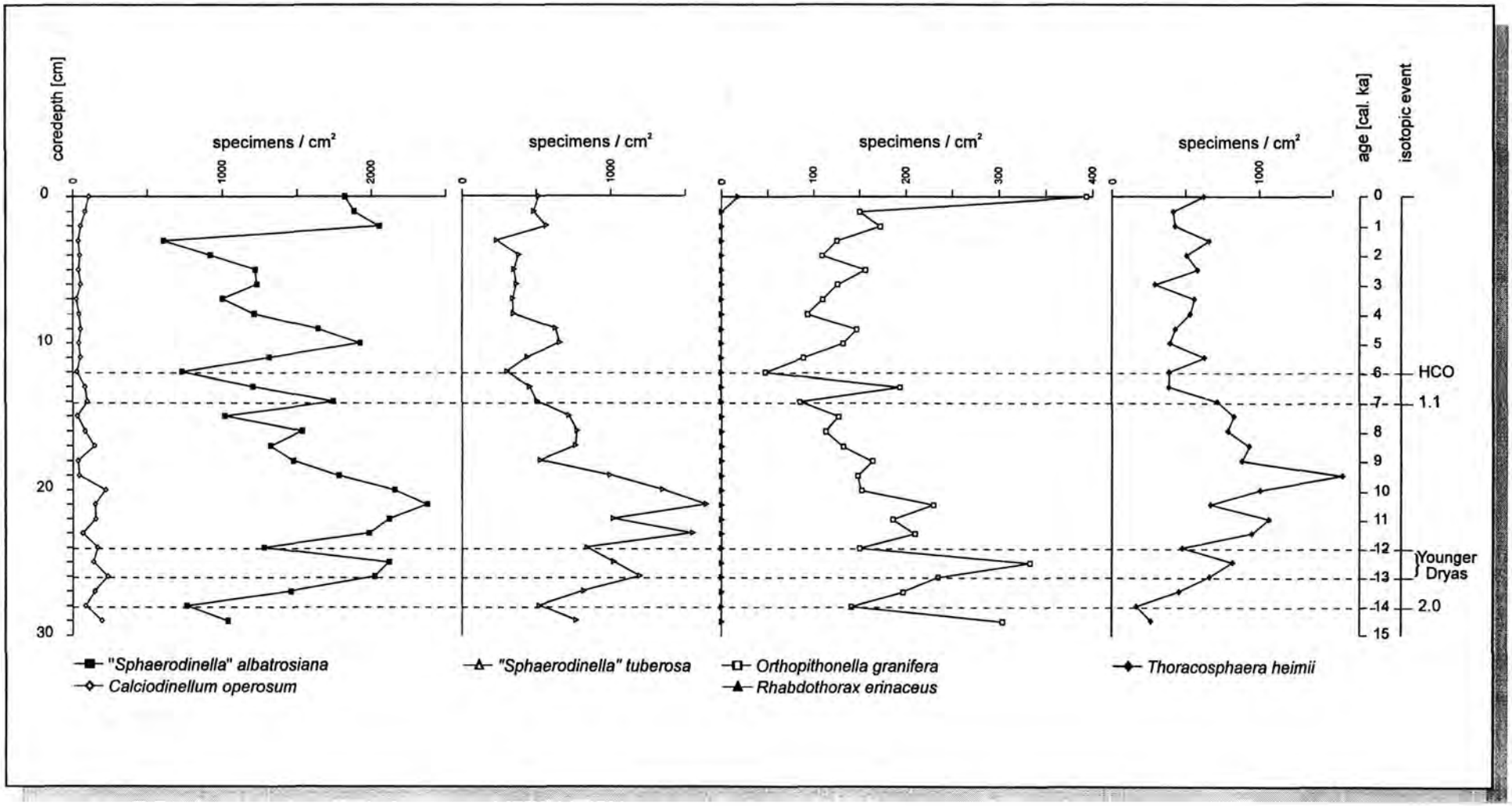

Fig.44: GeoB 1606-7 MUC Relative Amount of Species

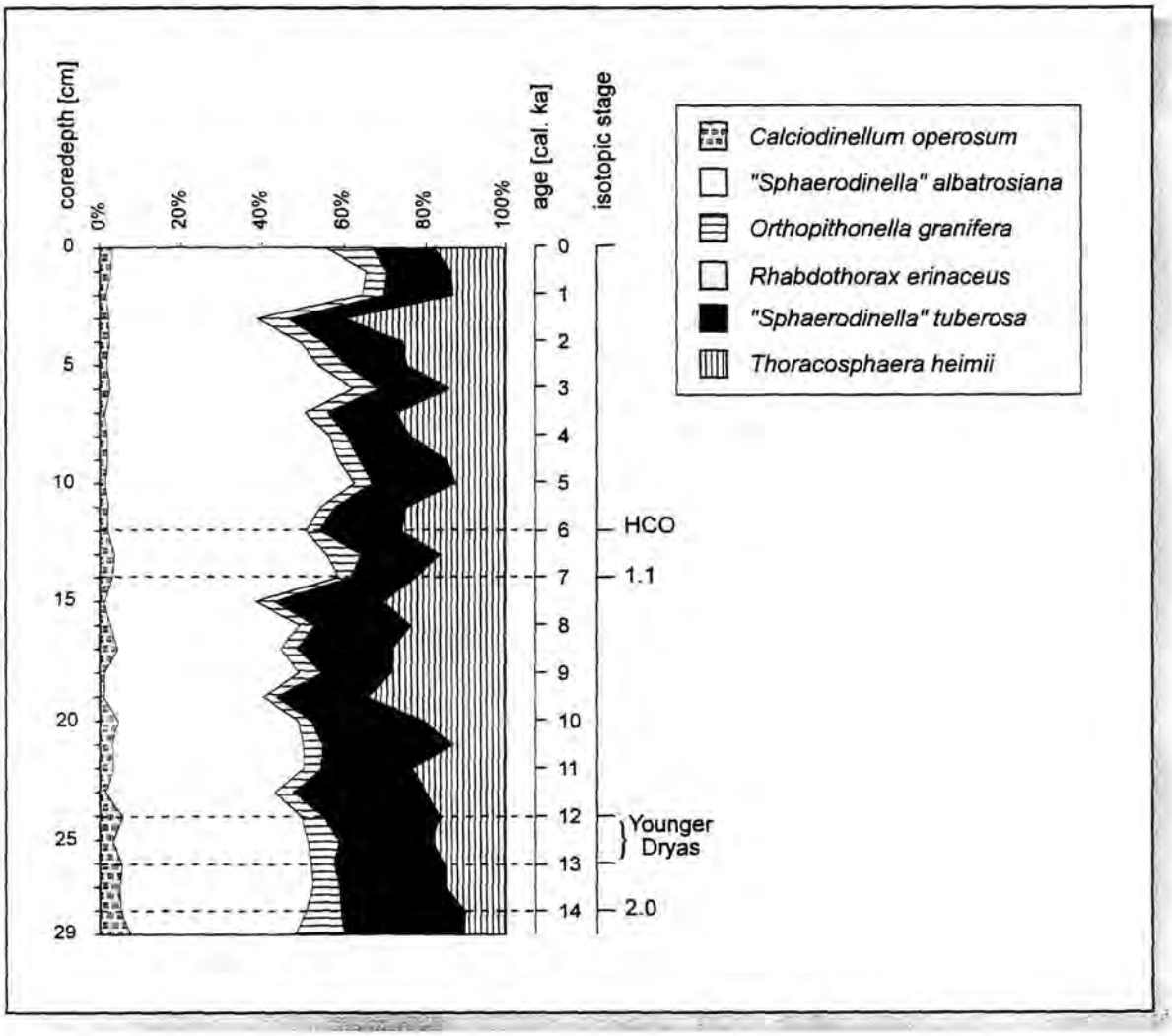

Fig. 44: Relative amount of recorded calcareous dinoflagellate species is plotted as cumulative curve for sediment core GeoB 1606-7 MUC (Guinea Basin).

5.2.3. DEGLACIATION STEP 2 (12.0-8.0 ka BP)

After the Younger Dryas cooling a second warming step led into the Preboreal warm period, representing the earliest Holocene. Modern conditions for the global ocean were established at about 9.0 ka ago (CHAPMAN et al., 1996).The deep water circulation pattern differed only little from the average of the last 4.0 ka (SARNTHEIN et al., 1994). The NADW originated from the Norwegian-Greenland Sea and its main stream moved southward passing west of the Rockall Plateau to the Mid-Atlantic Ridge. An intrawarm stage variation in deep water ventilation during the middle Holocene was recorded by Samthein et al. (1994) and interpreted as a weakened NADW flow at 2000-3000 m depth from the Azores to the equator and an enhancement in AABW circulation.

RESULTS:

- **Off Cape Blanc** core GeoB 1602-7 MUC (Fig.42) covers the last 10.0 ka and displays an overall and heavy domination of *Th. heimii* which amounts to 75-90% of the calcareous dinoflagellate assemblage. There is a distinctive stepwise increase of specimen densities of "*Sph.*" *albatrosiana*,

"Sph." tuberosa, and *Th. heimii* from 10.0 ka BP to Isotopic Event 1.1 ka BP (Fig.41). *O. granifera* shows the maximum abundance at 9.3 ka BP decreasing slowly until 7.0 ka BP. *C. operosum* and *Rh. erinaceus* are rare species in this core, they exhibit only minor fluctuations during this interval.

- **In the Guinea Basin**, a considerable increase of specimen densities has been observed for all but one (*Rh. erinaceus*) species of calcareous dinoflagellates in GeoB 1606-7 MUC (Fig.43) from 12.0 ka BP to 10.5-9.5 ka BP. The maximum abundances of *"Sph." albatrosiana* and *O. granifera* occurred 10.5 ka BP. *C. operosum* has shown its maximum 10.0 ka BP. The maximum abundance of *"Sph." tuberosa* happened 9.5 ka BP. This was followed by an interval of substantial abundance decline until Isotopic Event 1.1.

In GeoB1607-8 MUC, a general abundance decrease has been observed for all species during the entire time interval (Fig.45).

These fluctuations can be traced within the relative species assemblages as well (Fig.44, Fig.46).

DISCUSSION:

- **Offshore NW Africa** CHAPMAN et al. (1996) estimated a slight mean annual SST increase from 20.9°C to 21.3°C and seasonality of 7°C. MIX et al. (1986a) suggested cooler conditions with SST below 16°C and strong advections of CC and an increase in upwelling. According to DUPLESSY et al. (1992) substantial SSS shifts occurred off NW Africa after the Younger Dryas. SSS increased from 35.0‰ to 36.5‰ within 1.0 ka, declined by 1‰ within the next 1.0 ka, followed by another increase of more than 2‰. In GeoB 1602-7 these SSS fluctuations may be reflected by a *"Sph." tuberosa* increase during 10.0-8.3 ka BP, and a considerable decline until 8.0 ka BP, resulting in a slight increase. *"Sph." albatrosiana* shows a moderate rise in abundance which points to a slightly higher SST than today. The abundance of *Th. heimii* rises constantly to a specimen density three times as high. *O. granifera* shows high specimen densities from 9.3 ka BP to 7.7 ka BP, but so far this abundance could not be correlated to any environmental parameter.

- **In the eastern equatorial Atlantic**, early Holocene (7-10 ka BP) reconstructions of SIKES & KEIGWIN (1994) have indicated MA SST of 27.2-32.4°C which are much higher than present conditions. SST estimates of MIX et al. (1986a) and MCINTYRE et al. (1989) have suggested considerably lower temperatures (mean annual SST: 23-25°C, Tc: 23.5°C, Tw: 26.0°C). A temperature minimum along the equator separated very warm waters (>26°C) at 2-8°N in the western Atlantic and warm waters in the Gulf of Guinea and south of the equator (MIX et al., 1986a). These cooler SST estimates have indicated a weak equatorial divergence. *"Sph." albatrosiana* abundance has steadily decreased from 12.0 ka BP to 8.0 ka BP despite substantial fluctuations. *"Sph." tuberosa* displays the same pattern of decline, thus suggesting higher SST at the beginning and lower temperatures at the end of this time interval.

5.3. MODERN OCEAN (8-0 ka BP)

A third relatively minor warming step, between 8.0-6.0 ka BP, marked the Boreal-Atlantic boundary, and introduced the mild climate of the early Holocene (BERGER, 1990). During this warming step the orbitally forced strengths of the trade wind and monsoon adjusted and waters from the NAST advanced toward the NW African continental margin at the HCO (MIX et al., 1986a; MCINTYRE et al., 1989). During the last 9.0 ka, humidity decreased considerably for the North African continent and adjacent seas (MATTHEWSON et al., 1995).

According to SARNTHEIN et al. (1994) the NADW flow pattern was similar to the modern Atlantic Ocean and can be traced all along the Portuguese and African continental margin. North of the equator it has associated with high organic carbon content and fluff layers of the sediment, owing to coastal-upwelling productivity. In the south the local productivity was triggered by nutrient rich waters discharging from the tropical rivers. Below 3800-4000 m the AABW flowed northward along the east Atlantic continental margin and into the Canary basin. The MOW was traced southeast of Gibraltar between 800 m and 1800 m.

5.3.1. ISOTOPIC EVENT 1.1 (7 ka BP)

RESULTS:

- **Off Cape Blanc**, in core GeoB 1602-7, *Th. heimii* adds up to 85% of the species assemblage; *"Sph." albatrosiana*, *"Sph." tuberosa*, and *O. granifera* amount to about 5% each; the other two species are extremely rare (Fig.42). Specimen density of *"Sph." albatrosiana* is similar to present abundance; *"Sph." tuberosa*, *O. granifera*,

and *Th. heimii* show a dramatically higher abundance than today (Fig.41).

- **In the Guinea Basin**, the assemblage is dominated by *"Sph." albatrosiana* (~50%), *"Sph." tuberosa* amounts to 15-20%, *Th. heimii* adds up to 25-30%, *C. operosum* and *O. granifera* amount to ~5% each (Fig.44, Fig.46). All species but one display more or less the same abundance as today (Fig.43, Fig.45). In core GeoB 1606-7 the abundance of *O. granifera* is much lower than at present.

DISCUSSION:

- **Offshore NW Africa** the temperature estimates indicated mean annual SST of 20.0-21.4°C and seasonality of about 7-8°C, which would be near modern conditions (MIX et al., 1986a, b; CHAPMAN et al., 1996). SSS reconstructions of DUPLESSY et al. (1992) implied high salinity above 37‰. With the exception of *"Sph." albatrosiana*, every calcareous dinoflagellate species displayed abundances two to seven times as high as at present which may be interpreted as reflecting the influence of oligotrophic NAST waters. The absolute highest abundance of *Th. heimii* is a strong evidence of invading NAST waters. After 7.7 ka BP, *O. granifera* abundance decreased rapidly to zero abundance within 1.3 ka.

- **In the eastern equatorial Atlantic** temperature reconstructions exhibit slightly lower mean annual SST (24-25°C; MIX et al., 1986a) than at present. Seasonality may have been similar to today (BILLUPS & SPERO, 1996, Tc: 23.8°C, Tw: 28.5°C) or involved considerably lower temperatures (MCINTYRE et al., 1989, Tc: 23.4°C, Tw: 25.9°C). The calcareous dinoflagellate abundances suggest oceanographic conditions similar to the present ones.

5.3.2. HOLOCENE CLIMATIC OPTIMUM (6 ka BP) TO PRESENT OCEAN CONDITIONS

At the HCO, 6 ka BP, the NE trade wind intensity was at a minimum (SARNTHEIN et al., 1981; HOOGHIEMSTRA, 1988); but a stable circulation pattern over the last 6 ka has been suggested in agreement with the SST data (CHAPMAN et al., 1996).

RESULTS:

- **Off Cape Blanc** (Fig.41), there are distinctive maximum abundances for *"Sph." albatrosiana*, *C. operosum*, *"Sph." tuberosa*, and *Th. heimii* at the beginning of the HCO (6.3 ka BP); specimen densities later generally decrease stepwise to present abundances. *O. granifera* exhibits a rapid decline to zero abundance until 5.7 ka BP; from this time onwards these cysts have only been found rarely. Other rare species are *C. operosum* and *Rh. erinaceus*. The former has a maximum at the HCO as well; and the latter displays only minor fluctuations throughout the core.

- **In the Guinea Basin** (Fig.43, Fig.45), *"Sph." albatrosiana* shows major abundance oscillations throughout this time interval with high specimen densities four times the low ones. *C. operosum*, *"Sph." tuberosa*, and *Th. heimii* abundances fluctuate as well but in minor dimensions. For *O. granifera*, a stepwise increase has been observed with the maximum abundance of core GeoB 1606-7 in the uppermost sample. *Rh. erinaceus* has been recorded only in the uppermost samples.

The relative amounts of the species reflect the abundance patterns (Fig.42, Fig.44, Fig.46).

DISCUSSION:

- **Offshore NW Africa** the Middle Holocene estimates indicate warmer SST than modern conditions, and the thermal equator reached a stable northern hemisphere position (MIX et al., 1986a). The maximum specimen densities between Isotopic Event 1.1 and the HCO are three to seven times as high as the present ones. The SST is suggested to have favoured the "warm water cysts" and thus led to maximum abundances; followed by a stepwise decrease as the mean annual temperature dropped to the modern level. If modern oceanographic conditions were established at 6.0 ka BP (CHAPMAN et al., 1996) the cause for these maxima would be uncertain.

-**In the eastern equatorial Atlantic** middle Holocene SST estimates may indicate cooler waters (MIX et al., 1986a; MCINTYRE et al., 1989) or suggest present warmth (BILLUPS & SPERO, 1996). 6.0-5.0 ka BP, after the HCO, small peaks for the "warm water cysts", such as seen in the sediments off NW Africa, have been observed, which may imply warm SST conditions. The modern oceanographic conditions, with their high SST and low SSS, are considered to have been achieved about 1.5-2.0 ka ago.

»

Fig.45: The specimen densities of calcareous dinoflagellates on SEM stubs are plotted for core GeoB 1607-8 MUC (Guinea Basin).

Fig.45: GeoB 1607-8 MUC Specimen Densities

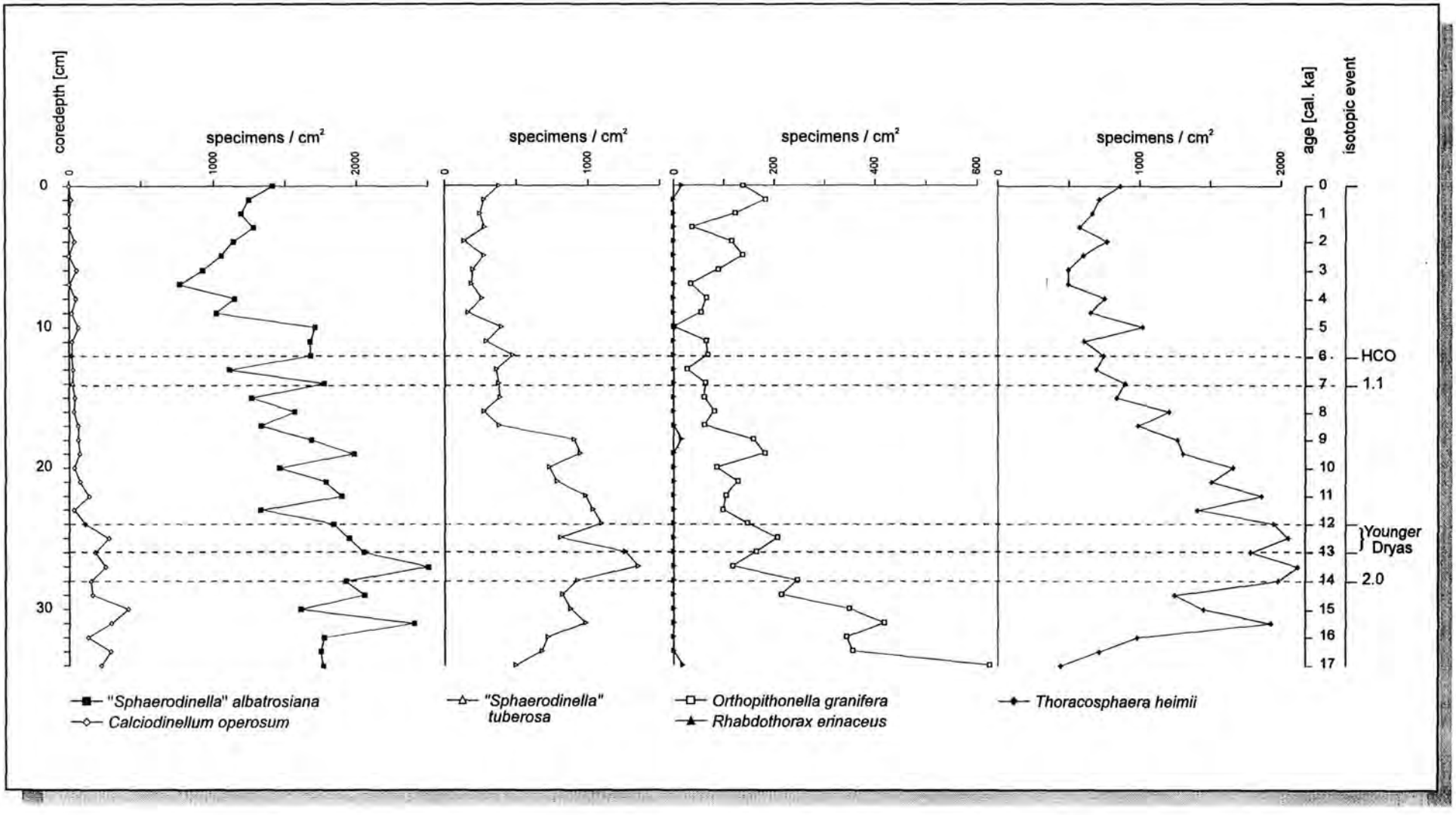

Fig.46: GeoB 1607-8 MUC Relative Amount of Species

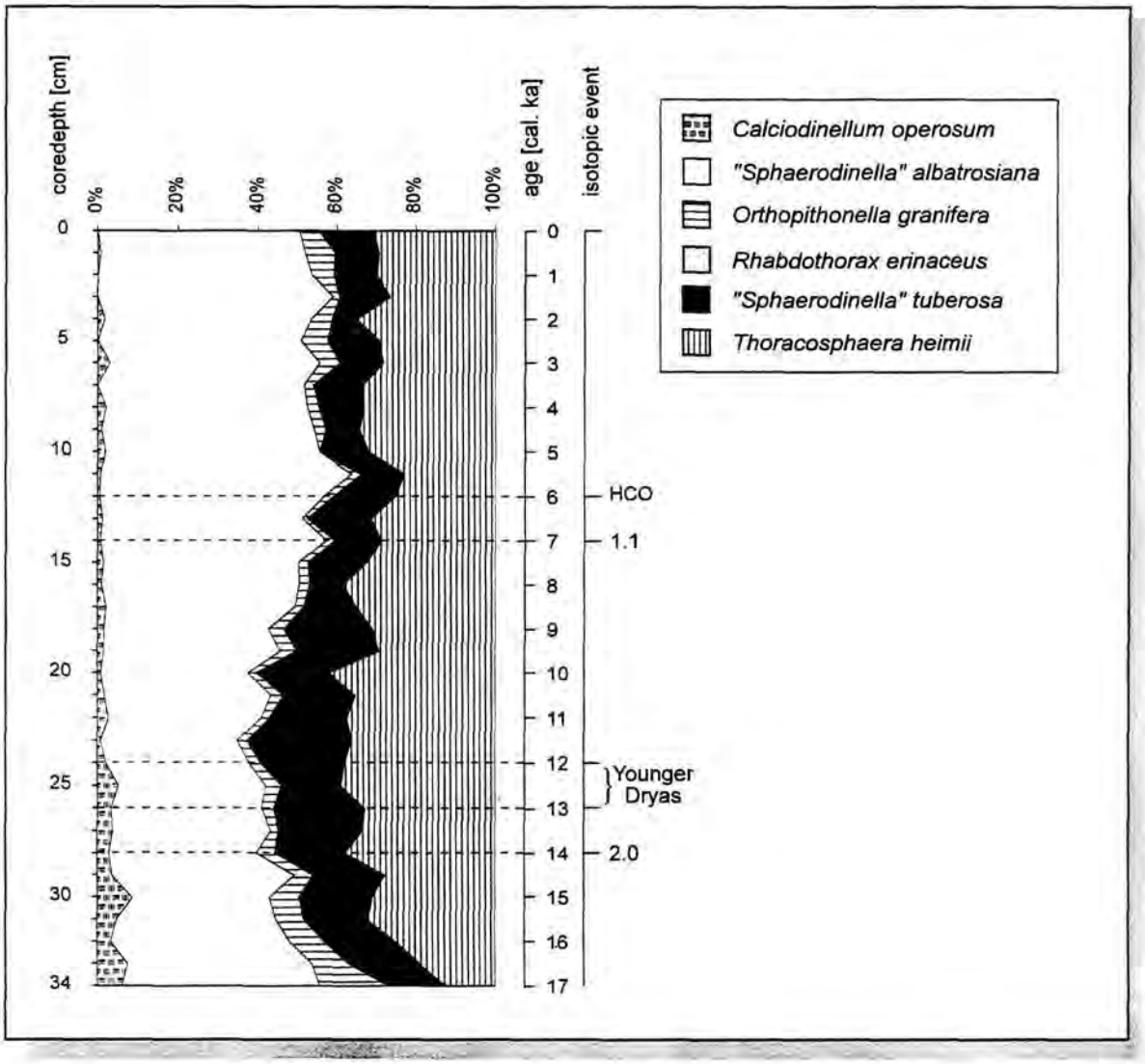

Fig. 46: Relative amount of recorded calcareous dinoflagellate species is plotted as cumulative curve for sediment core GeoB 1607-8 MUC (Guinea Basin).

It is uncertain whether the oceanographic parameters of the directly overlying surface waters are reflected in the sediment samples, or if unknown amounts of calcareous dinoflagellates have been transported by lateral currents within the water column.

The modern Atlantic at the site position off Cape Blanc is primarily influenced by the CC and the local upwelling regime. This area has a relatively low MA SST (~21°C, LEVITUS, 1982), but shows high seasonality with Tc 19°C and Tw 24°C (MITTELSTAEDT, 1991). The MA SSS is 36.0-36.5 (LEVITUS, 1986) with a seasonality of 1‰ (MITTELSTAEDT, 1991; DESSIER & DONGUY, 1994). This site shows very high productivity rates (>125gC/m²·a, BERGER, 1989).

In the Guinea Basin, with the modern equatorial current system, the waters have the highest MA SST of the Atlantic (~27°C, LEVITUS, 1982) with considerable seasonality (6-8°C, HASTENRATH & LAMB, 1977; PETERSON & STRAMMA, 1991). The high annual precipitation rate and river run-off into the Guinea Basin causes a low SSS year-round (MA SSS: 35.0‰, LEVITUS, 1986) with seasonal variations from 34.75‰ to

35.75‰ (DESSIER & DONGUY, 1994). Here, the productivity rates are slightly lower (90-125gC/m²·a, BERGER, 1989) than offshore NW Africa.

In the sub-Recent sediments, the abundance curves of "*Sph.*" *albatrosiana* and "*Sph.*" *tuberosa* are clearly linked with productivity and SST increase during deglaciation. An overall higher SSS is assumed for the Last Glacial Maximum which has decreased to the present low salinity conditions. This may have only a secondary effect on "*Sph.*" *tuberosa* abundance during deglaciation, but is clearly reflected in the limited abundances of the later Holocene.

From the present state of knowledge, the following biogeographic situation may be assumed for the calcareous cyst species assemblages in the Atlantic Ocean:

- In the sediments off Cape Blanc [low MA SST (~21°C) and high MA SSS (36.0-36.5‰)] "*Sph.*" *albatrosiana* and "*Sph.*" *tuberosa* are found in low numbers. "*Sph.*" *albatrosiana* dominates the assemblage with 56%. "*Sph.*" *tuberosa* amounts to 41% of the calcareous cyst assemblage.

- In the Guinea Basin [very high MA SST (~27°C) and severely reduced MA SSS (35.0-35.5‰)], "*Sph.*" *albatrosiana* clearly dominates the assemblage (74-78%). "*Sph.*" *tuberosa* is present in relatively low numbers and amounts to 21%.

- At Station E, offshore the northern coast of South America [high MA SST (26°C) and strong SSS seasonality (35.0-36.5‰, DESSIER & DONGUY, 1994)], very high fluxes of "*Sph.*" *albatrosiana* and inferior flux rates of "*Sph.*" *tuberosa* have been recorded (DALE & DALE, 1992).

- At Station S, in the western NAST [low MA SST (22°C) and high very MA SSS (36.5-37.0‰)], fluxes of "*Sph.*" *albatrosiana* decreased and "*Sph.*" *tuberosa* flux rates have increased in relation to Station E (DALE & DALE, 1992).

- In the western South Atlantic off Recife [high MA SST (>27°C) and high MA SSS (36.0-36.5‰)] the calcareous cyst assemblage is overwhelmingly dominated by "*Sph.*" *tuberosa* (83%), with "*Sph.*" *albatrosiana* amounting to only 17% (KARWATH, 1995).

It may therefore be implied from these data that the calcareous dinocysts may be used as indicators for distinctive oceanographic parameters of different water masses and major ocean currents. Future plankton studies will have to confirm, whether the 24°C-isotherm may generally be regarded as the SST margin of the "warm water cysts", and whether the "*Sph.*" *tuberosa*-cysts definitely show a second limitation to high SSS ocean areas defined by the 35.5‰-isoline.

And subsequently, sediment analyses will have to establish, whether the calcareous "warm water cysts" in the sediments may be used as proxies for warm water sea surface currents from low to higher latitudes, for current changes in the lower water column, or whether the glacial SST shifted below the "critical" 24°C-limit. "*Sph.*" *tuberosa*, as a possible salinity indicator, could be of high value for reconstructing past ocean SSS conditions, especially for glacial-interglacial salinity fluctuations. The relative abundances of *Th. heimii*-shells may give further information on dinoflagellate palaeo-productivity.

Thus, the distribution pattern of calcareous dinocysts may be used as a further palaeo-climatic indicator, whereas the fossil vegetative, coccoid *Th. heimii*-shells potentially offer a direct record of dino-phyceae primary productivity. Furthermore, the dinoflagellate fossil record could be re-evaluated on the basis of calcareous dinocysts and *Th. heimii*-shell remains, at least from the Tertiary onward.

6. CONCLUSIONS

In the studied area about 22-60% of the shelled phytoplankton organisms are dinoflagellates of various life stages. The cellulosic vegetative-thecate dinoflagellates form up to 25-55% of the shelled phytoplankton. 114 species were recorded. The SEM examinations of the plankton filters have shown that a large amount of very small vegetative-thecate dinoflagellate organisms which are very difficult to observe and to identify with a LM.

The development of the species associations discussed here is certainly related to various oceanographic parameters of the corresponding surface water environment. Species associations were defined for the equatorial Atlantic, for the area offshore NW Africa, and for the region around the Canary Isles. Relationships were established between planktic distribution patterns of recorded dinoflagellate species and oceanographic parameters such as sea surface temperature (SST), sea surface salinity (SSS), productivity, biogeography, and the distributing currents of the hydrodynamic system.

While investigating planktic distribution patterns of thecate dinoflagellates, several distinctive features have been observed in this study:

Many species usually found in higher latitudes or neritic parts of the Atlantic have been found in the fully oceanic waters of the study area, thus including the equatorial Atlantic into their distribution areas. The extended distribution areas are reflected in enlarged SST and SSS ranges. A better tolerance of higher SST is suggested.

Some species may be excellent biomarkers for distinctive surface water masses. *Ceratium gibberum, C. teres, Dinophysis micropterygia, D. parva, Oxytoxum crassum,* and *O. ovale* may be considered as characteristic for the equatorial Atlantic. *Ceratium azoricum, C. furca, C. minutum, C. tripos, Dinophysis caudata, Goniodoma sphaericum, Prorocentrum rostratum,* and *Protoperidinium oviforme* are suggested to be characteristic for the area offshore NW Africa. A huge amount of species are considered to be ubiquitous in the investigated area; amongst these are most species of the cyst-producing genus *Gonyaulax*. *Ornithocercus magnificus, O. steinii,* and *Ceratocorys horrida* are suggested to be "oceanic" dinoflagellates which are adapted to oligotrophic waters.

The proportional amount of the calcareous vegetative-coccoid species, *Thoracosphaera heimii*, averages 2-7% of the shelled phytoplankton and reaches a maximum of 12% at the Canary Isles. This ubiquitous species is found frequently to abundantly in the plankton within the entire recorded temperature and salinity range.

In tropical waters less than 10% of the vegetative-thecate dinoflagellate species are capable of cyst production. Even though the majority of species are known to form organic-walled cysts, these dinosporin cysts were not recorded during the study.

The planktic cyst assemblages are clearly dominated by calcareous forms, which were found in great abundances. In the equatorial Atlantic calcareous dinocysts average 2-5% of the shelled phytoplankton; offshore NW Africa (11.5°N/21°W) a maximum of 15% was recorded, decreasing rapidly to the north. At the Canary Isles no cysts were recorded.

Of the calcareous dinocysts, "*Sphaerodinella*" *albatrosiana* is the most abundant species in the equatorial Atlantic. It was found in waters warmer than 24°C, together with the rarer cyst species "*Sph.*" *tuberosa*. "*Sph.*" *albatrosiana* generally occurred in waters with salinities below 36.3‰; "*Sph.*" *tuberosa* was found within a salinity range of 35.5-36.3‰. A strong temperature dependence of both species is suggested, and these cysts may be regarded as thermophytes or "warm water cysts". Their planktic distribution is restricted to low-latitude waters with SST >24°C. "*Sph.*" *tuberosa* shows an additional restriction to waters with SSS >35.5‰.

The vegetative-thecate species *Scrippsiella trochoidea*, together with its calcareous cyst *Rhabdothorax erinaceus*, was frequently found in the plankton within an extended SST and SSS range. The calcareous cyst *Orthopithonella granifera* was recorded in small numbers, but occurred within wide temperature and salinity ranges throughout the investigated region.

Of these planktic dinoflagellates only the calcareous dinoflagellates are preserved in the sediments and may be regarded as reflecting the tropical fully oceanic dinoflagellate population.

Sub-Recent multicorer sediment samples of the tropical East Atlantic were investigated for calcareous dinoflagellates. The species association in the sediments offshore NW Africa is heavily dominated by *Th. heimii*-

shells (relative amount 78-90%); the calcareous dinocysts are present but only in small amounts (max. 15%). In the sediments of the Guinea Basin, however, the species association is dominated by the "warm water cysts" "*Sph.*" *albatrosiana* (50-55%) and "*Sph.*" *tuberosa* (12-20%). *Th. heimii*-shells amount to 20-40%.

The sediment core GeoB 1602-7 from offshore NW Africa covers the last 10.0 ka. There is a distinctive stepwise increase of specimen densities of "*Sph.*" *albatrosiana*, "*Sph.*" *tuberosa*, and *Th. heimii* from 10.0 ka BP to the beginning of the Holocene Climatic Optimum (HOC) at ~6.3 ka BP. The maximum specimen densities are three to seven times as high as the present ones. The oceanographic conditions at the HCO are suggested to have favoured *Th. heimii* and the "warm water cysts", and thus have led to maximum abundances. In the sediments of modern oceanographic conditions, with low mean annual SST (~21°C) and high SSS (36.25-37.0‰), both "*Sph.*" *albatrosiana* and "*Sph.*" *tuberosa* are found in low but approximately the same numbers. It is unclear why *O. granifera* shows a maximum from 9.3 ka BP to 7.7 ka BP, and decreases rapidly until 5.7 ka BP; from this time onwards these cysts were rarely found. Other rare species are *C. operosum* and *Rh. erinaceus*.

The sediment cores of the Guinea Basin cover the last 15 ka BP (GeoB 1606-7) and 17.0 ka BP (core GeoB1607-8) respectively, including Isotopic Event 2.0 and the Younger Dryas period. *Rh. erinaceus* is an extremely rare species, only some specimens were found occasionally. Just before and after Isotopic Event 2.0, at about 14.0 ka BP, all the other calcareous dinoflagellates have minimum specimen densities, increasing to maxima during the Younger Dryas chronozone. In the early Holocene some small maxima occur, but there is a general decrease until Isotopic Event 1.1. At the end of the HCO a shallow peak, such as seen in the sediments off NW Africa, is observed. The modern oceanographic conditions, very high mean annual SST (~28°C) and severely reduced SSS (34.75-35.75‰), are considered to have been achieved about 1.5-2.0 ka ago. "*Sph.*" *albatrosiana* dominates the modern assemblage and "*Sph.*" *tuberosa* is present in relatively low numbers.

Provided that the calcareous "warm water cysts" are strictly temperature dependent but tolerate high SSS seasonality, which is probable for "*Sph.*" *albatrosiana*, the area of maximum abundance in sediments should be related to maximum mean annual SST. In the East Atlantic, lateral transport by cold surface currents should restrict the area of maximum abundance to areas of low latitudes. In the West Atlantic, the cysts should be more widely distributed by warm surface currents and it should be possible to find them even in higher latitudes. In the lower water column an unknown amount of cysts may be transported by deep water masses.

For "*Sph.*" *tuberosa*, a second dependency on SSS above 35.5‰ besides SST is likely. The area of maximum "*Sph.*" *tuberosa*-abundance in the sediments should be related to ocean areas that display a mean annual optimum combination of these two oceanographic parameters (i.e. with high mean annual SST and SSS rates), and to the local distributing currents within the water column.

In the sub-Recent sediments, the abundancy curves of "*Sph.*" *albatrosiana* and "*Sph.*" *tuberosa* may be linked primarily to productivity and SST increase during deglaciation. An overall higher SSS (> ~1‰) is assumed for the Last Glacial Maximum which decreased thereafter to the present lower salinity conditions. This may have only a secondary effect on "*Sph.*" *tuberosa* abundancy during deglaciation, but is clearly reflected in the limited abundances during the later Holocene.

Therefore, from these data it may be implied that calcareous dinocysts can be used as indicators for distinctive oceanographic parameters of different water masses and major ocean currents. Future plankton studies have to confirm whether the 24°C-isotherm can be generally regarded as the SST margin of the "warm water cysts", and if the "*Sph.*" *tuberosa*-cysts definitely show a second limitation to high SSS ocean areas defined by the 35.5‰-isoline.

In addition, sediment analyses have to establish, if the calcareous "warm water cysts" in the sediments can be used as a proxy for warm water sea surface currents from low to higher latitudes, for current changes in the water column, or if the glacial SST shifted below the "critical" 24°C-limit. "*Sph.*" *tuberosa*, as a possible salinity indicator, could be a valuable tool for reconstructing past ocean SSS conditions, especially for glacial-interglacial salinity fluctuations. The relative abundances of *Th. heimii*-shells may give further information on dinoflagellate palaeoproductivity.

Thus, the distribution pattern of calcareous dinocysts may be used as a further palaeoclimatic indicator, whereas the fossil vegetative, coccoid *Th. heimii*-shells potentially offer a direct record of dinophyceae primary productivity. Furthermore, the dinoflagellate fossil record could be re-evaluated on the basis of calcareous dinocysts and *Th. heimii*-shell remains, at least from the Tertiary onwards.

ACKNOWLEDGEMENTS

Accomplishment of this study has spanned several years and numerous people and organizations have provided extensive assistance and support:

My parents and relatives have encouraged and supported my "university career".

Prof. Dr. Helmut Willems has initiated and supervised this doctoral thesis.

The research was funded by a grant of the *Graduierten Kolleg: "Stoff-Flüsse in marinen Geosystemen"* (i.e. "Particle Fluxes in Marine Geosystems") which is associated with the *Sonderforschungsbereich 261: "Der Südatlantik im Spätquartär: Rekonstruktion von Stoffhaushalt und Stromsystemen"* (i.e. Special Research Project 261: "Reconstructing Mass Budgets and Current Systems of the South Atlantic during the Late Quaternary").

I am grateful to all the members of the *Historische Geologie / Paläontologie* (i.e. Historical Geology / Palaeontology) and the other departments of the *Fachbereich 5 - Geowissenschaften* (i.e. Geosciences Faculty) at the University of Bremen, to all the people on board RV METEOR, and to all scientists who provided their assistance in many aspects.

Technical advice and assistance has been provided by i.a. Angelica Freesemann, Erna Friedel, Monika Kirsch, Dr. Hartmut Mai, and Anne Meyer.

Special recognition is due to Prof. Dr. John D. Dodge for providing his knowledge and experience in identifying thecate dinoflagellates with a SEM, and Dr. Dorothea Janofske for her continuing support, encouragement, and the invention of the "Horner Daiquiri".

REFERENCES:

ABÉ, T.H. (1981) (Prepared by Saito,M.): Studies on the family Peridiniidae, an unfinished monograph of the armoured dinoflagellata. *Kyoto Univ. Publ. Seto mar. biol. Lab., Spec. Publ.*, **6**: 409 pp.

ABRAHAMS, M.V. & TOWNSEND, L.D. (1993): Bioluminescence in dinoflagellates: a test of the burglar alarm hypothysis. *Ecology*, **74**: 258-260.

AKSELMAN, R. & KEUPP, H. (1990): Recent obliquipithonelloid calcareous cysts of *Scrippsiella patagonica* sp.nov. (Peridiniaceae, Dinophyceae) from plankton of the Golfo San Jorge (Patagonia, Argentina). *Mar. Micropaleont.*, **16**: 169-179.

AMADI, I., SUBBA RAO, D.V. & PAN, Y. (1992): A *Gonyaulax digitale* red water bloom in the Bedford Basin, Nova Scotia, Canada. *Bot. Mar.*, **35**: 451-455.

ANDERSEN, N. (1996): Biogeochemische Characterisierung von Sinkstoffen und Sedimenten aus ostatlantischen Produktionssystemen mit Hilfe von Biomarkern. *Berichte, Fachbereich Geowissenschaften, Universität Bremen*, **73**: 215 pp.

ANDRIÉ, C. (1996): Chlorofluoromethanes in the Deep Equatorial Atlantic Revisited. *In*: WEFER, G., BERGER, W.H., SIEDLER, G. & WEBB, D.J. (eds.) (1996): *The South Atlantic: Present and Past Circulation*. Springer, Berlin: 273-288.

BALECH, E. (1963): La familia Podolampadaceae (Dinoflagellata). *Bol. Inst. Biol. Mar.* Mar del Plata, **2**: 1-27.

BALECH, E. (1974): El genero *Protoperidinium* Bergh, 1881 (*Peridinium* Ehr., 1831, *partim*). *Rev. Mus. Argent. C. Nat.*, Hidrobiología, **4** (I): 1-79.

BALECH, E. (1988): Los dinoflagellados del Atlantico sudoccidental. *Inst. Esp. Oceanogr.*, Madrid, 310 pp.

BALECH, E. (1990): Four new dinoflagellates. *Helgoländer Meeresunters.*, **44**: 387-396.

BALSAM, W.L., OTTO-BLIESNER, B.L. & DEATON, B.C. (1995): Modern and last glacial maximum eolian sedimentation patterns in the Atlantic Ocean interpreted from sediment iron oxide content. *Paleoceanography*, **10** (3): 493-507.

BARD, E., ARNOLD, M., FAIRBANKS, R.G. & HAMELIN, B. (1993): ^{230}Th-^{234}U and ^{14}C ages obtained by mass spectrometry on corals. *Radiocarbon*, **35** (1): 191-199.

BARD, E., HAMELIN, B., FAIRBANKS, R.G. & ZINDLER, A. (1990): Calibration of the ^{14}C timescale over the past 30,000 years using mass spectrometric U-Th ages from Barbados corals. *Nature*, **345**: 405-410.

BARDOUIL,M., BERLAND, B., GRZEBYK, D. & LASSUS, P. (1991): L'existence de kystes chez les Dinophysiales. *C.R. Acad. Sci. Paris* Ser. 3, **312**: 663-669.

BELOW, R. (1987): Evolution und Systematik von Dinoflagellaten-Zysten aus der Ordnung Peridiniales. *Palaeontographica*, **B 205**: 1-164.

BERGER, W.H. & WEFER, G. (1996): Central Themes of South Atlantic Circulation. *In*: WEFER, G., BERGER, W.H., SIEDLER, G. & WEBB, D.J. (eds.) (1996): *The South Atlantic: Present and Past Circulation*. Springer, Berlin: 1-11.

BERGER, W.H. (1989): Global maps of ocean productivity. *In*: BERGER, W.H., SMETACEK, V.S.& WEFER, G. (eds.): *Productivity of the Ocean: Present and Past. Dahlem Workshop Reports*, J. Wiley & Sons, Chichester: 429-455.

BERGER, W.H. (1990): The Younger Dryas cold spell - a quest for causes. *Palaeogeogr., Palaeoclimatol., Palaeoecol. (Global Planet. Change Sect.)*, **89**: 219-237.

BERGER, W.H., FISCHER, K., LAI, C. & WU, G. (1987): Ocean productivity organic carbon flux. Part I. Overview and maps of primary production and exportproduction. *Univ. of California, San Diego, SIO Reference* 87-30.

BERGER, W.H., SMETACEK, V.S. & WEFER, G., editors (1989): Productivity of the Ocean: Present and Past. *Dahlem Workshop Reports*, J. Wiley & Sons, Chichester, New York, Brisbane, Toronto, Singapore, 470 pp.

BEVERIDGE, N.A.S., ELDERFIELD, H. & SHACKLETON, N.J. (1995): Deep thermohaline circulation in the low-latitude Atlantic during the last glacial. *Paleoceanography*, **10** (3): 643-660.

BILLUPS, K. & SPERO, H.J. (1996): Reconstructing the stable isotope geochemistry and paleotemperatures of the equatorial Atlantic during the last 150,000 years: Results from individual foraminifera. *Paleoceanography*, **11** (2): 217-238.

BLANCO, J. (1995): The distribution of dinoflagellate cysts along the Galician (NW Spain) coast. *J. Plankton Res.*, **17**: 283-302.

BOLCH, C.J. & HALLEGRAEFF, G.M. (1990): Dinoflagellate cysts in Recent marine sediments from Tasmania, Australia. *Bot. Mar.*, **33**: 173-192.

BOZIN, S.A. & FILIMOV, V.S. (1985): Spontaneous bioluminescence of dinoflagellates in Vostok Bay, Sea of Japan. *Oceanology*, **25**: 395-397.

BRASSEL, S.C., EGLINTON, G., , MARLOWE, I.T., PFLAUMANN, U. & SARNTHEIN, M. (1989): Molecular stratigraphy: A new tool for climatic assessment. *Nature*, **320**: 129-133.

BROECKER, W.S. (1989): The salinity contrast between the Atlantic and Pacific Oceans during glacial time. *Paleoceanography*, **4** (2): 207-212.

BROECKER, W.S., BLANTON, S., SMETHIE JR., W.M. & OSTLUND, G. (1991): Radiocarbon decay and oxygen utilization in the deep Atlantic Ocean. *Global Biogeochem. Cycles*, **5**: 87-117.

BUJAK, J.P. & DAVIES, E.H. (1983): Modern and fossil Peridiniineae. *AASP Contrib. Ser.*, **13**: 203 pp.

BUSKEY, E., MILLS, L. & SWIFT, E. (1983): The effects of dinoflagellate bioluminescence on the swimming behavior of a marine copepod. *Limnol. Oceanogr.*, **28**: 575-579.

CARBONELL-MOORE, M.C. (1992): *Blepharocysta hermosillai*, sp.nov. a new member of the family Podolampodaceae Lindemann (Dinophyceae). *Bot. Mar.*, **35**: 273-281.

CARBONELL-MOORE, M.C. (1994a): On the biogeography of the family Podolampadaceae Lindemann (Dinophyceae) - vertical and latitudinal distribution. *Rev. Palaeobot. Palynol.*, **84**: 23-44.

CARBONELL-MOORE, M.C. (1994b): On the taxonomy of the family Podolampadaceae Lindemann (Dinophyceae) with descriptions of three new genera. *Rev. Palaeobot. Palynol.*, **84**: 73-99.

CARBONELL-MOORE, M.C. (1996a): *Ceratocorys anacantha*, sp. nov.., a New Member of the Family Ceracocoryaceae Lindemann (Dinophyceae). *Bot. Mar.*, **39**: 1-10.

CARBONELL-MOORE, M.C. (1996b): On *Spiraulax jolliffei* (Murray *et* Whitting) Kofoid and *Gonyaulax fusiformis* Graham (Dinophyceae). *Bot. Mar.*, **39**: 347-370.

CHAPMAN, M.R. SHACKLETON, N.J., ZAO, M. & EGLINTON, G. (1996): Faunal and alkenone reconstructions of subtropical North Atlantic surface hydrography and paleotemperatures over the last 28 kyr. *Paleoceanography*, **11** (3): 343-357.

CLARK, P.U., ALLEY, R.B., KEIGWIN, L.D., LICCIARDI, J.M., JOHNSEN, S.J. & WANG, H. (1996): Origin of the first global mletwater pulse following the last glacial maximum. *Paleoceabography*, **11** (5): 563-577.

CLIMATE: LONG-RANGE INVESTIGATION, MAPPING AND PREDICTION (CLIMAP) PROJECT MEMBERS (1981) (A. McIntyre comp.): Seasonal reconstructions of the Earth's surface at the last glacial maximum. *GSA Map and Chart Ser.*, **MC-36**: 18pp.

COLEBROOK, J.M. (1982): Continuous plankton records: seasonal variations in the distribution and abundance of plankton in the North Atlantic Ocean and the North Sea. *J. Plankton Res.*, **4** (3): 435-462.

CURRY, W.B. & LOHMANN, G.P. (1990): Reconstructing past particle fluxes in the tropical Atlantic Ocean. *Paleoceanography*, **5** (4): 487-505.

DALE, B. & DALE, A.L. (1992): Dinoflagellate contributions to the deep sea. *Ocean Biocoenosis Series*, **5**: 75 pp.

DALE, B. (1976): Cyst formation, sedimentation, and preservation: factors affecting dinoflagellate assemblages in Recent sediments from Trondheimsfjord, Norway. *Rev. Palaeobot. Palynol.*, **22**: 39-60.

DALE, B. (1983): Dinoflagellate resting cysts: "benthic plankton". *In*: FRYXELL, G.A.(ed.), *Survival Stratigies of the Algae*, Cambridge University Press, N.Y.: 69-136.

DE VERNAL, A., MUDIE, P.J., HARLAND, R., MORZADEC-KERFOURN, M.T., TURON, J.-L. & WRENN, J.H. (1992): Quarternary organic-walled dinoflagellate cysts of the North Atlantic Ocean and adjecent seas: Ecostratigraphy and Biostratigraphy. *In*: HEAD, M.J. & WRENN, J.H. (ed.), Neogene and Quarternary Dinoflagellates and Acritarchs. *AASP Foundation*: 289-328.

DEFLANDRE, G. (1947): *Calciodinellum* nov. gen., premier répresentant d'une famille nouvelle de Dinoflagellés fossiles a theque calcaire. *C. R. Acad. sci.*, **224**: 1781-1782.

DEFLANDRE, G. (1948): Les Calciodinellidès - dinoflagellés fossiles a theque calcaire. *Le Botaniste*, **34**: 191-219.

DESSIER, A. & DONGUY, J.R. (1994): The sea surface salinity in the tropical Atlantic between 10°S and 30°N - seasonal and annual variations (1977-1989). *Deep-sea Research*, **41** (1): 81-100.

DODGE, J.D. & HARLAND, R. (1991): The distribution of planktonic dinoflagellates and their cysts inthe eastern and northeastern Atlantic Ocean. *New Phytol.*, **118**: 593- 603.

DODGE, J.D. & MARSHALL, H.G. (1994): Biogeographic analysis of the armored planktonic dinoflagellate *Ceratium* in the North Atlantic and adjecent sea. *J. Phytol.*, **30**: 905-922.

DODGE, J.D. & PRIDDLE, J. (1987): Species composition and ecology of dinoflagellates from the Southern Ocean near South Georgia. *J. Plankton Res.*, **9** (4): 685-697.

DODGE, J.D. & SAUNDERS, R.M. (1985): A partial revision of the genus *Oxytoxum* (Dinophyceae) with the aid of scanning electron microscopy. *Bot. Mar.*, **28**: 99-122.

DODGE, J.D. (1981): Three new generic names in the Dinophyceae: *Herdmania, Sclerodinium,* and *Triadinium* to replace *Heteraulacus* and *Goniodoma*. *Br. phycol. J.*, **16**: 273-280.

DODGE, J.D. (1982): *Marine dinoflagellates of the British Isles*. H.M.S.O., London: 303 pp..

DODGE, J.D. (1988): An SEM study of thecal division in *Gonyaulax* (Dinophyceae). *Phycologia*, **27** (2): 241-247.

DODGE, J.D. (1989a): Some revisions of the family Gonyaulacaceae (Dinophyceae) based on scanning electron microscopy. *Bot. Mar.*, **32**: 275-298.

DODGE, J.D. (1989b): Records of marine dinoflagellates from the North Sutherland (Scotland). *Br. phycol. J.*, **24**: 385-389.

DODGE, J.D. (1993): Armoured dinoflagellates in the NE Atlantic during the BOFS cruises, 1988-90. *J. Plankton Res.*, **15** (5): 465-483.

DODGE, J.D. (1994): Biogeography of marine armoured dinoflagellates and dinocysts in the NE Atlantic and North Sea. *Rev. Palaeobot. Palynol.*, **84**: 169-180.

DÜING, W., HISARD, P., KATZ, E., MEINCKE, J., MILLER, L., MOROSHKIN, K.V., PHILANDER, G., RIBNIKOV, A.A., VOIGT, K. & WEISBERG, R. (1975): Meanders and long waves in the equatorial Atlantic. *Nature*, **257**: 280-284.

DÜING,W., OSTAPOFF, F. & MERLE,J. (1980) (prepared by Lee,V.): Physical Oceanography of the Tropical Atlantic during GATE. *Global Atmospheric Research Program (GARP) Atlantic Tropical Experiment*, University of Miami:

DUPLESSY, J.-C., LABEYRIE, L., ARNOLD, M., PATERNE, M., DUPRAT, J. & VAN WEERING, T.C.E. (1992): Changes in surface salinity of the North Atlantic Ocean during the last deglaciation. *Nature*, **358**: 485-488.

DUPLESSY, J.-C., LABEYRIE, L., PATERNE, M., HOVINE, S., FICHFET, T., DUPRAT, J. & LABRACHEERIE, M. (1996): High Latitude Deep Water Sources During the Last Glacial Maximum and the Intensity of the Global Oceanic Circulation. *In*: WEFER, G., BERGER, W.H., SIEDLER, G. & WEBB, D.J. (eds.) (1996): *The South Atlantic: Present and Past Circulation*. Springer, Berlin: 445-460.

DUPLESSY, J.-C., SHACKLETON, N.J., FAIRBANKS, R., LABEYRIE, L., OPPO, D. & KALLEL, N. (1988): Deep water source variations during the last climatic cycle and their impact on the global deepwater circulation. *Paleoceanography*, **3**: 343-360.

EDWARDS, L.E. & ANDRLE, V.A.S. (1992): Distribution of selected dinoflagellate cysts in modern marine sediments. *In*: HEAD, M.J. & WRENN, J.H. (ed.), Neogene and Quarternary Dinoflagellates and Acritarchs. *AASP Foundation*: 259-288.

EDWARDS, L.E. (1992): New semiquantitative (paleo)temperature estimates using dinoflagellate cysts , an example from the North Atlantic Ocean. *In*: HEAD, M.J. & WRENN, J.H. (ed.), Neogene and Quarternary Dinoflagellates and Acritarchs. *AASP Foundation*: 69-87.

EDWARDS, L.E., MUDIE, P.J. & DE VERNAL, A. (1991): Pliocene paleoclimatic reconstruction using dinoflagellate cysts: Comparison of methods. *Quaternary Science Reviews*, **10**: 259-274.

ELLEGARD, M.; CHRISTENSEN, N.F. & MOESTRUP, O. (1994): Dinoflagellate cysts from recent Danish marine sediments. *Eur. J. Phycol.*, **29**: 183-194.

EPPLEY, R.W., HOLM-HANSEN, O. & STRICKLAND, J.D.H. (1968): Some observations on the vertical migration of dinoflagellates. *J. Phycol.*, **4**: 333-340.

EPPLEY,R.W., REID, F.M.H., CULLEN, J.J., WINANT, C.D. & STEWART, E. (1984): Subsurface patch of a dinoflagellate (*Ceratium tripos*) off Southern California: patch length, growth rate, associated vertically migrating species. *Mar. Biol. (Berl.)*, **80**: 207-214.

EVITT, W.R. (1985): Sporopollenin dinoflagellates cysts: their morphology and interpretation. *AASP Mon. Ser.*, **1**: 333pp.

FAIRBANKS, R.G. (1989): A 17,000-year glacio-eustatic sea level record: influence of glacial melting rates on the Younger Dryas event and deepocean circulation. *Nature*, **342**: 637-642.

FAIRBANKS, R.G., SVERDLOVE, M., FREE, R., WIEBE, P.H. & BÉ, A.W.H. (1982): Vertical distribution and isotopic fractionation of living planktonic foraminifera from the Panama Basin. *Nature*, **298**: 841-844.

FAIRBANKS, R.G., WIEBE, P.H. & BÉ, A.W.H. (1980): Vertical distribution and isotopic composition of living planktonic foraminifera in the western North Atlantic. *Science*, **207**: 61-63.

FENSOME, R.A., TAYLOR, F.J.R., NORRIS, G., SARJEANT, W.A.S., WHARTON, D.I. & WILLIAMS, G.L. (1993): A classification of living and fossil dinoflagellates. *Micropaleontology, Spec. Publ.*, **7**: 351 pp.

FENSOME, R.A., MACRAE, R.A., MOLDOWAN, J.M., TAYLOR, F.J.R. & WILLIAMS, G.L. (1996): The early Mesozoic radiation of dinoflagellates. *Paleobiology*, **22**(3): 329-338.

FISCHER, G. & WEFER, G. (1996): Long-term Observation of Particle Fluxes in the EasternAtlantic: Seasonality, Changes of Flux with Depth and Comparison with the Sediment Record. *In*: WEFER, G., BERGER, W.H., SIEDLER, G. & WEBB, D.J. (eds.) (1996): *The South Atlantic: Present and Past Circulation*. Springer, Berlin: 325-344.

FÜTTERER, D.K. (1976): Kalkige Dinoflagellaten ("Calciodinelloideae") und die systematische Stellung der Thoracosphaeroideae. *N. Jb. Geol. Paläont. Abh.*, **151** (2): 119-141.

FÜTTERER, D.K. (1977): Distribution of calcareous dinoflagellates in Cenozoic sediments of Site 366, eastern North Atlantic. *In*: LANCELOT, Y. et al., *Init. Repts. DSDP*, **41**: 709-737.

FÜTTERER, D.K. (1983): The modern upwelling record off Northwest Africa. *In*: SUESS, E. & THIEDE, J. (eds.): *Coastal Upwelling. Ist Sediment Record, Part B: Sedimentary Records of Ancient Coastal Upwelling*, Plenum Press, New York, 105-121.

FÜTTERER, D.K. (1990): Distribution of calcareous dinoflagellates at the Cretaceous-Tertiary boundary of Queen Maud Rise, eastern Wedell Sea, Antarctica. *In*: BARKER, P.F. et al., *Proc. ODP, Sci. Results*, **113**: 533-548.

GAINES, G. & ELBRÄCHTER, M. (1987): Heterotrophic nutrition. *In*: TAYLOR, F.J.R. (ed.), The Biology of Dinoflagellates. *Bot. Monogr.*, **21**: 224-268.

GAO, X., DODGE, J.D. & LEWIS, J. (1989): An ultrastrctural study of planozygotes and and encystment of a marine dinoflagellate, *Scrippsiella* sp. *Br. phycol. J.* **24**: 153-165.

GAO,X. & DODGE, J.D. (1991): The taxonomy and ultrastructure of a marine dinoflagellate, *Scrippsiella minima* sp.nov. *Br. phycol. J.* **26**: 21-31.

GILBERT, M.W. & CLARK, D.L. (1983): Central Arctic Ocean paleoceanographic interpretation based on Late Cenozoic calcareous dinoflagellates. *Mar. Micropaleont.*, **17**: 385-401.

GORDON, A.L. (1996): Comment on the South Atlantic#s Role in the Global Circulation. *In*: WEFER, G., BERGER, W.H., SIEDLER, G. & WEBB, D.J. (eds.) (1996): *The South Atlantic: Present and Past Circulation*. Springer, Berlin: 121-124.

GORDON, N., ANGEL, D.L., NEORI, A., KRESS, N. & KIMOR, B. (1994): Heterotrophic dinoflagellates with symbiotic cyanobacteria and nitrogen limitation in the Gulf of Aqaba. *Mar. Ecol. Prog. Ser.*, **107**: 83-88.

GOULD, R.W, jr. & FRYXELL, G.A. (1988): Phytoplankton species composition in a Gulf Stream warm core ring. I. Changes

over a five month period. *J. mar. Res.*, **46**: 367-398.

HALLEGRAEFF, G.M. & LUCAS, I.A.N. (1988): The marine dinoflagellate genus *Dinophysis* (Dinophyceae): photosynthetic, neritic and non-photosynthetic, oceanic species. *Phycologia*, **27** (1):25-42.

HANSEN, P.J. (1991): *Dinophysis* - a planktonic dinoflagellate genus which can act both as a prey and a predator of a ciliate. *Mar. Ecol. Prog. Ser.*, **69**: 201-204.

HARLAND, R. (1973): Dinoflagellate cysts and arcritarchs from the Bearpaw Formation (Upper Campanian) of southern Alberta, Canada. *Palaeontology*, **16**: 665-706.

HARLAND, R. (1983): Distribution maps of recent dinoflagellate cysts in bottom sediments from the North Atlantic Ocean and adjacent seas. *Palaeontology*, **26** (2): 321-387.

HARLAND, R. (1988): Dinoflagellates, their cysts and Qaternary stratigraphy. *New Phytologist*, **108**: 111-120.

HASTENRATH, S. & LAMB, P.J. (1977): *Climatic Atlas of the Tropical Atlantic and Eastern Pacific Oceans*. The University of Wisconsin Press, Madison, 15pp.

HASTENRATH, S. & MERLE, J. (1987): Annual cycle of subsurface thermal structure in the tropical Atlantic Ocean. *J. Phys. Oceanogr.*, **17**: 1518-1538.

HEAD, E.J.H., HARRISON, W.G., IRWIN, B.I., HORNE, E.P.W. & LI, W.K.W. (1996): Plankton dynamics and carbon flux in an area of upwelling off the coast of Morocco. *Deep-Sea Res.*, **43** (11-12): 1713-1738.

HEAD, M.J. & WRENN, J.H. (1992): A forum on Neogene and Quarternary dinoflagellate cysts: The edited transcript of a round table discussion held at the Second Workshop on Neogene Dinoflagellates. *In*: HEAD, M.J. & WRENN, J.H. (ed.), Neogene and Quarternary Dinoflagellates and Acritarchs. *AASP Foundation*: 1-31.

HEAD, M.J. (1989): Dinoflagellate cysts from the Pliocene Coralline Crag deposits of Suffolk, eastern England: An SEM / LM study including new observations of wall ultrastructure for selected species. *Fourth International Conference on Modern and Fossil Dinoflagellates, Woods Hole MA, Program and Abstracts*: p. 57.

HENTSCHEL, E. (1936): Allgemeine Biologie des Südatlantischen Ozeans. *In:* DEFANT, A. (edt.): *Wissenschaftliche Ergebnisse der Deutschen Atlantischen Expedition auf dem Forschungs- und Vermessungsschiff "METEOR" 1925-1927*. Band XI, De GRUYTER & Co., Berlin, 344 pp.

HÖLL, C., ZONNEVELD, K.A.F. & WILLEMS, H. (in press): On the ecology of calcareous dinoflagellates: The Quarternary eastern equatorial Atlantic.

HOLLIGAN, P.M., MADDOCK, L. & DODGE, J.D. (1980): The distribution of dinoflagellates around the British Isles in July 1977: A multivariate analysis: *J. mar. biol. Ass. U. K.*, **60**: 851-867.

HOOGHIEMSTRA, H. (1988): Changes of major wind belts and vegetation zones in NW Africa 20,000-5,000 YR B.P. as deduced from marine pollen record near Cap Balnc. *Rev. Palaeobot. Palynol.*, **55**: 101-140.

HOUGHTON, R.W. (1989): Influence of local and remote wind forcing in the Gulf of Guinea. *J. Geophys. Res.*, **94** (C4): 4816-4828.

HOUGHTON, R.W. (1991): The relationships of sea surface temerature to thermocline depth at annual and interannual time scales in the tropical Atlantic Ocean. *J. Geophys. Res.*, **96** (C8): 15,173-15,185.

IMBRIE, J., BERGER,A., BOYLE, E.A., CLEMENS, S.C., DUFFY, A., HOWARD, W.R., KUKLA, G., KUTZBACH, J., MARTINSON, D.G., MCINTYRE, A., MIX, A.C., MOLFINO, B., MORLEY, J.J., PETERSON, L.C., PISIAS, N.G., PRELL, W.L., RAYMO, M.E., SHACKLETON, N.J., & TOGGWEILER, J.R. (1992b): On the structure and origin of major glaciation cycles - 2. The 100,000-year cycle. *Paleoceanography*, **8** (6): 699-735.

IMBRIE, J., BOYLE, E.A., CLEMENS, S.C., DUFFY, A., HOWARD, W.R., KUKLA, G., KUTZBACH, J., MARTINSON, D.G., MCINTYRE, A., MIX, A.C., MOLFINO, B., MORLEY, J.J., PETERSON, L.C., PISIAS, N.G., PRELL, W.L., RAYMO, M.E., SHACKLETON, N.J., & TOGGWEILER, J.R. (1992a): On the structure and origin of major glaciation cycles - 1. Linear responses to Milankovitch forcing. *Paleoceanography*, **7** (6): 701-738.

IMBRIE, J., MCINTYRE, A. & MIX, A. (1989): Oceanic response to orbital forcing in the late Quarternary: Observational and

experimental strategies. *In*: BERGER, A. et al. (eds.): *Climate and Geosciences*, Kluwer Acadamic, Boston Mass.: 121-164.

INOUYE, I. & PIENAAR, R.N. (1983): Observations on the life cycle and microanatomy of *Thoracosphaera heimii* (Dinophyceae) with special reference to its systematic position. *S. Afr. J. Bot.*, **2** (1): 63-75.

JACOBSON, D.M. & ANDERSON, D.M. (1986): Thecate heterotrophic dinoflagellates: Feeding behavior and mechanisms. *J. Phycol.*, **22**: 249-258.

JAFAR, S.A. (1979): Taxonomy, stratigraphy and affinities of calcareous nannoplankton genus *Thoracosphaera* KAMPTNER. *Proceed. IV. Int. Palynol. Congr.*, **2**: 1-21.

JANOFSKE, D. & KEUPP, H. (1992): Mesozoic and Cenozioc "calcispheres" - update in systematics. *INA Newsl.*, **14** (1): 14-16.

JANOFSKE, D. (1990): Eine neue "Calcisphaere" *Carnicalyxia tabellata* n. g. n. sp. aus den Cassianer Schichten (Cordevol, unteres Karn) der Dolomiten. *Berliner geowiss. Abh.*, **(A) 124**: 259-269.

JANOFSKE, D. (1992): Kalkiges Nannoplankton, insbesondere Kalkige Dinoflagellaten-Zysten der alpinen Obertrias: Taxonomie, Biostratigraphie und Bedeutung für die Phylogenie der Peridiniales. *Berliner geowiss. Abh.*; **(E) 4**: 53 pp.

JANOFSKE, D. (1996): Ultrastructure types in Recent "calcispheres". *Bull. Inst. océanogr. Monaco*, **14**: 295-303.

JANSEN, E. & VEUM, T. (1990): Evidence for two-step deglaciation and its impact on North Atlantic deep-water circulation. *Nature*, **343**: 612-616.

JANSEN, E. (1992): Deglaciation, Impact on Ocean Circulation. *Encyclopedia of Earth System Science*, **3**: 35-46.

JANSEN, J.H.F., UFKES, E. & SCHNEIDER, R.R. (1996): Late Quarternary Movements of the Angola-Benguela Front, SE Atlantic, and Implications fro Advection in the Equatorial Ocean. *In*: WEFER, G., BERGER, W.H., SIEDLER, G. & WEBB, D.J. (eds.) (1996): *The South Atlantic: Present and Past Circulation*. Springer, Berlin: 553-575.

JICKELLS, T.D.; NEWTON, P.P.; KING, P.; LAMPITT, R.S. & BOUTLE, C. (1996): A comparison of sediment trap records of particle fluxes from 19 to 48°N in the northeast Atlantic and their relation to surface water productivity. *Deep-Sea Res. I*, **43**: 971-986.

KAMPTNER, E. (1927): Beitrag zur Kenntnis adriatischer Coccolithophoriden. *Arch. Protistenk.*, **58**: 173-184.

KAMPTNER, E. (1937): Neue und bemerkenswerte Coccolithineen aus dem Mittelmeer. *Arch. Protistenk.*, **89**: 279-316.

KAMPTNER, E. (1944): Coccolithineen-Studien im Golf von Neapel. *Wiener bot. Zschr. (Österr. bot. Zschr.)*, **93**: 138-147.

KAMPTNER, E. (1946): Zur Kenntnis der Coccolithineen-Gattung *Thoracosphaera* KPT. *Anz. Akad. Wiss. Wien, Math.-naturwiss. Kl.*, **83**: 100-103.

KAMPTNER, E. (1955): Fossile Coccolithineen-Skelettreste aus Insulinde. *Verh. K. Ned. Akad. Wet. Afd. Nat. R., 2 Deel L*, **2**: 106.

KAMPTNER, E. (1958): Betrachtungen zur Systematik der Kalkdinoflagellaten, nebst Versuch einer neuen Gruppierung der Chrysomonadales. *Ann. Naturhistor. Mus. Wien*, **71**: 117-198.

KAMPTNER, E. (1963): Coccolithineen-Skelettreste aus Tiefseeablagerungen des Pazifischen Ozeans. *Ann. Naturhistor. Mus. Wien*, **66**: 139-204.

KAMPTNER, E. (1967): Kalkflagellaten-Skelettreste aus dem Tiefseeschlamm des Südatlantischen Ozeans. *Ann. Naturhistor. Mus. Wien*, **71**: 117-198.

KAMYKOWSKI, D. & MCCOLLUM, S.A. (1986): The temperature acclimatized swimming speed of selected marine dinoflagellates. *J. Plankton Res.*, **8**: 275-287.

KARWATH, B. (1995): Verteilung kalkiger Dinoflagellaten der letzten 170 000 Jahre im westlichen Brasil-Becken (Südatlantik, Kern GeoB 2204-2). *Unpubl. Diplomarbeit, FB 5 Geowissenschaften, Universität Bremen*: 109 pp.

KEMLE-VON MÜCKE, S. (1994): Obeflächenwasserstruktur und -zirkulation des Südostatlantiks in Spätquartär. *Berichte, Fachbereich Geowissenschaften, Universität Bremen*, **55**: 151 pp.

KEUPP, H. & KOHRING, R. (1993): Kalkige Dinoflagellatenzysten aus dem Obermiozän von El Medhi (Algerien). *Berliner geowiss. Abh.*, **(E) 9**: 25-43.

KEUPP, H. & KOHRING, R. (1994): Kalkige Dinoflagellaten-Zysten aus dem Rupelton (Mittel-Oligozän) des Mainzer Beckens und der Niederrheinischen Bucht. *Mainzer geowiss. Mitt.*, **23**: 159-184.

KEUPP, H. & MUTTERLOSE, J (1984): Organismenverteilung in den D-Beds von Speeton (Unterkreide, England) unter besonderer Berücksichtigung der kalkigen Dinoflagellaten-Zysten. *Facies*, **10**: 153-178.

KEUPP, H. & VERSTEEGH, G. (1989): Ein neues systematisches Konzept für kalkige Dinoflagellaten-Zysten der Subfamilie Orthopithonelloideae KEUPP 1987. *Berliner geowiss. Abh.*, **106**: 207-219.

KEUPP, H. (1981): Die kalkigen Dinoflagellaten-Zystsn der borealen Unter-Kreide (Unter-Hauterivium bis Unter-Albium). *Facies*, **5**: 190 pp.

KEUPP, H. (1984): Revision der kalkigen Dinoflagellaten-Zysten G. DEFLANDRES, 1948. *Paläont. Z.*, **58** (1/2): 9-31.

KEUPP, H. (1987): Die kalkigen Dinoflagellatenzysten des Mittelalb bis Untercenoman von Escalles/Boulonnais (N.-Frankreich). *Facies*, **16**: 37-88.

KEUPP, H., MONNET, B. & KOHRING,R. (1991): Morphotaxa bei kalkigen Dinoflagellaten-Zysten und ihre problematische Systemisierung. *Berliner geowiss. Abh.*, **(A) 134**: 161-185.

KOFOID, C.A. (1907): The plates of *Ceratium* with a note on the unity of the genus. *Zool. Anzeiger*, **32**: 177-183.

KOFOID, C.A. (1909): On *Peridinium steini* Jörgensen, with a note on the nomenclature of the skeleton of the Peridinidae. *Arch. Protistenk.*, **16** (1): 25-47.

KOHRING, R: (1993): Kalkdinoflagellaten aus dem Mittel- und Obereozän von Jütland (Dänemark) und dem Pariser Becken (Frankreich) im Vergleich mit anderen Tertiär-Vorkommen. *Berliner geowiss. Abh.* **(E) 6**: 1-164.

KRASNOW, R., DUNLAP, J.C., TAYLOR, W., HASTINGS, J.W., VETTERLING, W. & GOOCH, V. (1980): Circadian spontaneous bioluminescent glow and flashing of *Gonyaulax polyedra*. *J. Comp. Physiol.*, **138**: 19-26.

LANGE, C.B., TREPPKE, U.F. & FISCHER, G: (1994): Seasonal diatom fluxes in the Guinea Basin and their relationships to trade winds, hydrography and upwelling events. *Deep-Sea Res. 1*, **41** (5/6): 859-878.

LATASA, M. (1995): Pigment composition of *Heterocapsa* sp. and *Thalassiosira weissflogii* growing in batch cultures under different irradiances. *Sci. Mar.*, **59** (1): 25-37.

LATZ, M.I. & LEE, A.O. (1995): Spontaneous and stimulated bioluminescence of the dinoflagellate *Ceratocorys horrida* (Peridiniales). *J. Phycol.*, **31**: 120-132.

LESSARD, E.J. & SWIFT, E. (1986): Dinoflagellates from the North Atlanic classified as phototrophic and heterotrophic by epiflourescence microscopy. *J. Plankton Res.*, **8** (6): 1209-1215.

LEVITUS, S. (1982): Climatological Atlas of the World Ocean. *NOAA Prof. Pap.*, **13**:173 pp.

LEVITUS, S. (1986): Annual Cycle of Salinity and Salt Storage in the World Ocean. *J. Phys. Oceanogr.*, **16**: 322-343.

LEVITUS, S. (1989): Interpendatal variability of salinity in the upper 150 m of the North Atlantic Ocean, 1970-1974 versus 1955-1959. *J. Geophys. Res.*, **94**: 9679-9685.

LEWIS, J. (1991): Cyst-theca Relationships in *Scrippsiella* (Dinophyceae) and Related Orthoperidinoid Genera. *Bot. Mar.*, **34**: 91-106.

LEWIS, J., DODGE, J.D. & POWELL,A.J. (1990): Quaternary dinoflagellate cysts from the upwelling system offshore Peru, Hole 686B, ODP Leg 112. *Proc. ODP, Sci. Results*, **112**: 323-327.

LOEBLICH, A.R., III. (1982): Dinophyceae. *In:* PARKER, S.P. (ed.): *Synopsis and Classification of Living Organisms*. Vol.1, McGraw-Hill, New York: 101-115.

LOHMANN, H. (1912): Untersuchungen über das Pflanzen- und Tierleben der Hochsee in Atlantischen Ozean während der Ausreise der "Deutschland". *Sitzber. Ges. naturforsch. Freunde*, Berlin: 32 pp.

LOHMANN, H. (1920): Die Bevölkerung des Ozeans mit Plankton nach den Ergebnissen der Zentrifugenfänge während der Ausreise der "Deutschland" 1911, zugleich ein Beitrag zur Biologie des Atlantischen Ozeans. *Arch. Biontol.*, **4**: 1-617.

LONGHURST, A. (1993): Seasonal cooling and blooming in tropical oceans. *Deep-Sea Res. I*, **40**: 2145-2165.

LONGHURST, A., SATHYENDRANATH, S., PLATT, T. & CAVERHILL, C. (1995): An estimate of global primary production in the ocean from satellite radiometer data. *J. Plankton Res.*, **17** (6): 1245-1271.

MARRET, F. (1994): Distribution of dinoflagellate cysts in recent marine sediments from the east Equatorial Atlantic (Gulf of Guinea). *Rev. Palaeobot. Palynol.*, **84**: 1-22.

MARTINSON, D.G., PISIAS, N.G., HAYS, J.D., IMBRIE, J., MOORE, T.C. & SHACKLETON, N.J. (1987): Age dating and the orbital theory of the ice ages: Development of a high-resolution 0 to 3000,000-year chronostratigraphy. *Quat. Res.*, **27**: 1-29.

MATSUOKA, K. (1983): List of synonyms of late Pleistocene to Holocene dinoflagellate cysts. I. *Gonyaulax* group. *News of Osaka Micropaleontologists*, **11**: 1-32.

MATSUOKA, K., KOBAYASHI, S. & GAINS, G. (1990): A new species of the genus *Ensiculifera* (Dinophyceae), its cyst and motile forms. *Bull. Plankton Soc. Japan*, **37** (2): 127-143.

MATTHEWSON, A.P., SHIMMIELD, G.B., KROON, D. & FALLICK, A.E. (1995): A 300 kyr high-resolution aridity record of the North African continent. *Paleoceanography*, **10** (3): 677-692.

MATTHIESSEN, J. (1991): Dinoflagellaten-Zysten im Spätquartär des Europäischen Nordmeeres: Palökologie und Paläo-Ozeanographie. *GEOMAR Report*, **7**: 104pp.

MCINTYRE, A., RUDDIMAN, W.F., KARLIN, K. & MIX, A.C. (1989): Surface water response of the equatorial Atlantic Ocean to orbital forcing. *Paleoceanography*, **4** (1): 19-55.

MCKENZIE, L. (1991): Does *Dinophysis* (Dinophyceae) have a sexual life cycle? *J. Phycol.*, **28**: 399-406.

MEESON, B.W. & SWEENEY, B.M. (1982): Adaptation of *Ceratium furca* and *Gonyaulax polyedra* (Dinophyceae) to different temperatures and irradiances: growth rates and cell volume. *J. Phycol.*, **18**: 241-245.

MEINECKE, G. (1992): Spätquartäre Oberflächenwassertemperaturen im östlichen äquatorialen Atlantik. *Berichte, Fachbereich Geowissenschaften, Universität Bremen*, **29**: 181 pp.

MITTELSTAEDT, E. (1991): The ocean boundary along the northwestern African coast: Circulation and oceanographic properties at the sea surface. *Progr. Oceanogr.*, **26**: 307-355.

MIX, A.C. & MOREY, A.E. (1996): Climate Feedback and Pleistocene Variations in the Atlantic South Equatorial Current. *In*: WEFER, G., BERGER, W.H., SIEDLER, G. & WEBB, D.J. (eds.) (1996): *The South Atlantic: Present and Past Circulation*. Springer, Berlin: 503-525.

MIX, A.C. (1989): Pleistocene paleoproductivity: evidence from organic carbon and foraminiferal species. *In*: BERGER, W.H., SMETACEK, V.S. & WEFER, G. (eds.): *Productivity of the Ocean: Present and Past. Dahlem Workshop Reports*, J. Wiley and Sons, Chichester: 313-340.

MIX, A.C., RUDDIMAN, W.F. & MCINTYRE, A. (1986a): Late quarternary paleoceanography of the tropical Atlanic, 1: Spatial variability of annual mean sea-surface temperatures, 0 - 20,000 years b.p.. *Paleoceanography*, **1** (1): 43-66.

MIX, A.C., RUDDIMAN, W.F. & MCINTYRE, A. (1986b): Late quarternary paleoceanography of the tropical Atlantic, 2: The seasonal cycle of the sea surface temperature, 0 - 20,000 years b.p.. *Paleoceanography*, **1** (3): 339-353.

MÖHN, E. (1984): System und Phylogenie der Lebewesen. Band 1: Physikalische, chemische und biologische Evolution. Prokaryonta. Eukaryonta (bis Ctenophora). *Schweizerbart, Stuttgart*: 884 pp.

MOITA, M.T. & SAMPAYO, M.A. (1993): Are there cysts in the genus *Dinophysis*. *In*: SMAYDA, T.J. & SHIMIZU, Y. (eds.), *Toxic Phytoplankton Blooms in the Sea*. Elsevier, Amsterdam: 153-158.

MOLFINO, B., KIPP, N.G. & MORLEY, J.J. (1982): Comparison of foraminiferal, coccolithophorid, and radiolarian paleotemperature equations: Assemblage coherency and estimate concordancy. *Quat. Res.*, **17**: 279-313.

MOLINARI, R.L. (1982): Observations of eastward currents in the tropical South Atlantic Ocean: 1978-1980. *J. Geophys. Res.*, **87**: 9707-9714.

MOLINARI, R.L., VOITURIEZ, B. & DUNCAN, P. (1981): Observations in the subthermocline undercurrent of the equatorial South Atlantic Ocean. *Oceanol. Acta*, **4** (4): 451-456.

MONTRESOR, M. & ZINGONE, A. (1988): *Scrippsiella precaria* sp. nov. (Dinophyceae), a marine dinoflagellate from the Gulf of Naples. *Phycologia*, **3**: 387-394.

MONTRESOR, M., JANOFSKE, D., WILLEMS, H. (1997): The cyst-theca relationship in *Calciodinellum operosum* emend. (Peridiniales, Dinophyceae) and a new approach for the study of calcareous cysts. *J. Phycol.*, **33** (1): 122-131.

MONTRESOR, M., MONTESARCHIO, E., MARINO, D. & ZINGONE, A. (1994): Calcareous dinoflagellate cysts in marine sediments of the Gulf of Naples (Mediterranean Sea). *Rev. Palaeobot. Palynol.*, **84**: 45-56.

MONTRESOR, M., ZINGONE, A. & MARINO, D. (1993): The calcareous resting cyst of *Pentapharsodinium tyrrhenicum* comb. nov. (Dinophyceae). *J. Phycol.*, **29**: 223-230.

MUDIE, P.J. (1989): Palynology and dinocyst biostratigraphy of the late Miocene to Pleistocen, Norwegian Sea ODP Leg 104, Sites 642 to 644. *In:* ELDHOLM, O., THIEDE, J., TAYLOR, E. et al., *Proc. ODP, Sci. Results*, **104**: 587-610.

MULITZA, S. (1994): Spätquartäre Variationen der oberflächennahen Hydrographie im westlichen äquatorialen Atlantik. *Berichte, Fachbereich Geowissenschaften, Universität Bremen*, **57**: 97 pp.

MÜLLER, P.J., SCHNEIDER, R. & RUHLAND, G. (1994): Late Quarternary PCO_2 variations in the Angola Current: Evidence from organic carbon $\delta^{13}C$ and alkenone temperatures. *In:* ZAHN, R., KAMINSKI, M.A., LABEYRIE, L. & PEDERSEN, T.F. (eds.), *Carbon Cycling in the Glacial Ocean: Constraints on the Ocean's Role in Global Change*: 343-366.

NEHRING, S. (1995): Dinoflagellate resting cysts in phytoplankton ecology in the North Sea. *Helgoländer Meeresunters.*, **49**: 375-392.

PETERSON, R.G. & STRAMMA, L. (1991): Upper-level circulation in the South Atlantic Ocean. *Prog. Oceanog.*, **26**: 1-73.

PFLAUMANN, U., DUPRAT, J., PUJOL, C. & LABEYRIE, L.D. (1996): SIMMAX: A modern analog technique to deduce Atlantic sea surface temperatures from planktonic foraminifera in deep-sea sediments. *Paleoceanography*, **11** (1): 15-35.

PHILANDER, S.G.H. & PACANOWSKI, R.C. (1986): The mass and heat budget in a model of the tropical Atlantic Ocean. *J. Geophys. Res.*, **91** (C12): 14,212-14,220.

PLATT, T.; SATHYENDRANATH, S. & LONGHURST, A. (1995): Remote sensing of ocean colour: a vehicle for estimation of marine primary production at a regional scale. *Phil. Trans. R. Soc. London Ser. A*, **348**: 191-202.

POWELL, A.J., DODGE, J.D. & LEWIS, J. (1990): Late Neogene to Pleistocene palynological facies of the Peruvian continental margin upwelling, Leg 112. *Proc. ODP, Sci. Results*, **112**: 297-321.

PRELL, W.L., IMBRIE, J., MARTINSON, D.G., MORLEY, J.J., PISIAS, N.G., SHACKLETON, N.J. & STREETER, H.F. (1986): Graphic correlation of oxygen isotope stratigraphy application to the Late Quarternary. *Paleoceanography*, **1** (2): 137-162.

PRÉZELIN, B. (1987): Photosynthetic physiology of dinoflagellates. *In:* TAYLOR, F.J.R. (ed.), The Biology of Dinoflagellates. *Bot. Monogr.*, **21**: 174-223.

RAVELO, A.C., FAIRBANKS, R.G. & PHILANDER, S.G.H. (1990): Reconstructing tropical Atlantic hydrography using planktonic foraminifera and an ocean model. *Paleoceanography*, **5** (3): 409-431.

REGUERA, B., BRAVO, I. & FRAGA, S. (1990): Distribution of *Dinophysis acuta* at the time of a DSP outbreak in the Rías of Pontovedra and Vigo (Galicia, NW Spain). *International Council for the Exploration of the Sea* C.M. 1990/L: 14.

REGUERA, B., BRAVO, I. & FRAGA, S. (1995): Autoecology and some life history stages of *Dinophysis acuta* Ehrenberg. *J. Plankton Res.*, **17** (5): 999-1015.

REID, J.L., Jr. (1964a): Evidence of a South Equatorial Counter Current in the Atlantic Ocean in July 1963. *Nature*, **203**: 182.

REID, J.L., Jr. (1964b): A transequatorial Atlantic oceanographic section in July 1963 compared with other Atlantic and Pacific sections. *J. Geophys. Res.*, **69**: 5205-5215.

REID, P.C. & HARLAND, R. (1977): Studies of Quaternary dinoflagellate cysts from the North Atlantic. *AASP Contrib. Series*, **5A**: 147-169.

REID, P.C. (1978): Dinoflagellate cysts in the plankton. *New Phytologist*, **80**: 219-229.

RICHARDSON, P.L. & PHILANDER, S.G.H. (1987): The seasonal variations of surface currents in the tropical Atlantic Ocean: A comparison of ship drift data with results from a general circulation model. *J. Geophys. Res.*, **92** (C1): 715-724.

RUDDIMAN, W.F., RAYMO, M.E., MARTINSON, D.G., CLEMENT, B.M. & BACHMAN, J. (1989): Pleitocene evolution: Northern hemisphere ice sheets and North Atlantic Ocean. *Paleoceanography*, **4**: 353-412.

SARJEANT, W.A.S. (1982): Dinoflagellate cyst terminology: a discussion and proposals. *Can. J. Bot.*, **60**: 922-945.

SARNTHEIN, M., PFLAUMANN, U., ROSS, R., TIEDEMANN, R. & WINN, K. (1992): Transfer functions to reconstruct ocean palaeoproductivity: a comparison. *In:* Summerhays, C.P., PRELL, W.L. & Emeis, K.C. (eds.): *Upwelling Systems: Evolution since the Early Miocene*, Geological Society Special Publication, **64**: 411-427.

SARNTHEIN, M., TETZLAFF, G., KOOPMANN, B., WOLTER, K. & PFLAUMANN, U. (1981): Glacial and interglacial wind regimes over the eastern subtropical Atlantic and North-West Africa. *Nature*, **293**: 193-196.

SARNTHEIN, M., WINN, K., DUPLESSY, J.-C. & FONTUGNE, R. (1988): Global variations of surface ocean productivity in low and mid latitudes: influence on CO_2 reservoirs of the deep ocean and atmosphere during the last 21,000 years. *Paleoceanography*, **3** (3): 361-399.

SARNTHEIN, M., WINN, K., JUNG, S.J.A., DUPLESSY, J.-C., LABEYRIE, L., ERLENKEUSER, H. & GANSSEN, G. (1994): Changes in east Atlantic deepwater ciculation over the last 30,000 years: Eight time slice reconstructions. *Paleoceanography*, **9** (2): 209-267.

SATHYENDRANATH, S.; LONGHURST, A.; CAVERHILL, C.M. & PLATT, T. (1995): Regionally and seasonally differentiated primary production in the North Atlantic. *Deep-Sea Res. I*, **42**: 1773-1802.

SCHNEIDER, R.R., MÜLLER, P.J. & RUHLAND, G. (1995): Late Quaternary surface circulation in the east equatorial South Atlantic: Evidence from alkenone sea surface temperatures. *Paleoceanography*, **10** (2): 197-219.

SCHNEIDER, R.R., MÜLLER, P.J. & RUHLAND, G., Meinecke, G., Schmidt, H. & Wefer, G. (1996): Late Quarternary Surface Temerature and Productivity in the East-Equatorial Atlantic: Response to Changes in Trade/Monsoon Wind Forcing and Surface Water Advection. *In*: WEFER, G., BERGER, W.H., SIEDLER, G. & WEBB, D.J. (eds.) (1996): *The South Atlantic: Present and Past Circulation*. Springer, Berlin: 527-551.

SIKES, E.L. & KEIGWIN, L.D. (1994): Equatorial Atlantic sea surface temperature for the last 30 kyr: A comparison of $U^{k'}_{37}$, $\delta^{18}O$ and foraminiferal assemblage estimates. *Paleoceanography*, **9** (1): 31-45.

SIKES, E.L. & KEIGWIN, L.D. (1996): A reexamination of northeast Atlantic sea surface temperature and salinity over the last 16 kyr. *Paleoceanography*, **11** (3): 327-342.

SOURNIA, A. (1982): Is there a shade flora in the marine plankton? *J. Plankton Res.*, **4** (2): 391-399.

SOURNIA, A. (1986): Volume 1: Introduction, Cyanophycées, Dictyochophycées, Dinophycées et Raphidophycées. *In:* Atlas du Phytoplancton Marin. *Edition du Centre National de la Recherche Scietifique*: 216 pp.

STEIDINGER, K.A. & TANGEN, K. (1996): Dinoflagellates. *In:* Tomas, C.R. (ed.): *Identifying marine diatoms and dinoflagellates*. Acadamic Press, Inc., San Diego: 387-597.

STEINMETZ, J.C. (1991): Calcareous Nannoplankton Biocoenosis: Sediment Trap Studies in the Equatorial Atlantic, Central Pacific, and Panama Basin. *Ocean Biocoenosis Series*, **1**: 85 pp.

STOTT, L.D. & TANG, C.M. (1996): Reassessment of foraminiferal-based tropical sea surface $\delta^{18}O$ paleotemperatures. *Paleoceanography*, **11** (1): 37-56.

STOVER, L.E. & EVITT, W.R. (1978): Analyses of Pre-Pleistocene organic-walled dinoflagellate cysts. *Stanford Univ. Pupl. Geol. Sci.*, **15**: 300 pp.

STRAMMA, L., IKEDA, Y. & PETERSON, R.G. (1990): Geostrophic transports in the Brazil Current region north of 20°S. *Deep-Sea Res.*,

STREET-PERROTT, F.A. & PERROTT, R.A. (1990): Abrupt climate fluctuations in the tropics: the influence of Atlantic Ocean circulation. *Nature*, **343**: 607-612.

TANGEN, K., BRAND, L.E., BLACKWELDER, P.L. & GUILLARD, R.R.L. (1982): *Thoracosphaera heimii* (LOHMANN) KAMPTNER is a dinophyte: Observations on its morphology and life cycle. *Marine Micropaleont.*, **7**: 193-212.

TAYLOR, F.J.R. (1976): Dinoflagellates from the International India Expedition. *Bibliotheca Botanica*, **132**: 1-234.

TAYLOR, F.J.R. (1980): On dinoflagellate evolution. *Biosystems*, **13**: 65-108.

TAYLOR, F.J.R. (1987b): Ecology of dinoflagellates: A. General and marine ecosystems. *In:* TAYLOR, F.J.R. (ed.), The Biology of Dinoflagellates. *Bot. Monogr.*, **21**: 399-501.

TAYLOR, F.J.R. (ed.) (1987a): The Biology of Dinoflagellates. *Bot. Monogr.*, **21**: pp.

THIEDE, J. & JÜNGER, B. (1991): Faunal and floral indicators of ocean coastal upwelling (NW African and Peruvian Continental Margins). *In:* SUMMERHAYES, C.P., PRELL, W.L. & EMEIS, K.C. (eds.), Upwelling Systems: Evolution since the Early Miocene. *Geol. Soc. Spec. Publ.*, **64**: 47-76.

THOMAS, W.H., VERNET, M. & GIBSON C.H. (1995): Effects of small-scale turbulance on photosynthesis, pigmentation, cell division, and cell size in the marine dinoflagellate *Gonyaulax polyedra* (Dinophyceae). *J. Phycol.*, **31**: 50-59.

TREPPKE, U.F. (1996): Saisonalität im Diatomeen- und Silikoflagellatenfluß im östlichen tropischen und subtropischen Atlantik. *Berichte, Fachbereich Geowissenschaften, Universität Bremen*, **74**: 200 pp.

TREPPKE, U.F., LANGE, C.B. & WEFER, G. (1996): Vertical fluxes of diatoms and silicoflagellates in the eastern equatorial Atlantic, and their contribution to sedimentary record. *Marine Micropaleontol.*, **28**: 73-96.

VAN BENNEKOM, A.J. (1996): Silica Signals in the South Atlantic. *In*: WEFER, G., BERGER, W.H., SIEDLER, G. & WEBB, D.J. (eds.) (1996): *The South Atlantic: Present and Past Circulation*. Springer, Berlin: 345-354.

VERARDO, D.J. & MCINTYRE, A. (1994): Production and destruction: Control of biogenous sedimentation in the tropical Atlantic 0-300,000 years B.P. *Paleoceanography*, **9** (1):63-86.

VERSTEEGH, G.J.M. (1993): New Pliocene and Pleitocene calcareous dinoflagellate cysts from southern Italy and Crete. *Rev. Palaeobot. Palynol.*, **78**: 353-380.

VERSTEEGH, G.J.M. (1994): Recognition of non-cyclic environmental changes in the Mediterranean Pliocene: A palynological approach. *Marine Micropaleont.*, **23**: 147-183.

WALL, D. & DALE, B. (1968,a): Modern dinoflagellate cysts and evolution of the Peridiniales. *Micropaleontology*, **14** (3): 265-304.

WALL, D. & DALE, B. (1968,b): Quarternary calcareous dinoflagellates (Calciodinellideae) and their natural affinities. *J. Paleont.*, **42** (6): 1395-1408.

WALL, D., DALE, B. & HARADA, K. (1973): Descriptions of new fossil dinoflagellates from the Late Quarternary of the Black Sea. *Micropaleontology*, **19** (1): 18-31.

WALL, D., DALE, B., LOHMANN, G.P. & SMITH, W.K. (1977): The environmental and climatic distribution of dinoflagellate cysts in modern marine sediments from regions in the North and South Atlantic Oceans and adjcent seas. *Marine Micropaleont.*, **2**: 121-200.

WALL, D., GUILLARD, R.R.L., DALE, B., SWIFT, E. & WATABE, N. (1970): Calcitic resting cysts in *Peridinium trochoideum* (STEIN) LEMMERMANN, an autotrophic marine dinoflagellate. *Phycologia*, **9** (2): 151-156.

WEFER, G. & FISCHER, G. (1993): Seasonal pattern of vertical particle fluxes in equatorial and coastal upwelling areas of the eastern Atlantic. *Deep-Sea Res.*, **40**: 1613-1645.

WEFER, G., BEESE, D., BERGER, W.H., BLEIL, U., BUSCHHOFF, H., FISCHER, G., KALBERER, M., KEMLE-VON MÜCKE, S., KERNTOPF, B., KOTHE, C., LUTTER, D., PIOCH, B., POTOTZKI, F., RATMEYER, V., ROSIAK, U., SCHMIDT, W., SPIEß, V. & VÖLKER, D. (1993): Bericht über die METEOR-Fahrt M20/1, Bremen - Abidjan, 18.11.1991 - 22.12.1991. *Berichte, Fachbereich Geowissenschaften, Universität Bremen*, **24**: 73 pp.

WEFER, G., BEESE, D., BERGER, W.H., BUSCHHOFF, H., CEPEK, M., DIEKAMP, V., FISCHER, G., HOLMES, E., KEMLE-VON MÜCKE, S., KERNTOPF, B., LANGE, C., MULITZA, S., OTTO, S., PLUGGE, R., RATMEYER, V., RÜHLEMANN, C., SCHMIDT, W., SCHWARZE, M., WALLMANN, K., &

ZABEL, M. (1994): Report and preliminary results of METEOR-cruise M23/3, Recife - Las Palmas, 21.3.1993 - 12.4.1993. *Berichte, Fachbereich Geowissenschaften, Universität Bremen*, **44**: 71 pp.

WEFER, G., BERGER, W.H., BICKERT, T., DONNER, B., FISCHER, G., KEMLE-VON MÜCKE, S., MEINICKE, G., MÜLLER, P.J., MULITZA, S., NIEBLER, H.-S., PÄTZOLD, J., SCHMIDT, H., SCHNEIDER, R.R. & SEGL, M. (1996a): Late Quarternary Surface Circulation of the South Atlantic: The Stable Isotope Record and Implications for Heat Transport and Productivity. *In*: WEFER, G., BERGER, W.H., SIEDLER, G. & WEBB, D.J. (eds.) (1996): *The South Atlantic: Present and Past Circulation*. Springer, Berlin: 461-502.

WEFER, G., BERGER, W.H., SIEDLER, G. & WEBB, D.J. editors (1996b): The South Atlantic: Present and Past Circulation. *Springer, Berlin*: 644 pp.

WILLEMS,H. (1985): *Tetramerosphaera lacrima* eine intern gefächerte Calcisphaere aus der Ober-Kreide. *Senckenberg. Leth.*, **66** (3/5): 177-201.

WILLEMS,H. (1988): Kalkige Dinoflagellaten-Zysten aus der oberkretazischen Schreibkreide-Fazies N-Deutschlands (Coniac-Maastricht). *Senckenberg. Leth.*, **68** (3/5): 433-477.

WILLEMS,H. (1990): *Tetratropis*, eine neue Kalkdinoflagellaten-Gattung (Pithonelloideae) aus der Ober-Kreide von Lägerdorf (N-Deutschland). *Senckenberg. Leth.*, **70** (1/3): 239-257.

WILLEMS,H. (1992): Kalk-Dinoflagellaten aus dem Unter-Maastricht der Insel Rügen. *Z. geol. Wiss.*, **20** (1/2): 155-178.

WILLEMS,H. (1994): New calcareous dinoflagellates from the Upper Cretaceous white chalk of northern Germany. *Rev. Palaeobot. Palynol.*, **84**: 57-72.

WOOD, E.J.F. (1968): Dinoflagellates of the Caribbean Sea and adjacent areas. *University of Miami Press, Coral Gables, Florida*, 144 pp.

ZAO, M., BEVERIDGE, A.S., SHACKLETON, N.J., SARNTHEIN, M. & EGLINTON, G. (1995): Molecular stratigraphy of cores off northwest Africa: Sea surface temperature history over the last 80 ka. *Paleoceanography*, **10** (3):661-675.

ZÜGEL, P. (1994): Verbreitung kalkiger Dinoflagellaten-Zysten im Cenoman/Turon von Westfrankreich und Norddeutschland. *Cour. Forsch.-Inst. Senckenberg*, **176**: 159 pp.

PLATES

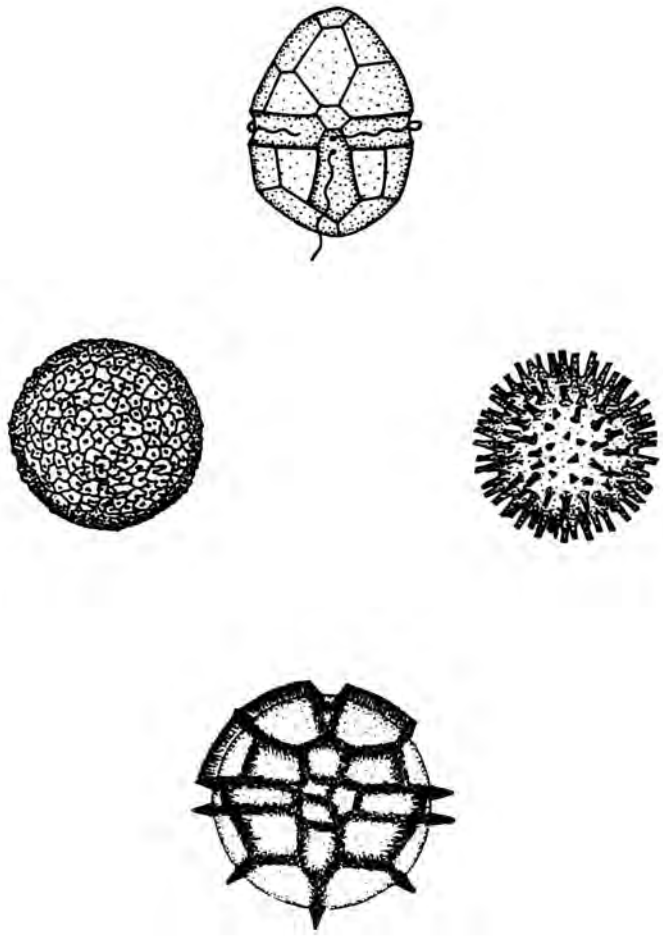

PLATE 1:

FAMILY PROROCENTRACEAE STEIN, 1883

MESOPORUS LILLICK, 1937

Fig.1: ***Mesoporus perforatus*** (GRAN) LILLICK, 1937; lateral view, one main round thecal plate, anterior end at bottom, characteristic depression (the "pore") in centre of plate, plates joined at edges with sutural bands, plate ornamented with "pimples", pores around periphery of each main plate, sample 22-S17, #01114.

PROROCENTRUM EHRENBERG, 1834

Fig.2: ***Prorocentrum balticum*** (LOHMANN) LOEBLICH, 1970; oblique valve view, anterior end shows the flagellar pore complex with minute apical spines, ridged sutural bands between the two plates, plates covered with small "pimples", sample 22-S08, #01328.

Fig.3: ***P. compressum*** (BAILEY) ABÉ ex DODGE, 1975; lateral view, anterior end at the left with small projections, plates covered with pores in characteristic depressions, sample 22-S17, #01115.

Fig.4: ***P. gracile*** SCHÜTT, 1895; lateral view, theca lanceolated, anterior end rounded with broad-lanceolate apical spine at the right, pointed posterior end at the left, thecal plates ornamented with shallow depressions and perforated by trichocyst pores, sample 22-S08, #01291.

Fig.5: ***P. rostratum*** STEIN, 1883; lateral view, cell elongated, characteristic two-pointed spine at anterior part to the right, two-pointed anterior end to the left, thecal plates covered with tiny spines and perforated by pores, sample 22-S27, #02342.

Fig.6: ***P. lebourae*** SCHILLER, 1928; oval theca in lateral view, anterior end with broad-lanceolate spine in upper right corner, plates ornamented with small depressions and perforated by numerous pores arranged in radial rows in a typical pattern, sample 22-S08, #01422.

Fig.7: ***P. micans*** EHRENBERG, 1833; lateral view, anterior part rounded with spine in the upper right corner, posterior end pointed, theca covered with shallow depressions and perforated by trichocyst pores, sample 22-S32, #02754.

Fig.8: ***P. nanum*** SCHILLER, 1918; lateral view, thecal plate smooth and rounded with trichocyst pores at periphery, anterior end with blunt spine in upper right corner, sample 22-S27, #02339.

Fig.9, 10: ***P. sphaeroideum*** SCHILLER, 1928; sample 22-S24, #02715

9. oblique lateral view, resembles *P. balticum* but larger, anterior part up, thecal plates covered with minute spines,

10. flagellar pore area with small apical spine, ridged sutural bands between the two main plates.

Plate 1: Family Prorocentraceae

1 3µm

2 3µm

3 10µm

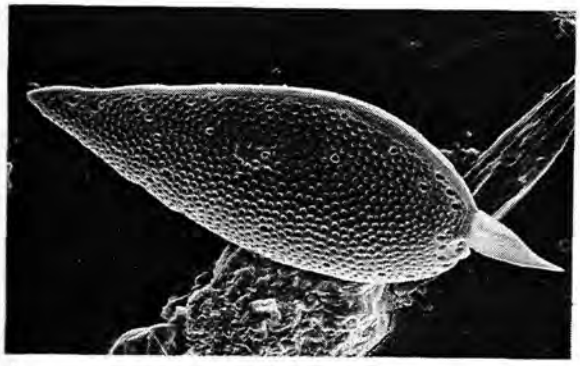

4 10µm

5 10µm

6 10µm

7 10µm

8 10µm

9 10µm

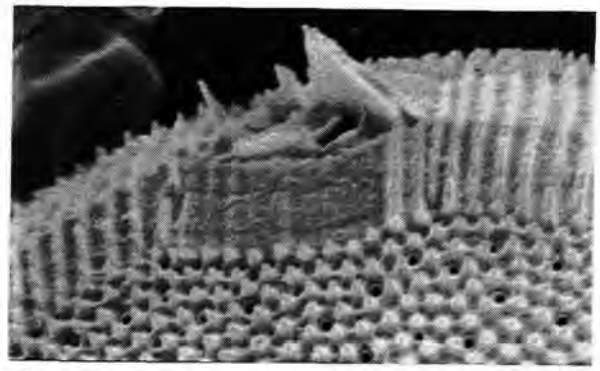

10 1µm

PLATE 2:

FAMILY DINOPHYSIACEAE STEIN, 1883

DINOPHYSIS EHRENBERG, 1839

Fig.1: sample 22-S17,

a. *Dinophysis amphora* BALECH, 1971 (lower specimen); right lateral view, cell round, cingulum wide not excavated with large anterior list, left sulcal list broad and sustained by three ribs, posterior rib visible, right sulcal list ends at rib theca covered with depressions, #01122,a;

b. *D. pulchella* (LEBOUR) BALECH, 1967 (upper specimen); right lateral view, tiny species: ~10 µm, epitheca distinctive, cingulum wide with relatively narrow lists, sulcal lists small, left sulcal list supported by ribs, thecal surface with depressions, #01122,b.

Fig.2, 3: ***D. caudata*** SAVILLE-KENT, 1881; sample 22-S33, #02751,

2. right lateral view, cell with long ventral hypothecal projection, epitheca reduced sloping to the ventral side with large anterior cingular list, dorsal posterior cingular list small, on ventral side joining into wing-like left sulcal list with three supporting ribs, right sulcal list small,

3. thecal plate surface showing hexagonal areolation with central pores.

Fig.4: ***D. caudata* var. *tripos*** (GOURRET) GAIL, 1950; lateral view, pair of cells after longitudinal division, still joined at dorsal edges of hypothecae, long ventral hypothecal projections and shorter dorsal projections, both sulcal lists already developed, sample 22-S27, #02383.

Fig.5, 6, 7: ***D. cuneus*** (SCHÜTT) ABÉ, 1967; sample 22-S35,

5. right lateral view, cingular and sulcal lists subequal in size with ridges, #02784, (in dark upper right corner a specimen of *Thoracosphaera heimii*),

6. plate ornamentation reticulate with pores in centre of areolae, same specimen as Fig.5.

7. antapical view, #02847.

Fig.8, 9: ***D. dens*** PAVILLARD, 1915; sample 22-S33, #02743

8. right lateral view, species "sac-shaped", epitheca flat and obscured by anterior cingular list twice as large as posterior list, both inclined anteriorly, left sulcal list supported by three spines, much larger and twice as long as right sulcal list,

9. smooth plate surface with numerous pores.

Plate 2: Family Dinophysiaceae

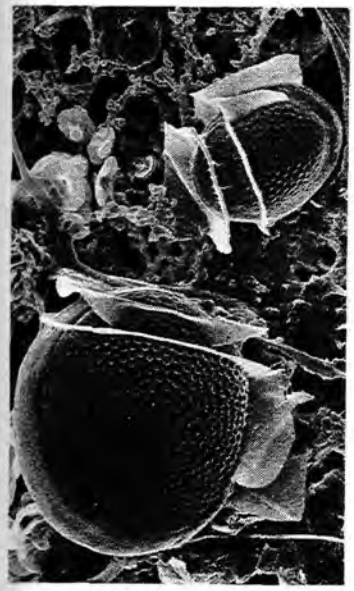

1 10µm

2 10µm

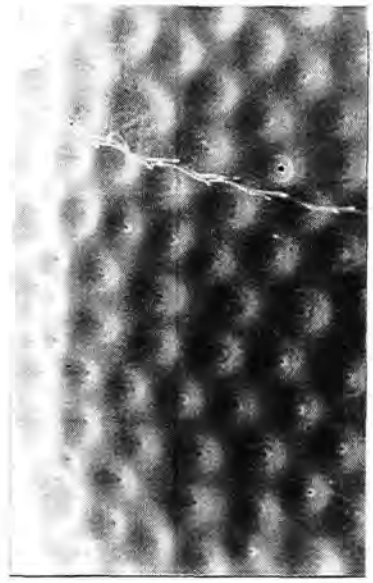

3 3µm

4 30µm

5 10µm

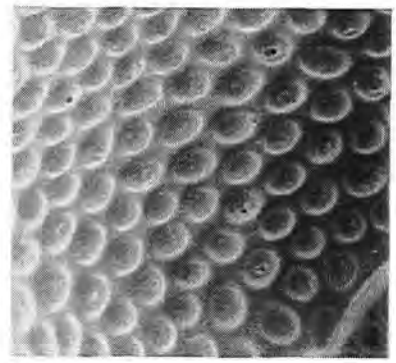

6 3µm

7 10µm

8 10µm

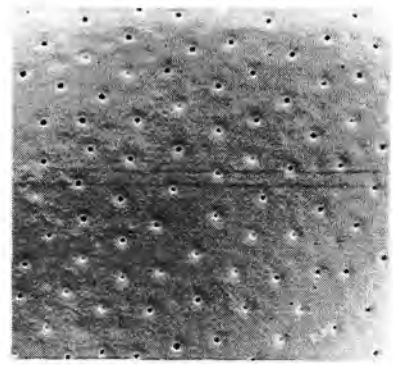

9 10µm

PLATE 3:

FAMILY DINOPHYSIACEAE STEIN, 1883

DINOPHYSIS EHRENBERG, 1839

Fig.1: ***Dinophysis fortii*** PAVILLARD, 1923; right lateral view, epitheca reduced and obscured by curved anterior girdle lists, cingulum excavated, left sulcal list wide on 4/5 of hypotheca, right sulcal list much shorter, plate ornamented with circular areolations, sample 22-S25, #02291.

Fig.2, 5: ***D. hastata*** STEIN, 1883; sample 22-S34, #02732,

2. right lateral view, cell with triangular spine at posterior end of hypotheca (at bottom), epitheca flat sloping ventrally, cingulum not excavated, anterior girdle list broader and with ribs, left sulcal list wide and wing-like supported by ribs, lowest rib visible,

5. thecal surface hexagonal with reticulations and pores in centre of some areolae.

Fig.3: ***D. parva*** SCHILLER, 1928; right lateral view, cell ovoid, epitheca very small, anterior cingular list wide supported by ribs with a "crown-like" appearance, posterior list very narrow; cingulum wide and not excavated, sulcal lists relatively small, thecal plates smooth and perforated with pores parallel to suture of hypothecal plates, sample 22-S16, #02538.

Fig.4: ***D. micropterygia*** DANGEARD, 1927; oblique right lateral view, cingular and sulcal lists small, reticulate plate ornamentation continues on right sulcal list, sample 22-S25, #02271.

Fig.6: ***D. ovum*** SCHÜTT, 1895; left lateral view, cell ovoid, epitheca reduced and concealed by anterior girdle list, hypotheca rounded, left sulcal list extended and sustained by three ribs, thecal surface smooth with circular areolations and pores in centre, sample 22-S37, #02884.

Fig.7: ***D. parvula*** (SCHÜTT) BALECH, 1967; left lateral view, cell nearly spherical, epitheca domed, girdle lists small, cingulum not excavated, left sulcal list moderate, thecal plates smooth with pores parallel to plate sutures, sample 22-S11, #02405.

Fig.8: ***D. rotundatum*** CLAPARÈDE & LACHMANN, 1859; oblique right lateral view on rounded epitheca, cingulum wide and not excavated, girdle lists subequal in width, medium size left sulcal list with three ribs, narrower right sulcal list, thecal surface covered with shallow depressions some carrying a single pore, sample 22-S16, #01232.

Plate 3: Family Dinophysiaceae

1 10µm

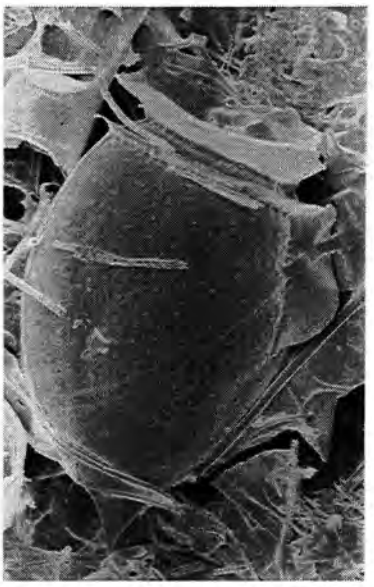

2 10µm

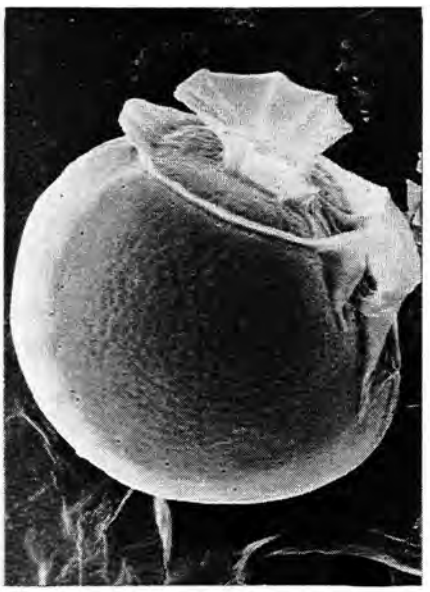

3 10µm

4 10µm

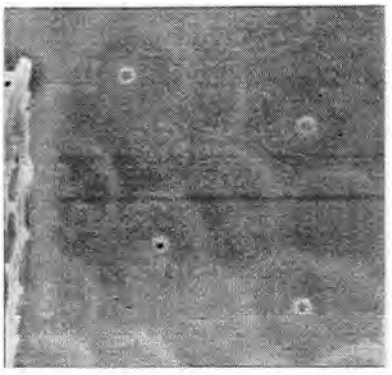

5 3µm

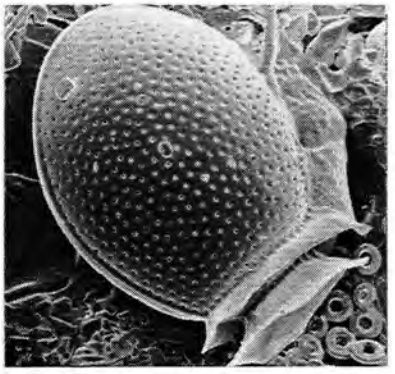

6 10µm

7 10µm

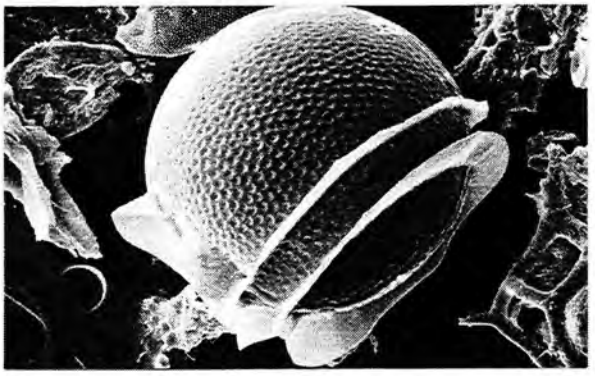

8 10µm

PLATE 4:

FAMILY ORNITHOCERCACEAE KOFOID & SKOGSBERG, 1928

ORNITHOCERCUS STEIN, 1883

Fig.1: ***Ornithocercus magnificus*** STEIN, 1883; left lateral view, cell strikingly ornamented with huge "sail-like" left sulcal list supported by four ribs (with a specimen of *Thoracosphaera heimii* on top), "parachute-like" posterior cingular list with radial ribs inclined anteriorly and concealing small epitheca, hypotheca round, plates covered with large depressions, sample 22-S18, #01995.

Fig.2: ***O. steinii*** SCHÜTT, 1900; left lateral view, epitheca slightly inclined to ventral side and obscured by large and ribbed posterior cingular list, left sulcal list extensively ridged, reaching dorsal side of hypotheca and touching posterior girdle list, hypotheca ovoid to round, thecal depressions large, sample 22-S18, #02150.

PARAHISTIONEIS KOFOID & SKOGSBERG, 1928

Fig.3: ***Parahistioneis acuta*** KOFOID & SKOGSBERG, 1928; right lateral view, species intermediate in list development between *Ornithocercus* and *Histioneis* (HALLEGRAEFF & LUCAS, 1988), reduced epitheca inclined ventrally and concealed by wide and strongly ribbed anterior cingular list, posterior girdle list "collar-like" and flared with radial ribs, cingulum wider dorsally than ventrally, left sulcal list ample with large pointed rib at posterior end of hypotheca, plates ornamented by depressions extending to right sulcal list, sample 22-S14, #01015.

FAMILY AMPHISOLENIACEAE LINDEMANN, 1928

AMPHISOLENIA STEIN, 1883

Fig.4, 5: ***Amphisolenia* cf. *globifera*** STEIN, 1883; sample 22-S23, #02580,

4. left lateral view, cell needle-shaped with extremely elongated hypotheca with a "swelling" in the upper part,
5. the "head": very much reduced epitheca and excavated cingulum with lists, sulcus not discernible.

FAMILY CALCIODINELLACEAE DEFLANDRE, 1949 *emend.* BUJAK & DAVIES, 1983

SCRIPPSIELLA BALECH, 1959

Fig.6, 7: ***Scrippsiella* cf. *trochoidea*** (STEIN) LOEBLICH III, 1976;

6. left specimen: ventral view, equatorial cingulum offset one width on right side, thecal plates smooth and relatively delicate with pores, sample 22-S10, #01375,a;

   right specimen: apical view on conical epitheca and apical pore complex, sample 22-S10, #01375,b.

7. oblique antapical view of sulcal area, hypotheca rounded without spines, sample 22-S08, #01324.

Plate 4:

Family Dinophysiaceae

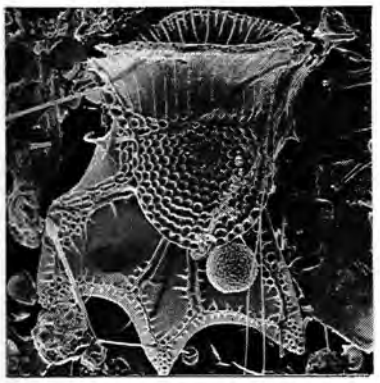

1 30µm

2 30µm

3 10µm

Family Amphisoleniaceae

4 100µm

5 10µm

Family Calciodinellaceae

6 10µm

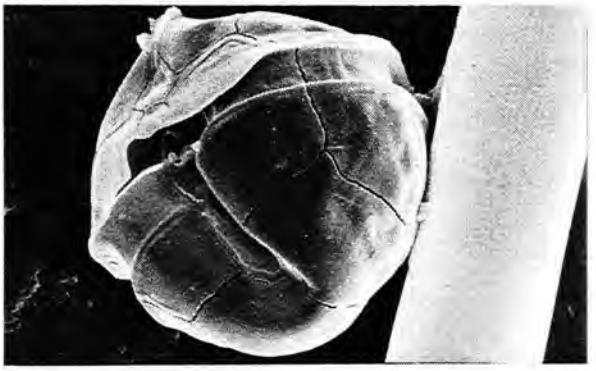

7 10µm

PLATE 5:

FAMILY CERATIACEAE WILEY & HICKSON, 1909

CERATIUM SCHRANK, 1793

Fig.1, 2: ***Ceratium azoricum*** CLEVE, 1900;

1. ventral view, cell relatively small flattened dorso-ventrally, apical horn shorter than body, hypotheca rounded with two posterior horns pointing to the anterior and just barely exceeding body, sample 22-S27, #02324;
2. dorsal view, plate surface smooth, no cingular lists, horns ornamented with low ridges, sample 22-S32, #02633.

Fig.3, 4: ***C. candelabrum*** (EHRENBERG) STEIN, 1883;

3. ventral view, cell "stubby", body broader than high, epitheca tapering obliquely, apical horn straight and short, (*Prorocentrum lebourae* in lower left corner) sample 22-S08, #01427;
4. dorsal view, hypotheca triangular with two straight antapical horns, left horn longer than right horn, cingulum with lists, thecal surface ornamented with low latitudinal ridges and perforated with pores, (*Prorocentrum gracile* on top) sample 22-S08, #01294.

Fig.5, 6: ***C. trichoceros*** (EHRENBERG) KOFOID, 1908;

5. ventral view, cell delicate, body small with long and thin horns, antapical horns at base almost at right angles to line of apical horn, then curved until being parallel to apical horn, length of antapicals almost the same as apical, sample 22-S27, #02388;
6. epitheca rounded, base of hypotheca almost flat, thecal plates smooth, no cingular lists, sample 22-S27, #02379.

Fig.7, 8: ***C. declinatum*** KARSTEN, 1907;

7. ventral view, body longer than broad and flattened dorsoventrally, all horns within body plane, , sample 22-S 11, #02465;
8. epitheca high and obliquely conical, apical horn straight but not at right angle to cingulum, hypotheca short, base round and stretching into antapical spines, left antapical horn shorter and more robust than right antapical, cingulum with lists on left side but without lists on right side, sample 22-S11, #02428.

Plate 5: Family Ceratiaceae

1 30µm

2 10µm

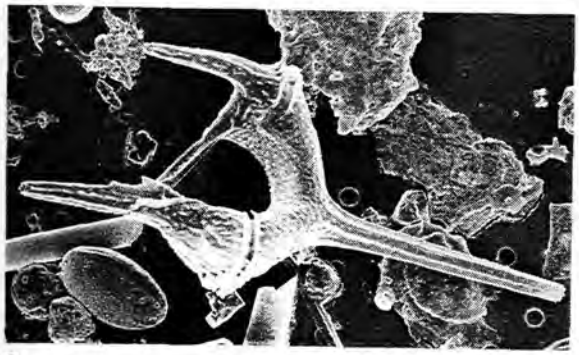

3 30µm

4 30µm

5 100µm

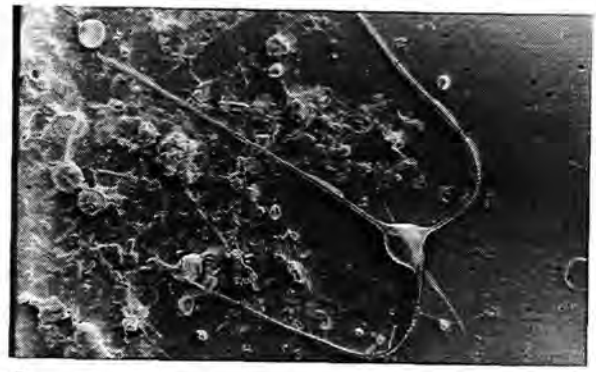

6 100µm

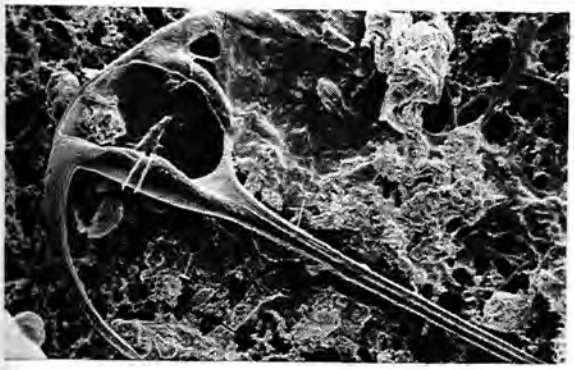

7 30µm

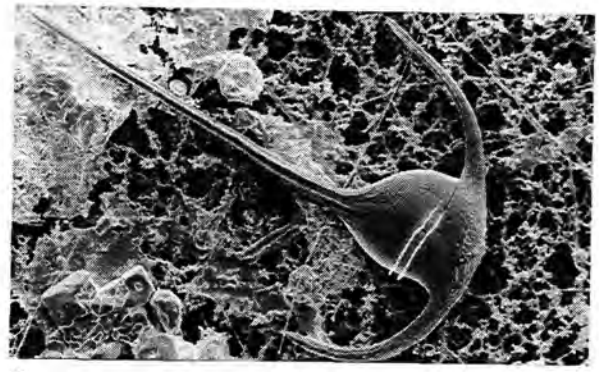

8 30µm

PLATE 6:

FAMILY CERATIACEAE WILEY & HICKSON, 1909

CERATIUM SCHRANK, 1793

Fig.1, 2: ***Ceratium furca*** (EHRENBERG) CLAPARÈDE & LACHMAN, 1858;

1. ventral view, body elongated and straight, epitheca high tapering gradually into apical horn, sample 22-S27, #02325;
2. dorsal view, hypothecal sides parallel, antapical horns sub-parallel and strong, left antapical longer than right one, cingulum incised with lists, thecal plates ornamented with reticulations and longitudinal ridges with pores in between, antapical horns slightly toothed along the sides, sample 22-S25, #02303.

Fig.3, 4: ***C. fusus*** (EHRENBERG) DUJARDIN, 1841;

3. ventral view, cell needle-shaped, epitheca high tapers gently to long straight apical horn, hypotheca tapering into long left antapical horn, right antapical absent, left antapical slightly toothed posteriorly, sample 22-S13, #01265;
4. ventral view, (with *Gonyaulax turbynei, G. striata, Thoracosphaera heimii*) sample 22-S08, #01293.

Fig.5, 6: ***C. gibberum*** GOURRET, 1883;

5. ventral view, cell rather bulbous, body thick, hypotheca rounded to gibbous and longer than epitheca, sample 22-S14, #01073;
6. dorsal view, epitheca low, apical horn asymmetrically bend to the left, right antapical horn bend around dorsally and almost touching epitheca, left antapical evenly bend anteriorly, thecal plates with pores and ridges mainly at sutures, (additionally: *Thoracosphaera heimii*) sample 22-S16, #02529.

Fig.7: ***C. hexacanthum*** GOURRET, 1883; dorsal view, cell large, antapical horns twisted, epitheca tapering into straight apical horn, thecal plates covered with characteristic large reticulations, sample 22-S27, #02366.

Fig.8: ***C. cf. horridum*** GRAN, 1902; ventral view, cell pentangular, epitheca short with steep right side and rounded left side tapering into long slender apical horn, hypotheca depressed posteriorly, antapical horns at angles 45° (left) and 90° (right) to the apical horn bending around in anterior direction, (additionally: *Oxytoxum sceptrum*, *Prorocentrum rostratum*) sample 22-S27, #02385.

Plate 6: Family Ceratiaceae

1 30µm

2 30µm

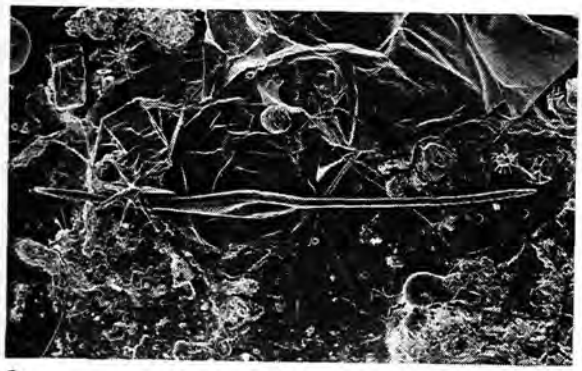

3 30µm

4 30µm

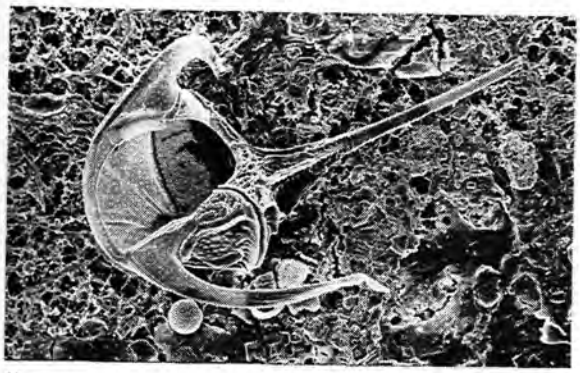

5 30µm

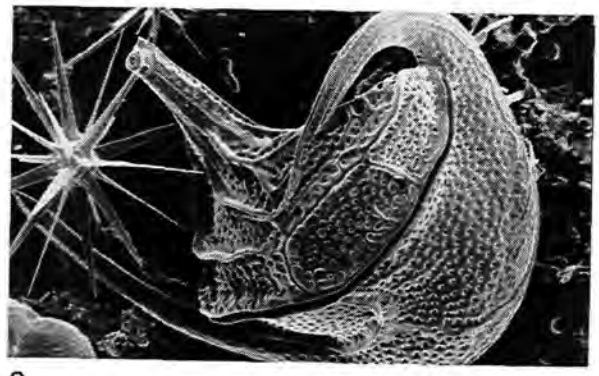

6 30µm

7 100µm

8 30µm

PLATE 7:

FAMILY CERATIACEAE WILEY & HICKSON, 1909

CERATIUM SCHRANK, 1793

Fig.1, 2: ***Ceratium karsteni*** PAVILLARD, 1907;

1. ventral view, cell with long apical horn, base of hypotheca flat, antapical horns in line then curving anteriorly and parallel to apical horn, left antapical much longer than right one and tip is bend toward the apical, (*Oxytoxum stropholatum* at apical horn) sample 22-S16, #01255;
2. dorsal view, theca almost triangular, base of apical horn slightly curved and with ridges, cingulum has lists, thecal plates perforated with pores, sample 22-S17, #01664.

Fig.3, 4: ***C. lineatum*** (EHRENBERG) CLEVE, 1899;

3. ventral view, cell rather delicate, apical horn long and straight, hypotheca rectangular with sides tapering into two straight antapical horns, left antapical horn longer than right one, (*Gonyaulax turbynei* at right bottom corner) sample 22-S13, #01274;
4. dorsal view, epitheca triangular and tapering into apical horn, cingulum slightly depressed with lists, thecal plates with longitudinal ridges and pores, sample 22-S27, #02362.

Fig.5: ***C. macroceros*** (EHRENBERG) VANHOFFEN, 1897; dorsal view, cell large and delicate, body small and pentangular, apical horn slender and even, two antapical horns pointing posteriorly then turning parallel to apical horn, left antapical horn at base in line with apical horn, right antapical horn emerges at 130° to apical horn, cingulum with lists, thecal surface smooth, (*Oxytoxum scolapax, Protoperidinium divergens* at left) sample 22-S37, #02878.

Fig.6: ***C. massiliense*** (GOURRET) JÖRGENSEN, 1911; ventral view, species very similar to *C. macroceros*, base contour of hypotheca is straight, both antapical horns arise at right angles to each other, neither one runs far posteriorly before bending sharply to the anterior, cingulum with lists, (*C. furca, Dinophysis dens, Prorocentrum micans* at the right) sample 22-S33, #02742.

Fig.7, 8: ***C. minutum*** JÖRGENSEN, 1920;

7. ventral view, cell small, base of hypotheca angled leading into very short antapical horns, right antapical shorter than left one, sample 22-S33, #02760;
8. dorsal view, epitheca rounded at cingulum then concavely tapering into short apical horn, thecal plates ornamented with longitudinal ridges and perforated by pores, sample 22-S32, #02631.

Plate 7: Family Ceratiaceae

1 100µm

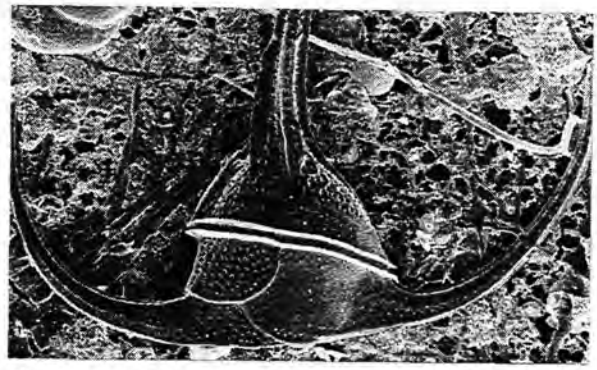

2 30µm

3 30µm

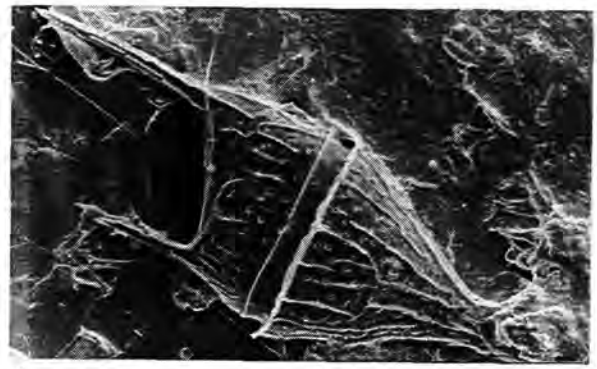

4 10µm

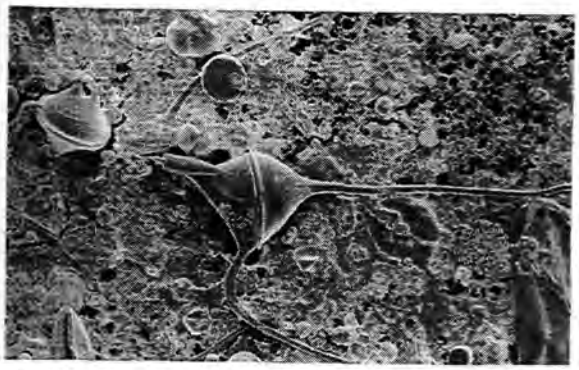

5 100µm

6 100µm

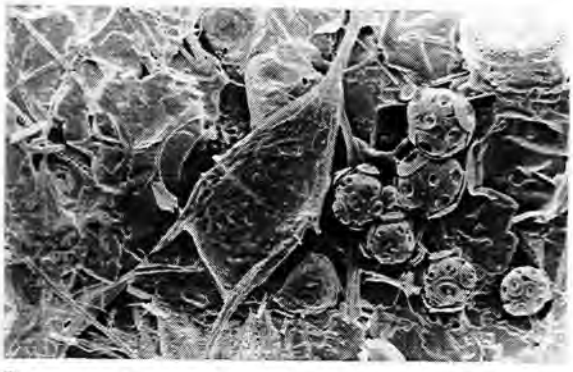

7 10µm

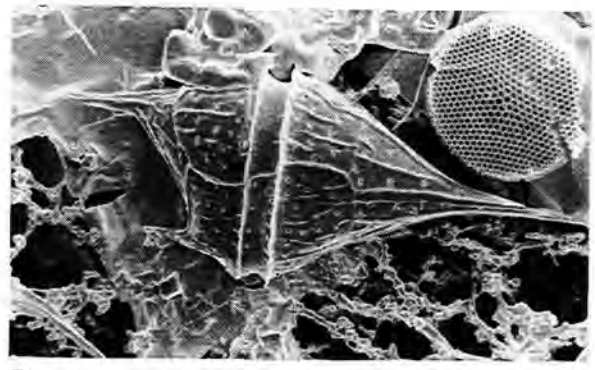

8 10µm

PLATE 8:

FAMILY CERATIACEAE WILEY & HICKSON, 1909

CERATIUM SCHRANK, 1793

Fig.1, 2, 3: ***Ceratium cf. pavillardii*** JÖRGENSEN, 1911;

1. ventral view, cell rather large with long and straight apical horn, sample 22-S18, #02155;
2. dorsal view, base of right antapical horn transverse then sharply bending ventral-anteriorly, base of left antapical horn directed dorsally then ventral-anteriorly at 30-50° with apical horn, sample 22-S18, #02153,
3. dorsal side shows almost triangular epitheca tapering into apical horn, base of hypotheca at angle to longitudinal axis, base of horns winged and toothed, same specimen as Fig.2.

Fig.4, 5: ***C. pentagonum*** GOURRET, 1883;

4. ventral view, cell with broad pentagonal body, epitheca triangular and tapering into straight apical horn, sample 22-S25, #02294;
5. dorsal view, hypotheca with slightly angular base ending into short and thick antapical horns, antapical horns slightly directed posteriorly, cingulum excavated with lists, thecal plates covered with longitudinal ridges and pores, sample 22-S25, #02236.

Fig.6, 7: ***C. teres*** KOFOID, 1907;

6. ventral view, cell with long straight apical horn, base of hypotheca angular tapering into two pointed antapical horns, left antapical "swollen" in the middle, (*Gonyaulax turbynei* at right side of cingulum) sample 22-S16, #01229;
7. dorsal view of slightly rounded body, epitheca drawn out and triangular, cingulum insignificantly depressed with lists, thecal plates ornamented with irregular and rudimentary longitudinal ridges and pores, (additionally: "*Sphaerodinella*" *albatrosiana*) sample 22-S16, #01247.

Fig.8: ***C. carriense*** GOURRET, 1883; dorsal view, species similar to *C. trichoceros* and *C. massiliense*, body small and almost triangular, antapical horns at right angles to line of apical horn curving gently to the anterior and ending 45° to apical horn, thecal surface smooth, no cingular lists, (*Oxytoxum sceptrum* at apical horn) sample 22-S27, #02373.

Fig.9, 10: ***C. tripos*** (O.F. MÜLLER) NITZSCH, 1817;

9. ventral view, cell with rounded epitheca tapering sharply into long apical horn, hypotheca flattened posteriorly, pointed antapical horns sharply bending to the anterior and almost parallel to apical horn, sample 22-S25, #02253;
10. dorsal view, base of apical horn slightly bend, cingulum with lists, thecal plates with pores, sample 22-S25, #02252.

Plate 8: Family Ceratiaceae

1 100µm

2 100µm

3 30µm

4 30µm

5 30µm

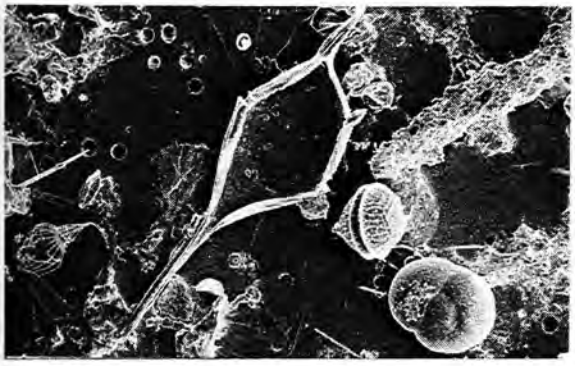

6 30µm

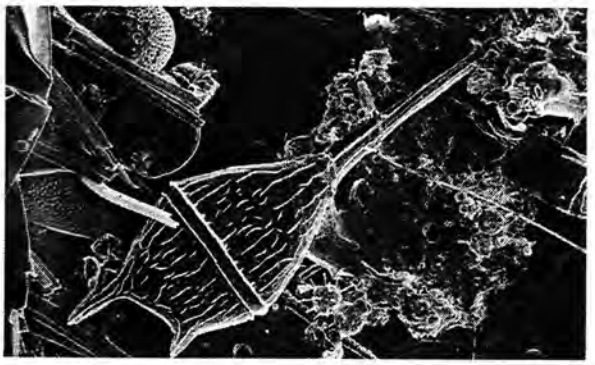

7 30µm

8 100µm

9 30µm

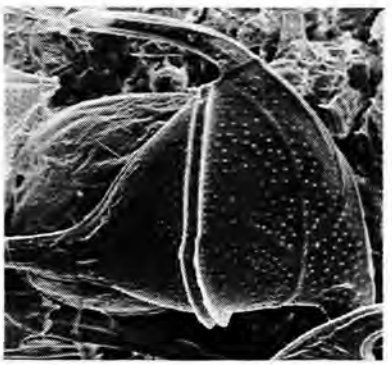

10 30µm

PLATE 9:

FAMILY CERATOCORYACEAE LINDEMANN, 1928

CERATOCORYS STEIN, 1883

Fig.1, 2: ***Ceratocorys horrida*** STEIN, 1883;

1. right lateral view, cell looks like a gladiator's helmet, hypotheca angular with sutural ridges extended into strong toothed spines, cingulum deeply excavated with strongly ribbed lists, sulcus with lists, left list drawn out into a spine, sample 22-S18, #01998;
2. oblique ventral view on flat epitheca with high sutural ridges, thecal plates with depressions and pores forming regular reticulations, sample 22-S16, #02551.

FAMILY CLADOPYXIDACEAE STEIN, 1883

MICRACANTHODINIUM DEFLANDRE, 1937

Fig.3, 4: ***Micracanthodinium setiferum*** (LOHMANN) DEFLANDRE, 1937;

3. oblique ventral view, cell small rounded, cingulum widely depressed and slightly displaced, sulcus deep and wide, thecal plates with numerous small spines and a few long and fine processes, sample 22-S11, #02461;
4. oblique apical view of epitheca with small ovoid apical pore, sample 22-S13, #01262.

PALAEOPHALACROMA SCHILLER, 1928

Fig.5, 6: ***Palaeophalacroma unicinctum*** SCHILLER, 1928;

5. ventral view, cell small and ovoid, species characterized by cingulum with pronounced anterior list, cingulum slightly depressed and left-handed lacking a posterior list, sulcus not depressed with small lists, hypotheca rounded without any projections, sample 22-S11, #02393;
6. apical view on rounded epitheca with apical pore complex, 1' is long and narrow posteriorly touching sulcus, thecal plates smooth with pores, sample 22-S23, #02564.

Plate 9:

Family Ceratocoryaceae

1 30µm

2 30µm

Family Cladopyxidaceae

3 3µm

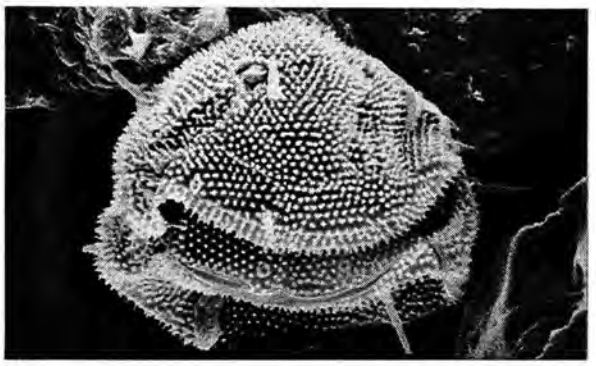

4 3µm

5 3µm

6 3µm

PLATE 10:

FAMILY GONYAULACACEAE LINDEMANN, 1928

AMPHIDOMA STEIN, 1883

Fig.1, 2: ***Amphidoma nucula*** STEIN, 1883;

1. right lateral view, cell small and biconical, cingulum broadly excavated and slightly displaced with small lists, sample 22-S32, #02639;
2. dorsal view, epitheca larger than hypotheca, epitheca with small apical horn, characteristic thecal plate reticulation, sample 22-S32, #02629.

LINGULODINIUM WALL, 1967 *emend.* DODGE, 1989

Fig.3, 4: ***Lingulodinium polyedrum*** (STEIN) DODGE, 1989;

3. ventral view, cell polyhedral, cingulum median depressed and offset one width but without overlap, cingular lists narrow, sulcus straight widening posteriorly, sample 22-S32, #02630;
4. oblique ventral view of hypotheca, sides straight, antapex flat without spines, thecal plates thick with ridges along sutures, plates covered with characteristic reticulations and numerous pores, sample 22-S11, #02426.

PERIDINIELLA KOFOID & MICHENER, 1911

Fig.5, 6: ***Peridiniella sphaeroidea*** KOFOID & MICHENER, 1911;

5. oblique dorsal view on epitheca with apical pore complex, cell nearly spherical, cingulum with prominent lists and ribs, thecal plates strongly reticulated, sample 22-S14, #01046;
6. thecal surface with reticulations, each enclosing a cluster of very small poroids, girdle not excavated, sample 22-S35, #02769.

PROTOCERATIUM BERGH, 1882

Fig.7, 8: ***Protoceratium reticulatum*** (CLAPARÈDE & LACHMAN) BÜTSCHLI, 1885; sample 22-S34, #02675,

7. oblique dorsal view, cell sub-spherical, cingulum deeply incised with small lists,
8. plate surface heavily reticulated with pores.

Plate 10: Family Gonyaulacaceae

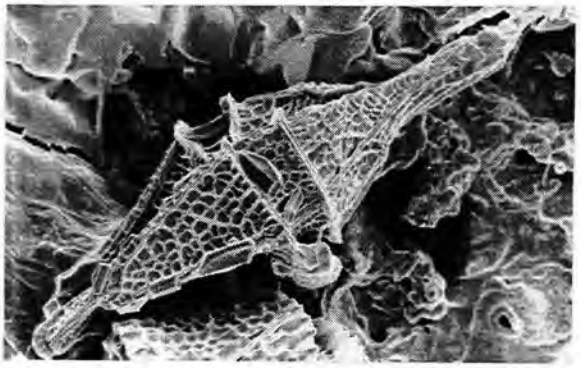

1 3µm

2 10µm

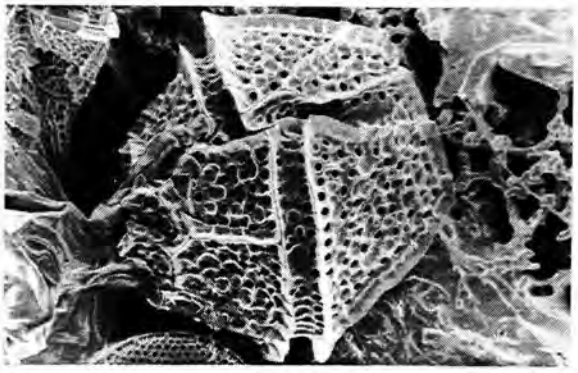

3 10µm

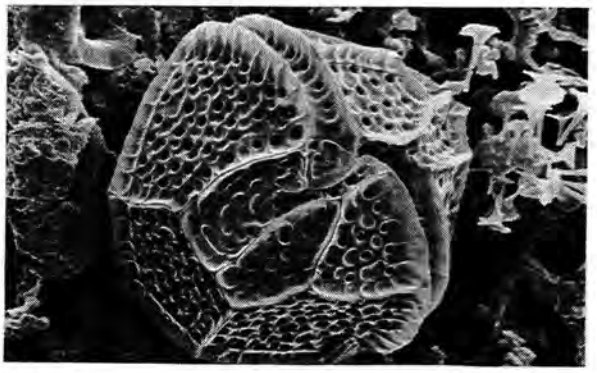

4 10µm

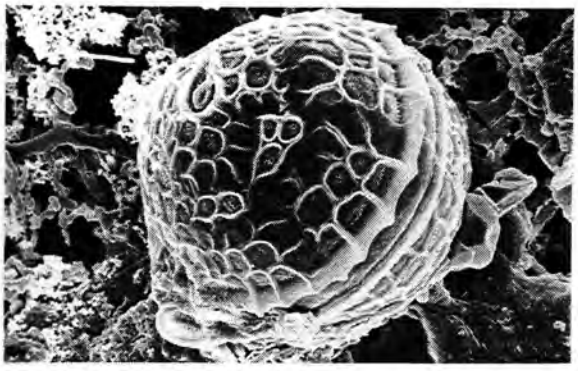

5 10µm

6 3µm

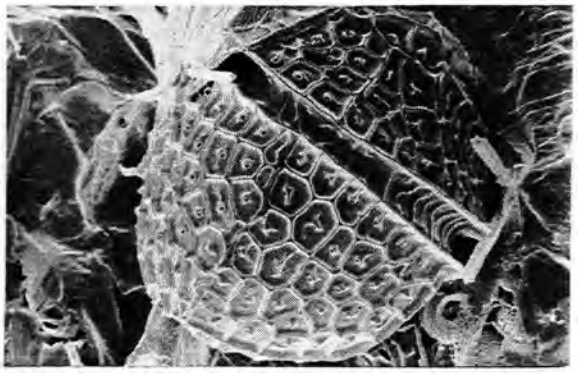

7 10µm

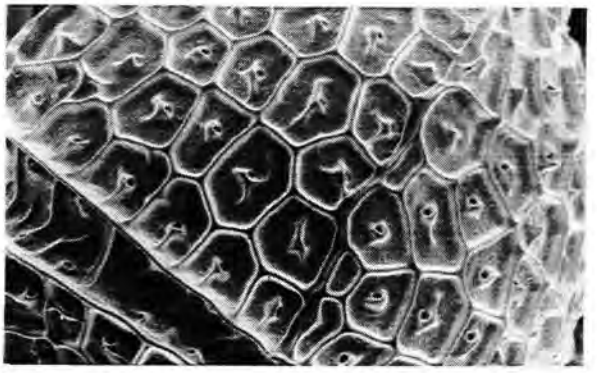

8 3µm

PLATE 11:

FAMILY GONYAULACACEAE LINDEMANN, 1928

GONIODOMA STEIN, 1883

Fig.1, 3, 5: ***Goniodoma polyedricum*** (POUCHET) JORGENSEN, 1899;

1. oblique right lateral view, cell polygonal, plate margins with distinctive angular ridges, thecal plates perforated with pores, cingulum slightly offset with wide lists, sample 22-S27, #02335;
3. epitheca with characteristic 1' plate and apical pore directed to the left, sample 22-S23, #02601;
5. hypotheca with distinctive arrangement of three plates at antapex, sulcus deep but narrow with lists, sample 22-S35, #02767.

Fig.2, 4, 6, 7: ***G. sphaericum*** MURRAY & WHITTING, 1899;

2. oblique dorsal view on epitheca, cell rounded, thecal plates smooth without any projections but with small cingular and sulcal lists, plates covered with pores, sample 22-S27, #02375;
4. hypotheca with radially symmetric plate pattern, sulcus deep and short with lists, sample 22-S32, #02616;
6. epitheca with characteristic 1' plate and apical pore complex, sample 22-S35, #02805,
7. distinct elongate apical pore directed to the left, same specimen as Fig.6.

Plate 11: Family Gonyaulacaceae

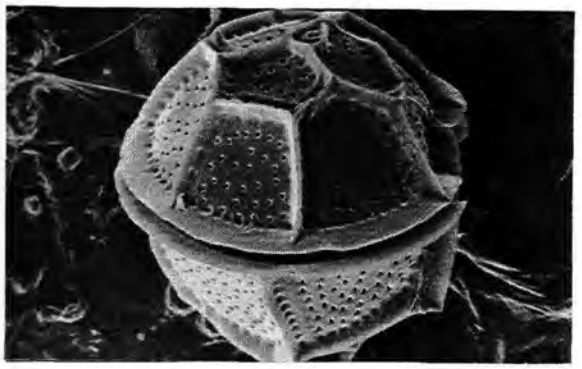

1 10µm

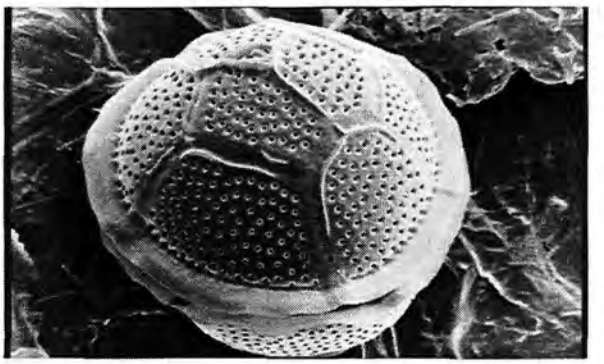

2 10µm

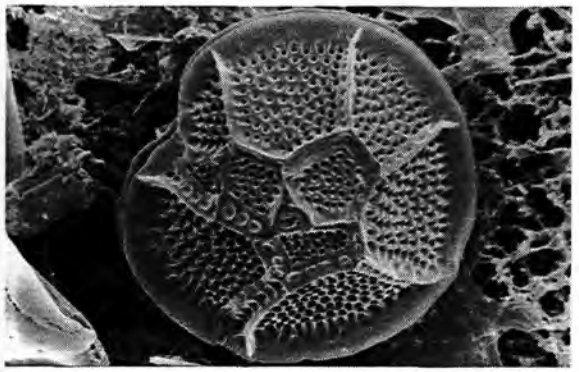

3 10µm

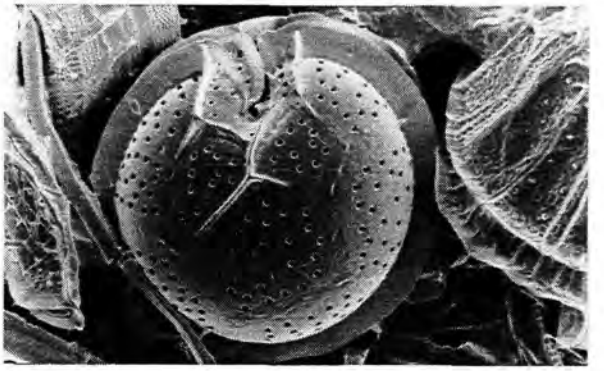

4 10µm

5 30µm

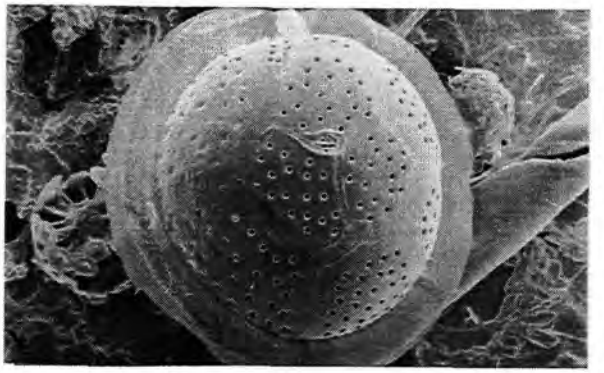

6 10µm

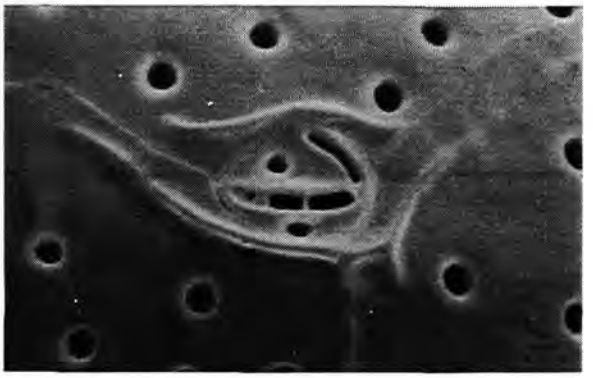

7 1µm

PLATE 12:

FAMILY GONYAULACACEAE LINDEMANN, 1928

SPIRAULAX KOFOID, 1911 *emend.* CARBONELL-MOORE, 1996

Fig.1: ***Spiraulax jolliffei*** (MURRAY & WHITTING) KOFOID, 1911 *emend.* CARBONELL-MOORE, 1996; oblique left lateral view, cell spindle-shaped, epitheca and hypotheca extended into horn-like processes, cingulum excavated and displaced nearly two widths, girdle lists broad, thecal plates perforated by huge pores (on top part of "*Sphaerodinella*" *albatrosiana*), sample 22-S16, #02523.

GONYAULAX DIESING, 1866

Fig.2: ***Gonyaulax digitalis*** (POUCHET) KOFOID, 1911; ventral view, cell rhomboidal with distinct apical horn and two stout antapical spines, cingulum depressed and displaced by two widths with an overlap, sulcus narrow anteriorly and broad at posterior end with smooth sulcal lists, thecal plates perforated by numerous large pores, sample 22-S16, #02549.

Fig.3, 4: ***G.* cf. *hyalina*** OSTENFELD & SCHMIDT, 1901; sample 22-S27, #02311,

3. collapsed theca, theca delicate and deformed,
4. characteristic plate ornamentation: small lines and ridges between thin longitudinal ribs.

Fig.5, 6: ***G. monospina*** RAMPI, 1951;

5. ventral view, cell ovoid with small apical horn and single antapical spine, median cingulum wide and offset with slight overlap, sulcus broad posteriorly with two short sulcal lists, sample 22-S16, #02557;
6. left lateral view on cingulum with short lists displaced one width, hypotheca rounded, thecal plates smooth with circular depressions and some pores, sample 22-S10, #01403.

Fig.7, 8: ***G. polygramma*** STEIN, 1883;

7. right lateral view, cell elongated, epitheca conical tapering to apical horn, plates ornamented with series of distinctive longitudinal ridges, reticulations between ridges with circular depressions and pores, sample 22-S27, #02368;
8. ventral view showing median cingulum excavated and with narrow lists, cingulum displaced less than one width with slight overlap, sulcus depressed widening posteriorly with lists, hypotheca with square antapex and spine, sample 22-S10, #01347.

Plate 12: Family Gonyaulacaceae

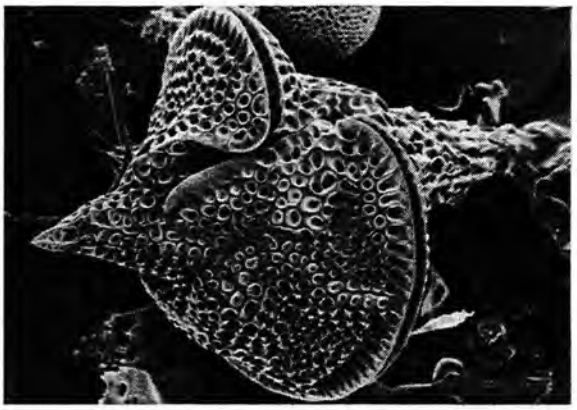

1 30µm

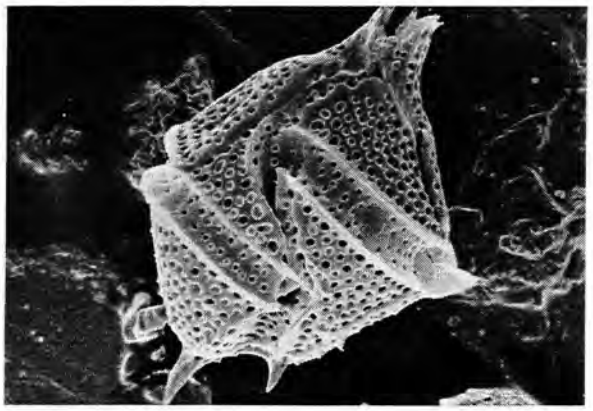

2 10µm

3 10µm

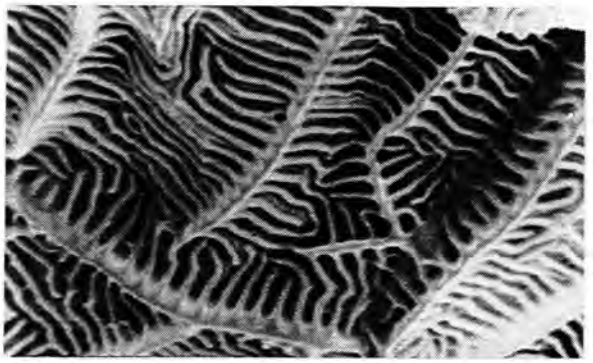

4 1µm

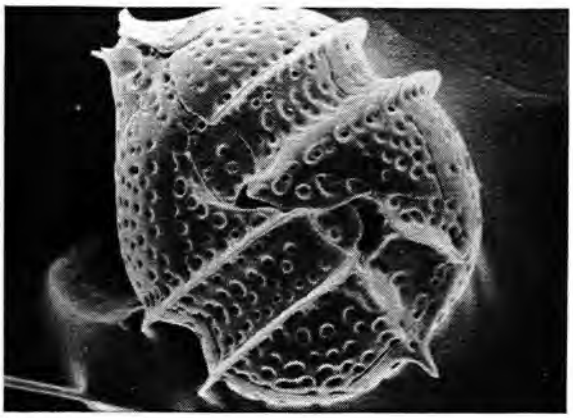

5 3µm

6 3µm

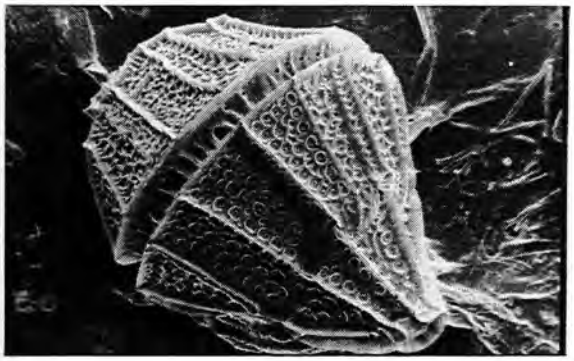

7 10µm

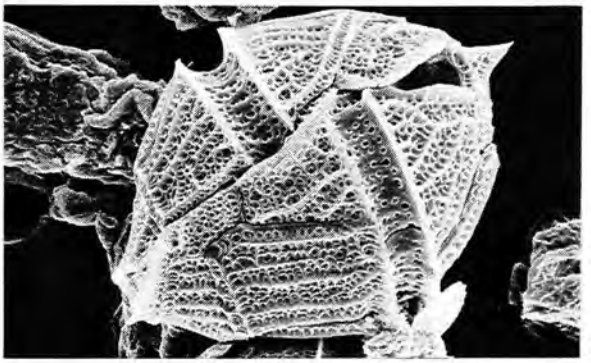

8 10µm

PLATE 13:

FAMILY GONYAULACACEAE LINDEMANN, 1928

GONYAULAX DIESING, 1866

Fig.1: ***Gonyaulax polygramma*** STEIN, 1883; ventral view, cell after division, division plane oblique from anterior right to posterior left, left half of theca from parent cell, right half in process of development (DODGE, 1988), sample 22-S35, #02766.

Fig.2, 4: ***G. spinifera*** (CLAPARÈDE & LACHMANN) DIESING, 1866;

2. oblique ventral view on epitheca with curved sides, apical pore area oval, 2a plate with distinctive ventral pore at anterior end, thecal plates with reticulations and numerous pores, sample 22-S13, #01271;
4. ventral view on median cingulum offset at least two widths with large overlap, cingulum deeply excavated with small lists, sulcus very narrow anteriorly widening posteriorly, hypotheca square to rounded with short spines at antapex, sample 22-S17, #01118.

Fig.3, 5, 6: ***G. striata*** MANGIN, 1926;

3. ventral view, epitheca conical with low apical horn, median cingulum widely excavated and displaced one width but without overlap, sulcus narrow anteriorly but broad posteriorly, sample 22-S14, #02476;
5. left lateral view of hypotheca with straight sides and rounded posterior end, sample 22-S10, #01415,
6. characteristic plate ornamentation: longitudinal ridges with reticulations and smaller ribs and bars in between, cingulum partially with vertical ribs, same specimen as Fig.5.

Fig.7, 8, 9: ***G. turbynei*** MURRAY & WHITTING, 1899;

7. ventral view, cell ovoid with convex epitheca and short apical horn, cingulum broadly excavated with vertical ridges offset one width and slight overlap, cingular lists with ribs, sulcus deep and vertical widening posteriorly, sample 22-S13, #02513;
8. oblique ventral view of hypotheca with rounded posterior end and very small spines, sample 22-S08, #01295;
9. apical view on epitheca and oval apical pore, thecal plates ornamented with longitudinal ridges and reticulations in between, sample 22-S23, #01176.

Plate 13: Family Gonyaulacaceae

1 10µm

2 10µm

3 10µm

4 10µm

5 10µm

6 3µm

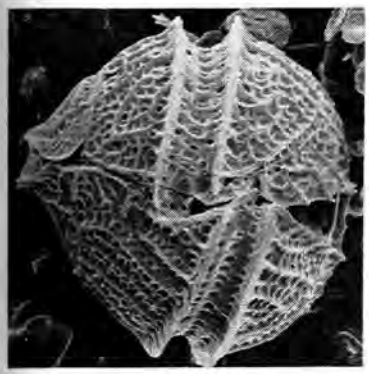

7 10µm

8 3µm

9 3µm

PLATE 14:

FAMILY OXYTOXACEAE LINDEMANN, 1928

OXYTOXUM STEIN, 1883

Fig.1: ***Oxytoxum constrictum*** (STEIN) BÜTSCHLI, 1885; left lateral view, cell biconical, ridged hypotheca with characteristic constriction, epitheca cap-like with straight sides and blunt tip, hypotheca with curved sides tapering to short antapical horn, cingulum depressed and smooth but with ridges, thecal plates with reticulations and pores, ornamentation changes on either side of constriction, epitheca perforated with pores showing growth bands, sample 22-S11, #02466.

Fig.2, 5: ***O. crassum*** SCHILLER, 1937;

2. oblique ventral view, cell rounded with deep and wide cingulum, length of sulcus one width of cingulum, small epitheca gently domed covered with "pimples" and some pores, apical process short, hypotheca with scattered clover-leaf patterning, sample 22-S13, #01270;

5. oblique lateral view on ovoid hypotheca with small blunt antapical process, thecal plates reticulated with longitudinal ridges forming hexagons, smooth growth bands, sample 22-S08, #01311.

Fig.3, 4: ***O. laticeps*** SCHILLER, 1937;

3. right lateral view, cell with deep and wide cingulum, sulcus covered with large wing, hypotheca shortly conical with short vertical ridges and pores forming an overall irregular reticulation, antapical protrusion broad-pointed, sample 22-S17, #01676;

4. apical view, epitheca very small with convex apex and slightly ridged projection, cingulum is excavated and ornamented with reticulations and has small ridged lists, epitheca covered with reticulated ridges and perforated with pores, sulcus covered by large wing, sample 22-S32, #02614.

Fig.6, 8: ***O. challengeroides*** KOFOID, 1907;

6. ventral view, cell spindle-shaped with curved hypotheca tapering into antapical spine, spine with ridges, sulcus one width of cingulum on both epitheca and hypotheca partly covered with a wing, plain growth bands, sample 22-S11, #02424;

8. oblique right lateral view on triangular epitheca ornamented with pores and strong ridges, cingulum very deep and wide and strongly ridged, thecal plates with short vertical ridges and pores, sample 22-S08, #01320.

Fig.7, 9: ***O. ovale*** SCHILLER, 1937;

7. oblique dorsal view on small hat-like epitheca, 4' plate with distinctive pore, cingulum deeply excavated and very wide with lists, growth bands smooth, sample 22-S16, #01233;

9. left lateral view, cell ovoid with convex hypotheca tapering posteriorly into small sharp projection, sulcus deeply recessed with list, thecal plates with regular wide reticulations and pores, sample 22-S35, #02865.

Fig.10: ***O. stropholatum*** DODGE & SAUNDERS, 1985; oblique left lateral view, cell with convex hypotheca, cingulum depressed ending in wing projecting over sulcus, sulcus with lists, sample 22-S11, #02394.

Plate 14: Family Oxytoxaceae

1 10µm

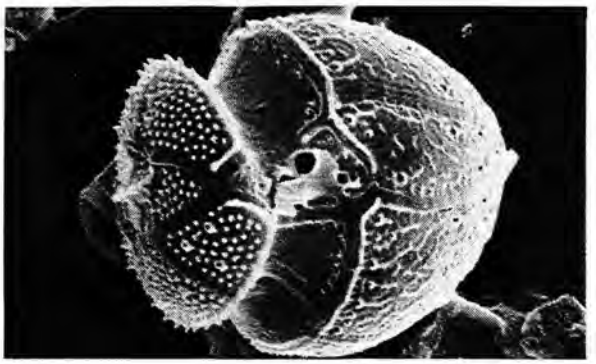

2 3µm

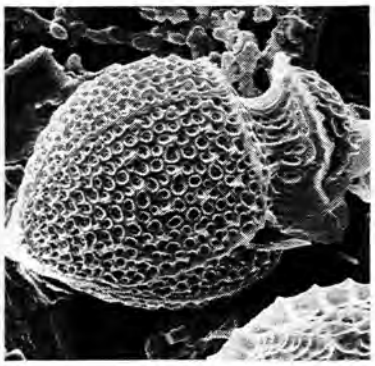

3 3µm

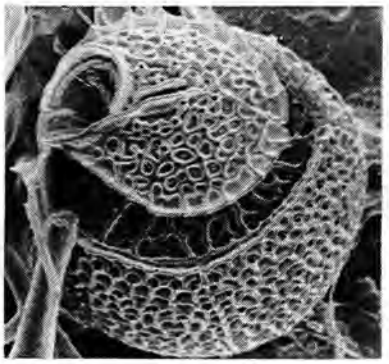

4 3µm

5 3µm

6 10µm

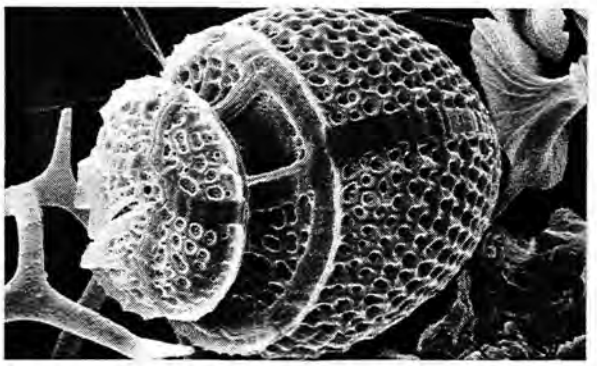

7 3µm

8 10µm

9 10µm

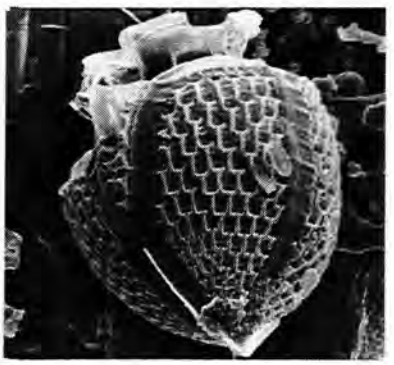

10 3µm

PLATE 15:

FAMILY OXYTOXACEAE LINDEMANN, 1928

OXYTOXUM STEIN, 1883

Fig.1: ***Oxytoxum stropholatum*** DODGE & SAUNDERS, 1985; oblique lateral view on hypotheca with short antapical spine, thecal plates with short vertical ridges and pores forming a characteristic reticulation, sample 22-S10, #01396.

Fig.2: ***O. reticulatum*** (STEIN) SCHÜTT, 1895; oblique dorsal view, cell biconical, epitheca with straight sides and blunt apex, hypotheca with curved sides tapering posteriorly into a short spine, cingulum depressed with vertical ridges, thecal plates with deep circular depressions and pores, sample 22-S35, #02866.

Fig.3, 4: ***O. sceptrum*** (STEIN) SCHRÖDER, 1906;

3. right lateral view, thecal plates with continuous longitudinal ridges and pores in between, sample 22-S35, #02867;
4. left lateral view, cell similar in shape to *O. challengeroides* but a little bit more bulbous, growth bands plain, sample 22-S27, #02315.

Fig.5, 6: ***O. scolapax*** STEIN 1883;

5. right lateral view, cell spindle-shaped with pointed ends, epitheca triangular with prominent apical spine, hypotheca covered with numerous short vertical ridges and pores, sample 22-S08, #01301;
6. ventral view, cingulum deeply excavated, sulcus short covered with a large wing, hypotheca ending in antapical plate with four ridges, sample 22-S37, #02881.

Fig.7, 8: ***O. tesselatum*** (STEIN) SCHÜTT, 1895;

7. left lateral view, cell asymmetrically biconical, hypotheca with convexly curved sides and strong antapical spine, plate ornamentation characteristic with longitudinal ridges and short transverse ridges in between bordered by pores, cingulum excavated with vertical ridges, sample 22-S17, #01672;
8. oblique dorsal view on short and concave epitheca with radial ridges and irregular reticulations, sample 22-S17, #01671.

Plate 15: Family Oxytoxaceae

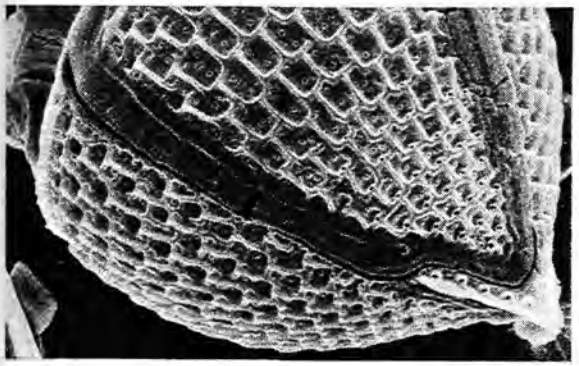

1 3µm

2 10µm

3 10µm

4 10µm

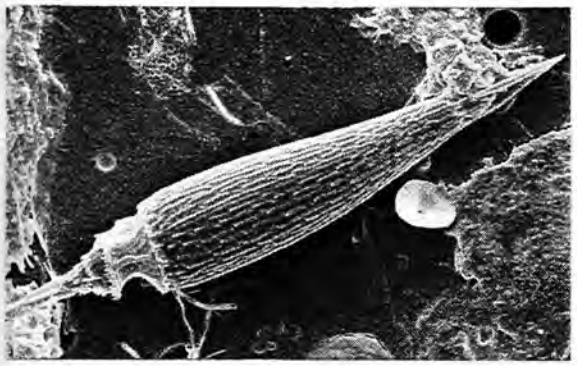

5 10µm

6 10µm

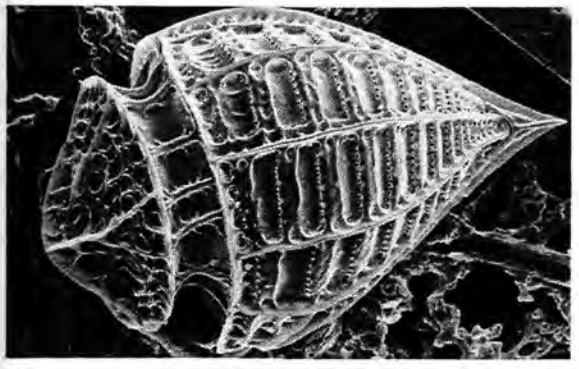

7 10µm

8 10µm

PLATE 16:

FAMILY PROTOPERIDINIACEAE BUJAK & DAVIES, 1983

PROTOPERIDINIUM BERGH, 1882

Fig.1: ***Protoperidinium* cf. *cerasus*** (PAULSEN) BALECH, 1973; ventral view, cell globular with small apical horn and two antapical spines, cingulum slightly displaced with lists and spines, thecal plates smooth with pores, sample 22-S13, #02511.

Fig.2, 3: ***P. depressum*** (BAILEY) BALECH, 1974; sample 22-S34, #02739,

2. ventral view, cell large flattened dorsoventrally, cingulum laterally expanded with lists, sulcus deeply excavated, apical and antapical horns prominent, (specimen of *Gonyaulax turbynei* in upper left corner),
3. plate 1' reticulated with pores.

Fig.4, 5, 6: ***P. diabolum*** (CLEVE) BALECH, 1974;

4. ventral view, apical horn large, antapical spines lanceolate and winged, cingulum not depressed with insignificant displacement, girdle and sulcal lists with spines, sample 22-S33, #02745,
5. plate 1' with fine and rudimentary vermiculate reticulation and intercalary growth bands, same specimen as in Fig.4;
6. dorsal view, 3''' plate broad, left antapical spine with accessory spine at base, sample 22-S34, #02665.

Fig.7, 8: ***P. divergens*** (EHRENBERG) BALECH, 1974;

7. oblique ventral view, cingulum not offset but excavated with lists supported by spines, sulcus widening posteriorly and with lists, plates with spiny reticulations, sample 22-S25, #02251;
8. oblique dorsal view, hypotheca with characteristic diverging antapical horns, apical horn prominent but here obscured, sample 22-S16, #01245.

Fig.9, 10: ***P. elegans*** (CLEVE) BALECH, 1974; sample 22-S11,

9. ventral view, cell large with prominent apical and antapical horns, dorsoventrally flattened, cingulum equatorial but depressed and with spiny lists, sulcus deep with lists, (to the left: *Oxytoxum challengeroides*, lower right corner: *Palaeophalacroma unicinctum*) #02427;
10. oblique dorsal view, 3''' plate narrow, antapical horns very large, ornamentation reticulate with spines, #02400.

Plate 16: Family Protoperidiniaceae

1 10µm

2 30µm

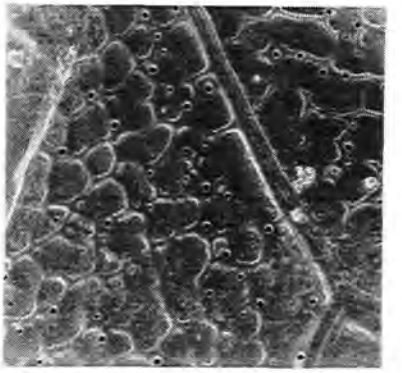

3 3µm

4 10µm

5 3µm

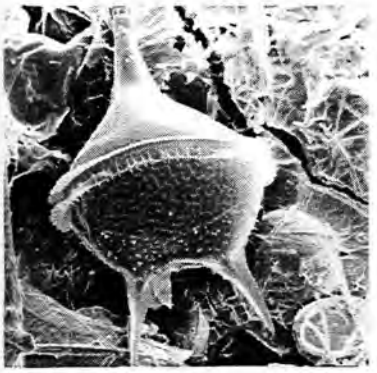

6 30µm

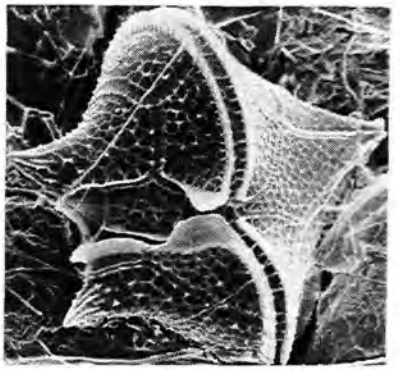

7 10µm

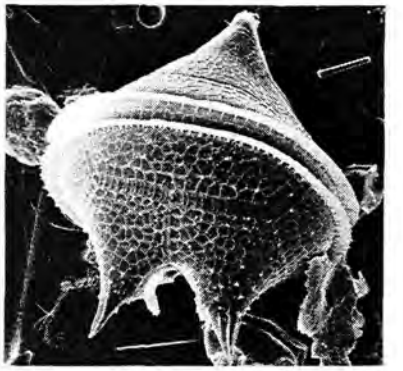

8 10µm

9 30µm

10 30µm

PLATE 17:

FAMILY PROTOPERIDINIACEAE BUJAK & DAVIES, 1983

PROTOPERIDINIUM BERGH, 1882

Fig.1, 2, 3: ***Protoperidinium globulus*** (STEIN) BALECH, 1974, *sensu* ABÉ (1981);

1. oblique ventral view, cell almost spherical, no projections except cingular and sulcal lists, no spines, cingulum displaced two width, sample 22-S27, #02389;
2. oblique view on dorsal epitheca and apical pore complex, intercalary growth bands broad, sample 22-S34, #02678;
3. thecal plate surface granular but otherwise smooth, sample 22-S35, #02792.

Fig.4, 5: ***P. minutum*** (KOFOID) LOEBLICH III, 1969; sample 22-S34, #02730,

4. oblique view on dorsal epitheca, cell rounded, apical horn low surrounded by pores, intercalary growth bands present,
5. distinctive plate covering with "pimples" in a polygonal pattern, pores present.

Fig.6, 7: ***P. oceanicum*** (VANHÖFFEN) BALECH, 1974;

6. oblique dorsal view, cell very large, apical and antapical horns long and narrow, cingulum with spiny lists, sample 22-S25, #02238;
7. thecal plates with shallow reticulations and pores, sample 22-S34, #02668.

Fig.8, 9: ***P. oviforme*** (DANGEARD) BALECH, 1974, *sensu* BALECH (1988); sample 22-S27

8. ventral view, cell oval with short apical horn and characteristic antapical three-winged spines, cingulum not excavated and displaced one width, cingular lists with spines, sulcus with right "lip-like" list, #02365;
9. oblique lateral view, antapical spines slightly angled ventrally, plate surfaces with small-scale reticulation, #02354.

Plate 17: Family Protoperidiniaceae

1 10µm

2 10µm

3 3µm

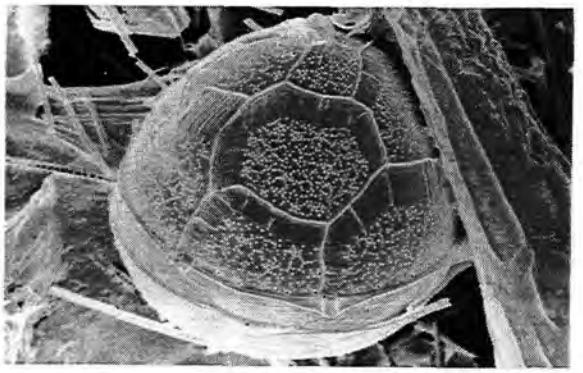

4 10µm

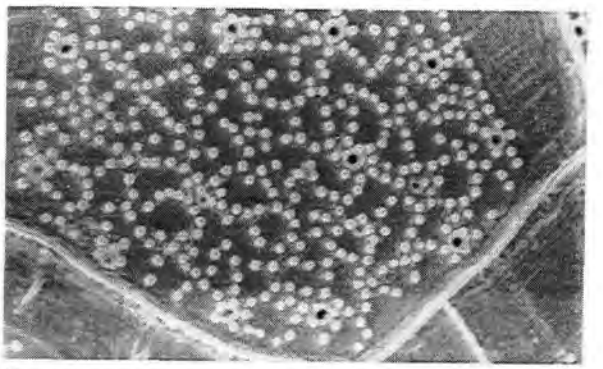

5 3µm

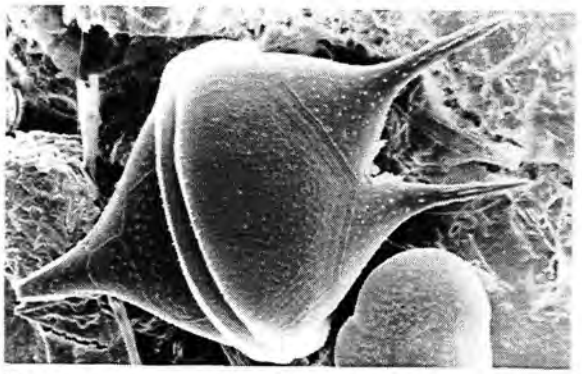

6 30µm

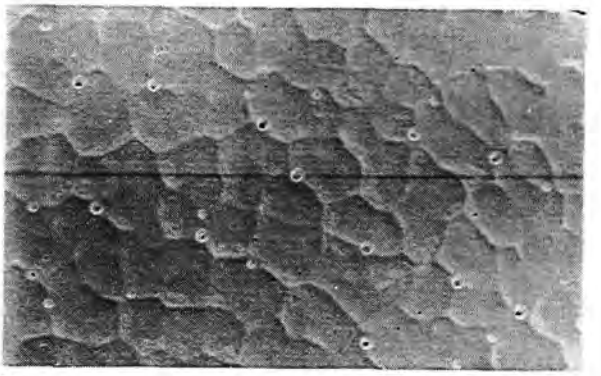

7 3µm

8 10µm

9 10µm

PLATE 18:

FAMILY PROTOPERIDINIACEAE BUJAK & DAVIES, 1983

PROTOPERIDINIUM BERGH, 1882

Fig.1: ***Protoperidinium ovum*** (SCHILLER) BALECH, 1974; oblique lateral view, cell "egg-shaped" with short apical horn, cingulum not depressed, plate surface plain but with pores, sample 22-S34, #02721.

Fig.2: ***P. parviventer*** BALECH, 1978; ventral view, cell very broad, epitheca larger than hypotheca, apical horn short, antapical spines equally short and tapering, cingulum not excavated and offset one width, girdle and sulcal lists with spines, plates ornamented with reticulation , sample 22-S14, #02478.

Fig.3: ***P. pentagonum*** (GRAN) BALECH, 1974; oblique view on ventral epitheca, characteristic "longitudinal" ridges bordering 1'-5' and 1"-7" plates, ventral area concave, cingular lists with spines, plate surface reticulated, sample 22-S20, #01668.

Fig.4: ***P. quarnerense*** (SCHRÖDER) BALECH, 1974; epitheca with brief apical horn, cingulum largely displaced, cingular lists supported by spines, thecal plate surface even but granular with pores, sample 22-S37, #02876.

Fig.5, 6: ***P. cf. punctulatum*** (PAULSEN) BALECH, 1974; sample 22-S33, #02747,

5. antapical view of collapsed theca, no antapical spines or horns, cingulum not displaced but depressed and with spiny lists, sulcus narrow,
6. plate ornamentation characteristic with short spines or "pimples" and pores in between.

Fig.7, 8: ***P. rectum*** (KOFOID) BALECH, 1974, *sensu* BALECH (1988); sample 22-S35, #02803,

7. oblique lateral view, cell oval with high cylindrical apical horn and antapical spines, cingulum not excavated,
8. thecal plates covered with small vermiculate depressions with pores, giving an overall impression of very small reticulations.

Plate 18: Family Protoperidiniaceae

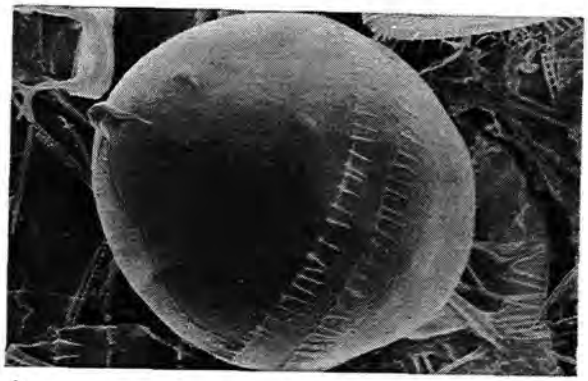

1 10µm

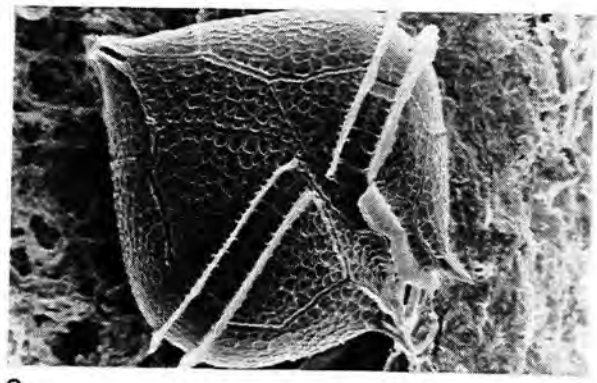

2 10µm

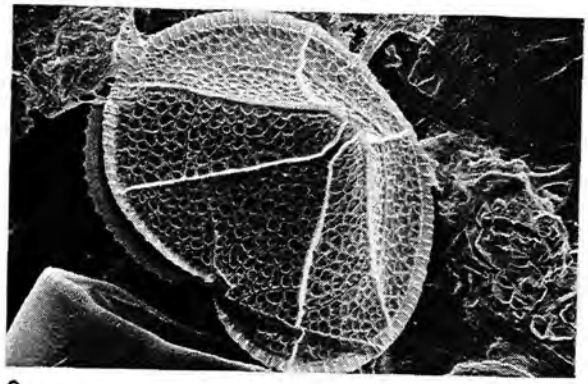

3 10µm

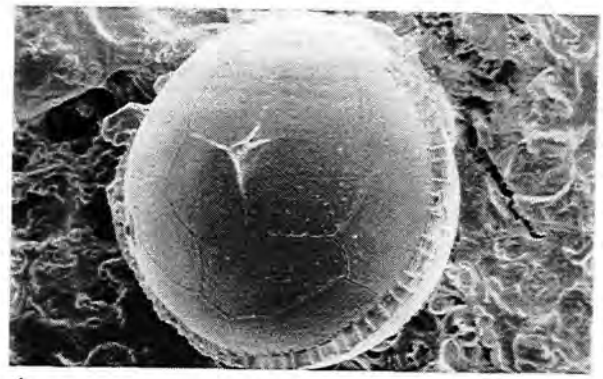

4 10µm

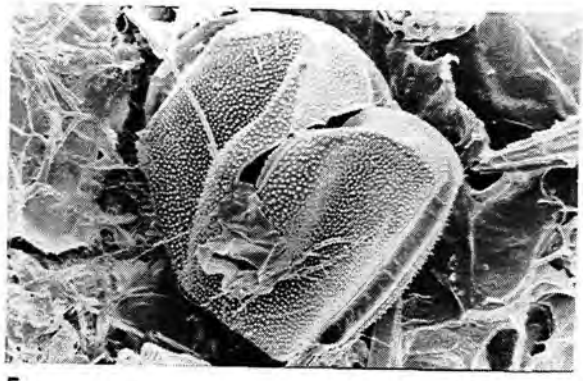

5 10µm

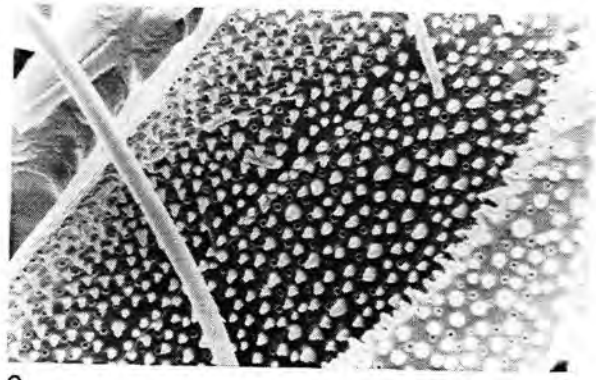

6 3µm

7 10µm

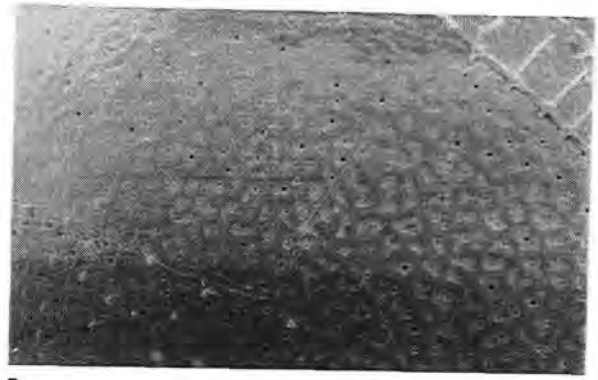

8 3µm

PLATE 19:

FAMILY PROTOPERIDINIACEAE BUJAK & DAVIES, 1983

PROTOPERIDINIUM BERGH, 1882

Fig.1, 2: ***Protoperidinium steinii*** (JORGENSEN) BALECH, 1974;

1. oblique ventral view, hypotheca rounded with two distinctive three-winged spines, cingulum slightly offset, sulcus bordered by lists, left sulcal list merging into left antapical spine, right sulcal list "lip-like", sample 22-S14, #02479;
2. oblique ventral view on epitheca with prominent apical horn, girdle lists with spines, thecal plates covered with reticulations, sample 22-S10, #01417.

Fig.3, 4, 6: ***P. subcurvipes*** (LEBOUR) BALECH, 1974;

3. oblique ventral view, cell rounded, cingulum displaced by one width, sulcus with prominent list on left side, short curved spine at right posterior end of sulcus, extensive intercalary growth bands present, sample 22-S17, #02819;
4. oblique dorsal view on epitheca (*Gonyaulax monospina* at bottom), anterior girdle list wide with spines, sample 22-S35, #02819,
6. right lateral side of epitheca with apical pore complex, thecal plates with reticulations perforated by pores in the middle of areolae, same specimen as Fig.4.

Fig.5: ***P. tenuissimum*** (KOFOID) BALECH, 1974; oblique ventral view, cell large with elongated body and long apical horn, hypotheca rounded with three-winged spines, length of antapical spines equals diameter of cell, cingulum slightly displaced with very short lists, sulcus with lists, left sulcal list extending posteriorly below base, thecal plates plain with irregular vermiculate reticulations sample 22-S25, #02302.

Fig.7, 8: ***P.* cf. *tuba*** (SCHILLER) BALECH, 1974; sample 22-S24, #02685,

7. lateral view, body rounded with long cylindrical "tube-like" apical horn, antapical spines long partly obscured by body,
8. thecal plates with reticulations and pores, cingulum wide with narrow lists.

Plate 19: Family Protoperidiniaceae

1 10µm

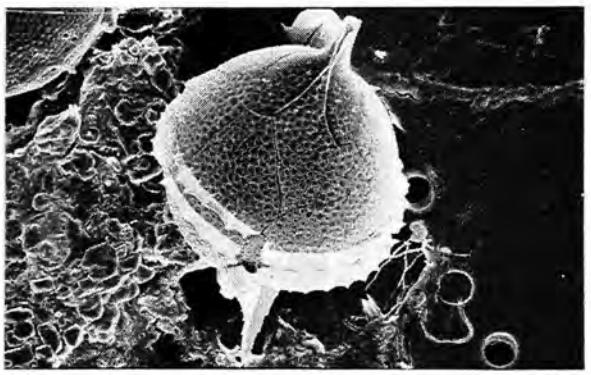

2 10µm

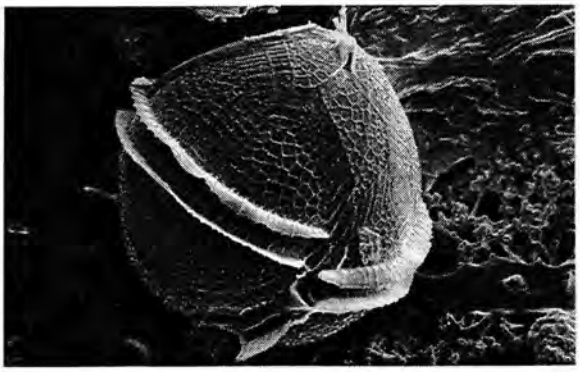

3 10µm

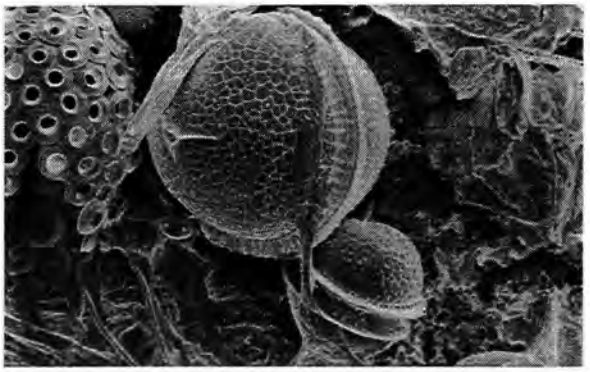

4 10µm

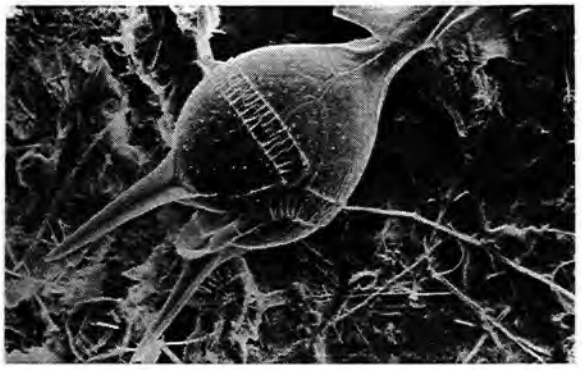

5 10µm

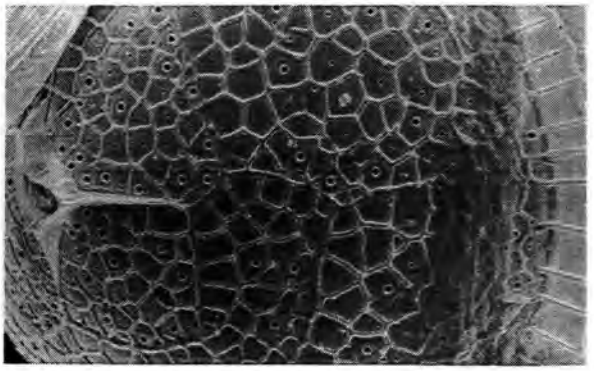

6 3µm

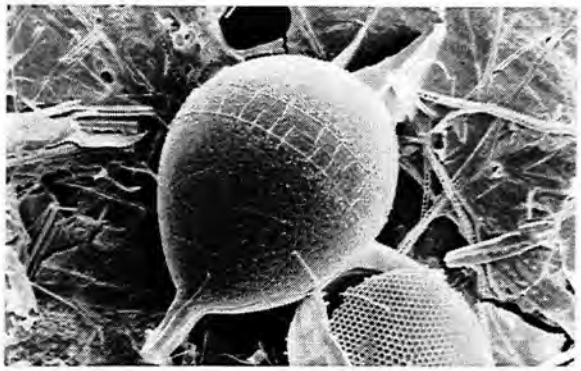

7 10µm

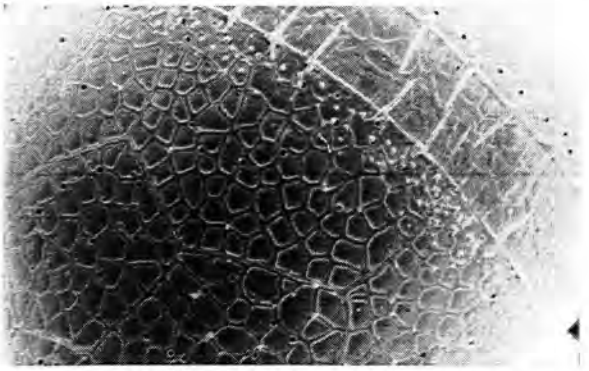

8 3µm

PLATE 20:

FAMILY PODOLAMPADACEAE LINDEMANN, 1928

BLEPHAROCYSTA EHRENBERG, 1873

Fig.1, 2: ***Blepharocysta cf. paulsenii*** SCHILLER, 1937; sample 22-S35, #02813,

1. apical view, thecal plates plain perforated by pores, growth bands wide,
2. apical pore complex.

PODOLAMPAS STEIN, 1883

Fig.3: ***Podolampas bipes*** STEIN, 1883; ventral view, cell lacking cingulum, epitheca with short apical horn, hypotheca broad and rounded with two winged antapical spines, sulcus small not depressed covered by left antapical wing, thecal plates with broad shallow depressions and pores, rows of pores at plate sutures, sample 22-S27, #02381.

Fig.4: ***P. palmipes*** STEIN, 1883; left lateral view, cell pyriform, epitheca drawn out into long apical horn, hypotheca round with two winged antapical spines, left one much longer than right one and covering short sulcus, sample 22-S27, #02378.

FAMILY THORACOSPHAERACEAE SCHILLER, 1930 *emend.* TANGEN, 1982

THORACOSPHAERA KAMPTNER, 1927

Fig.5, 6, 7, 8: ***Thoracosphaera heimii*** (LOHMANN) KAMPTNER, 1927 **in the plankton**

5. shell "empty" with oblique view on aperture, no outer organic layer present, sample 22-S17, #01711;
6. detail of distal shell surface of "mature" specimen without visible aperture, crystals are up to 1µm big concealed by outer organic wall layer, phragma covers most of the pseudo-pores as well, sample 22-S10, #01377;
7. detail of outer shell surface, specimen without aperture, crystals very small covered with outer organic "skin", most pseudo-pores covered, sample 22-S13, #01264;
8. detail of distal shell surface, specimen without outer organic covering, crystals very small arranged around "pores", crystals getting smaller to the periphery of "rosettes" and are not completely interconnected, sample 22-S10, #01383.

Plate 20: Family Podolampadaceae

1 10µm

2 3µm

3 30µm

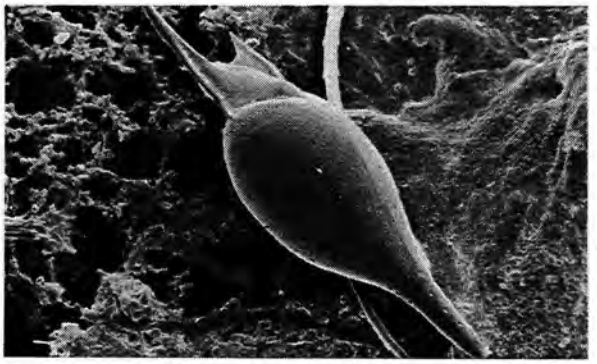

4 10µm

Family Thoracosphaeraceae:

Thoracosphaera heimii

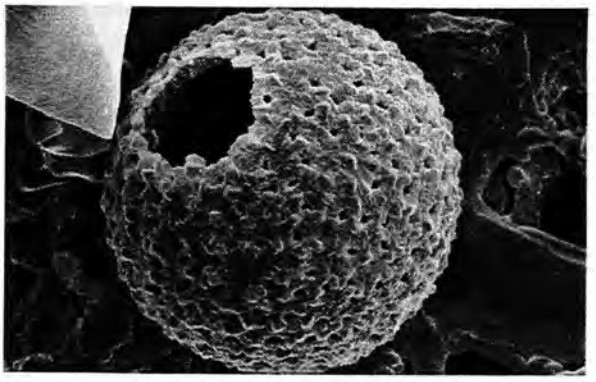

5 3µm

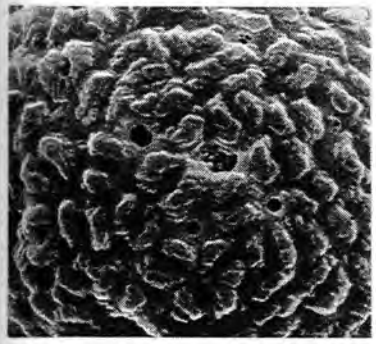

6 3µm

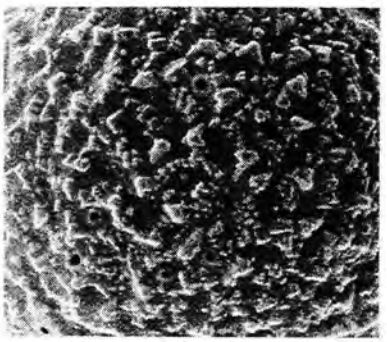

7 3µm

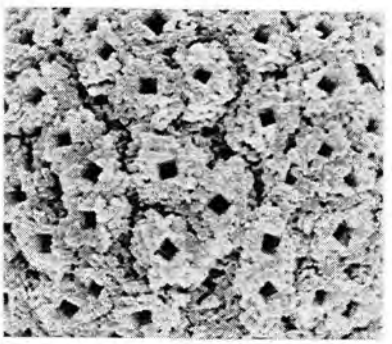

8 3µm

PLATE 21:

FAMILY THORACOSPHAERACEAE SCHILLER, 1930 *emend.* TANGEN, 1982

THORACOSPHAERA KAMPTNER, 1927

Thoracosphaera heimii (LOHMANN) KAMPTNER, 1927 **in the sediments** (exception: Fig.5)

Fig.1, 2: sample 1602-7 MUC 17-18cm, #01891,

1. overall view, specimen without visible aperture,
2. detail of distal shell surface, crystals polygonal granular of average size, crystallites arranged around rectangular pseudo-pores;

Fig.3, 4: sample 1602-7 MUC 16-17cm, #01887,

3. overall view, specimen without discernible aperture,
4. detail of outer shell surface with large crystals covering some of pseudo-pores;

Fig.5: oblique view on aperture of an empty specimen, crystals around margin of aperture irregularly serrated, no visible outer organic phragma, plankton sample 22-S17, #01711 (see Pl.20, Fig.5);

Fig.6: oblique view, specimen with open aperture, rim-crystallites of aperture bend distally, sample 1602-7 MUC 0-1cm, #01721;

Fig.7: detail of disintegrated shell showing polygonal fragmentation on distal shell surface, fragments composed of crystals arranged "rosette-like" around a pseudo-pore, sample 1602-7 MUC 17-18cm, #01893;

Fig.8: detail of half of a shell showing polygonal fragments with view on inner surface and wall cross section, proximal shell surface even with small vermiculate crystallites and irregular poroids, wall cross section shows "spongious" crystallites with poroids branching into very small and irregular conduits, sample 1602-7 MUC 13-14cm, #01855.

Plate 21: Family Thoracosphaeraceae: *Thoracosphaera heimii*

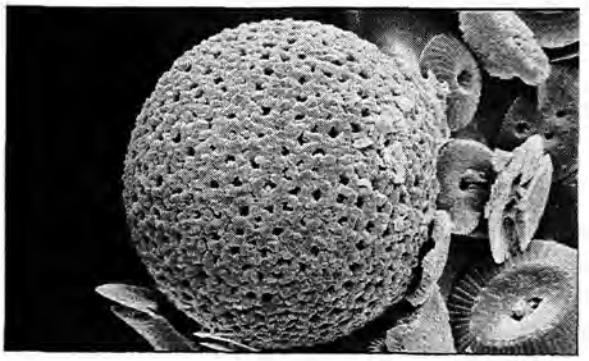

1 3µm

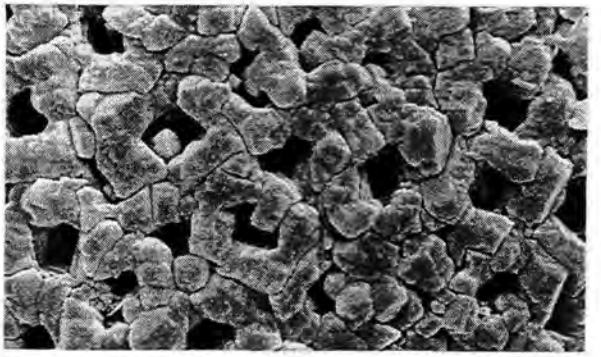

2 1µm

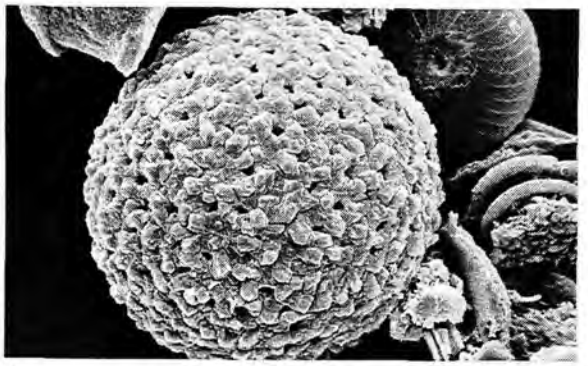

3 3µm

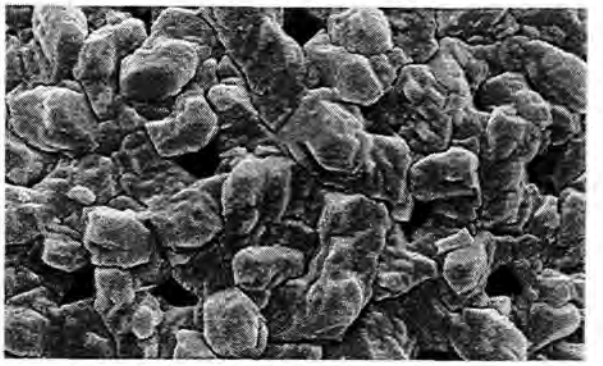

4 1µm

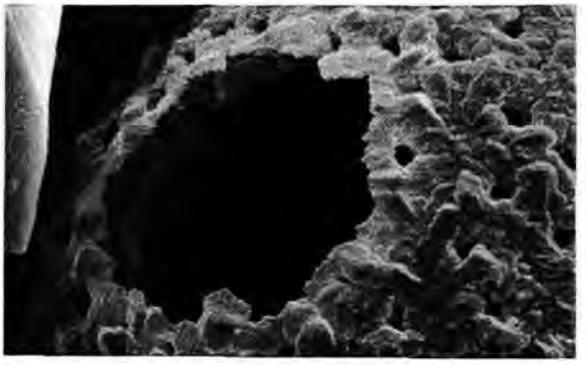

5 1µm

6 1µm

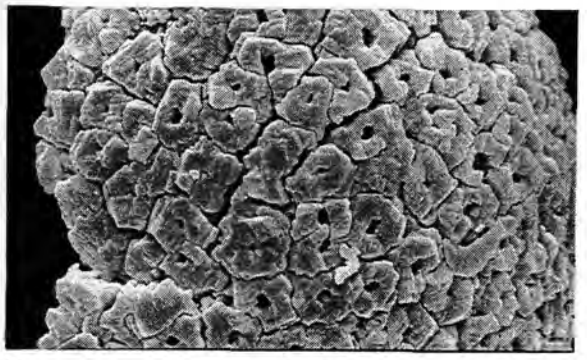

7 1µm

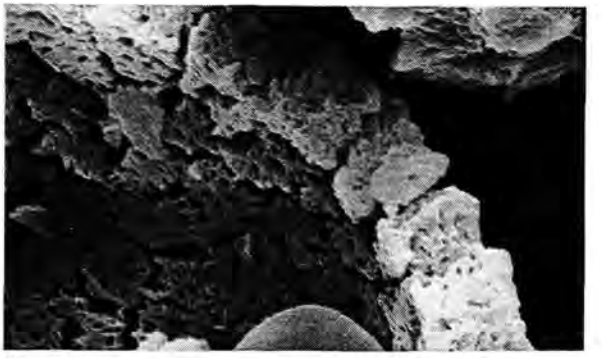

8 1µm

PLATE 22:

FAMILY CALCIODINELLACEAE DEFLANDRE, 1947 *emend.* BUJAK & DAVIS, 1983

CALCIODINELLUM DEFLANDRE, 1947 and

"*SPHAERODINELLA*" KEUPP & VERSTEEGH, 1989 **in the sediments**

Morphological Transitions between

Calciodinellum operosum DEFLANDRE, 1947 and

"*Sphaerodinella*" *albatrosiana* (KAMPTNER) KEUPP & VERSTEEGH, 1989

Fig.1, 2: ***Calciodinellum operosum***, sample 1606-7 MUC 1-2cm, #00705,

1. ventral view, *C. operosum* with operculum still attached, crystallite ridges well developed (apical end at bottom of photograph),
2. detail of parasulcus with crystallite ridges and enlarged pores, paraplates sa+1c clearly discernible at left bottom corner, sinistral and dextral sulcal paraplates merge into one paraplate, part of paraplate sp visible at top, and part of paraplate 1' at bottom;

Fig.3, 4: ***C. operosum***, sample 1606-7 MUC 14-15cm, #02203,

3. ventral view, specimen complete with operculum, crystallite ridges terminate as "blocky" rhomboids,
4. detail of sulcal area with paraplates defined by crystallite ridges and large pores, paraplates 1´+sa at top, paraplate 1c merges into sinistral and dextral sulcal paraplates, paraplate sp (at bottom) clearly defined by crystallite ridge;

Fig.5, 6: ***C. operosum***, sample 1606-7 MUC 15-16cm, #02209,

5. ventral view, specimen with open archaeopyle, crystallite ridges only a fraction of a micrometer high,
6. detail of parasulcus, paraplates 1´+sa+1c+sp discernible by rudimentary crystallite ridges and large pores;

Fig.7, 8: **"*Sphaerodinella*" *albatrosiana***, sample 1606-7 MUC 0-1cm, #01598,

7. ventral view, specimen without operculum, no visible crystallite ridges,
8. detail of sulcal area, outlines of paraplates 1´+sa+1c defined by enlarged pores.

Plate 22: Family Calciodinellaceae: *Calciodinellum operosum*

1 10µm

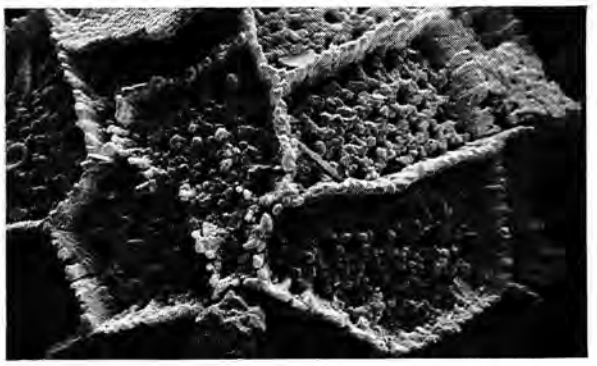

2 3µm

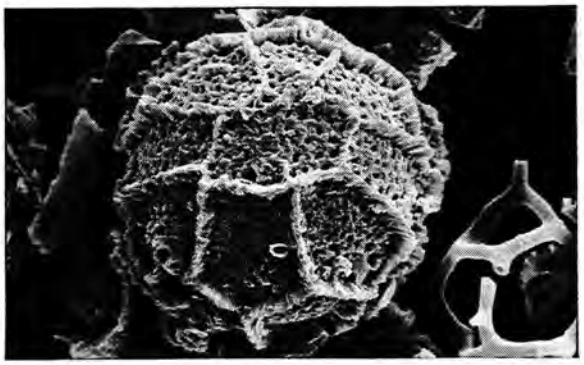

3 10µm

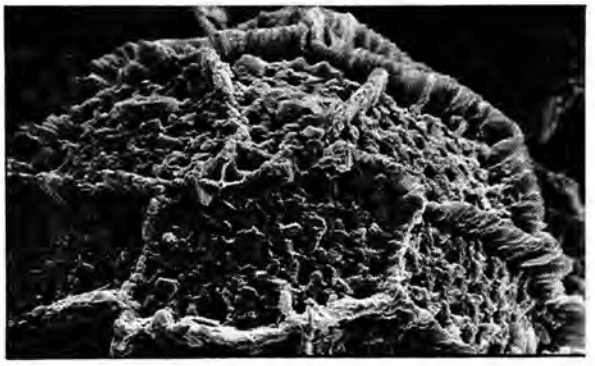

4 3µm

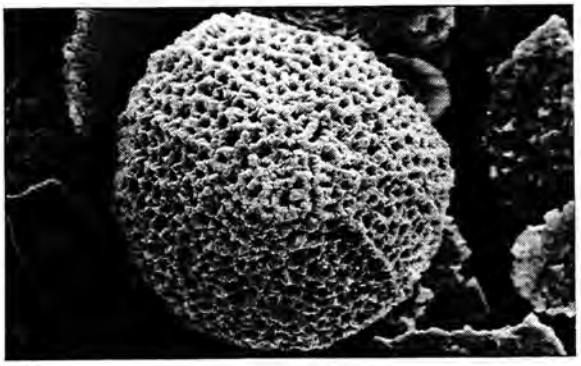

5 10µm

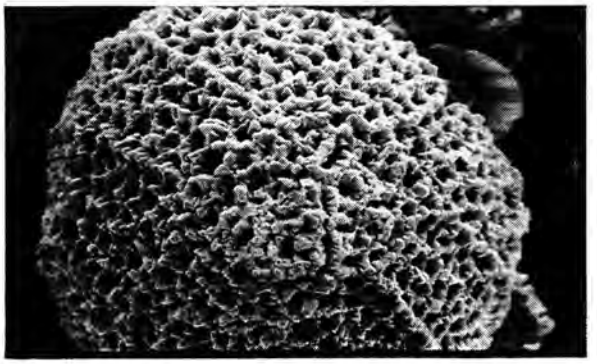

6 3µm

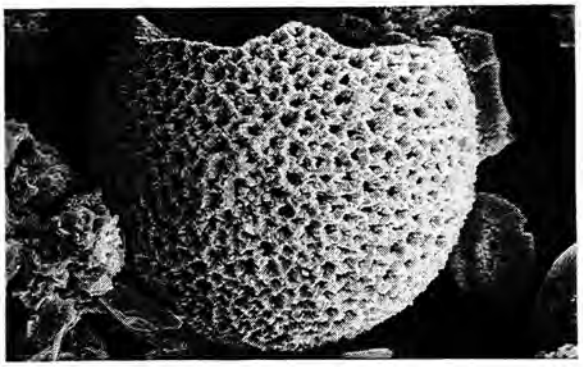

7 10µm

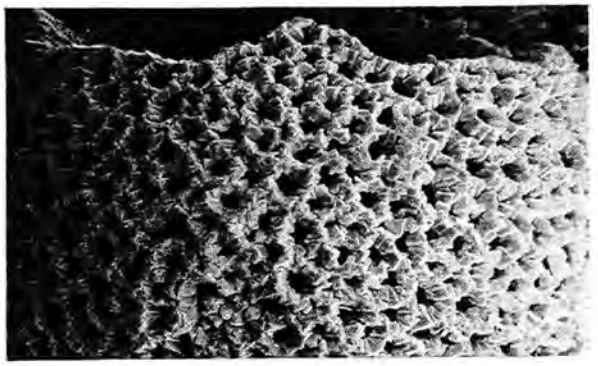

8 3µm

PLATE 23:

FAMILY CALCIODINELLACEAE DEFLANDRE, 1947 *emend.* BUJAK & DAVIS, 1983

CALCIODINELLUM DEFLANDRE, 1947 and

"*SPHAERODINELLA*" KEUPP & VERSTEEGH, 1989 **in the sediments**

Morphological Transitions between

Calciodinellum operosum DEFLANDRE, 1947 and

"*Sphaerodinella*" *albatrosiana* (KAMPTNER) KEUPP & VERSTEEGH, 1989

Fig.1, 2: ***Calciodinellum operosum***, sample 1606-7 MUC 0-1cm, #01490,

1. overall view on distal surface of lone big operculum, paraplates Po+2'-4'+1a-3a defined by crystallite ridges,
2. detail of apical pore paraplate;

Fig.3: ***C. operosum***, overall view on outer surface of single operculum, paraplates Po+2'-4'+1a-3a discernible by means of crystallite ridges, part of paraplate 2a missing, sample 1606-7 MUC 0-1cm, #01659;

Fig.4: ***C. operosum***, overall view on distal surface of isolated operculum, paraplates Po+2'-4'+1a-3a defined by two lines of low crystallite ridges, sample 1606-7 MUC 22-23cm, #02886;

Fig.5, 6: ***"Sphaerodinella" albatrosiana***, sample 1606-7 MUC 0-1cm, #01523,

5. oblique ventral view of solitary operculum without visible crystallite ridges,
6. detail of apical pore equivalent;

Fig.7: ***"Sph." albatrosiana***, apical view, specimen with operculum still attached, two thirds of archaeopyle boundary show suture, apical pore paraplate clearly discernible, no crystallite ridges visible, sample 1606-7 MUC 0-1cm, #01459;

Fig.8: ***"Sph." albatrosiana***, overall view on proximal surface of separated operculum, apical pore equivalent visible, sample 1606-7 MUC 0-1cm, #01525 (see Pl.25, Fig.6).

Plate 23: Family Calciodinellaceae: *Calciodinellum operosum*

1 10µm

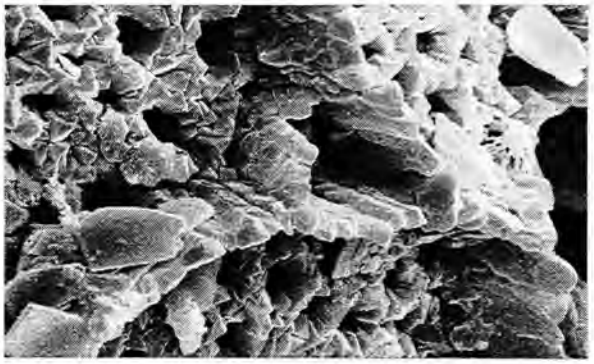

2 3µm

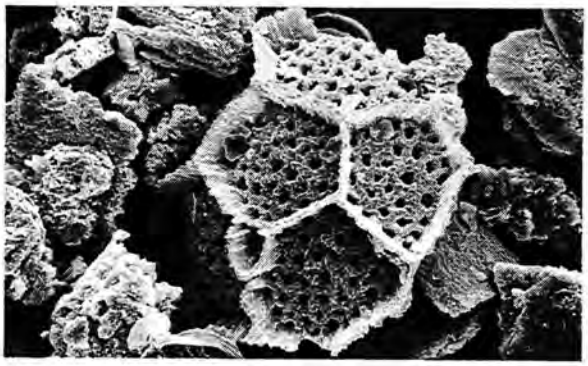

3 3µm

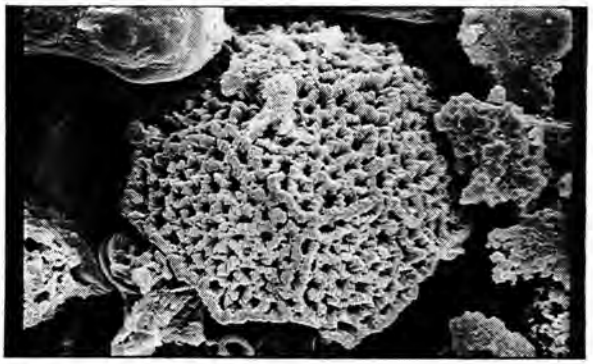

4 3µm

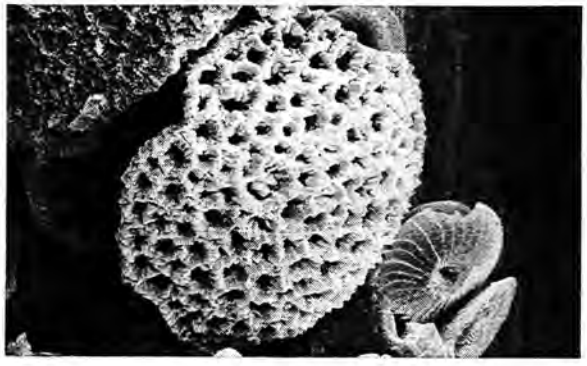

5 3µm

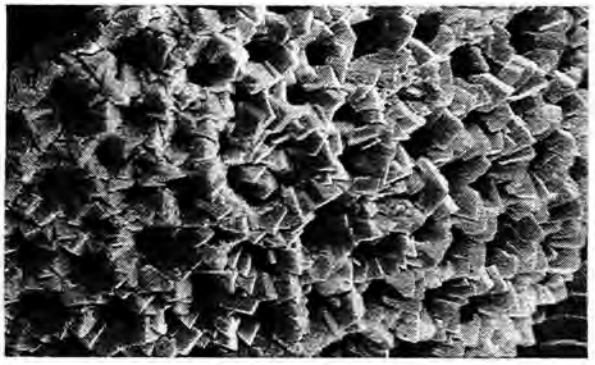

6 3µm

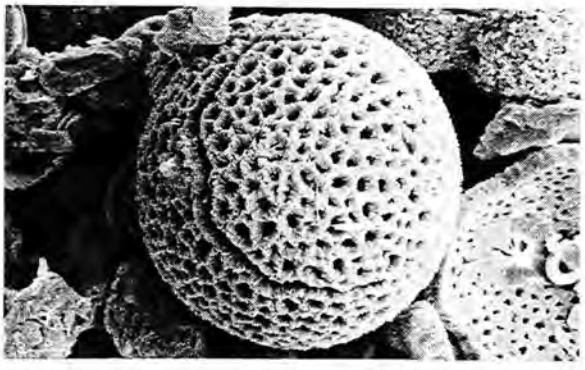

7 10µm

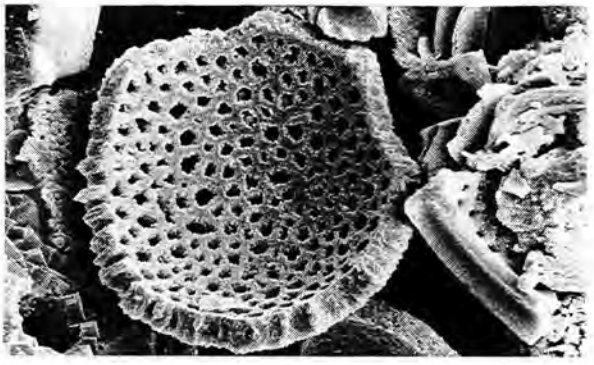

8 3µm

PLATE 24:

FAMILY CALCIODINELLACEAE DEFLANDRE, 1947 *emend.* BUJAK & DAVIS, 1983

CALCIODINELLUM DEFLANDRE, 1947

Calciodinellum operosum DEFLANDRE, 1947 **in the sediments**

Fig.1, 2: sample 1607-8 MUC 1-2cm, #00934,

1. antapical view, specimen with only rudimentary crystallite ridges, paraplate sp at right bottom corner,
2. detail of paraplate sutures, suture of paraplates 1""+2"" includes two lines of slightly longer crystals bordering one serie of pores, suture of paraplates 2""+sp consists of one line of elongated crystals, ridges not solid with gaps between crystallites;

Fig.3, 4: sample 1602-7 MUC 12-13cm, #01845,

3. right lateral view, specimen with open archaeopyle and low crystallite ridges,
4. detail of sutural junction of paraplates 5c+6c+4'''+5''', crystallite ridges low but solid with one line of densely packed "blocky" rhomboids;

Fig.5, 6: sample 1602-7 MUC 8-9cm, #01818,

5. right lateral view, specimen with solid and well preserved crystallite ridges,
6. detail of dorsal part of paraplate 2"", crystallite ridges compact terminating in "blocky" rhomboids,

Fig.7, 8: sample 1607-8 MUC 18-19cm, #02912,

7. left lateral view, specimen without operculum, crystallite ridges long and slender but damaged in many places,
8. detail, lateral view of crystallite ridge between paraplates 3c+4c, crystallites long and flat with "feathery" texture.

Plate 24: Family Calciodinellaceae: *Calciodinellum operosum*

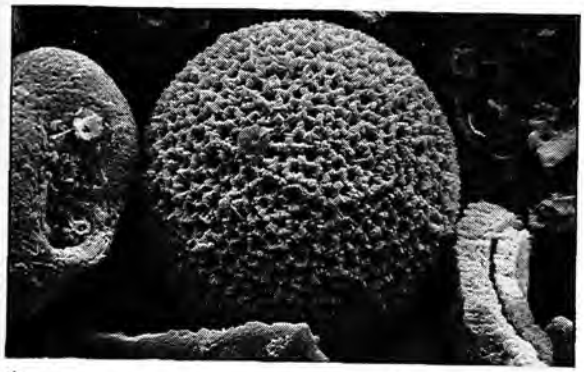

1 10µm

2 3µm

3 10µm

4 1µm

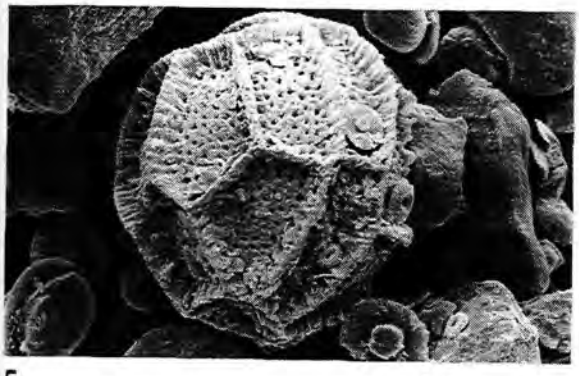

5 10µm

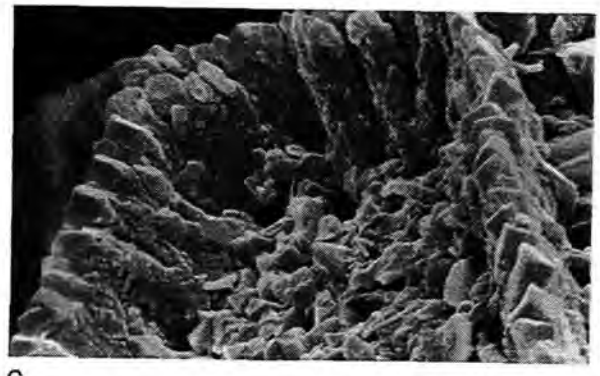

6 1µm

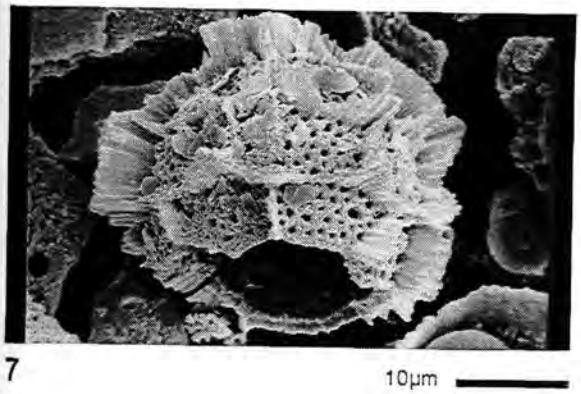

7 10µm

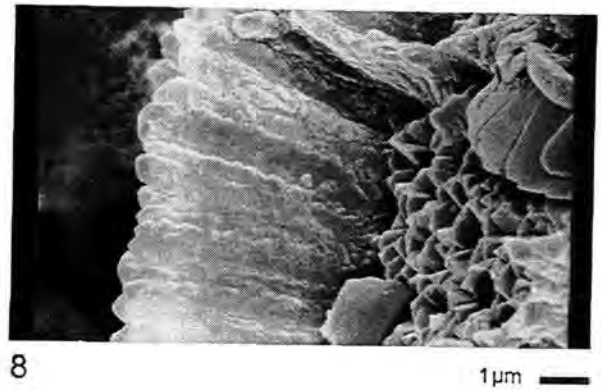

8 1µm

PLATE 25:

FAMILY CALCIODINELLACEAE DEFLANDRE, 1947 *emend.* BUJAK & DAVIS, 1983

CALCIODINELLUM DEFLANDRE, 1947 and

"*SPHAERODINELLA*" KEUPP & VERSTEEGH, 1989

Calciodinellum operosum DEFLANDRE, 1947 **in the sediments**

Fig.1, 2: sample 1606-7 MUC 9-10cm, #02093,

1. apical view, specimen with open archaeopyle and long "feathery" crystallite ridges,
2. detail of dorsal archaeopyle suture, paraplate 2a split within most dorsal and posterior serie of pores, this part remained with main cyst body;

Fig.3, 4: sample 1602-7 MUC 17-18cm, #01899,

3. dorsal view of specimen without operculum, crystallite ridges low and solid with "blocky" rhomboids,
4. detail of dorsal archaeopyle suture, paraplate 2a ruptured anteriorly of most dorsal and posterior serie of pores, this part remained with main cyst body;

Fig.5: detail of solitary operculum with well developed crystallite ridges, proximal surface with reticulation pattern, cross section of rim shows one layer of slightly brighter crystallites representing skeletal ultrastructure of main cyst body, on top of these onset of crystallite ridge discernible by slightly darker crystals, sample 1602-7 MUC 14-15cm, #01863;

"Sphaerodinella" albatrosiana (KAMPTNER) KEUPP & VERSTEEGH, 1989 **in the sediments**

Fig.6: detail of proximal surface of lone operculum, crystal bases even, crystallites circularly arranged around pores blending laterally into overall reticulate pattern, sample 1606-7 MUC 0-1cm, #01525 (see Pl.28, Fig.8);

Fig.7: detail of distal cyst surface of specimen with open archaeopyle, ultrastructural crystallites very small arranged around pores, crystallites interconnected laterally in an overall reticulate pattern, sample 1606-7 MUC 0-1cm, #01536;

Fig.8, 9: sample 1606-7 MUC 12-13cm,

8. overall view on distal surface of single operculum,
9. detail of outer surface showing "overgrowth" of small rhombic crystals (slightly brighter crystallites).

Plate 25: Family Calciodinellaceae: *Calciodinellum operosum*

1 10µm

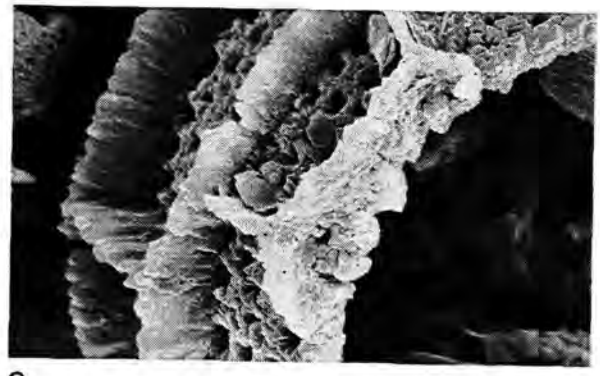

2 3µm

3 10µm

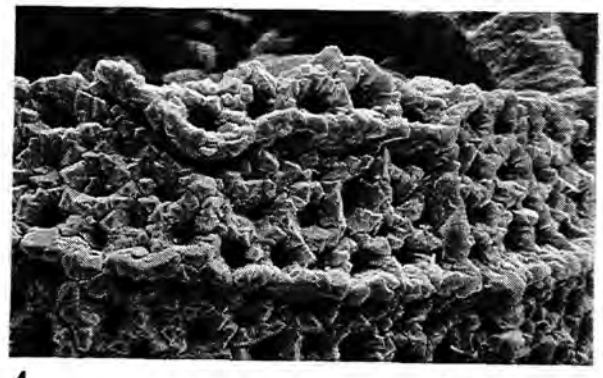

4 3µm

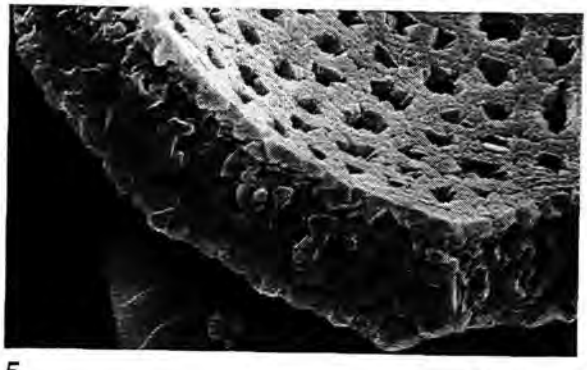

5 1µm

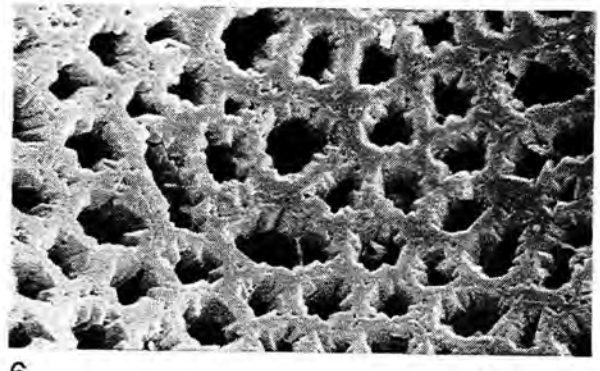

6 1µm

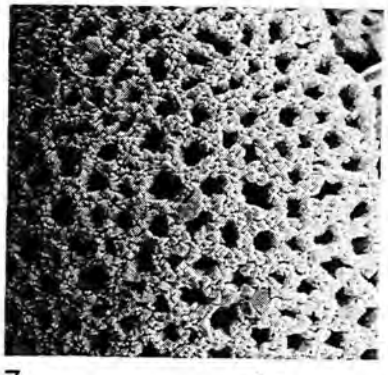

7 3µm

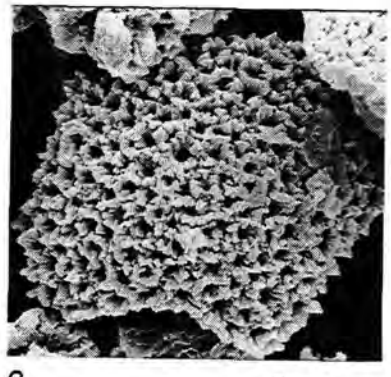

8 3µm

9 1µm

PLATE 26:

FAMILY CALCIODINELLACEAE DEFLANDRE, 1947 *emend.* BUJAK & DAVIS, 1983

"*SPHAERODINELLA*" KEUPP & VERSTEEGH, 1989

"*Sphaerodinella*" *albatrosiana* (KAMPTNER) KEUPP & VERSTEEGH, 1989 **in the plankton**

Fig.1, 2: sample 22-S14, #01077,

1. left lateral view, specimen with cell content, operculum still attached with part of archaeopyle suture visible,
2. detail of distal cyst surface, outer organic wall layer or phragma present, crystallites form ring-like structures around pores, crystals loosely attached to adjacent "*ringlets*";

Fig.3: detail of outer cyst surface of complete specimen, crystallites and part of pores covered with outer organic phragma, crystallites arranged around pores only moderately connected to neighbouring ring-like crystal structures, sample 22-S10, #01370;

Fig.4, 5: sample 22-S08, #01322,

4. oblique apical view of specimen with operculum still attached,
5. detail of operculum with archaeopyle suture, pores covered with outer organic wall layer, apical pore equivalent visible on left side of photograph, crystallites circularly arranged around pores and fairly linked;

Fig.6: detail of outer cyst surface, specimen with very small wall crystallites, crystallites not visible underneath outer organic phragma, phragma covers pores as well, sample 22-S08, #01309;

Fig.7: detail of distal cyst surface, specimen complete, "ringlets" of crystallites blending more or less into overall reticulate pattern, circular arrangement of crystallites still visible, sample 22-S16, #01238;

Fig.8: detail of specimen with operculum still attached, "mature" crystals linked building reticulate pattern, outer organic wall layer present but not covering pores, sample 22-S14, #01022;

Fig.9: detail of outer cyst surface, specimen with very small wall crystallites, outer organic phragma somewhat reduced revealing crystallites arranged around pores, sample 22-S16, #01234;

Fig.10: detail of outer cyst surface with a boring perforating cyst wall, operculum still attached with archaeopyle suture visible at uppermost part, cell content gone even though remains of outer organic phragma still covering crystals and some pores, sample 22-S16, #01196;

Fig.11, 12: sample 22-S16, #01254,

11. overall view, specimen crushed with collapsed cell content,
12. detail of wall cross section, pores proximally completely covered by inner organic wall layer or phragma and distally partly covered by outer organic wall layer or phragma.

Plate 26: Family Calciodinellaceae: "*Sphaerodinella*" *albatrosiana*

1 10µm

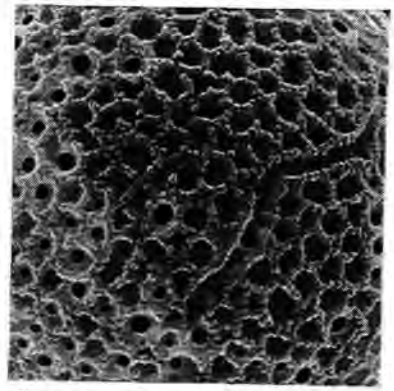

2 3µm

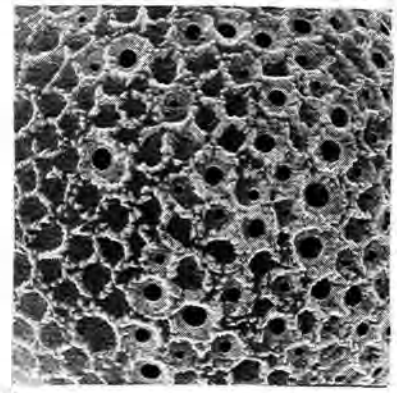

3 3µm

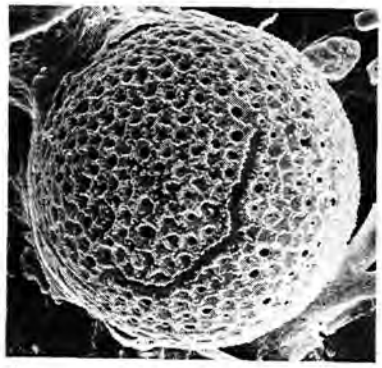

4 10µm

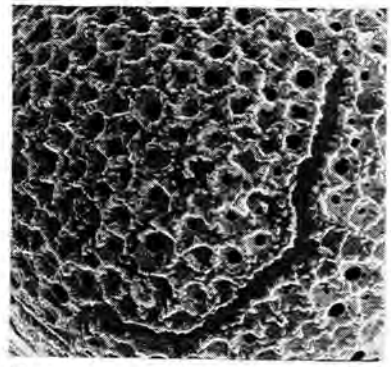

5 3µm

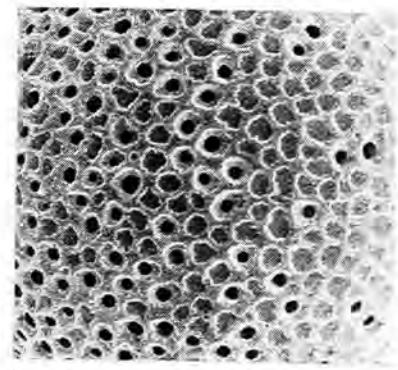

6 3µm

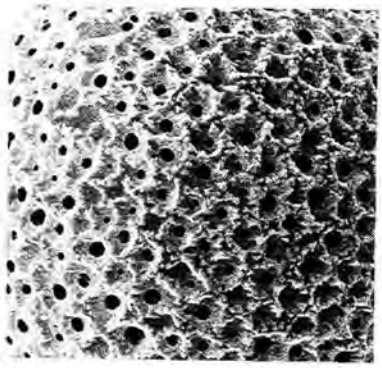

7 3µm

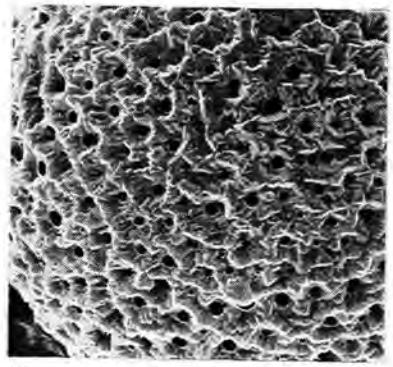

8 3µm

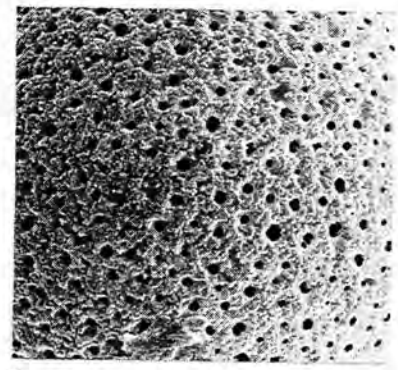

9 3µm

10 3µm

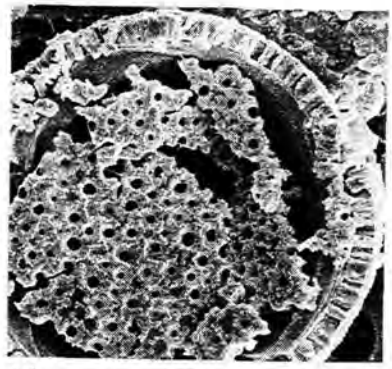

11 10µm

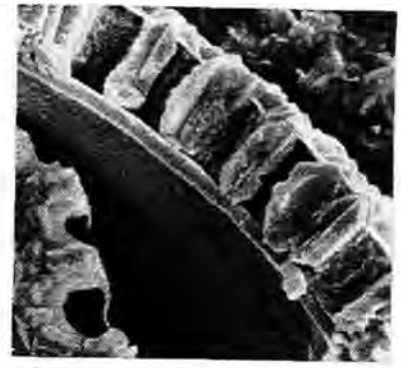

12 1µm

PLATE 27:

FAMILY CALCIODINELLACEAE DEFLANDRE, 1947 *emend.* BUJAK & DAVIS, 1983

SPHAERODINELLA KEUPP & VERSTEEGH, 1989

"Sphaerodinella" tuberosa (KAMPTNER) KEUPP & VERSTEEGH, 1989 **in the plankton**

Fig.1, 2: sample 22-S14, #00991,

1. left lateral view, specimen with cell content, operculum still attached (at right bottom of specimen), archaeopyle suture covered with outer organic wall layer or phragma,
2. detail of outer cyst surface, crystals show three-sided pyramids with flattened top, crystal faces hidden under outer organic phragma, phragma perforated by some pores between crystal pyramids;

Fig.3, 4: sample 22-S23, #01155,

3. oblique antapical view, specimen completely wrapped in outer organic layer,
4. detail of distal cyst surface, outer organic phragma without pores obscures lower part of crystals, crystal pyramids show furrowed edges,

Fig.5, 6: sample 22-S23, #01155,

5. oblique antapical view, specimen with outer organic phragma,
6. detail of outer cyst surface, crystallite pyramid tips serrated barely visible underneath outer organic wall layer;

"Sph." tuberosa **in the sediment**

Fig.7, 8: sample 1602-7 MUC 11-12cm, #01842,

7. lateral view, specimen slightly ovoid with missing operculum,
8. detail of distal cyst surface showing big loosely packed "buckle"-crystals with large pseudo-pores in lower crystal faces.

Plate 27: Family Calciodinellaceae: "*Sphaerodinella*" *tuberosa*

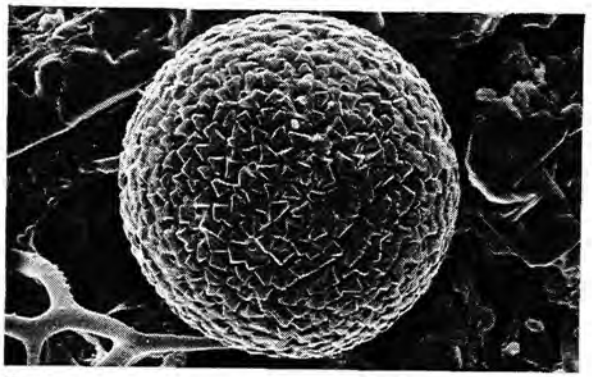

1 10µm

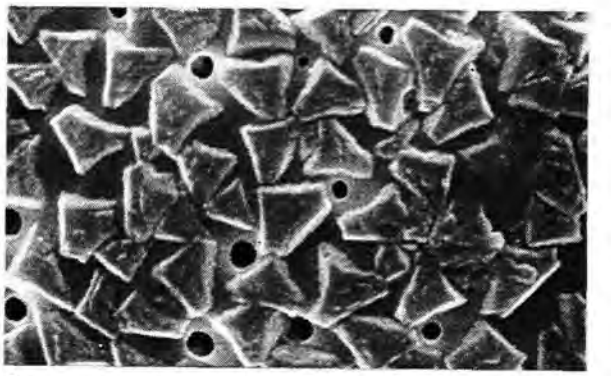

2 1µm

3 10µm

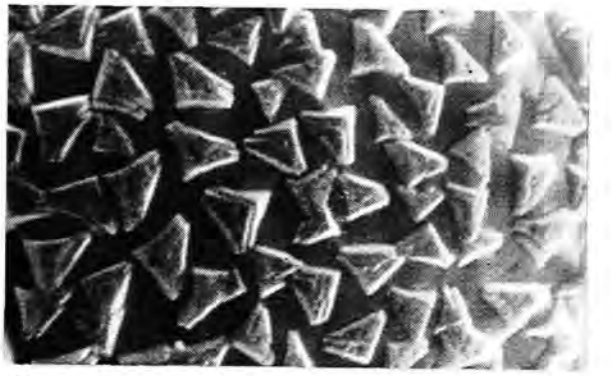

4 1µm

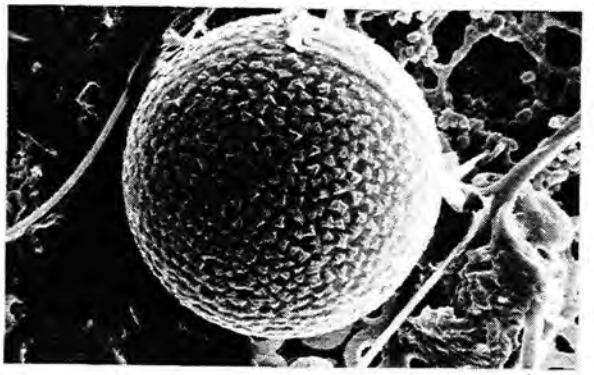

5 10µm

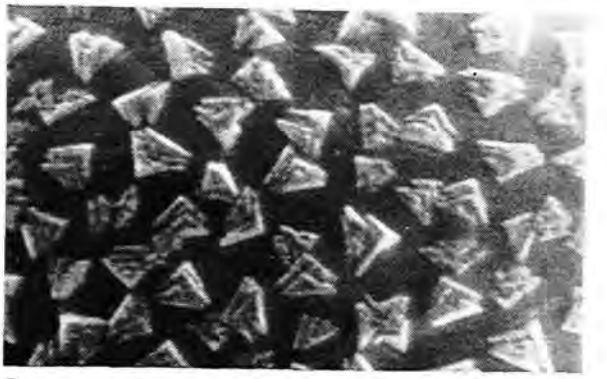

6 1µm

7 10µm

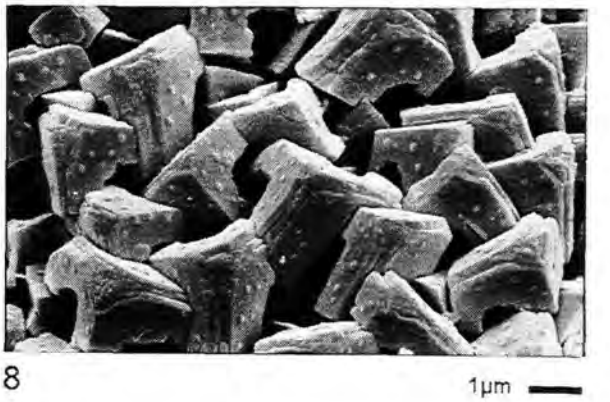

8 1µm

PLATE 28:

FAMILY CALCIODINELLACEAE DEFLANDRE, 1947 *emend.* BUJAK & DAVIS, 1983

SPHAERODINELLA KEUPP & VERSTEEGH, 1989

"Sphaerodinella" tuberosa (KAMPTNER) KEUPP & VERSTEEGH, 1989 **in the sediments**

Fig.1: oblique antapical view, distal crystal faces showing "buckle-like" framework, sample 1606-7 MUC 1-2cm, #00708;

Fig.2: apical view, specimen with operculum still attached, two thirds of archaeopyle boundary shows clear suture, sample 1606-7 MUC 0-1cm, #00606;

Fig.3, 4: sample 1606-7 MUC 12-13cm, #02175,

3. overall view on distal surface of isolated operculum with distinct outlines of plates 2'-4' + 1a-3a,

4. detail of operculum composed of "buckle"-crystals of average proportions and with grooved pyramid edges, tips clearly flattened, big pseudo-pores in lower crystal faces;

Fig.5: left lateral view, specimen with missing operculum, big archaeopyle open with plain margins, outer cyst surface shows transition between "buckle"- and "blocky"-crystals, sample 1606-7 MUC 1-2cm, #00732;

Fig.6: oblique lateral view, specimen without operculum, archaeopyle almost circular but frayed, crystals with solid "blocky" contour, sample 1602-7 MUC 19-20cm, #01924 (see Pl.26, Fig.7);

Fig.7, 8: sample 1602-7 MUC 24-25cm, #02055,

7. overall view on distal surface of single operculum, outline nearly circular,

8. detail of operculum composed of tightly crammed "blocky" crystals, small pseudo-pores visible, tips of rhombic "blocks" flattened.

Plate 28: Family Calciodinellaceae: "*Sphaerodinella*" *tuberosa*

1 10µm

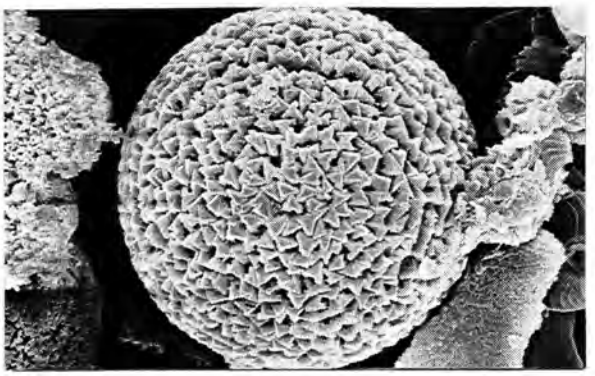

2 10µm

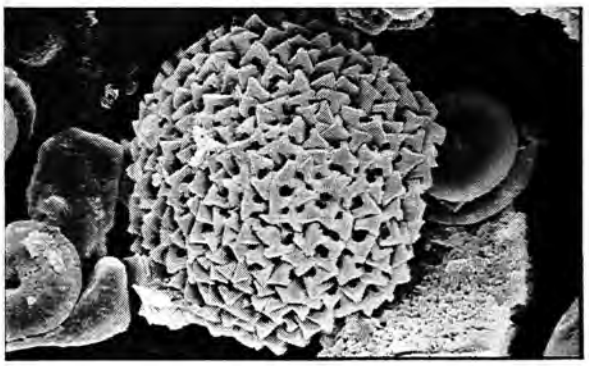

3 3µm

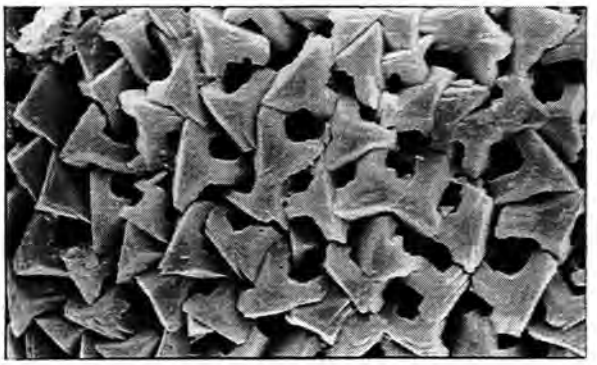

4 1µm

5 10µm

6 10µm

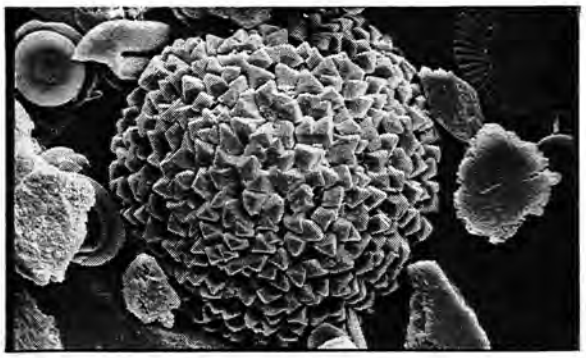

7 10µm

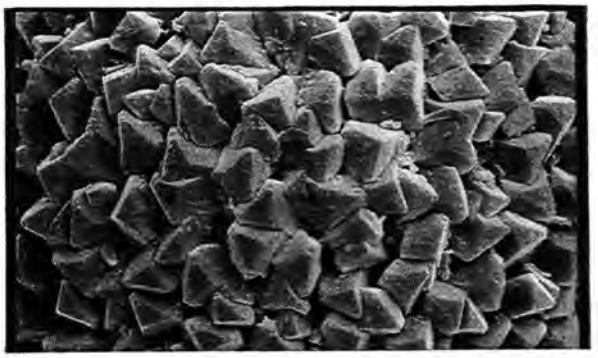

8 3µm

PLATE 29:

FAMILY CALCIODINELLACEAE DEFLANDRE, 1947 *emend.* BUJAK & DAVIS, 1983

SPHAERODINELLA KEUPP & VERSTEEGH, 1989

"Sphaerodinella" tuberosa (KAMPTNER) KEUPP & VERSTEEGH, 1989 **in the sediments**

Fig.1, 2: sample 1606-7 MUC 7-8cm, #02083,

1. lateral view, specimen without operculum, archaeopyle big nearly circular, distal faces of wall crystals with "cap-like" appearance,
2. detail of proximal cyst surface with plain polygonal sharp-edged crystal bases, bases with central poroid and "spade of cards" contour;

Fig.3, 4: sample 1606-7 MUC 18-19cm, #02217,

3. overall view, specimen without visible operculum, outer cyst surface shows "cap-like" crystals,
4. detail of distal cyst surface with "wavy" crystal edges;

Fig.5, 6: sample 1602-7 MUC 12-13cm, #01847,

5. overall view on proximal surface of single operculum with approximately circular outline,
6. detail of crystal bases and rim cross section of operculum, crystal bases even with small poroid in centre, most outlines resemble "spade of cards", crystal rhomboids of rim have clear edges;

Fig.7: detail of archaeopyle rim cross section, lower edges of crystals "sheared off", sample 1602-7 MUC 19-20cm, #01924 (see Pl.25, Fig.6);

Fig.8: proximal surface of broken specimen, crystal bases with central poroids and typical "spade of cards" outline, sample 1602-7 MUC 0-1cm, #00341.

Plate 29: Family Calciodinellaceae: "*Sphaerodinella*" *tuberosa*

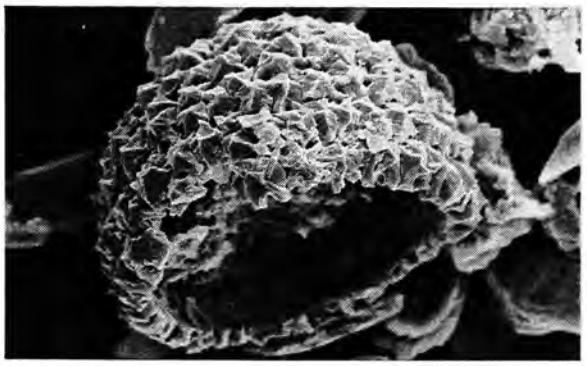

1 10µm

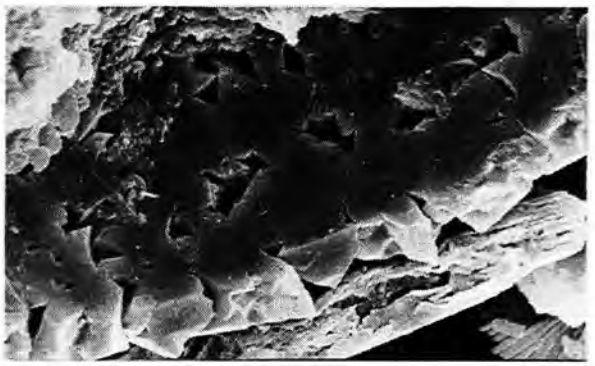

2 3µm

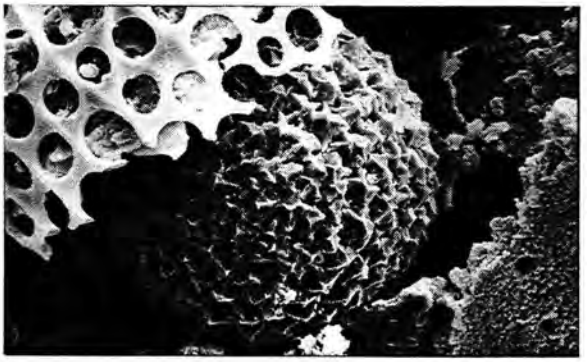

3 10µm

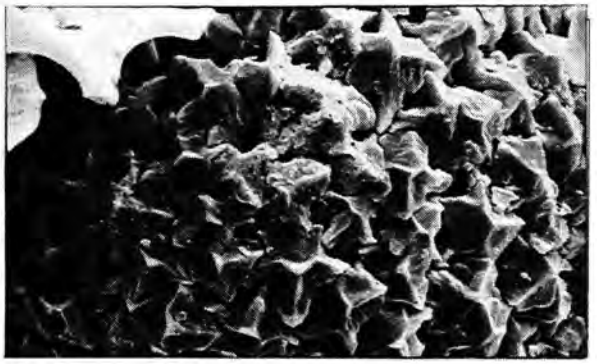

4 3µm

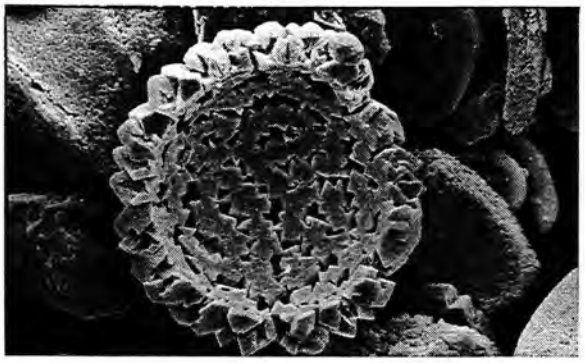

5 10µm

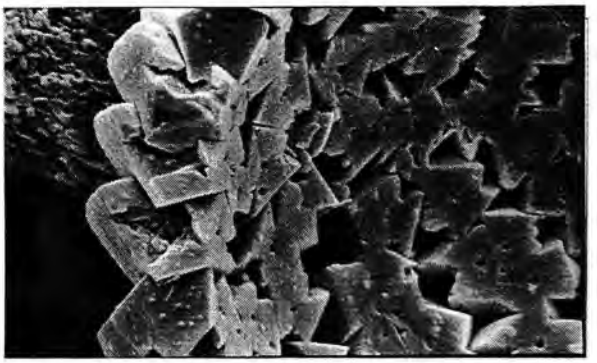

6 1µm

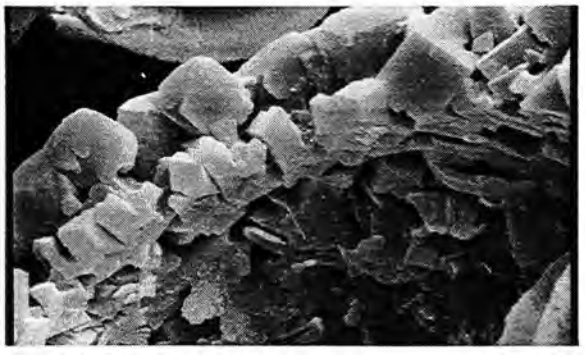

7 1µm

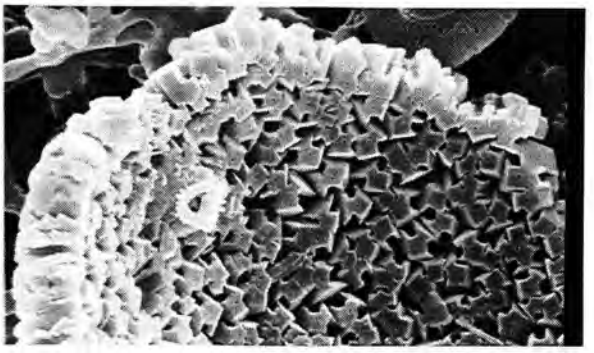

8 3µm

PLATE 30:

FAMILY CALCIODINELLACEAE DEFLANDRE, 1947 *emend.* BUJAK & DAVIS, 1983

RHABDOTHORAX KAMPTNER, 1958

Rhabdothorax erinaceus (KAMPTNER) KAMPTNER, 1958 **in the plankton**

Fig.1, 2, 3: sample 22-S10, #01407,

1. overall view, "perfect specimen" with long spines and spherical central body, no visible operculum,
2. detail of distal cyst surface with triangular, "clover leaf" crystal bases well developed and interconnected to form rigid central body,
3. triangular spines rise from centre of crystal bases tapering to pointed pyramid-like tip;

Fig.4: overall view of ovoid specimen with short spines ending in a small "knobby" pyramid, sample 22-S32, #02611;

Fig.5, 6: sample 22-S17, #01087,

5. overall view of slightly damaged specimen with short spines,
6. detail of outer cyst surface, crystal bases only loosely packed, central cyst body broken up in several places revealing cell content underneath, small triangular spines ending in "knobby" pyramids;

Fig.7, 8: sample 22-S32, #02650,

7. overall view of ovoid specimen with very short spines,
8. detail of distal cyst surface, crystals with rudimentary bases and serrated margins, spines show triangular outline tapering into small three-sided pyramids.

Plate 30: Family Calciodinellaceae: *Rabdothorax erinaceus*

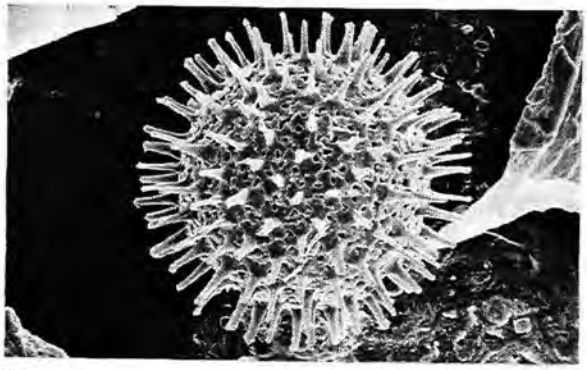

1 10µm

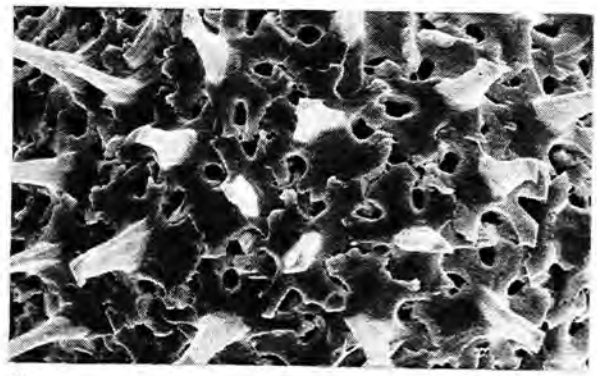

2 3µm

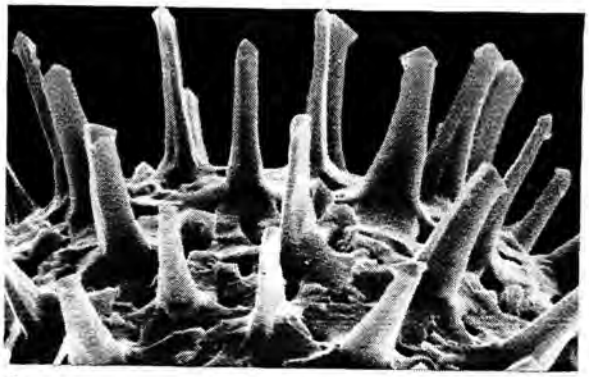

3 3µm

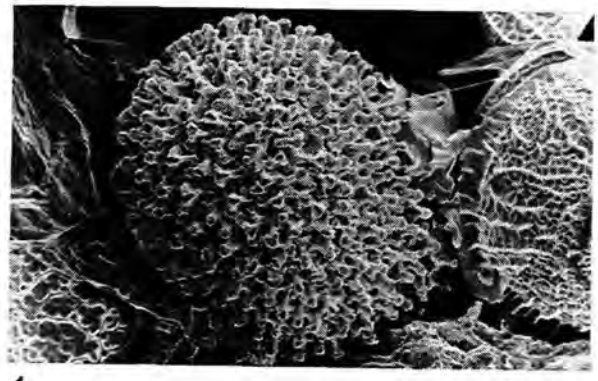

4 10µm

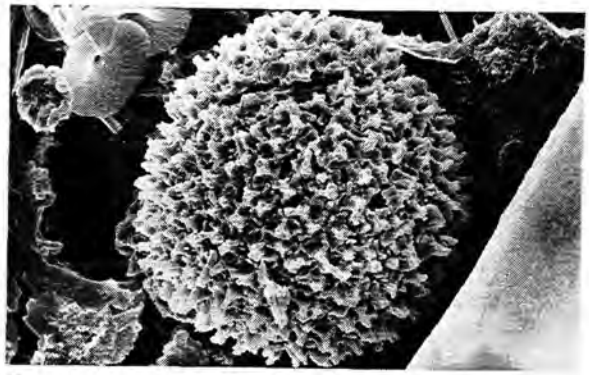

5 10µm

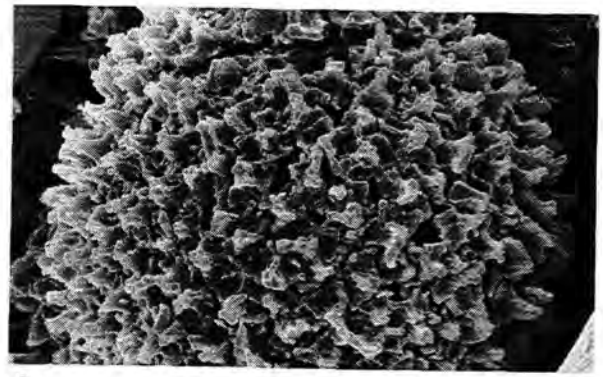

6 3µm

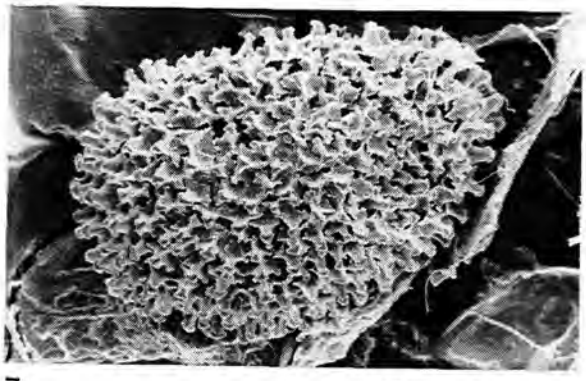

7 10µm

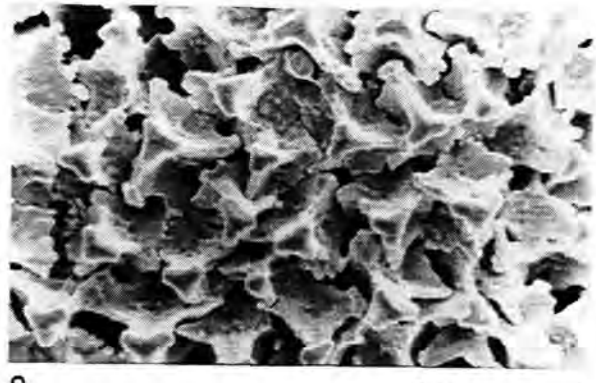

8 3µm

PLATE 31:

FAMILY CALCIODINELLACEAE DEFLANDRE, 1947 *emend.* BUJAK & DAVIS, 1983

RHABDOTHORAX KAMPTNER, 1958

Rhabdothorax erinaceus (KAMPTNER) KAMPTNER, 1958 **in the sediments**

Fig.1, 2: sample 1607-8 MUC 0-1cm, #02897,

1. oblique lateral view, specimen spherical with big circular archaeopyle,
2. detail of archaeopyle rim showing crystals with well developed and linked "clover leaf" bases and long triangular pointed spines;

Fig.3, 4: sample 1602-7 MUC 21-22cm, #02034,

3. overall view, specimen with round central body and long, but sometimes broken, spines,
4. detail of distal cyst surface with joined crystal bases, central spines long triangular and may be broken;

Fig.5, 6: sample 1602-7 MUC 23-24cm, #02039,

5. oblique apical view, spherical specimen without operculum and broken spines,
6. detail of archaeopyle rim showing well attached crystal bases and broken spines;

Fig.7: overall view, specimen ovoid with short "knobby" spines, sample 1606-7 MUC 0-1cm, #02070;

Fig.8: detail of proximal surface, specimen damaged, crystal bases smooth with small central poroid, outline "star-like" with blunt edges, sample 1602-7 MUC 18-19cm, #01903.

Plate 31: Family Calciodinellaceae: *Rabdothorax erinaceus*

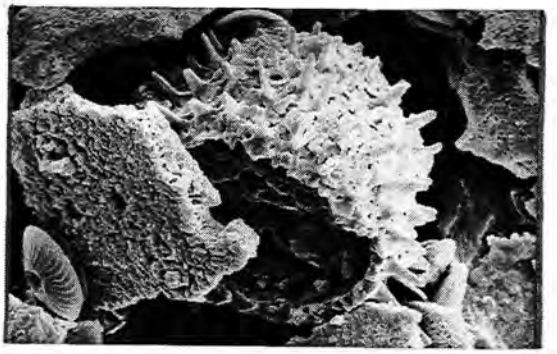

1 10µm

2 3µm

3 10µm

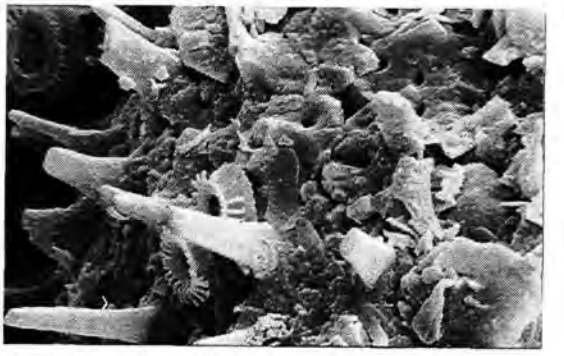

4 3µm

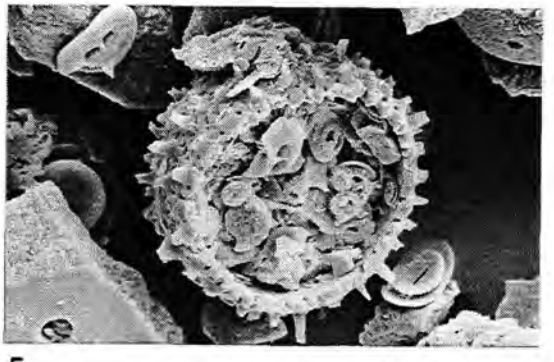

5 10µm

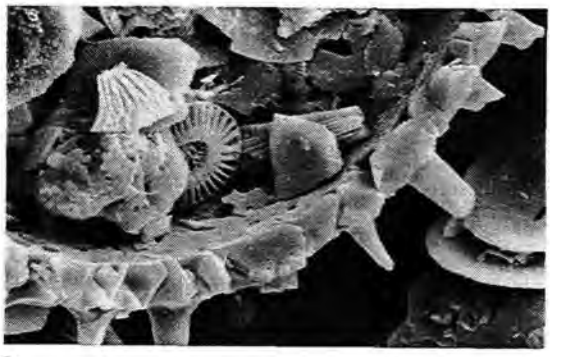

6 3µm

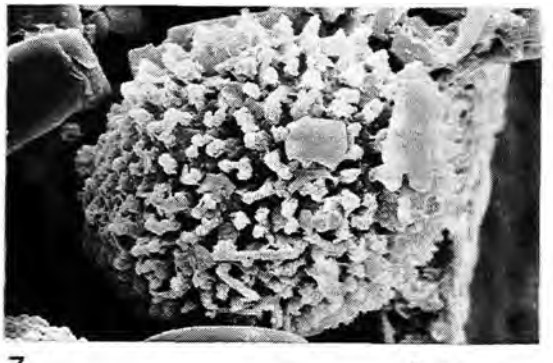

7 3µm

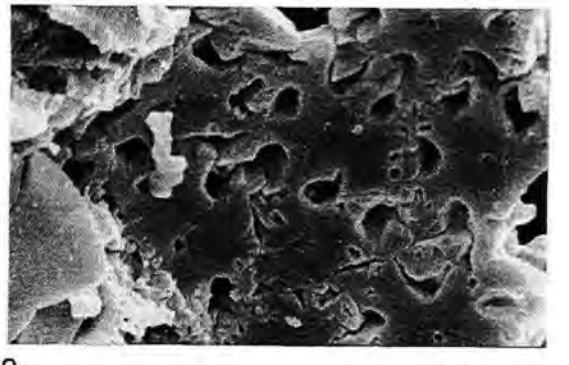

8 1µm

PLATE 32:

FAMILY CALCIODINELLACEAE DEFLANDRE, 1947 *emend.* BUJAK & DAVIS, 1983

ORTHOPITHONELLA KEUPP, 1984 *emend.* KEUPP & VERSTEEGH, 1989

Orthopithonella granifera (FÜTTERER) KEUPP & KOHRING, 1993 **in the plankton**

Fig.1, 2: sample 22-S17, #01673,

1. oblique lateral view, specimen with missing operculum,
2. oblique view of circular archaeopyle, tiny crystallites of distal cyst wall obscured by outer organic wall layer or phragma, proximal wall surface smooth hidden by inner organic wall layer;

Fig.3: close lateral view, specimen without operculum, archaeopyle with serrated margin, sample 22-S23, #01172;

Fig.4: detail of specimen without visible operculum, outer organic phragma reduced exposing needle-like crystals of outer cyst wall, sample 22-S17, #01100.

O. granifera **in the sediments**

Fig.5, 6: sample 1606-7 MUC 12-13cm, #02194,

5. apical view, with operculum still attached,
6. detail of sub circular operculum, crystallites densely packed with a "solid-blocky" margin;

Fig.7, 8: sample 1602-7 MUC 13-14cm, #01852,

7. lateral view, specimen complete and slightly ovoid, outer cyst wall shows segmentation into irregular plate-like elements,
8. lateral view of operculum showing elevation of "knobby" central feature and "flattened" sutural rim surrounding the archaeopyle.

Plate 32: Family Calciodinellaceae: *Orthopithonella granifera*

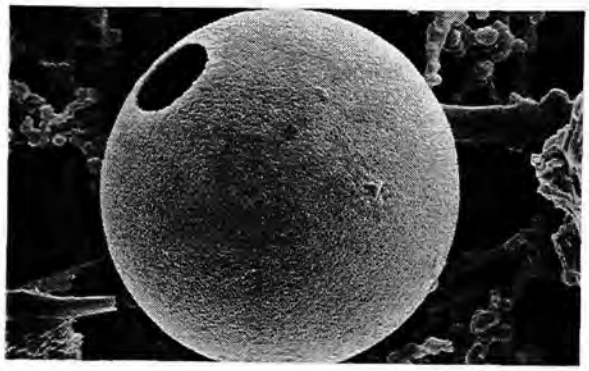

1

3µm

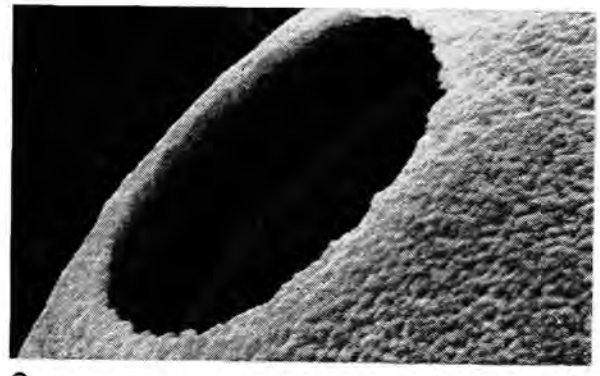

2

1µm

3

3µm

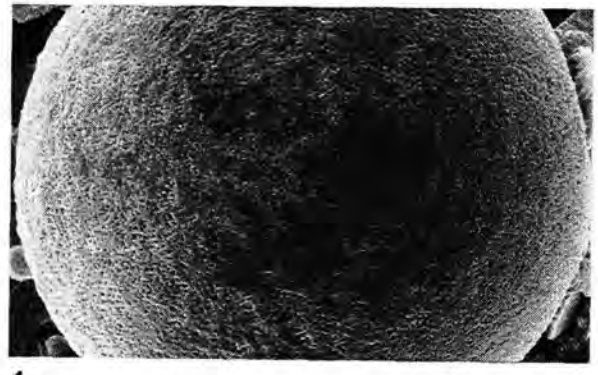

4

3µm

5

3µm

6

3µm

7

3µm

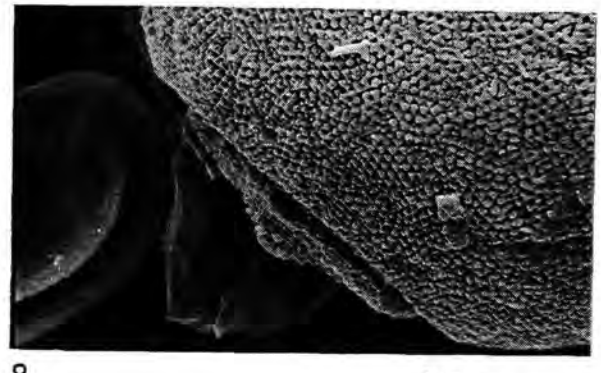

8

3µm

PLATE 33:

FAMILY CALCIODINELLACEAE DEFLANDRE, 1947 *emend.* BUJAK & DAVIS, 1983

ORTHOPITHONELLA KEUPP, 1984 *emend.* KEUPP & VERSTEEGH, 1989

Orthopithonella granifera (FÜTTERER) KEUPP & KOHRING, 1993 **in the sediments**

Fig.1, 2, 3: sample 1606-7 MUC 7-8cm, #02090,

1. oblique apical view, specimen with open archaeopyle, outer cyst surface shows less pronounced segmentation,
2. oblique view of archaeopyle with tightly packed crystallites at sub-circular sutural rim area;
3. detail of distal cyst surface, some crystallites arranged in single file whereas others blending laterally and forming reticulate pattern;

Fig.4: detail of outer cyst surface with "big" crystallites merging to reticulate pattern, sample 1606-7 MUC 0-1cm, #01717;

Fig.5: detail of distal cyst surface, crystallites tiny densely stacked forming a granular surface with poroids, sample 1602-7 MUC 21-22cm, #02032;

Fig.6: detail of outer cyst surface, crystallites tightly packed with slight secondary overgrowth of small calcite rhomboids, sample 1602-7 MUC 23-24cm, #02050;

Fig.7, 8: sample 1606-7 MUC 22-23cm, #02890,

7. detail of wall cross section, specimen damaged, crystallites small elongated rhomboids packed on top of each other, poroids between rhomboids,
8. detail of proximal cyst wall with even surface, crystallites have vermiculate outline with poroids in between.

Plate 33: Family Calciodinellaceae: *Orthopithonella granifera*

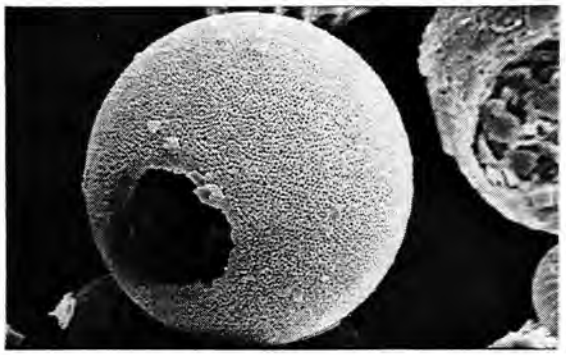

1 3µm

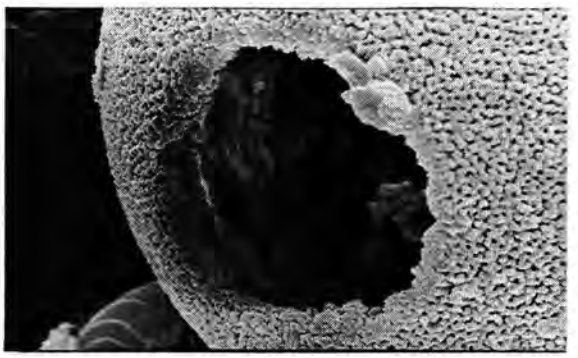

2 3µm

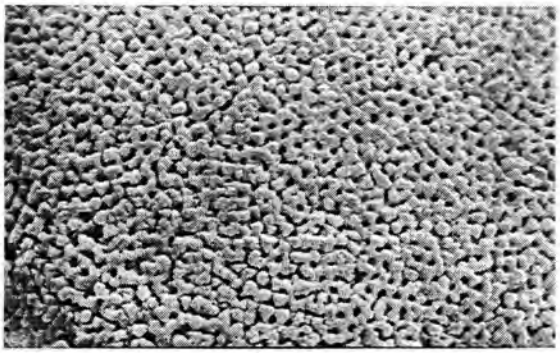

3 1µm

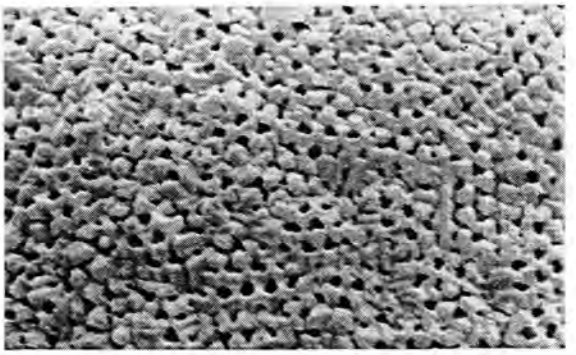

4 1µm

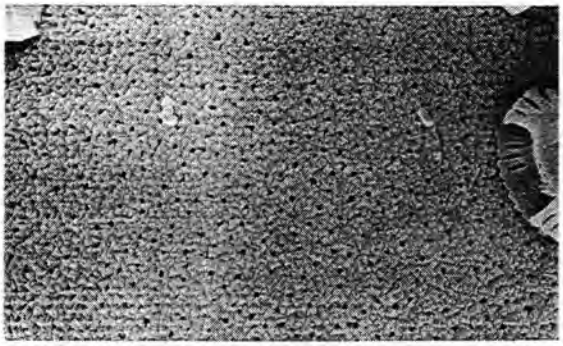

5 1µm

6 1µm

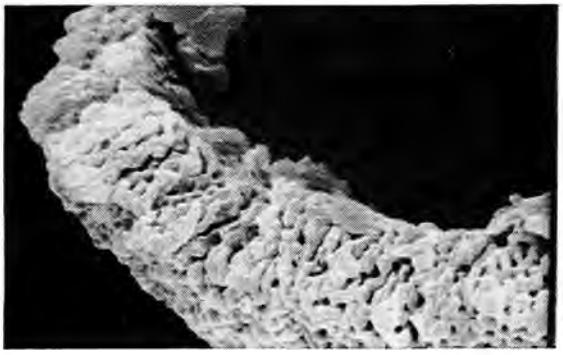

7 1µm

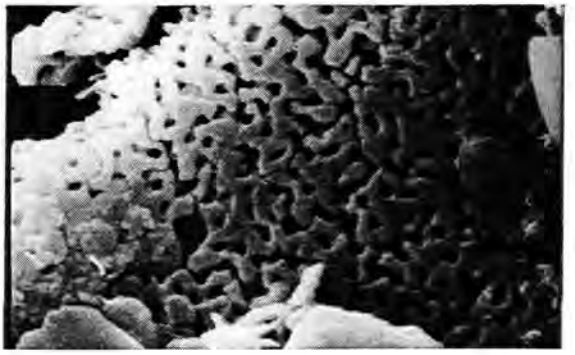

8 1µm

Appendix A:

Alphabetic list of the vegetative-thecate dinoflagellates and their cysts recorded during cruise M 23/3.
The nutritional mode (Nut.) is listed (as a: autotrophic, h: heterotrophic, s: with endo/episymbionts).
The thecate species are recorded as present (dark shaded bars) or absent (blank).
The respective cyst names are listed for species known to produce cysts and the occurrence of cysts in the plankton samples is marked with an X.
The presence of the vegetative-coccoid species is recorded with black bar graphs.

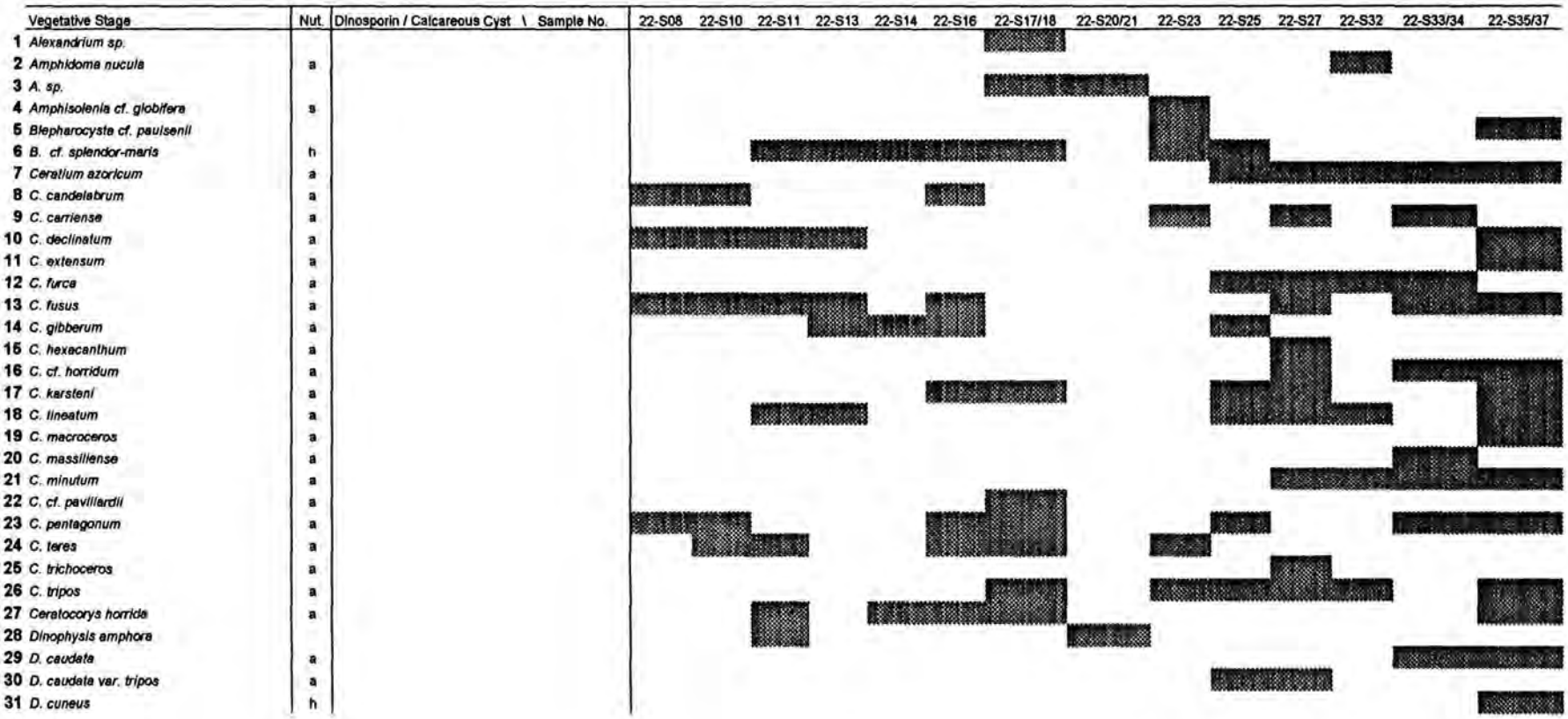

Appendix A:

Alphabetic list of the vegetative-thecate dinoflagellates and their cysts recorded during cruise M 23/3.
The nutritional mode (Nut.) is listed (as a: autotrophic, h: heterotrophic, s: with endo/episymbionts).
The thecate species are recorded as present (dark shaded bars) or absent (blank).
The respective cyst names are listed for species known to produce cysts and the occurrence of cysts in the plankton samples is marked with an X.
The presence of the vegetative-coccoid species is recorded with black bar graphs.

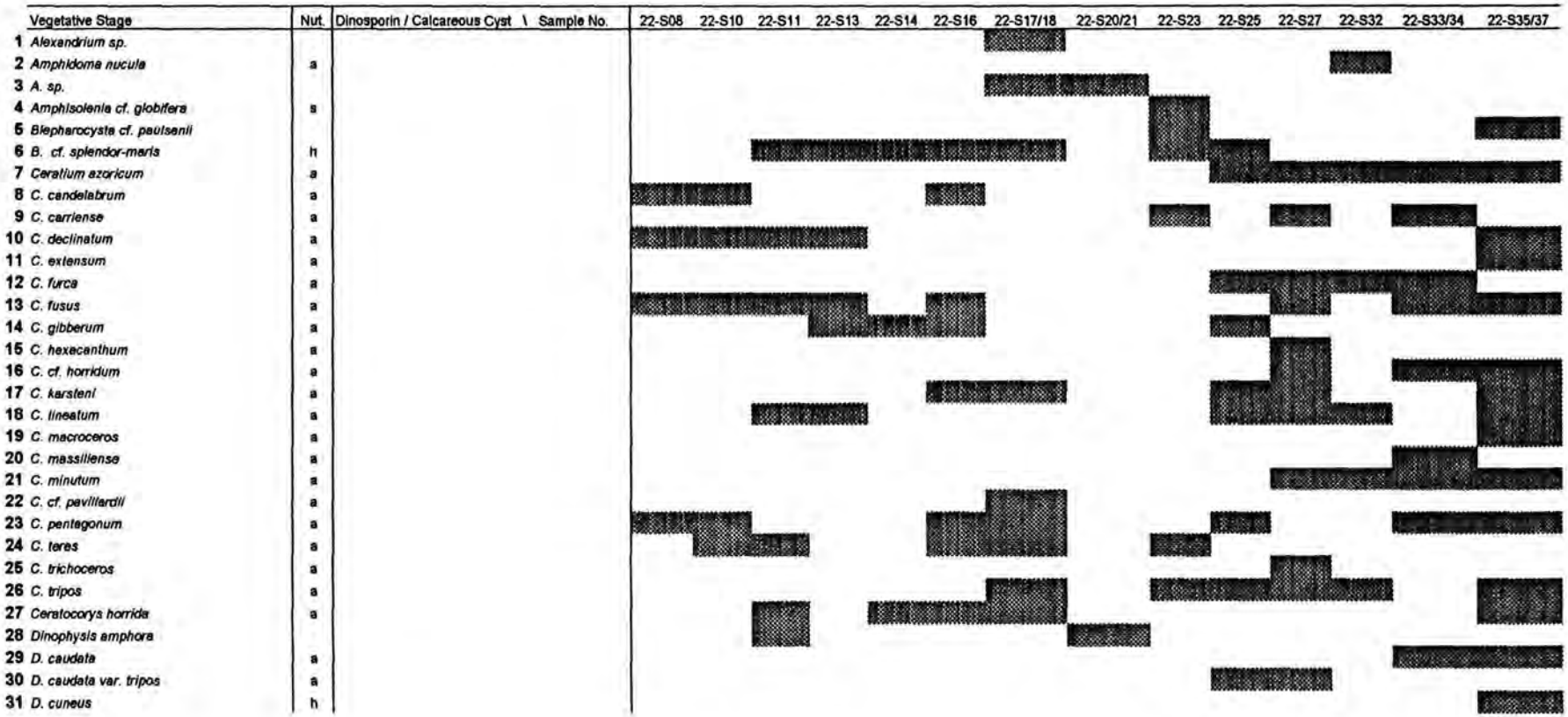

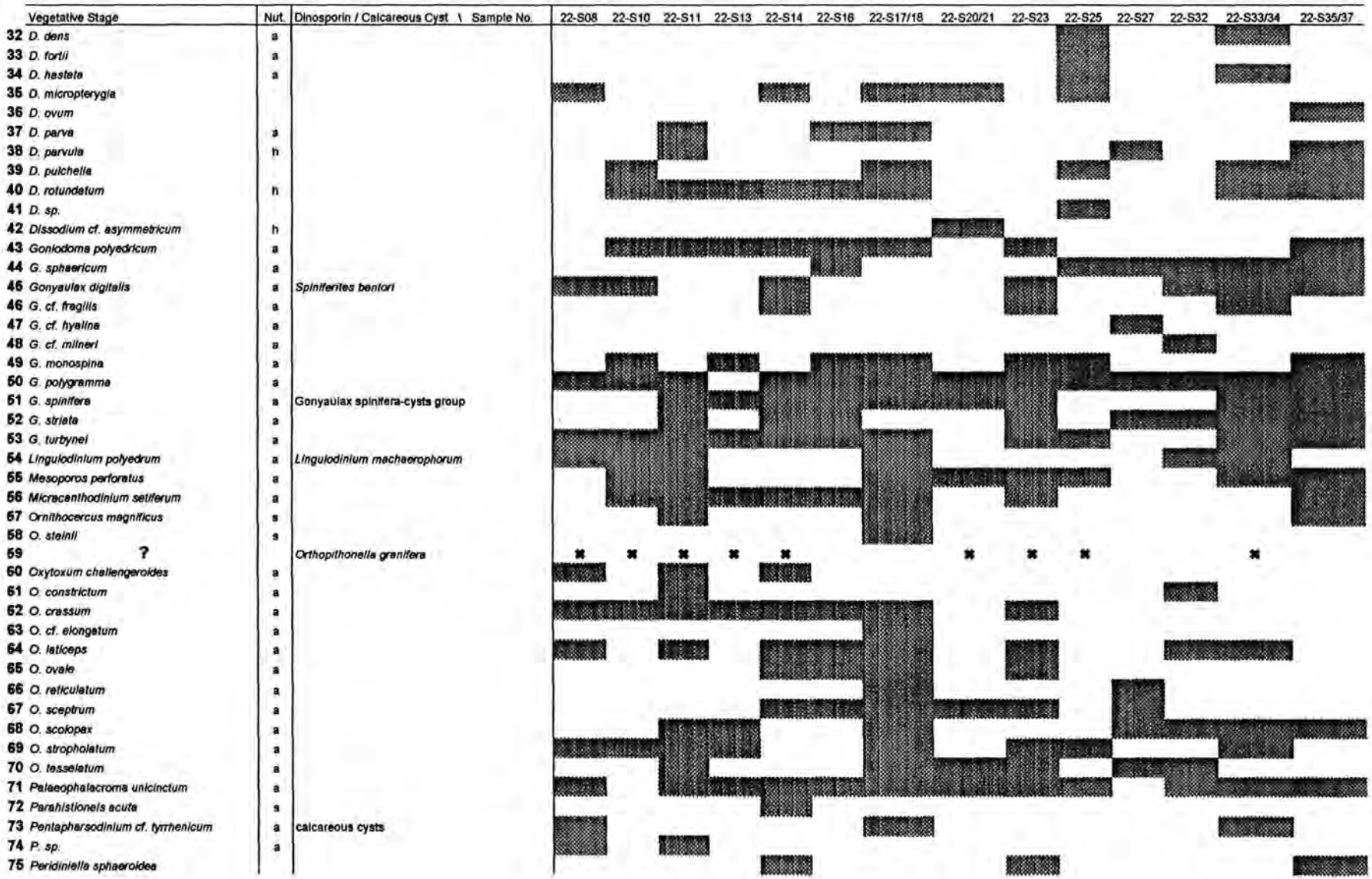
Vegetative Stage
Nut.
Dinosporin / Calcareous Cyst \ Sample No.
22-S08
22-S10
22-S11
22-S13
22-S14
22-S16
22-S17/18
22-S20/21
22-S23
22-S25
22-S27
22-S32
22-S33/34
22-S35/37
32 D. dens
33 D. fortii
34 D. hastata
35 D. micropterygia
36 D. ovum
37 D. parva
38 D. parvula
39 D. pulchella
40 D. rotundatum
41 D. sp.
42 Dissodium cf. asymmetricum
43 Goniodoma polyedricum
44 G. sphaericum
45 Gonyaulax digitalis
46 G. cf. fragilis
47 G. cf. hyalina
48 G. cf. milneri
49 G. monospina
50 G. polygramma
51 G. spinifera
52 G. striata
53 G. turbynei
54 Lingulodinium polyedrum
55 Mesoporos perforatus
56 Micracanthodinium setiferum
57 Ornithocercus magnificus
58 O. steinii
59 ?
60 Oxytoxum challengeroides
61 O. constrictum
62 O. crassum
63 O. cf. elongatum
64 O. laticeps
65 O. ovale
66 O. reticulatum
67 O. sceptrum
68 O. scolopax
69 O. stropholatum
70 O. tesselatum
71 Palaeophalacroma unicinctum
72 Parahistionels acuta
73 Pentapharsodinium cf. tyrrhenicum
74 P. sp.
75 Peridiniella sphaeroidea
a
h
s
Spiniferites bentori
Gonyaulax spinifera-cysts group
Lingulodinium machaerophorum
Orthopithonella granifera
calcareous cysts

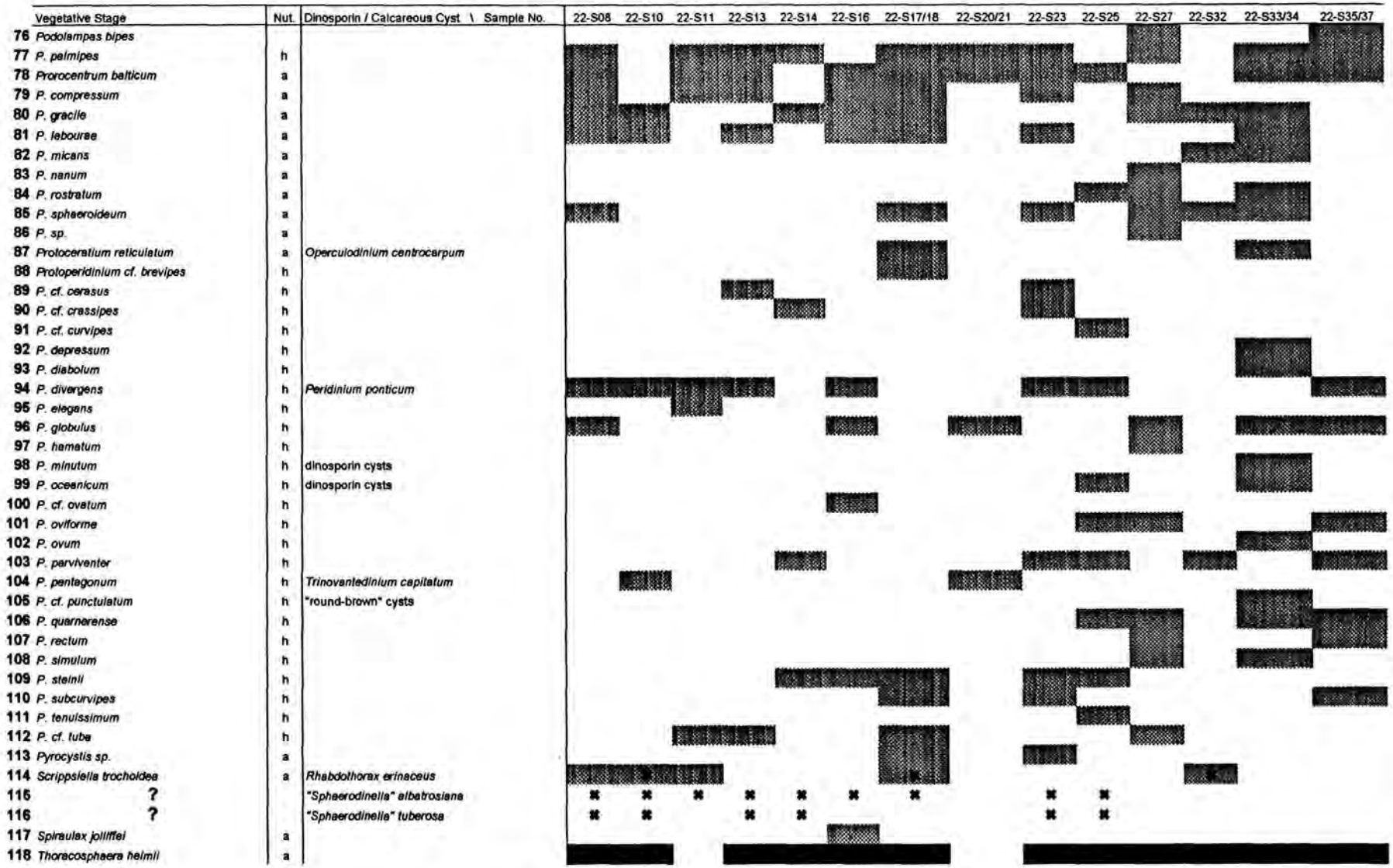
Vegetative Stage
Nut.
Dinosporin / Calcareous Cyst \ Sample No.
22-S08
22-S10
22-S11
22-S13
22-S14
22-S16
22-S17/18
22-S20/21
22-S23
22-S25
22-S27
22-S32
22-S33/34
22-S35/37
76 Podolampas bipes
77 P. palmipes h
78 Prorocentrum balticum a
79 P. compressum a
80 P. gracile a
81 P. lebourae a
82 P. micans a
83 P. nanum a
84 P. rostratum a
85 P. sphaeroideum a
86 P. sp. a
87 Protoceratium reticulatum a Operculodinium centrocarpum
88 Protoperidinium cf. brevipes h
89 P. cf. cerasus h
90 P. cf. crassipes h
91 P. cf. curvipes h
92 P. depressum h
93 P. diabolum h
94 P. divergens h Peridinium ponticum
95 P. elegans h
96 P. globulus h
97 P. hematum h
98 P. minutum h dinosporin cysts
99 P. oceanicum h dinosporin cysts
100 P. cf. ovatum h
101 P. oviforme h
102 P. ovum h
103 P. parviventer h
104 P. pentagonum h Trinovantedinium capitatum
105 P. cf. punctulatum h "round-brown" cysts
106 P. quarnerense h
107 P. rectum h
108 P. simulum h
109 P. steinii h
110 P. subcurvipes h
111 P. tenuissimum h
112 P. cf. tuba h
113 Pyrocystis sp. a
114 Scrippsiella trochoidea a Rhabdothorax erinaceus
115 ? "Sphaerodinella" albatrosiana
116 ? "Sphaerodinella" tuberosa
117 Spiraulax jolliffei a
118 Thoracosphaera heimii a

Appendix B:

Calculated specimen densities on the SEM stubs of surface sediment samples from offshore NW Africa (GeoB 1602-7 MUC) and from the eastern equatorial Atlantic (GeoB 1606-7 MUC, GeoB 1607-8 MUC).

GeoB 1602-7 MUC (Off Cape Blanc)

Depth [cm]	Age Calender ka	Event	*C. operosum*	*"Sph." albatrosiana*	*O. granifera*	*Rh. erinaceus*	*"Sph." tuberosa*	*Th. heimii*
0			8	146	15	0	107	1472
1			15	68	53	8	114	1430
2			0	100	0	0	108	689
3			0	120	0	0	64	1518
4			0	107	0	0	64	1093
5			0	43	0	9	113	1541
6			0	97	0	0	177	1329
7			0	51	0	0	87	1148
8			8	50	0	0	83	1533
9			7	150	0	0	157	1450
10			0	164	16	8	109	1570
11			0	189	8	0	189	1754
12			16	110	0	0	118	1795
13			15	145	7	0	225	3106
14			9	144	0	0	171	3594
15			0	177	0	0	129	3772
16			7	147	0	0	110	3404
17			7	160	0	0	240	3533
18	6.00	HCO	30	170	30	10	290	5100
19			47	422	94	0	453	9984
20			11	160	117	0	330	5787
21	7.00	1.1	8	143	191	8	278	5770
22			0	198	186	12	314	6744
23			0	100	262	15	169	4231
24			0	123	239	0	123	4215
25			9	73	264	9	246	3673
26			9	55	236	0	173	3309
27			10	80	270	10	90	3020
28			18	18	282	0	91	2636
29			0	36	127	0	91	2491
30			0	33	142	0	58	1017

GeoB 1606-7 MUC (Guinea Basin)

Depth [cm]	Age Calender ka	Event	*C. operosum*	*"Sph." albatrosiana*	*O. granifera*	*Rh. erinaceus*	*"Sph." tuberosa*	*Th. heimii*
0			107	1821	393	18	518	625
1			83	1883	150	0	483	417
2			52	2052	172	0	569	431
3			36	607	125	0	232	661
4			46	918	109	0	382	509
5			39	1221	156	0	351	584
6			53	1232	126	0	368	295
7			24	1000	110	0	342	561
8			40	1213	93	0	347	533
9			53	1642	147	0	632	432
10			40	1925	132	0	660	396
11			51	1317	89	0	443	633
12	6.00	HCO	28	731	48	0	304	393
13			83	1208	194	0	458	389
14	7.00	1.1	99	1747	85	0	507	718
15			28	1014	127	0	718	831
16			81	1532	113	0	774	790
17			145	1319	132	0	763	934
18			33	1475	164	0	525	885
19			42	1780	148	0	996	1568
20			219	2155	152	0	1347	1010
21			148	2377	230	0	1639	672
22			153	2119	186	0	1017	1068
23			65	1984	210	0	1548	952
24	12.00		165	1278	150	0	842	481
25		Younger	138	2118	333	0	1020	824
26	13.00	Dryas	235	2020	235	0	1196	667
27			148	1459	197	0	820	459
28	14.00	2.00	85	761	141	0	521	169
29			196	1036	304	0	768	268

GeoB 1607-8 MUC (Guinea Basin)

Depth [cm]	Age Calender ka	Event	*C. operosum*	*"Sph." albatrosiana*	*O. granifera*	*Rh. erinaceus*	*"Sph." tuberosa*	*Th. heimii*
0			0	1414	128	17	379	862
1			18	1248	184	0	275	716
2			0	1193	123	0	246	667
3			0	1278	37	0	278	574
4			39	1135	115	0	135	769
5			0	1052	138	0	276	604
6			53	922	89	0	195	496
7			0	763	34	0	186	492
8			49	1148	66	0	262	754
9			18	1018	55	0	164	655
10			63	1708	0	0	396	1021
11			21	1674	65	0	292	609
12	6.00	HCO	17	1678	68	0	475	746
13			27	1107	27	0	360	693
14	7.00	1.1	21	1771	63	0	375	896
15			41	1265	61	0	388	837
16			32	1565	81	0	274	1210
17			61	1329	61	0	378	988
18			64	1683	159	16	905	1270
19			73	1982	182	0	946	1309
20			34	1458	85	0	729	1661
21			73	1782	127	0	782	1509
22			138	1897	104	0	983	1862
23			33	1328	98	0	1033	1410
24	12.00		109	1836	146	0	1091	1946
25		Younger	276	1948	207	0	810	2052
26	13.00	Dryas	180	2049	164	0	1262	1787
27			250	2500	117	0	1350	2117
28	14.00	2.00	151	1925	245	0	925	1981
29			161	2054	214	0	821	1250
30			409	1606	349	0	879	1455
31			291	2400	418	0	982	1927
32			131	1771	344	0	721	984
33			288	1746	356	0	678	712
34			220	1762	634	18	495	440